



# ScuDo

Scuola di Dottorato ~ Doctoral School  
WHAT YOU ARE, TAKES YOU FAR

Doctoral Dissertation  
Doctoral Program in Architectural and Landscape Heritage (29<sup>th</sup> Cycle)

# Dynamic characterization of high performance materials for application to cultural heritage

By

**Elena Pinotti**

\*\*\*\*\*

**Supervisor:**

Prof. Rosario Ceravolo

**Doctoral Examination Committee:**

Prof. Stefano Gabriele, Referee, University of Roma Tre

Prof.ssa Giuseppa Novello, Referee, Politecnico di Torino

Prof. Francesco Romeo, Referee, University of Roma La Sapienza

Prof. Salvatore Russo, Referee, University of IUAV

Prof.ssa Cecilia Surace, Referee, Politecnico di Torino

Politecnico di Torino  
2017

## Declaration

I hereby declare that, the contents and organization of this dissertation constitute my own original work and does not compromise in any way the rights of third parties, including those relating to the security of personal data.

Elena Pinotti

2017

\* This dissertation is presented in partial fulfillment of the requirements for **Ph.D. degree** in the Graduate School of Politecnico di Torino (ScuDo).



## **Acknowledgment**

All my gratitude to my supervisor Prof. Rosario Ceravolo and Prof. Andrea De Marchi for placing their confidence in me and inspiring my work with their precious advices. My most affectionate thanks to the researchers Luca Zanotti Fragonara and Antonino Quattrone for their helps and supports during these years.

The work presented in this dissertation is the result of a "Youth Project", a PhD grant funded by the Italian Ministry of Education and Scientific Research, with the subject on "Advanced materials for structural applications in the cultural heritage field".





## **Abstract**

Natural hazards, such as earthquakes, can compromise the integrity of the cultural heritage with potentially devastating effects. The reduction of the seismic vulnerability of the cultural heritage constitutes a question of maximum importance especially in countries where vast cultural heritage combines with a medium or high seismic risk, such as in Italy. From the second half of the last century, the scientific community edited a number of important documents and charts for the conservation, reinforcement and restoration of the cultural heritage. The aim is to mitigate the seismic vulnerability of the cultural heritage.

This research focused on high performance materials for applications aimed to structural and seismic protection of cultural heritage, with a special focus on historical masonry structures. In particular, the final aim is to define a self-diagnosis strategy for fibres, yarns and ties in view of efficient, non-invasive and reversible interventions on cultural heritage buildings.

In order to set up the scene, the present thesis starts by introducing the reader to the seismic protection of cultural heritage thorough an extensive review on high performance materials, strengthening techniques and systems, taking care to highlight real world applications and limitations of their use.

The second step of this work concerns in the mechanical and rheological characterization of high performance material fibres. The materials investigated are essentially Kevlar® 29 (para-aramid), Carbon and Silicon Carbide. To reach this goal, an extensive experimental testing campaign was conducted on fibres and

yarns in accordance with specific protocols. A further step was defining appropriate damage indices for different materials, with a special focus on Kevlar® 29. Within the same research programme, a novel testing machine was also designed in cooperation with the Laboratory of Electronic Measurements of the Politecnico di Torino. A prototype-testing machine for dynamic testing on high resistance fibres was built using recycled materials and components. A distinctive feature of this machine is that it can apply to the sample any kind of dynamic excitation (random, impulse, harmonic etc.).

A second testing campaign concerned the durability of Kevlar® 29 fibres, which are known to be sensitive to long-term exposure to UV radiation. Accordingly, for this campaign, the samples were artificially damaged by using UV lamps. The analysis of the resonance profiles allowed for the extraction of parameters such as the elastic moduli, quality factors, and non-linear coefficient for a set of fibres. In particular, non-linearity parameters derived from the Krylov-Bogoliubov method demonstrated to be consistent with the damage affecting the fibres.

The final chapter of the dissertation concerns a new concept for a tie endowed with self-diagnosis properties, which are obtained by integrating a low cost testing device into the tie model. The self-diagnosis properties system of existing structures has an important role in the preservation of the cultural heritage because the best therapy is preventive maintenance. Specifically, the para-aramid tie system proposed for the reinforcement of historic building constitutes a non-invasive, reversible and repeatable intervention, as required by the main guidelines on preservation of cultural heritage.



# Contents

1. Structural conservation and repair of the cultural heritage.....	2
1.1 National and international deontological guidelines for the protection of cultural heritage.....	2
1.1.1 International context .....	2
1.1.2 The Italian national context .....	6
1.2 Safety assessment of the architectural heritage .....	7
1.3 Introduction to high performance fibre materials for historical constructions .....	9
1.3.1 Why use high performance fibre materials .....	9
1.3.2 Application of high performance fibre materials to masonry constructions.....	12
1.3.3 Limitations in the use of high performance fibre materials on masonry constructions .....	15
2. High performance materials.....	22
2.1 Definition of composite materials .....	23
2.2 Composite materials: classification .....	24
2.3 High performance materials: fibres .....	24
2.3.1 Fibre types.....	25
2.3.2 Fibre architecture .....	28
2.4 High performance materials: matrix.....	31
2.5 Why choose a high performance material .....	33
2.6 Commonly used fibres for structural applications.....	39
2.6.1 Glass fibres .....	39

2.6.2 Carbon fibres.....	43
2.6.3 Aramid fibres .....	47
2.7 Brief history of polymers and composites used in construction industry .....	50
2.7.1 First generation (1930s-1940s) .....	50
2.7.2 Second generation (1950s-1960s).....	53
2.7.3 Third generation (1970s-1980s).....	54
2.7.4 Fourth generation (1990s).....	55
2.8 Composites for engineering applications .....	57
3. Using high performance materials for strengthening interventions: a literature review.....	60
3.1 Background.....	60
3.2 Strengthening actions .....	62
3.3 Repairing and strengthening techniques.....	64
3.3.1 Injection .....	64
3.3.2 Local reconstruction named “cuci-scuci” .....	64
3.3.3 External or internal reinforcement .....	66
3.3.4 Stitching and local tying .....	66
3.3.5 Repointing and reinforced repointing .....	66
3.3.6 Tie bars .....	67
3.3.7 Structural and element substitution.....	68
3.3.8 Dismantling and remounting .....	69
3.3.9 Continuous and discrete confinement (jacketing).....	69
3.3.10 Reinforced concrete and masonry edge-beams .....	70
3.3.11 Enlargement .....	70
3.3.12 Buttrressing, suspension and strutting.....	70
3.3.13 Frictional contact, post-tension, and pre-compression .....	72
3.3.14 Anchoring .....	72
3.3.15 Direct intervention on foundations .....	73
3.3.16 Interventions on soil beneath foundation.....	73

3.3.17 Seismic isolation .....	73
3.4 Repairing and strengthening systems .....	74
3.4.1 Externally bonded reinforcement.....	75
3.4.2 Near surface mounted reinforcement.....	76
3.4.3 Mechanically fastened FRP-system.....	76
3.5 Interventions on masonry buildings using FRP.....	77
3.5.1 Improvement of Connections to Activate Box Behaviour.....	78
3.5.2 Increase of Strength and Compactness of Walls.....	81
3.5.3 Strengthening of arches and vaults .....	86
3.5.4 Strengthening and stiffening of floors .....	91
3.5.5 Confinement of masonry columns .....	92
3.6 Numerical investigations on the possible use of aramid fibres for a permanent strengthening intervention on the Fossano belfry .....	95
3.6.1 The Fossano belfry description.....	95
3.6.2 Finite Element (FE) model calibration .....	97
3.6.3 The AFRP strengthening intervention .....	99
3.6.4 Analysis and results.....	101
3.6.5 Comparison with traditional strengthening techniques.....	104
4. A prototype-testing machine for the dynamic characterization of high performance materials.....	106
4.1 Introduction .....	107
4.2 Prototype-testing machine description .....	110
4.3 The resonant spring-mass approach .....	114
4.4 The containment structure and its effects .....	118
4.5 Quality Factor limitations .....	121
5. Experimental investigation on high-strength fibres and results.....	126
5.1 Experimental investigation on pristine samples .....	127
5.1.1 Samples investigated.....	128
5.1.2 Test procedure of forced tests .....	129
Survey on nonlinear system identification in structural dynamics .....	140

5.1.3 Nonlinear identification of the backbone curve.....	149
5.1.4 Dissipation properties and quality factor: experimental evaluation .....	152
6. Experimental investigation and results on damaged Kevlar® 29 samples....	156
6.1 Effects of UV exposure on high-strength materials: background .....	157
6.2 Experimental investigation on damaged Kevlar® 29 samples.....	159
6.2.1 Forced testing on the sample damaged for 792 hours.....	163
6.2.2 Forced testing on the sample damaged for 1272 hours.....	170
6.2.3 Forced testing on the sample damaged for 2040 hours.....	176
6.2.4 Comparison of the results obtained.....	185
7. A new concept for a tie element with self-diagnosis properties .....	190
7.1 Structural Health Monitoring .....	191
7.2 The concept of a tie with self-diagnosis properties .....	192
8. References.....	202



# List of Figures

Figure 1: market share of textile fibres and composite types. Source (Duflou, et al., 2012). .....	10
Figure 2: historic development (a) and geographical distribution (b) of articles dealing with LCC and HPM. Source (Ilg, et al., 2016). .....	17
Figure 3: classification scheme of composite materials. ....	24
Figure 4: types of fibres. Source (CNR-DT 200/2004, 2004). ....	26
Figure 5: classification scheme of the most widespread commercially available high-performance fibres. ....	27
Figure 6: fibre architecture. Source (Mallick, 1997). ....	28
Figure 7: braided fabrics. Source (Nivitex.Fibreglass.and.Resins, 2017) and (Composites, 2014). ....	30
Figure 8: disordered glass fibres and random mat. Source (CNR-DT 200/2004, 2004). ....	30
Figure 9: stress-strain curve of the main high-performance materials. Source (CNR-DT 200/2004, 2004). ....	35
Figure 10: glass fibre manufacture, a schematic representation. Source (Hollaway, 1993). ....	40
Figure 11: the basic tetrahedral structure of glass fibre Source (Gowayed, 2014). ....	43
Figure 12: Manufacturing process of carbon fibre. Source (Hollaway, 1993). ....	45
Figure 13: effect of heat treatment temperature compared to tensile strength and modulus of elasticity. Source (Campbell, 2010). ....	47
Figure 14: the chemical structure of Kevlar®. Source (Gowayed, 2014). ....	48
Figure 15: Schematic diagram showing the relative importance of ceramics, composites, polymers and metals, in mechanical and civil engineering as a function of time (The time scale is nonlinear). Source: (Ashby, 1987). ....	51
Figure 16: step in “cuci-scuci” strengthening intervention. ....	65
Figure 17: example of “cuci-scuci” intervention. Source (Modena, et al., 2011). ....	65
Figure 18: repointing technique, phases of intervention: placing of the rebars (a) and of the anchors (b); view of a joints after repointing (before the injection of the pins’ holes) (c); final view (d). Source (Valluzzi, et al., 2005). ....	67

Figure 19: the interventions on S. Giustina (PD, Italy) bell-tower: injections (a), partial rebuilding ('cuci-scuci) (b), insertion of bar (c). Source (Modena & Valluzzi, 2008).....	68
Figure 20: propping intervention of lateral wall of church of Onna (AQ). Source (Modena, et al., 2011).....	71
Figure 21: shoring of facade with cables and wooden frames (Chiesa di S. Marco, L'Aquila). Source (Modena, et al., 2011). ....	71
Figure 22: a) splitting failure for EB-FRP laminates; b) laminates used for MF-FRP systems. Source (Ascione, et al., 2009).....	76
Figure 23: fasteners used for MF-FRP systems. Source (Ascione, et al., 2009). ....	77
Figure 24: wet lay up system. Source (CNR-DT 200/2004, 2004).....	77
Figure 25: a), b) the north and west elevation of the masonry building, and position of CFRP wrapping interventions. Source (Borri & Castori, 2009).....	80
Figure 26: a), b) east and north elevation of the masonry building with horizontal and vertical SRG reinforcement. Source (Borri & Castori, 2009). ....	80
Figure 27: diagonal compression tests. Source (Borri, et al., 2009). ....	82
Figure 28: a) kerbs realised with carbon fibres placed up to the roof and the ceiling, and b) horizontal and vertical kerbs placed on internal and external walls. Source (Credali, 2009). ....	83
Figure 29: horizontal and vertical CFRP kerbs on internal and external walls. Source (Credali, 2009). ....	84
Figure 30: restoration intervention realised on the masonry external façade. Source (Credali, 2009). ....	85
Figure 31: strengthening intervention with hybrid reinforced carbon-aramid fibres systems. Source (Credali, 2009). ....	85
Figure 32: cracks and deformation in the vaults with relative displacement till 30cm. Source (Croci, 2000). ....	89
Figure 33: the new ribs, made of a central timber nucleus and external aramid fibres. In the background, the steel belt to anchor the base of the arches which sustain the roof is visible. Source (Croci, 2000). ....	90
Figure 34: Complesso di Venaria Reale (TO) – Strengthening intervention with strips placed to the intrados and extrados of the vaults. Source (Credali, 2002). ....	91
Figure 35: strengthening intervention with AFRP in Villa Reale in Monza (sx), and Real Albergo dei Poveri a Napoli (dx). Source (Olympus, 2016) and (ResinProget, 2012). ....	93
Figure 36: the Fossano belfry; wood ramps located inside the tower. ....	96

Figure 37: the belfry of the Fossano Cathedral with the strengthening intervention. ....	97
Figure 38: the FE model: subdivision in macroelements, and updated values of the elastic moduli. Source (Ceravolo, et al., 2014). ....	98
Figure 39: different position of the Kevlar® reinforcements investigated. ...	100
Figure 40: pushover curves, in x direction (Kevlar® 29 with E = 70GPa)...	101
Figure 41: pushover curves, in x direction (Kevlar® 49 with E = 160 GPa). ....	102
Figure 42: maximum displacement vs. ratio between the areas of the horizontal and vertical stripes. ....	103
Figure 43: maximum displacement vs. ratio between the areas of the vertical and horizontal stripes. ....	103
Figure 44: contour plots of the failure index for some load steps. ....	104
Figure 45: pushover curves relative to the unreinforced structure, the proposed intervention and the adoption of traditional techniques. ....	105
Figure 46: real prototype testing machine, and a schematic model. ....	111
Figure 47: schematic representation of the optical system. ....	112
Figure 48: schematic representation of the electromagnetic system. ....	113
Figure 49: the homemade magnetic circuit. ....	113
Figure 50: Schematic arrangement of tie-rods, with attachment errors. ....	115
Figure 51: Significant components in the prototype machine. ....	116
Figure 52: non-contact excitation and detection. ....	118
Figure 53: schematic representation of the containment structure. ....	119
Figure 54: the SiC (Type S) sample tested. ....	128
Figure 55: Kevlar® 29 sample tested. ....	128
Figure 56: carbon sample tested. ....	129
Figure 57: Silicon Carbide: values of frequency response recorded around resonance for increasing levels of driving force. ....	131
Figure 58: Silicon Carbide: frequency response measured around resonance for increasing levels of driving force. The maximum value is indicated by red dot. ....	131
Figure 59: Kevlar® 29: values of frequency response recorded around resonance for increasing levels of driving force. ....	133
Figure 60: Kevlar® 29: frequency response measured around resonance for increasing levels of driving force. The maximum value is indicated by red dot. ....	133
Figure 61: Carbon: values of frequency response recorded around resonance for increasing levels of driving force. ....	138

Figure 62: Carbon: frequency response measured around resonance for increasing levels of driving force. The maximum value is indicated by red dot.	138
Figure 63: flowchart of the general numerical procedure. Source (Song, et al., 2013).	147
Figure 64: amplitude-response curves for a varying strength of nonlinearities $\gamma$ . Source (Kalmar-Nagy & Balachandran, 2011).	149
Figure 65: Silicon Carbide: frequency response measured around resonance for increasing levels of driving force. The red dots highlight the maximum of the response curve and the dashed red line is the estimated backbone response curve.	150
Figure 66: Kevlar® 29: frequency response measured around resonance for increasing levels of driving force. The red dots highlight the maximum of the response curve and the dashed red line is the estimated backbone response curve.	151
Figure 67: Carbon: frequency response measured around resonance for increasing levels of driving force. The red dots highlight the maximum of the response curve and the dashed red line is the estimated backbone response curve.	151
Figure 68: weatherometer with a Xenon lamp, emitting UV rays at 340 nm at an irradiance of 1.1 W/m <sup>2</sup> used in an experimental tests. Source (Said, et al., 2006).	158
Figure 69: geometrical details of a UV lamp chosen to cause the damage on Kevlar®29 samples. Source (OSRAM, 2017).	160
Figure 70: power spectra distribution of Ultra-Vitalux® lightbulb subdivided for the different components of the electromagnetic spectrum. Source (OSRAM, 2017).	161
Figure 71: the experimental setup used to focus the light flux onto fibre samples.	162
Figure 72: damaged Kevlar® 29 sample (792 hours)	163
Figure 73: Sample exposed 792 hours: frequency response measured around resonance for increasing levels of driving force. The excitation range is 2 V – 10 V.	168
Figure 74: sample exposed 792 hours: frequency response measured around resonance for increasing levels of driving force. The excitation range is 2 V – 10 V. The red dots highlight the maximum of the response curve and the dashed red line is the estimated backbone response curve.	169
Figure 75: damaged Kevlar® 29 sample (1272 hours)	170

Figure 76: sample exposed 1272 hours: frequency response measured around resonance for increasing levels of driving force. The excitation range is 2 V – 10 V.....	174
Figure 77: sample exposed 1272 hours: frequency response measured around resonance for increasing levels of driving force. The excitation range is 2 V – 10 V. The red dots highlight the maximum of the response curve and the dashed red line is the estimated backbone response curve. ....	175
Figure 78: damaged Kevlar® 29 sample (2040 hours) .....	176
Figure 79: sample exposed 2040 hours: frequency response measured around resonance for increasing levels of driving force. The excitation range is 2 V – 10 V.....	181
Figure 80: sample exposed 2040 hours: frequency response measured around resonance for increasing levels of driving force. The excitation range is 2 V – 10 V. The red dots highlight the maximum of the response curve and the dashed red line is the estimated backbone response curve. ....	182
Figure 81: variations of measured nonlinear coefficient $X$ with respect to UV exposure time.....	184
Figure 82: measured variations of Q-factor versus drive level for different exposure times to UV. ....	186
Figure 83: typical Structural Health Monitoring strategy.. ....	191
Figure 84: possible setup configurations investigated: a) vertical sample, and suspended mass of 1.345 kg, b) horizontal sample, and mass of 0.150 kg, c) vertical sample, and suspended mass of 45 kg. ....	194
Figure 85: different setup investigated with different ball lens position.....	195
Figure 86: the concept of control and self-diagnosis system. ....	196
Figure 87: the concept of the system for self-diagnosis: demonstrative sketch of a possible application. ....	196
Figure 88: the belfry of the Fossano Cathedral with the strengthening intervention. ....	197
Figure 89: particular of the last safety measure works.....	197

# List of Tables

Table 1: cost of materials per unit force. Source (Burgoyne & Balafas, 2007)	19
Table 2: typical glass composition of glass fibres used to reinforced composite materials Source (Hollaway, 1994).	41
Table 3: Mechanical properties of some glass fibres. Source (Kinsella, et al., 2001)	42
Table 4: mechanical properties of some carbon fibres. Source (Hearle, 2001)	44
Table 5: mechanical properties of some carbon fibres. Source (Gowayed, 2014).	49
Table 6: typical mechanical properties for glass, aramid, and carbon fibres. Source (Hollaway, 1993).	49
Table 7: materials properties after model-updating. Source (Ceravolo, et al., 2014).	99
Table 8: Recap of the main features of samples tested.	129
Table 9: SiC: strain values calculated from the numerical data acquired during the forced tests.	132
Table 10: Kevlar® 29: strain values calculated from the numerical data acquired during the forced tests.	134
Table 11: Carbon: strain values calculated from the numerical data acquired during the forced tests.	139
Table 12: main Q and damping values, estimated using the half-power bandwidth method, was computed for the 5 V response, for Kevlar® 29 and carbon, and for 1V response for SiC, respectively.	154
Table 13: Technical details of an OSRAM Ultra-Vitalux®. Source (OSRAM, 2017).	160
Table 14: strain values calculated from the numerical data acquired during the forced tests.	164
Table 15: strain values calculated from the numerical data acquired during the forced tests.	170
Table 16: strain values calculated from the numerical data acquired during the forced tests.	176
Table 17: results recap.	187





# **Chapter 1**

## **Structural conservation and repair of the cultural heritage**

In this first chapter the main issues involved in the seismic protection and analysis of the cultural heritage are introduced. In particular, the most relevant Italian national and international codes, such as the Directive PCM 2011 and the ISCARSAH guidelines, are reviewed.

In a second part of this chapter the role of high performance materials for the structural conservation and repair of the architectural heritage is explained. Disadvantages and points of strengths were briefly discussed, and lacks of knowledge were underlined, with a special focus on masonry structures applications.

### **1.1 National and international deontological guidelines for the protection of cultural heritage**

#### **1.1.1 International context**

The difficulty, or even lack, of communication between architects, art historians and engineers has always been one of the main obstacles in the analysis and conservation of the cultural heritage. In 2003, during the 14<sup>th</sup> General Assembly of ICOMOS (International Council on Monuments and Sites), a very

important document was produced and approved. The ISCARSAH guidelines (ICOMOS, 2003) claim that the conservation, reinforcement and restoration of the architectural heritage require a multidisciplinary approach.

An example of interdisciplinary approach is the interaction that may occur between historical research and structural diagnosis. On the one hand, historical research could discover particular facts involving structural behaviour, on the other historical questions could be find answer taking into consideration the global or local structural behaviour.

The ISCARSAH guidelines combine the different approaches involved in the structural conservation. This combination of both qualitative and quantitative approaches, has been very difficult due to the different philosophies on traditional and innovative techniques. The guidelines introduce also the concept of holistic approach for the evaluation of a building as a whole entity, and not a combination of singular elements.

In addition, the ISCARSAH guidelines discriminate in a clear way four different phases: the data acquisition (the phase of information gathering and investigation of the structure), the study of the structural behaviour (the intermediate phase), and the diagnosis and safety evaluation (the last two phases). The data acquisition phase is particularly important in historic buildings.

The correct evaluation of the structural problems cannot be achieved if there is lack of information about the structure under investigation. For these reasons, the ISCARSAH guidelines specify that the “knowledge of the structure” may be reached by means of the following steps:

- definition, description and knowledge of the historic and cultural significance of the building;
- description of the original materials and construction techniques;
- historical research of the whole life of the structure. It includes the changes to its form and any previous structural interventions;
- description of the structure in its present state. It include the damage identification, decay and possible progressive phenomena. This knowledge may be reached using appropriate types of test;
- description of the actions involved, the structural behaviour and types of materials.

It is also important to emphasise that all these actions may be carried out at different levels of detail, but this study have to be cost efficient. It must be proportional to the importance of the structure/building and the level of knowledge desired.

Another important consideration is that the restoration of a historical building must not be considered a part of an end in itself, but a means to an end, which is the cultural heritage. In fact, no action must be undertaken without distinguished between benefit and harm to the architectural heritage (except in the case where urgent interventions are required) and having demonstrated that interventions are indispensable.

For the restoration, strengthening and conservation of the architectural heritage, both traditional and innovative methods can be used. Regard to the “innovative” methods and materials, the guidelines claim that their use has to be weighed up with “traditional” ones. The compatibility with original materials and long-term impacts has to be defined, in order to avoid side-effects.

In addition, the monitoring of existing structures has an important role in the preservation of the cultural heritage. It is clearly explain in the guidelines that **“the best therapy is preventive maintenance”** that can only be reached by means of a structural monitoring. It is necessary not only in the case of a gradual phenomenon occurring, but also during a “step-by-step procedure of structural renovation”.

Ian Hume (Forsyth, et al., 2007) claims that the principles of structural conservation of historic structures can be summarised in five main points:

- **Conserve as found.** Structures should ideally be conserved as they are found. They should not be taken back to the condition that it is supposed they might have been in at some period in their history. They must not be “improved” without well-argued justifications.
- **Minimal intervention.** In many cases it is necessary to make changes both because of excessive decay or distortion resulting in a problem to the structural stability, or because changes are necessary to ensure that the structure may have a future. Any time that changes are made, these have to be kept to a minimum. Traditional and tested techniques are nowadays preferable to new methods that could have negative effect on the structure at some time in the future.

- **Like-for-like repairs.** If a repairs are to be necessary, the best solution is that they are made using the same materials found in the original construction. Nevertheless, there are cases when to do this could cause a great loss of fabric, and consequently a loss of detail and history.
- **Repairs should be reversible.** If a repairs are to be necessary, they should be designed and carried out taking into account the possibility to remove them. It should be possible to remove repairs from a structure, should it later prove possible to make better repairs, or if for some reason, the repairs become redundant. This is the principle of conservation most difficult to achieve. However, in many cases is not possible to guarantee the reversibility of repairs.
- **Repairs should be sympathetic.** Repairs need to be in character with the structure. If it is decided to use modern materials and technique for the repair, it is necessary that the design fits the general style of the original structure.

Another author, Bernard Feilden (Feilden, 2003), defines the standard of ethics and the recommendations that should be taken into consideration in any conservation work:

- the historic evidence must not be destroyed, falsified or removed.
- any intervention must be the minimum needed.
- any intervention have to be regulated by respect for the aesthetic, historical and physical integrity of cultural property.
- all methods, technologies and materials used during treatment should be carefully documented.

In addition, all the interventions proposed for the conservation of a historic building have to be **reversible or repeatable**, if technically possible, or at least have not to prejudice a future intervention, in case this could become necessary. Moreover, the interventions must allow the maximum possible amount of original material to be conserved, must be compatible in colour, tone, texture, form and scale. In case additions are necessary and unavoidable, they should be less evident than original material but, at the same time, identifiable.

However, Feilden adds that the problems arising from historic buildings are often unique. These problems must be solved from first principles on a trial-and-error basis. In addition, Feilden claim that architectural conservation does not share all the objectives of artistic conservation. Indeed, the architectural fabric has

to function as a structure (resisting dead and live loadings), and have to provide a suitable internal environment protected against certain type of hazards, such as fire, earthquake, or vandalism.

In addition, Claudio Modena introduced the concept that structural repair of a historic building has to be “cautious”. The “cautiousness” principle have to lead the complete process of the conservation of historic architectural heritage buildings (Modena, 1995). Indeed, a great number of restorations failed due to not appropriate applications of modern technologies. These technologies can also have good performance from a technical point of view, but they can modify the cultural value of a restored building. From the designer’s point of view, the principle of “cautiousness” results in two fundamental rules. The first is avoiding non-essential interventions, and the second is choosing intervention technologies, which alter as less as possible the chemical, physical, and mechanical properties of original materials and structures (compatible technologies). In addition, usual safety and reliability concepts could become inadequate when immaterial values are involved. The case of human life or historic and artistic assets, is an example.

### **1.1.2 The Italian national context**

In Italy, the first operative documents which has explicitly addressed the problem of cultural heritage buildings in seismic regions was a regulation of the Italian Ministry of Cultural Heritage, sometimes referred to as “**Documento Ballardini**” (Circolare\_n°564., 1997). This document fixed some general criteria and provided a classification of different types of interventions on historic buildings in seismic areas. In addition, the document presented an outline regard the interaction between different disciplines, in order to obtain an adequate depth of the analysis of the building.

A more recent and important contribution for the seismic protection of cultural heritage is represented by the Italian Legislative Decree “**Codice dei Beni Culturali e del Paesaggio**” (Codice\_dei\_Beni\_Culturali\_e\_del\_Paesaggio, 2004). Article 29 of this decree, explicitly mentions the seismic protection requirements of cultural heritage. In addition it states that the seismic upgrade is a part of the restoration intervention. Moreover, Article 30 impose to the government and local authorities to provide for the safety and the conservation of historic buildings owned by them (Lagomarsino, et al., 2010).

Recent seismic regulations for cultural heritage structures, such as the **Directive PCM and successive guidelines** (Presidenza\_del\_Consiglio\_dei\_Ministri, 2011) (Consiglio\_superiore\_dei\_lavori\_publici, 2011) in Italy, introduce and encourage the attainment of an appropriate “level of knowledge”. It can be obtained only through extended tests and investigations. It is necessary that the level of knowledge should be appropriate for the type of analysis that the designer is carrying out. For example, the Directive distinguishes among three different “levels of evaluation” for the analysis methods: LV1, LV2 and LV3. While the lower level (LV1) must be applied in the case of seismic assessment at territorial or urban scale on the entire protected architectural heritage, LV2 must be applied when the building necessitate of local interventions. The last level (LV3), the most detailed, must be required in the case of intervention that modify the structural behaviour of the building, or in the case in which a seismic assessment of the building is required.

When dealing with a historic building, what is must be done in various steps include:

- identification of the structure
- geometric data gathering
- historical analysis
- survey of the materials and their state of preservation
- mechanical characterisation of the materials
- soil and foundation analysis
- monitoring.

Regarding geometric survey, sophisticated and accurate techniques are nowadays available, including: laser scanner, interferometry, thermography etc. It is worthless to say that the acquisition of knowledge meets with the difficulties normally associated with the assessment of existing structures that must be preserved (Ceravolo, et al., 2012) (Bednarz, et al., 2014).

## **1.2 Safety assessment of the architectural heritage**

Before undergoing any consideration on the structural safety of historic structures, it is still worth pointing out that ancient structures were not “designed” as we expect nowadays, but they were built using rules of the thumb (e.g. geometric proportions), that were verbally handed down. These rules have been often guarded as secrets by builder guilds during the middle age, as they were developed by trial and error, and were modified through the centuries. Some of

which were even incorporated in the first building codes and survived until the mid of twentieth century (Beckmann & Bowles, 2004). It is straightforward that historic structures will or will not (mostly will not) achieve the level of safety required by modern building codes for each type of structures.

The main rules used in the safety assessment of historic structures may be classified into different categories, such as:

- necessity to adapt structural safety requirements to conservation requirements (choice of the safety levels),
- necessity to adapt the structural safety assessment to the maintenance strategy, and to the temporal horizon of the intervention (choice of the nominal life of the intervention),
- geometrical and topological complexity (modelling requirements),
- mechanical response (mechanical and constitutive models).

Regarding the structural safety assessment, in modern codes the uncertainties in materials behaviour and actions are usually covered by safety factors, which are directly associated to the assumed safety level. This approach is possible because the generalised costs are considered to be acceptable to the community. In the case of historic structures, the standard approach could be inappropriate, because it may require very invasive rehabilitation works. As a consequence, the whole costs are of a cultural nature, and may not be generalised.

After these considerations, when dealing with historic buildings it is preferable to use a more flexible approach to safety assessment. The final aim is to guarantee both safety for the users, and reduction of the interventions to the minimum possible. Consequently, in historic structures, lower safety levels than in new buildings can be sometimes justified. This because it is possible to decrease the risks related to the use of the building (e.g. by limiting the access in some area of the building, or by investing in continuous or periodic monitoring programs etc.).

However, the most important consideration regarding safety is that the usual partial factors considered for new buildings (taking into account uncertainties related to strength of materials) depend on the “level of knowledge” of the building. Codes such as the Directive (Presidenza\_del\_Consiglio\_dei\_Ministri, 2011) in Italy, introduces in explicit way the concept of “confidence factor”. This factor is conventionally applied to the material strength side, in spite of it actually

is intended to cover also model uncertainties. In this case, greater is the level of knowledge, lower is the value of the “confidence factor”.

Another difference between monumental buildings and standard ones is that historic buildings are often place of activities that requires very long design life.

Cultural heritage buildings are so particular that is also possible to decide to do not intervene or to do only limited interventions that permit to achieve a design life of about few decades. The idea could be preserving the structure for a few decades, and then waiting for the development of less invasive technologies. Indeed, innovative technologies are in fact expected to be develop in the near future, able to ensure longer design life for the building without being too much invasive (Caprili, et al., 2015).

## **1.3 Introduction to high performance fibre materials for historical constructions**

### **1.3.1 Why use high performance fibre materials**

The employment of traditional materials for strengthening method cannot be the best solution in any circumstances. Some methods of seismic upgrading (i.e. addition of new structural frames or shear walls) have been proven to be impracticable because they could be either invasive, or too costly or restricted in use for certain types of structures. Other strengthening methods such as grout injection, insertion of reinforcing steel, pre-stressing, jacketing, and different surface treatments have been summarized by some authors (Hamid, et al., 1994) (Saileysh Sivaraja, et al., 2013) (Ravikumar & Thandavamoorth, 2014). These methods involve the use of skilled labour and interfere with normal functions of the building. These traditional and well-known techniques could be inadequate for applications that should protect the cultural heritage (Sivaraja, et al., 2013) (Marcari, et al., 2007).

High performance materials (HPM) are now used in different field for different applications. The acronym HPM is used to indicate a general characterization of fibre reinforcements for fibre-reinforced concrete (FRC), fibre-reinforced polymers (FRP), engineered cementitious composites (ECC), and others (Ilg, et al., 2016) (Lin, et al., 1999) (Li, 2003).

HPM are a class of advanced composite materials that emanated from the aircraft and space industries. They have been used extensively in the medical,

sporting goods, automotive and small ship industries and are now finding uses elsewhere (Shrive, 2006). Figure 1 shows how HPM are used in the different areas of applications.

HPM are now increasingly used in the construction industry, and offer considerable potential for greater use in buildings. Nowadays, bridges are the main application field (Ilg, et al., 2016). Holloway in 2003 (Holloway, 2003) gives an overview of many applications of FRP and FRP/traditional material composite structures, even though masonry are never mentioned.

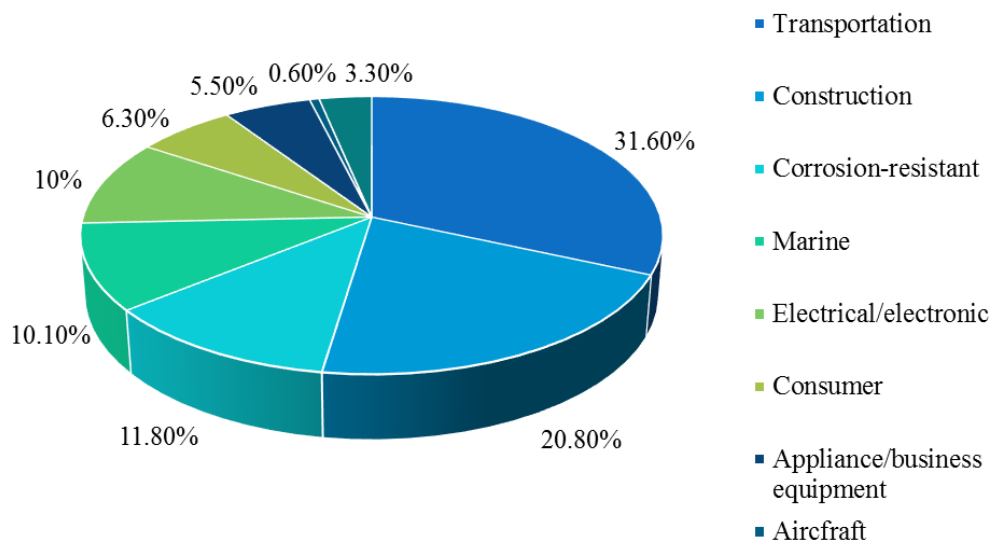


Figure 1: market share of textile fibres and composite types. Source (Duflou, et al., 2012).

HPM offer a set of advantages over traditional materials in building construction (Triantafillou & Fardis, 1993) (Oliveira, et al., 2010) (Kendall, 2007) (Saileysh Sivaraja, et al., 2013). The main features that encouraged the diffusion of these materials at different levels, are:

- high tensile strength,
- high stiffness-to-weight ratio,
- reduced mass,
- fatigue and corrosion resistance (superior durability),
- easy in-situ feasibility and adaptability,
- ability to mould complex forms, special surface finishes and effects,
- offsite fabrication,

- progressive reduction in production and distribution costs,
- modular construction,
- improved thermal insulation and lack of cold bridging (Kendall, 2007) (Sivaraja, et al., 2013) (Selin Ravikumar & Thandavamoorthy, 2014).

No structural failure may occur before fibres failure. Fibres activate their characteristics along their prevalent distribution, whereas have negligible properties in the other directions. Despite the large accessibility to various products (bars, strips, laminates, sheets, cords, grids), made of several reinforcing materials (carbon, glass, aramid, etc.), and applicable in different modalities on structures (embedded inside grooves or bed mortar joints, externally bonded or anchored), design rules for the interventions, feasibility recommendations and procedures aimed at checking the effectiveness of the technique and monitoring are still under definition (Valluzzi, 2008).

Given their properties, the main applications of HPM in construction industry are:

- to improve the global behaviour in seismic zone (tying, connections among components, strengthening),
- to counteract specific incipient or developed damage (high compression, shear and/or flexural conditions),
- to repair very specific local weaknesses depending on the peculiar construction typology.

Modern techniques of confinement consist of wrapping with FRP sheets or laminates. They were introduced in engineering practice as an innovative confinement technique during the last decade as an alternative to wood or steel ties adopted in the past.

Very thin layers of FRP are sufficient to yield strength and ductility improvements, thereby allowing for the reconstruction of heritage-protected buildings without changing the overall appearance (Aiello, et al., 2007) (Ilg, et al., 2016). More important is the poor invasiveness. An intervention realised with FRP could be also reversible (Triantafillou & Fardis, 1993) (De Lorenzis, et al., 2007), as the material applied on the surface is easily removable and do not require special restoration of the structure. It is important to take into consideration that the feature which characterize an historical building is the uniqueness. For this reason, a strengthening intervention is different case by case.

HPM are perfectly adapted to a specific case (ICOMOS, 2003) (Codice\_dei\_Beni\_Culturali\_e\_del\_Paesaggio, 2004).

### **1.3.2 Application of high performance fibre materials to masonry constructions**

In the previous sections the topics of the architectural heritage protection and conservation were introduced. In particular, the contents of now available guidelines were described, from national and international point of view. This because the preservation of cultural heritage buildings is considered a very important theme in the cultural life of modern societies. Nevertheless, this complex task requires the definition of proper methodologies, able to take into consideration, at the same time, their great architectural and cultural value, and their structural safety (ICOMOS 2001). One of the most important topic in current research, is the development of efficient and cost effective strengthening techniques. They have to be able to re-establish the original performance of cultural heritage buildings, and to prevent their brittle failure, in particular under earthquake loading (Oliveira, et al., 2010) (Oliveira, et al., 2011). The main challenge stays in a development of innovative techniques, advanced materials, and reinforcement processes, which will lead to discover suitable alternatives to the more traditional solutions that are incompatible in certain cases (technical-cultural incompatibilities).

Strengthening solutions, based on the external bonding realised with FRP composites, have become a popular option (both in new construction and for rehabilitation) (Bakis, et al., 2002) (Yuan, et al., 2004) (Shrive, 2006) (Oliveira, et al., 2011) (Oliveira, et al., 2010) (ICOMOS, 2003) ((FIB), 2001).

FRP composites have been now increasingly considered for strengthening and repair of both modern and historic masonry constructions, such as buildings, bridges, towers, and structural components, such as walls, arches and vaults, piers and columns.

Masonry structures constitute a significant part of historical constructions in Europe and particularly in Italy. Many of these structures are structurally inadequate for current or safe use respect to new seismic code regulations (Grande, et al., 2008). Older masonry buildings are often unreinforced, seismically vulnerable and should be retrofitted in order to provide higher strength and ductility.

Common causes of seismic inadequacy are due to (Oliveira, et al., 2010) (Cardoso, et al., 2005):

- structural degradation,
- insufficient design loads,
- structural damage sustained in a previous earthquake,
- improper design or construction,
- changes in building occupancy.

These causes involve the need to retrofit or upgrade historic masonry structures through strengthening techniques. Despite this, masonry structures were, until recently, largely been ignored as an area of interest for structural researchers (Garmendia, et al., 2011). In view of the importance of some masonry structures, the knowledge on this topic, assessment methods and reinforcement techniques should be acknowledged in comparison with other construction materials, such as concrete. A large number of analytical studies and experimental results allowed carry out of design recommendations that are commonly accepted by the scientific community (Aiello, et al., 2007) (Hamilton III & Dolan, 2001) (Oliveira, et al., 2011) (Bakis, et al., 2002).

Starting from extension of approaches proposed for concrete structures, and after the critical evaluation of the impact of generalised interventions on historical structures (Giuffrè, 1993) (Tomazevic, 1999), researches and studies have been more and more focused on the specific features of the masonry material, by recognizing its lack of homogeneity and the large variability of typologies and constituent basic materials and aggregations (brick, stones, mortar, mixed arrangements, etc.). This approach has led to a new impulse for the upgrading of standards devoted to masonry in seismic zone, which often include reference to specific codes or recommendations on the possible application of FRPs, unfortunately still very limited (e.g. (CNR-DT 200/2004, 2004) (ACI\_Committee\_440, 1996) (ACI\_Committee\_440., 2001) (Valluzzi, 2008).

A great contribution coming from researches on the reinforcement or upgrade of masonry structures regards the experimental behaviour of structural elements and different assemblages. Frequently, the final aim is to characterize the mechanical behaviour of strengthened elements, in order to define a simplified model for design and assessment.

The possibility of adopting FRP composites for strengthening masonry structures was initially investigated by Croci in 1987 (Croci, et al., 1987). In the

next three decades, great interest was devoted to the reinforcement of arches and vaults using FRP materials. Several experimental works show that it is a valid option for the strengthening and/or repair of masonry. Some of these works are reported below. After Croci's researches, also Schwegler (1994) (Schwegler, 1994) and Saadatmanesh (1997) (Saadatmanesh, 1997), addressed this topic. The first contributions about application on masonry structures concerned general aspects related to the improvement of the flexural capacity and the resistance to earthquakes (Triantafillou & Fardis, 1997) (Triantafillou, 1998) (Corradi, et al., 2002) (Shrive, 2006).

Following these initial studies, several experimental works have been carried out ( (Ehsani M.R., 1997) (Triantafillou, 1998)) showing that this technique is effectively a valid option to repair or strengthen masonry structures, in particular, arched ones (Valluzzi, et al., 2001) (Briccoli Bati & Rovero, 2001) (Foraboschi, 2004) (Briccoli Bati & Rovero, 2008). In particular, these research works address carbon and glass fibres. However, for strengthening old masonry structures, characterized by low strength and low stiffness values, the use of glass fibres (or aramid fibres) seems preferable (Oliveira, et al., 2010) (Oliveira, et al., 2011). If compared with carbon fibres, the lower axial stiffness of GFRP materials leads to less mechanical compatibility problems in combination with masonry and, thus, has the advantage of reducing stress concentrations along the (wider) GFRP-masonry interface. Experimental tests have shown that masonry arches strengthened with glass fibres exhibit better global ductility characteristics (Valluzzi, et al., 2001).

More specialised works including experimental campaign, analytical and numerical simulation on elements have been proposed. Hereafter, some bibliographical references, with special focus on masonry structures, are reported:

- **arches and vaults:** (Briccoli Bati & Rovero, 2001) (Briccoli Bati & Rovero, 2000) (Foraboschi, 2004) (Foraboschi, 2001) (Lourenço & Poças Martins, 2001) (Luciano, et al., 2001) (Valluzzi, et al., 2001) (Barbieri, et al., 2002) (Basilio, et al., 2004) (Oliveira, et al., 2006) (Borri, et al., 2007) (De Lorenzis, et al., 2007) (Baratta & Corbi, 2007);
- **columns and piers:** (Micelli, et al., 2004) (Aiello, et al., 2007) (Aiello, et al., 2005) (Krevaikas & Triantafillou, 2005) (Nurchi & Valdes, 2005) (Corradi, et al., 2007);

- **in-plane behaviour of wall panels:** (Ehsani M.R., 1997) (Luciano & Sacco, 1998) (Valluzzi, et al., 2002) (Haroun, et al., 2003) (Cecchi, et al., 2004) (Ascione, et al., 2005) (Hamid, et al., 2005) (ElGawady, et al., 2005) (El-Dakhakhni, et al., 2006);
- **out-of-plane behaviour of wall panels:** (Gilstrap & Dolan, 1998) (De Lorenzis, et al., 2000) (Velazquez-Dimas, et al., 2000) (Hamilton III & Dolan, 2001) (Hamoush, et al., 2001) (Kiss, et al., 2002) (Kuzik, 2003) (Li, et al., 2004) (Foster, et al., 2005) (Turco, et al., 2006) (Mosallam, 2007);
- **bond behaviour:** (Ehsani M.R., 1997) (De Lorenzis, et al., 2000) (Briccoli Bati & Rotunno, 2001) (Casareto, et al., 2003) (Tan, et al., 2003) (Aiello & Sciolti, 2006).

The choice of using strengthening technique is important because over-designing interventions on existing structures may usually involve unacceptable costs. In addition, in the case of architectural heritage, it could entail unacceptable losses of cultural values, from the historic and artistic point of view (Modena, et al., 2010).

In recent years, large investments have been concentrated on these topics, in order to investigate the modalities of application, and the efficacy of FRP reinforcing systems. A large number of developments have been performed. In addition, some guidelines for the strengthening and the conservation of existing structures have been formulated (Grande, et al., 2008) (CNR-DT 200/2004, 2004).

Safeguarding cultural values implies also appropriated selection and design of the intervention materials and technologies. Attention is to be paid to the possibilities offered by the traditional solutions and to their possible combinations with innovative ones.

### **1.3.3 Limitations in the use of high performance fibre materials on masonry constructions**

In spite of their advantages and versatility, composite materials have not seen widespread use in civil engineering owing to the lack of knowledge about their long-term behaviour and high initial costs involved (Richard, et al., 2007). Prediction of Life-Cycle Costs (LCC) for composites would depend on the

availability of a practical Life-Cycle Performance Model (LCPM) for composite materials in construction. Existing LCPM methods that rely on historical performance records are not useful in the case of composites materials. However, there is a wealth of information available on the performance of composites in other sectors such as aerospace, defence, and automobile field. These data-information may not be used for life-cycle modelling of composites in civil engineering because of critical differences in environmental exposure, operating conditions, and loading patterns. (Nystrom, et al., 2003) (Hastak & Halpin, 2000) (Mishalani & Madanat, 2002). For this reasons, they are quite widespread in infrastructure rehabilitation projects of concrete structures (Richard, et al., 2007) (Bakis, et al., 2002) (Ehlen, 1997) (Nystrom, et al., 2003) (Nishizaki, et al., 2006) (Kong & Frangopol, 2003) (Berg, et al., 2006) (Ehlen, 1999).

LCPM methods is a fundamental tool for the LCC evaluation. It has been defined as “economic assessment of an item, area, system, or facility, considering all the significant costs of ownership over its economic life, expressed in terms of equivalent dollars” (Ehlen, 1997) (Dell’Isola & Kirk, 1981). In generic terms, LCC would include:

- initial cost,
- maintenance costs,
- operating costs,
- replacement or refurbishment cost,
- retirement and disposal cost,
- other costs such as taxes, depreciation, and additional management costs (Dell’Isola & Kirk, 1981) (Ehlen, 1997).

In the case of composites, the various costs included under the LCC would depend on the application. For example, the LCC of a bridge would include (Burley & Rigden, 1997):

- construction costs,
- cost of work for each maintenance activity,
- road use delay costs from operation and maintenance requirements,
- the traffic management costs during maintenance operations.

The difficulty for costs’ evaluation, excluding the initial costs, arises from the lack of reference data or maintenance records for HPM-composite applications. The estimation should be made based on HPM properties and data available for

conventional material, at a component or system level. Consequently, it is important to develop a benefit-cost model that allows comparison of different alternatives, without the need to quantify the benefits in terms of dollar values (Hastak & Halpin, 2000).

A recent research conducted by Patrick Ilg et al. (Ilg, et al., 2016) addressed the topic of LCC applied to HPM. Figure 2 shows the trend for the number of cases that are published starting from 1997, as well as their geographic distribution. This is the demonstration that there is a growing interest respect to this high performance materials.

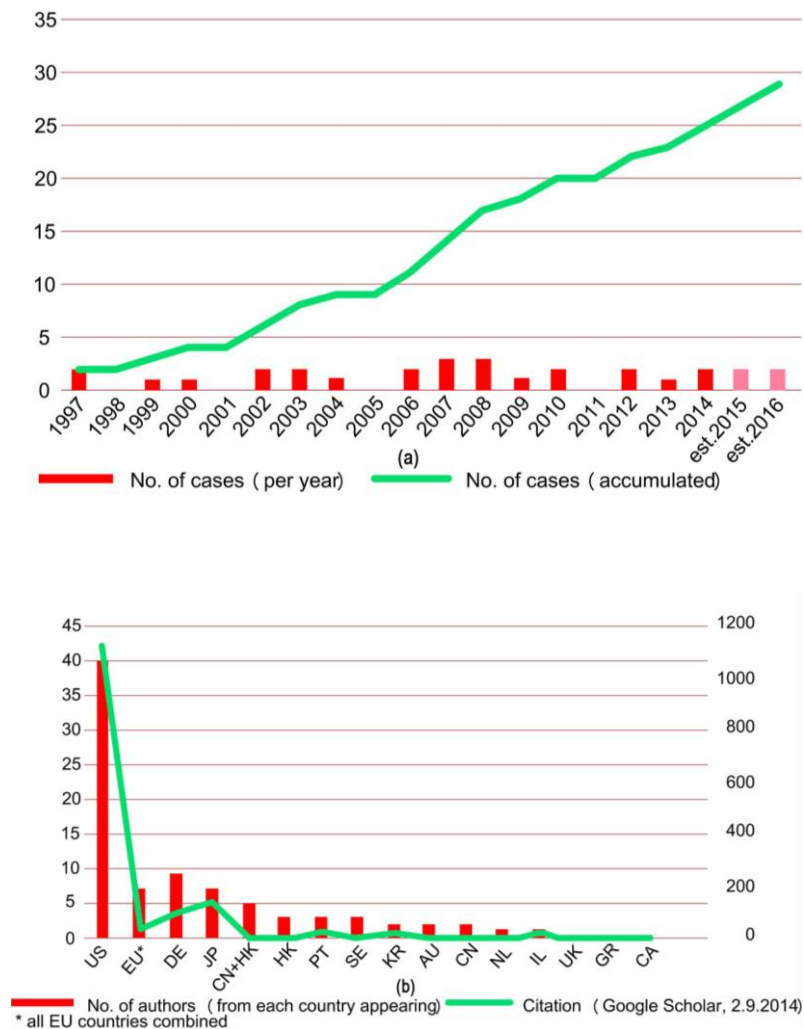


Figure 2: historic development (a) and geographical distribution (b) of articles dealing with LCC and HPM. Source (Ilg, et al., 2016).

The same research (Ilg, et al., 2016) shows that LCC is applied to HPM for structural applications with different levels of detail and quality. The initial results indicate that total life cycle costs for HPM are on average 10% higher. We urge the optimization of the cost structure of HPM to achieve the same level of LCC as conventional construction materials (steel or concrete in this specific case). In addition, these authors argue for a more holistic approach, which takes into consideration sustainability criteria throughout the life cycle of HPM based on the identified drivers of LCC:

- external costs, an extended life cycle,
- the discount rate and the expected service life.

The main problem is that the true costs of constructing, maintenance, and disposing of a HPM structures are less certain as compared to the same costs for traditionally used materials.

Burgoyne and Balafas in 2007 claimed that costs calculated, typically, are 5 or 6 times greater than the cost of steel. These costs were calculated on a cost/unit-force/unit-length basis. It was argued that those costs applied to materials in development and they would surely fall rapidly as manufacturing technology and the competitive market developed (Jungwirth & Windisch, 1995) (Burgoyne, 1991) (Burgoyne & Balafas, 2007). In addition, they claim that steel costs have recently risen, maybe because of significantly increased demand in Chinese economy. That should have improved the market for FRP, but it is clear in the following table (Table 1) (Burgoyne & Balafas, 2007) that the costs of new materials are higher in comparison to the costs of steel than they were 20 years ago and they are significantly higher than they were expected to be. It is widely believed that aramid and carbon fibre manufacturers have decided to concentrate on the small-volume, high-price, high-technology markets such as aerospace, rather than go for the high-volume, low-price, and basic-technology civil engineering market (Burgoyne & Balafas, 2007).

**Table 1:** cost of materials per unit force. Source (Burgoyne & Balafas, 2007).

<b>MATERIAL</b>	<b>STRENGTH [MPa]</b>	<b>COST [£/kN/m]</b>	<b>COST RATIO</b>	<b>NOTES</b>
Prestressing steel	1700	0.002	1	7-wire strand on coil
Reinforcing steel	460	0.006	3	Includes bending
GFRP	580	0.013	6.5	Excludes bending
Aramid fibre	2600	0.009	4.5	Fibre only
Aramid rope	2000	0.025	12.5	As a rope
AFRP	2000	0.025	12.5	As a pultrusion
CFRP	2000	0.025	12.5	As a pultrusion

(Based on £1 = US\$1.77 = €1.50, 2004 prices).

The initial-cost study here reported, shows that concrete structures reinforced with steel are less expensive than those reinforced with FRP, if only initial costs are considered. In case of steel structures that could corrode, the use of non-corrodible materials like FRPs could be a valid alternatives (Burgoyne & Balafas, 2007).

On the contrary, if average total life cycle costs for HPM are considered (eight cases in this work), they could be very competitive, with a cost that are 8.4% lower. The authors share the belief in a more eco-centric approach and, therefore, demand further research into a societal type of LCC that improves the mechanical properties while not ignoring sustainability criteria for new product systems such as HPM (Ilg, et al., 2016). The debate on this subject is still open.

In 2002 Bakis et al. (Bakis, et al., 2002) claimed that due to the importance of controlling risk in matters of public safety, standards and codes for FRP materials used in civil structures have been in development since the 1980s. FRP materials warrant separate treatment in standards and codes on account of their lower modulus and ductility in comparison with conventional materials such as metals. Without standards and codes, it is unlikely that FRP materials could make inroads beyond limited research and demonstration projects. Standardised test methods and material identification schemes minimise uncertainty in the performance and specification of FRP materials. Codes allow structures containing FRP materials to be designed, built, and operated with safety and confidence. A section of their

work describes the standard and code development activities in Japan, Canada, the United States, and Europe (Bakis, et al., 2002).

In 2007 Burgoyne and Balafas claimed that the reason because these materials were slow to take off was that there were no codes that could be applied. Various organisations have produced documents or are in the process of doing so. Despite the efforts of their authors they are all some extent flawed, since tests data are not available, particularly on the long-term properties, and the products are not yet standardized (Burgoyne & Balafas, 2007).



# Chapter 2

## High performance materials

High performance materials (HPM) in Fibre Reinforced Polymer (FRP), Synthetic Polymers (SP) and composite systems have become increasingly important in a various engineering fields. Since the middle of 20<sup>th</sup> century, high performance materials (or high-strength materials) have been used for a wide range of applications in civil and structural engineering.

The first part of this chapter provides an overview on composites made from high-strength materials. They are more beneficial than the conventional composites and their characteristics can be further enhanced by improving the design technology. The true innovation is that the engineer can design the composite material and the structural system at the same time, choosing the materials as needed. In natural form only very few materials exist which are composed of purely a single substance. The remaining materials are composed of numerous components, which when combined can form materials with better characteristics (Campbell, 2010). Synthetic polymer properties can be highly improved by adopting techniques used in nature.

In a second part of this chapter motivations about the choice of HPM for structural applications, and their properties are described. Strength and stiffness of materials are the critical characteristics for civil and structural applications. It is necessary to combine the polymer with other materials in order to obtain composites whose characteristics are better than those of its constituents. The most common used components are in particulates and fibrous forms. In case of

particulate composites specific material/materials are embedded and bonded together by polymers which is a continuous matrix with a low modulus of elasticity. On the other hand, in case of fibrous composites, fibres with high-strength and stiffness are enclosed. The fibre reinforcement may be oriented in such a way as to provide the greatest strength and stiffness in the required direction. The most efficient structural form may be selected by the mould-ability of the material (Campbell, 2010). On a less positive note, composite materials are expensive to fabricate, especially when sophisticated techniques are used to build them.

In conclusion, a brief history of polymers and composites used in construction industry and their usually applications are reported.

## **2.1 Definition of composite materials**

A composite material is a combination of two or more chemically different materials with a distinct interface between them. The constituent materials in the composite maintain at microscopic level their separate identities (phases). Based on the mechanical properties, each of these individual phases should perform certain essential functional requirements. The combination of different phases produces composites whose characteristics differ from those of the components (CNR-DT 200/2004, 2004). One of the principal components is the matrix, which is a continuous phase. The second major constituent is the reinforcement that can be in the form of fibres or particulates (high performance materials). Generally, the reinforcement is added to the matrix for improving or modifying one or more matrix properties. The reinforcement is a discontinuous phase, dispersed in uniform way into the matrix. The reinforcement surface may be chemically treated or coated with a very thin layer to protect it from environmental attack (moisture and chemical reaction), and for controlling or enhancing the interface bonding between the reinforcement and the matrix (Mallick, 1997).

For structural application, the composite reinforcement should be much stiffer and/or stronger than the matrix. Therefore, in composites materials, the main effect of fibre addition will be an important increase in the modulus and strength of the polymer matrix. However, the successful effect of the reinforcement in a composite depends also on the matrix chosen.

In recent years, reinforcements in particulate form have found considerable acceptance in metal and ceramics matrix composites. These reinforcements have approximately the same dimension in all directions. The most relevant parameters

is the particle volume fraction and the dispersion in the matrix. They can be incorporated into these matrices relatively easily. However, nowadays the most common reinforcements used in polymers, metals and ceramics are in a fibrous form (where their length is greater than the diameter).

Fibres can be used in both continuous and discontinuous lengths and generally occupies 30% - 70% of the matrix volume in the composites. Particulates can be of any geometrical shape, regular or irregular (spherical, plate like, angular etc.), and are generally less effective than fibres for reinforcing the matrix (Matthews & Rawlings, 1999) (Chou, et al., 1985) (Stacey, 1988).

## 2.2 Composite materials: classification

Composite materials are mainly divided as fibre and particle reinforced composites. Based on the orientation, particle reinforced composites can be divided as random and preferred orientation (Jones, 1998).

The classification of fibre reinforced composite is complex and is briefly reported in the following scheme (Figure 3).

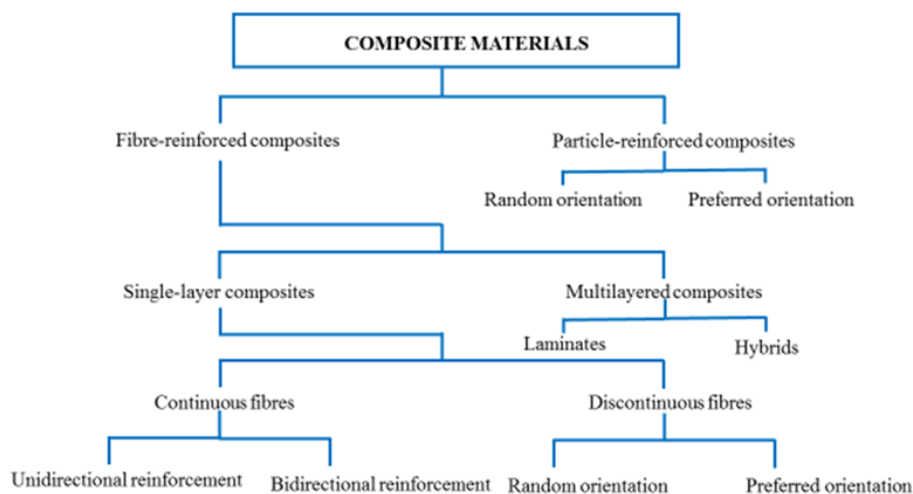


Figure 3: classification scheme of composite materials.

## 2.3 High performance materials: fibres

High performance fibres used in a fibre reinforced composites materials are usually very strong and stiff. These characteristics enable them to absorb the

tensile forces which acts on them during its intended use. High strength and high-modulus fibres are used as reinforcements for a low-modulus matrix in order to enable it to carry a higher load. The effectiveness of a fibre reinforcement is strictly related to type, length, volume fraction, and fibre orientation in the matrix. The selection of the fibre parameters for composite applications is very important. They influence one or more of the following characteristics of a fibre reinforced composites (Mallick, 1997) (Hollaway, 2010) :

- density
- tensile strength and modulus
- compressive strength and modulus
- fracture and fatigue performance
- response to impact loads
- electrical and thermal properties
- corrosion resistance
- cost.

It is necessary to take into account the anisotropic characteristics of such materials. In addition, at a microscopic level the properties of these composites depend on the fibre orientation and distribution, matrix properties, and their combination (CNR-DT 200/2004, 2004).

### **2.3.1 Fibre types**

Nowadays, a large variety of fibres with a wide range of densities, properties and cost are available commercially. These fibres can be manufactured in the form of long (continuous) or short (discontinuous) filaments. Short fibres are characterized by their length (in the range of 100  $\mu\text{m}$ -several mm). Most of these manufactured fibres are in the form of long continuous filaments and subsequently combined in various fashions such as strands, tows, rovings, yarns, fabrics, mats, etc. (Figure 4).

There are many types of long fibres used in structural engineering for strengthening like the glass, carbon, aramid, basalt and natural fibres (Pendhari, et al., 2008) (Codispoti, et al., 2015) . Generally, these types of fibres have much higher tensile strength than steel, titanium and aluminium. Moreover, short or discontinuous fibres are obtained by cutting the continuous fibres into lengths ranging from 3 to 50 mm. There is also another form of discontinuous fibres, called whiskers. They are single-crystal materials with diameters of about 10  $\mu\text{m}$ .

Whiskers are produced in extremely small lengths, and with a high length-to-diameter ratio ( $>100$ ). Nowadays, their cost is also very high.

Most of the commercially available fibres have approximately a circular cross-section or similar with a filament diameter in the range of 5-40  $\mu\text{m}$ . The boron fibres are an exception with a filament diameter of 140  $\mu\text{m}$  which gives a higher buckling resistance.

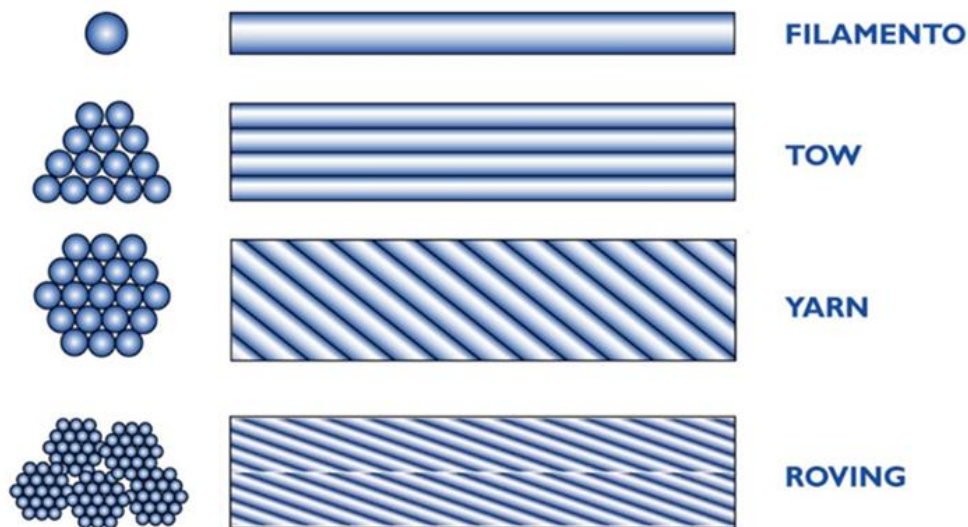


Figure 4: types of fibres. Source (CNR-DT 200/2004, 2004).

The high performance fibres also have a few common mechanical characteristics: they are generally brittle with a low elongation to failure of about 1-5%, and have a linear or a nearly linear elastic tensile stress-strain behaviour. In spite of these they have higher average tensile strength. It is possible to note a large variation in their strong points. Carbon and aramid fibres are highly anisotropic and are characterised by a significant difference in their longitudinal and radial thermal expansion coefficients. Others types of fibres such as glass and boron are instead isotropic (Mallick, 1997).

In addition to the well-known carbon, aramid and glass fibres, high-strength steel fibres are relatively a new kind of high-strength fibres (Corradi, et al., 2015). These fibres are characterised by better compatibility with organic matrices. But, they could be subjected to oxidation if not sufficiently protected. The use of

natural fibres made from plant, mineral or animal sources (such as jute, sisal, banana, hemp, ramie, coir, bamboo etc.) as reinforcements in plastics is increasing tremendously because they are usually cheap, have low environmental impact and offer useful mechanical properties (Pickering, et al., 2016). In recent years, the use of natural fibres for seismic upgrading and reinforcement of historic constructions is now limited to flax, hemp, and bamboo. Bamboo in particular is attractive as it is one of the fastest growing plants with a maturity cycle of 3–4 years (Janssen, 1991) (Amada, et al., 1997) (Corradi, et al., 2009) (Codispoti, et al., 2015).

In the following Figure 5 is shown a simple classification of the most widespread commercially available high performance fibres.

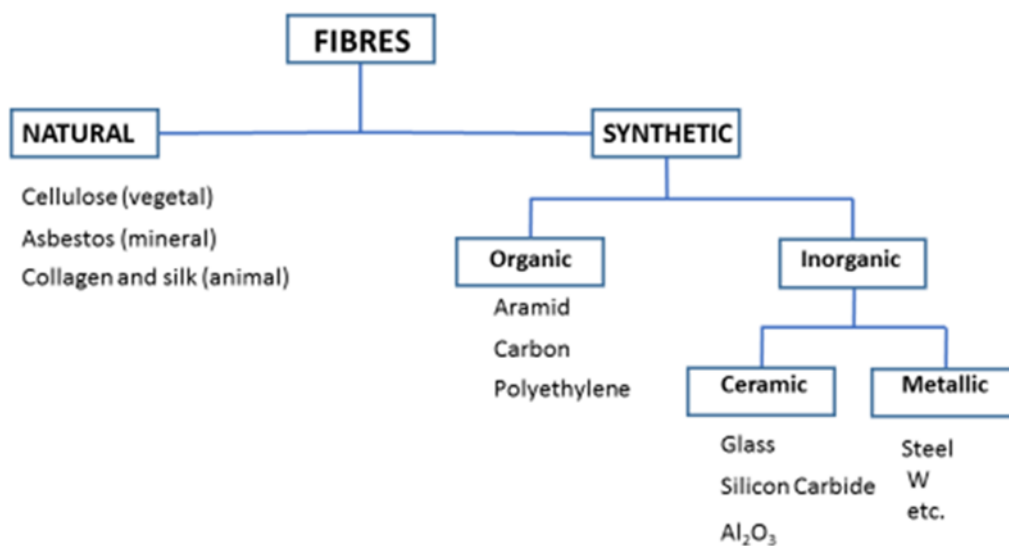


Figure 5: classification scheme of the most widespread commercially available high-performance fibres.

### 2.3.2 Fibre architecture

Fibre architecture indicate the arrangement of fibres, which can be one-dimensional (1D), two-dimensional (2D), or three-dimensional (3D) (Gokarneshan & Alagirusamy, 2009) (Figure 6). In the 1D form, the fibres can be either continuous or discontinuous. Continuous fibres (long fibres) are used in filament-wound, pultruded, or laminated structures. In these cases it is easy to precisely control the fibre orientation. Discontinuous fibres (short fibres or particles) are directly mixed into the matrix, and they are used for example in injection-moulded structures, or combined with a binder to form a planar mat. In these cases, it is very difficult to control the fibre orientation (Hull & Clyne, 1996) (Gowayed, 2014).

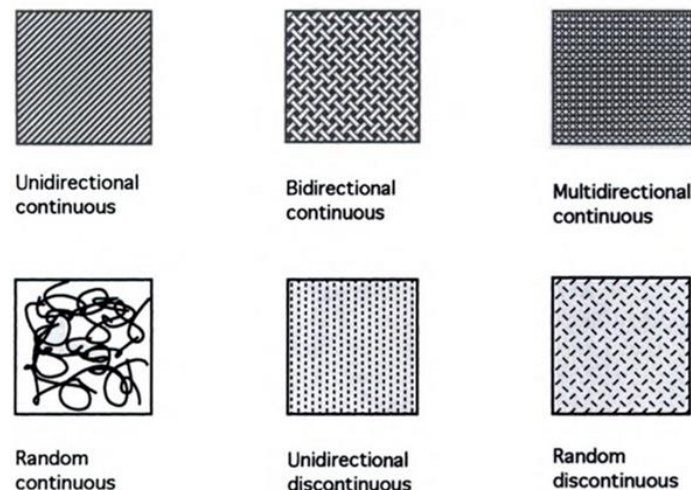


Figure 6: fibre architecture. Source (Mallick, 1997).

Woven fabrics represent one type of 1D architecture. Woven fabrics are planar textile obtained by weaving two sets of yarns at  $0^\circ$  and  $90^\circ$ . A planar weave provides a steady construction (very little slippage). Some of its advantages are as follows (Mallick, 1997) (Campbell, 2010):

- better drapability (ability for draping over irregular surfaces) than multi-directional laminates, which increases with the number of binders by unit area (lower harness)
- orthogonal in-plane properties
- lower susceptibility to inter-ply delamination

- larger design envelope (hybrid textiles, different fibre volume fraction in warp and weft directions, fabric type).

Disadvantages are the following:

- lower stiffness and strength (due to crimp) than multi-directional laminates
- higher processing costs than unidirectional laminates.

Two and three-dimensional architectures are produced by means of textile processes such as interlacing, intertwining, and interloping continuous fibres in textile machines. The textile is produced realised in mesh form with well-defined cell dimensions, which can be protected by a bituminous coat. It provides a good geometric stability, and works as a protective layer against a damaging agents (Gowayed, 2014).

Two-dimensional and three-dimensional products are knitted fabrics, braided fabrics, random mats, 3D woven fabrics, and non crimp-fabrics (Campbell, 2010) (Hollaway, 1993).

In detail:

- knitted fabrics are planar textile performs obtained by interloping one set of yarns (drawing loops of one yarn in the previous one, for example). Straight warp and/or filling yarns can be added to increase stiffness.
- Braided fabrics are textile pre-forms obtained by interlacing yarns in the bias direction. They are similar to rotated woven fabrics. Braided fabrics combine high torsional stiffness with large deformability in tension (Figure 7).
- Random mats are materials manufactured from a set of disordered fibres made by bonds of different nature such as simple entanglement, local thermal fusion or chemical binders. They are cheaper than their textile counterparts and have a lower strength and stiffness but higher deformability (Figure 8).

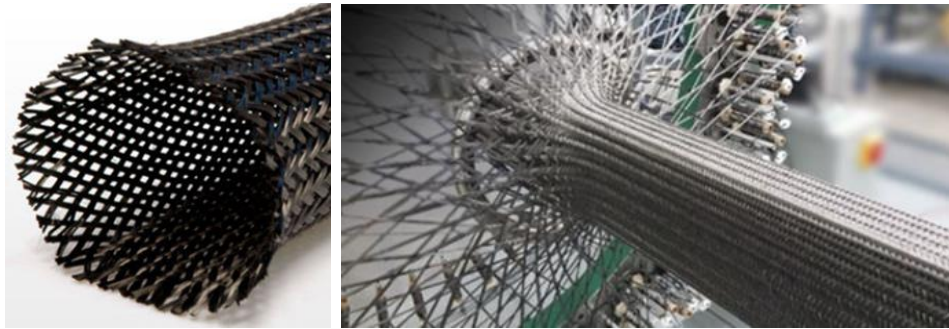


Figure 7: braided fabrics. Source (Nivitex.Fibreglass.and.Resins, 2017) and (Composites, 2014).



Figure 8: disordered glass fibres and random mat. Source (CNR-DT 200/2004, 2004).

- 3D woven fabrics are manufactured to improve the strength and the stiffness of textile pre-forms in the direction perpendicular to the fabric.
- Non crimp-fabrics are multidirectional laminates made up of unidirectional plies with different fibre orientation that are assembled and stitched together. In-plane mechanical properties are enhanced by the absence of crimp. Inter-ply delamination is inhibited by the 3D stitching.

Long textile fibres in composite materials of continuous length and usually 5-25 $\mu$ m in diameter are relatively stiff and strong. Their role is to absorb the tensile forces, mainly those parallel to their direction. Long textile fibre are characterise by high tensile strength, high length/diameter ratio, and by high ratio of strength to weight. Their mechanical behaviour is strictly related to some design parameters such as fibre angle, mesh size, wrap direction, etc.

Textile processes provide a good control over the fibre orientation, as well as fibre placement, and can be used to produce a variety of complex shapes or forms in a relatively short time. Two-dimensional architecture is used in laminated structures. A three-dimensional arrangement of continuous fibres is used when interlaminar failure or delamination becomes a problem with laminated structures that are made by stacking several laminae on top of one another. Laminated structures contain no fibres in the thickness direction and often fail by separation of laminae. Three-dimensional architecture can also be used to build composites with equal properties in the x, y, and z directions.

The fibre placement into a composite lamina can be unidirectional, bidirectional, multidirectional, or random. In the case of unidirectional placement of continuous fibres, the fibres are most efficient when the load in the composite is applied long the fibre direction (longitudinal direction). The strength and modulus of a unidirectional lamina are the highest in the direction of fibres and are much lower in other directions, particularly in the transverse direction (normal to the fibre). The matrix controls the properties perpendicular to the fibres.

A multidirectional laminates are built by stacking unidirectional lamina with different orientations. This placement is useful to reduce the variation of properties in different directions. Instead, when the fibres are randomly oriented, equal properties are obtained in all directions in the lamina plane. Consequently, the result of a randomly oriented arrangement of fibres is a quasi-isotropic lamina. The lamina properties will be much lower respect to the fibre direction properties of a unidirectional lamina.

## **2.4 High performance materials: matrix**

The matrix is the continuous phase in a composite material, and it plays several important uses as follows (Holloway, 2003) (Campbell, 2010) (CNR-DT 200/2004, 2004):

- prevents the reinforcement from moving
- makes possible the transfer of stress between fibres (when composite is under load)
- protects the reinforcements from harsh environment, damage during handling, and during the service life of the composite.

The matrix should disperse the fibres and separate them in order to avoid any catastrophic propagation of crack leading to failure of the composite, and finally to be chemically and thermally compatible with fibres over a long period.

The matrix plays only a minor role in the longitudinal tensile properties of a unidirectional continuous fibre composite while it is important in the transverse direction. The matrix selection influences some properties of a unidirectional fibre composite: the transverse tensile modulus and strength, longitudinal and transverse compressive properties and, shear modulus and strength. Moreover, it is important to highlight that for evaluating the mechanical properties of a composite material, the matrix has a great effect on its processing characteristics (Niroumand, 2009).

Matrix materials can be metallic, ceramic or polymeric. Polymeric materials are most widely used to produce composites as they are easy to infiltrate in the fibre perform, and are cheap when compared to other materials. Polymeric materials can be thermosets (resins) or thermoplastics.

Thermosets are polymers with branched chains. They are formed in situ by a chemical reaction (curing) between two polymers (resin-hardener or resin-catalyst), leading to three-dimensional network in which covalent bonds link different polymeric chains. Once cured, they do not become liquid again if heated, even if their mechanical properties decrease significantly over the glass transition temperature ( $T_g$ ). The molecular structure over  $T_g$  changes from a rigid to flexible network. This change is reversible. Thermoset polymers are low viscosity liquids at room temperature. They have high stiffness and strength, and good resistance to chemical attacks. Their main limitations are their brittleness and limited high-temperature capabilities (especially under hot/wet conditions) (Hollaway, 2010).

The most widespread thermoset polymers are:

- Polyester resins
- Vinylester resins
- Epoxy resins
- Phenolic resins
- Bismaleimides resins (BMI)
- Polymides resins.

Polyester resins are the most widely used matrices because of their low cost, good process ability, and environmental resistance. Particularly popular in marine industry are used in all applications that do not require extreme properties. Most polyester resins are viscous liquids consisting of a solution of a polyester in styrene. The addition of styrene (up to 50%) reduces the viscosity and enables resin curing by cross-linking of the polyester molecular chains.

The most common matrix used for FRP is an organic resin-based matrix. For structural engineering applications, polyester, vinylester, and epoxy are the widely used organic matrices. Epoxy matrix is widely used mainly because of its excellent adhesion to the fibres (due to its low viscosity), and due to the low amount of shrinkage during the curing process. It is important to notice that epoxy matrices have high-level of hardness, high-resistance to humidity and fatigue. It is possible to see that, after the curing period, a typical epoxy matrix has higher strength and stiffness properties than a polyester and vinylester matrix.

Thermoplastic polymers can have an amorphous or semi-crystalline structure. They alternate crystalline regions with amorphous ones in which the chains are approximate random coils. Thermoplastic polymers usually possess higher ductility and toughness when compared to thermoset polymers below glass transition temperature. Both properties increase very rapidly above  $T_g$  while the strength decreases. After the glass transition temperature, the amorphous chains change from glassy to a rubbery phase. Over melting temperature ( $T_m$ ), the viscosity gradually decreases without any distinct phase change, and thermoplastic polymers become viscous liquids that can be easily infiltrated into fibre performs. They can go through melting/freezing cycles repeatedly and can be re-melted and remoulded.

The most widely used thermoplastic polymers are (Das & Nizam, 2014):

- Polyolefins (PE, PP)
- Polyamides (Nylon)
- Polystyrene
- Polyphenylene Sulphide (PPS)
- Polyetheretherketone (PEEK)

## 2.5 Why choose a high performance material

Composites materials, especially FRP composites, offer many advantages compared to traditional materials for engineering applications (Karbhari & Zhao,

2000). The main advantage is that they are light as well as strong. Another significant advantage is that, by choosing an appropriate mix of matrix and reinforcement material, a new material can be made. Thus composite materials can precisely meet the requirements of a particular application and thus provide design flexibility. They can also be moulded into complex shapes.

Composite materials are perfect substitutes for steel, aluminium, titanium and other metals and are typically preferred because of their following properties (Niroumand, 2009) (Das & Nizam, 2014) (CNR-DT 200/2004, 2004):

**High-strength:** FRP composites are very effective in enhancing strength. They can be designed to provide a specific range of mechanical properties like tensile, flexural, impact and compressive strengths.

However, there are different kind of fibres commercially available, which different properties. For example, the aramid fibres have relatively low compressive strength compared to carbon fibre.

**Lightweight:** FRP composites have a higher specific strength compared to most materials used in similar applications. They can show more strength per weight than most metal alloys.

**High-strength to weight ratio:** the strength of a material is the force per unit area at failure per unit density. Any material that is strong and light has a higher strength/weight ratio. Materials such as aluminium, titanium, magnesium, carbon and glass fibre, and high-strength steel alloys all have good strength to weight ratios.

**Rigidity:** rigidity or stiffness of a material is measured in terms of Young's Modulus, and represents the deflection of a material under stress. Carbon fibre reinforced plastic is over 4 times stiffer than glass reinforced plastic (Figure 9).

**Tensile strength:** tensile strength or ultimate strength is the maximum stress that a material can withstand while being stretched. High performance fibre materials used in FRP are characterized by high tensile strength. However, brittle materials such as carbon fibre does not always fail at the same stress level because of internal flaws. Tensile strength of aramid fibres is slightly less than E-glass fibre (Hollaway & Head, 2001).

**Fatigue Resistance:** reduction in stiffness with large number of stress cycles is called fatigue which can lead to failure (unless the temperature is high).

Tests have shown that failure is unlikely to be a problem when cyclic stresses act in the direction of fibres. Carbon FRP (CFRP) is superior to glass FRP (GFRP) in fatigue and static strength and stiffness. But when CFRP fails, it will not show any significant exterior signs and thus the failure will be catastrophic.

The orientation of individual fibres and the fibre layer have a significant influence on the fatigue resistance. Different types of forces result in different failure modes.

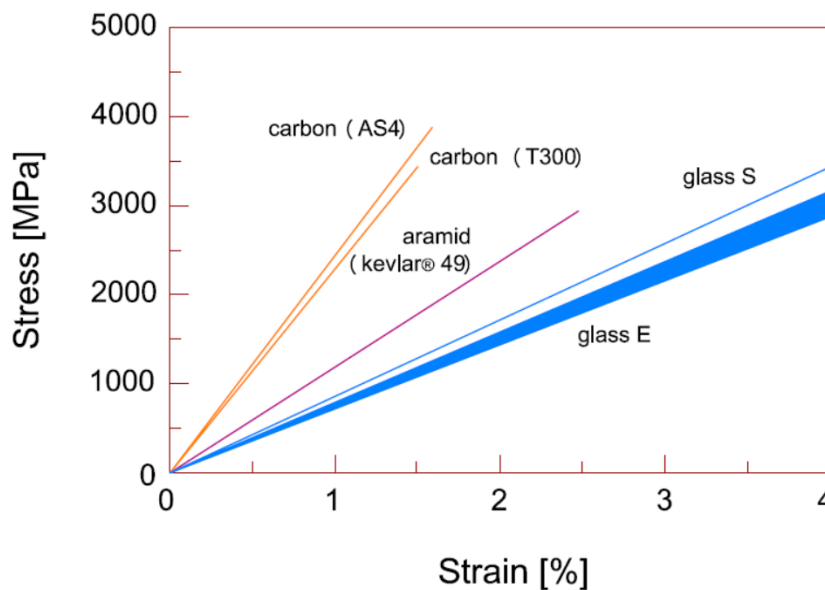


Figure 9: stress-strain curve of the main high-performance materials. Source (CNR-DT 200/2004, 2004).

**Impact and explosive loading:** the behaviour of FRP systems when subjected to impact or explosive loading is not yet completely understood. However, it is seen that aramid FRP (AFRP) are more resistant to impact than the CFRP.

Mechanical properties such as tensile strength, ultimate strain, and Elastic modulus of FRP systems degrade under aggressive conditions such as alkaline environment, moisture, extreme temperatures, thermal cycles, freeze and thaw cycles, and ultraviolet radiations (UV) (Karbhari, 2007).

**Effects of alkaline environment:** the water contained in the pores of concrete (or masonry) could cause deterioration of the resin and/or the interface between

FRP and the support. The damage caused by exposure to alkaline environment is typically more dangerous when compared to moisture exposure. The resins have to be completely cured before being exposed to an alkaline environment.

**Effects of moisture:** the main effects of moisture absorption are plasticization and reduction of glass transition temperature, strength and stiffness. The moisture absorption depends on the resin type, composition and quality of the laminate, thickness, curing conditions, resin-fibre interface, and finally the working conditions.

**Effects of temperatures variation and thermal cycles:** the viscous response of the resin and the composite depends on the temperature. With increase in temperature the modulus of elasticity of the resin decreases. The performance of FRP materials significantly decreases when the temperature is above T<sub>g</sub>. Thermal cycles do not have harmful effects on FRP composites. However they can cause micro-fractures in systems in which resins of high modulus of elasticity is used.

In civil infrastructure applications, undesired performance may be avoided by choosing a system in which the T<sub>g</sub> is always higher than the maximum operating temperature of the structure or component that is strengthened.

**Effects of freeze and thaw cycles:** exposure to freeze and thaw cycles does not have an impact on FRP performance, but reduces the performance of the resin and the fibre-resin interface. Polymer based resin systems can be improved, by providing higher strength and stiffness for temperatures lower than 0 °C. The effects of the decay induced in these cases, could be amplified by the presence of moisture.

**Effects of ultraviolet radiation (UV):** UV rays rarely deteriorate the mechanical performance of a systems strengthened with FRP. The most harmful effect related to UV exposure is the penetration of moisture and other aggressive agents through the damaged surface. Systems reinforced with FRP, could be protected from such damages by adding fillers to the resin or by providing appropriate coatings. AFRP will degrade particularly if exposed to sunlight and in high UV environment. Thus it is necessary to apply protective coatings to avoid the material degradation. Similarly epoxy resin is sensitive to UV ray and thus needs to be protected while carbon fibres will not deteriorate easily. This problem could involve other matrices.

The great sensitivity of Kevlar fibres to UV rays is a topic discussed in Chapter 6 of this work.

Mechanical properties such as tensile strength, ultimate strain, and elasticity modulus of systems strengthened with FRP, can also degrade due to creep, relaxation, and fatigue.

**Effects due to creep and relaxation:** both creep and relaxation depends in the properties of resins and fibres. Thermosetting resins are less viscous than thermoplastic resins. This phenomena is evident when the load is applied transverse to the fibres or when the composite has a low volume ratio of fibres, because the presence of fibres decrease the resin creep. Creep phenomena can be reduced ensuring low serviceability stresses. FRP systems made of carbon, aramid (e.g. Kevlar), and glass are the least, moderately, and most prone to creep rupture, respectively (Scott, et al., 1995).

**Fatigue effects:** the performance of FRP systems under fatigue conditions depends on the matrix composition and, on the fibre type. In the case of unidirectional composites, the fibres usually have some defects. This can delay the formation of cracks. They are also prevented by the action of adjacent fibres.

Other properties of composite materials which are useful for structural applications are the following:

**Corrosion Resistance:** FRP composites do not rust or corrode. If properly designed, the FRP composite components can have long service life and minimum maintenance when compared to traditional building materials. AFRP is not sensitive to organic solvents or oil, but are sensitive to strong acids, bases, and certain oxidizers. Exposure to these chemical substances could cause degradation of the fibres (Sen, 2003).

**Durability:** FRP composite technology is “new” compared with materials that it often replaces, such as concrete, masonry, steel or wood. Hence, many composite components have not yet attained their full life span. There are also some structures like FRP composite boats, tanks and certain other products that are in use for more than 50 years (CompositeBuild.com, 2014) (Karbhari, et al., 2003).

**Design Flexibility:** FRP composites can be fabricated into any kind of complex shape and configuration which can be large or small and can be used for structural, decorative or their combination. Composites materials do not bind the designers for any way, from prototype to production, based on the needs. Due to the design and fabrication flexibility of composites materials, single composite parts could replace complex assembly units of multiple parts that are produced with traditional materials such as wood, masonry, steel or aluminium. This property is very useful for applications on cultural heritage structures.

**Dimensional Stability:** FRP composite materials maintain their form and functionality with severe mechanical and environmental stresses.

**Good resistance to abrasion and cutting:** AFRP is often used for protection against cutting. Aramid materials are used worldwide for making armour and bullet proof materials, gloves, etc. which protect against sharp materials in construction industry (Bin Kabir & Ferdous, 2012).

**Strengthening limitation in case of fire:** composite materials are very sensitive to high-temperatures that can happen during a fire. When the temperature exceeds  $T_g$  of the resin (or the  $T_m$  in semi-crystalline materials), strength and stiffness of the FRP system are considerably reduced. While, in case of FRP used as external reinforcement for concrete or masonry structures, the exposure to high-temperature results in higher degradation of the bond between the composite system and the support (Katz, et al., 1999).

Composite parts can also be fabricated using appropriate polymer binder and filler technology for providing better performances for high-temperature applications. Using suitable manufacturing process and precursor materials, suitable carbon fibre composites can be designed to be used as protective clothing for firefighting (Keller, et al., 2006). As carbon fibres are chemically inert, they can also be used where the fire causes the release of corrosive agents. But these materials are costly. The resulting product is more efficient, but the raw materials are often expensive (Benichou, et al., 2010).

**Low Thermal Conductivity:** FRP composites are naturally poor conductors. But, thermally or electrically conductive materials can be incorporated into the composite part if high thermal or electrical conductivity is required. Thermal conductivity is a measure of how easily heat flows through a material.

Carbon fibres have high thermal conductivity in some forms. Since there are many variations on the theme of carbon fibre, it is not possible to identify exactly the thermal conductivity of the material. Some varieties of carbon fibres could be specifically designed for high or low thermal conductivity.

**Low coefficient of thermal expansion:** This is a quantitative measure of expansion and contraction of a material with rise and fall in temperature.

Low coefficient of thermal expansion makes CFRP suitable for applications where small movements can be critical such as for telescope and optical machinery.

**Electrical conductivity:** This is a critical property which has both merits and demerits. Carbon fibre conductivity can facilitate galvanic corrosion in fittings. A careful installation of the device may reduce the problem related to electrical conductivity.

Moreover, CFRP dust can accumulate and cause sparks or short circuits in electrical appliances and equipment.

**High Dielectric Strength:** FRP composites have excellent electrical insulating properties, making them an obvious choice for components in current carrying applications.

**Vandalism:** FRP composite materials are particularly sensitive to cuts and incisions produced by cutting tools. Hence, for protection of critical structures which may be subjected to vandalism adequate strengthening can be provided.

## 2.6 Commonly used fibres for structural applications

The most common type of fibres used for structural applications are the glass, carbon and aramid fibres. FRP are most attractive because they are cost-effective for their improved durability, the life-cycle maintenance costs are reduced, and they are easier for transporting and improving on-site productivity (CNR-DT 200/2004, 2004) (Christensen, et al., 1996) (Das & Nizam, 2014).

### 2.6.1 Glass fibres

Transforming glass into fibres is an ancient art. From the ancient times, these fibres were used to reinforce clay vessels and statues. Glass fibres are among the most versatile industrial materials known today (Wallenberger, et al., 2001).

They are typically amorphous fibres based on  $\text{SiO}_2$  (50-60%). Crystalline regions can be formed after prolonged heating at high temperatures (Gowayed, 2014).

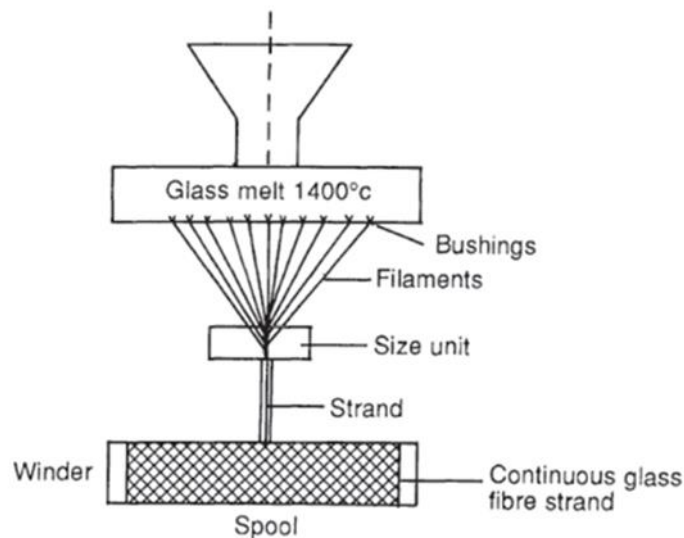


Figure 10: glass fibre manufacture, a schematic representation. Source (Hollaway, 1993).

Glass fibres are produced by melting several raw materials (Figure 10) many of which are abundant and cheap like silica and other salts. The main component of glass fibre is sand, but it also includes variable quantities of limestone, soda ash, borax, sodium sulphate, boric acid, etc. Various properties can be obtained by changing the chemical composition (Table 2). The transformation process is simple. Raw materials are heated in a furnace at temperatures ranging from 1500 to 1700°C, and later refined and transformed following a very precise sequence of chemical reactions, to obtain the molten glass. This molten glass is forced through a heated platinum spinneret containing extremely small holes. The fibres, which emerge from the spinneret, are immediately coated with a water-soluble sizing or a coupling agent. The coating provides a number of properties and functions to the glass. One important function is to prevent defects and fracture of the filaments during formation. It also protects the fibre from dust, which can scratch the fibre surface, and thus reduce its strength. The coupling agent could ensure a better interfacial adhesion of the fibre to matrix in a composite material. The coat also improves the yarn hand ability and protects it during the successive fabric forming processes.

**Table 2:** typical glass composition of glass fibres used to reinforced composite materials Source (Hollaway, 1994).

Component	Composition (%)- Type of glass			
	E	C	S	A
SiO <sub>2</sub>	52.4	63.6	64	72.5
Al <sub>2</sub> O <sub>3</sub> - Fe <sub>2</sub> O <sub>3</sub>	14.4	4.0	26	1.5
CaO - MgO	21.8	16.6	10	12.5
B <sub>2</sub> O <sub>3</sub>	10.6	6.7	-	-
Na <sub>2</sub> O - K <sub>2</sub> O	0.8	9.1	-	13.5

The fibres are manufactured into very fine filaments with diameters ranging from 2 to 13µm. Their strength and modulus may degrade with the increase of the temperature. Glass materials suffer from creep under a sustained loads, but despite this inconvenience, it can be designed to perform satisfactorily. The fibre itself is considered as an isotropic material with low thermal expansion coefficient than that of steel.

- **E-glass** (E for electrical use) is produced from lime-alumina-borosilicate, which can be easily obtained from raw materials like and which are available in abundance. The E-glass is the most common reinforcement material used in civil structures. Together with Advantex®, it represents over 90% of all GRP reinforcements produced today. It was launched successfully on the market in 1939.
- **C-glass** (C for corrosion) has a close chemical structure to that of E-glass but provides a high resistance to corrosion. It is not widely used in civil engineering application.
- **S-glass** (S for high strength) is an alumina silicate glass with a high tensile strength.

There are many others types of glass fibre which are commercially produced and used as a reinforcement:

- **Advantex®** is a calcium aluminosilicate glass, which is used as a boron free substitute for E-glass. It provides E-CR Glass acid resistance with the reinforcing characteristics of E-glass. It was succesfully introduced in the market in 1997.

- **AR-Glass** (Alkali resistant glass) is composed of alkali zirconium silicates. It was developed for use in concrete. It is mainly used for GRC (Glass Reinforced Cement) roofing, and sheeting panels.
- **D-glass** (Borosilicate glass) is characterized by a low dielectric constant. It is used for special applications requiring permeability to electromagnetic waves.
- **E-CR Glass** (Calcium aluminosilicate glass) is produced with a high alkali content. It is used where high acid corrosion resistivity is needed in addition to strength and electrical resistivity. It is commercially available since 1980.
- **R-glass** (Calcium aluminosilicate glass) is characterised by higher strength and temperature resistance when compared to E-CR Glass or Advantex®.

Glass fibres typically used to reinforce composite materials are divided into three main classes and is shown in Table 3 (Kinsella, et al., 2001).

The basic structure of glass fibre is composed of tetrahedral structural unit of silica ( $\text{SiO}_4$ ) (Figure 11). The silica atom forms a tetrahedral shape with four oxygen atoms.

**Table 3:** Mechanical properties of some glass fibres. Source (Kinsella, et al., 2001).

	<b>Tensile Modulus</b> [GPa]	<b>Tensile strength</b> [GPa]	<b>Poisson's ratio</b>	<b>Density</b> [g/cm <sup>3</sup> ]	<b>Strain to failure</b> [%]
E - Glass	72	3.45	0.22	2.55	1.8-3.2
C - Glass	69	3.3	-	2.49	-
S - Glass	87	3.5	0.23	2.5	4

The presence of calcium (Ca), sodium (Na), and potassium (K) breaks the silica network, reducing the stiffness and strength of the fibre. This improve the formability of the melt to form the fibres (Gowayed, 2014).

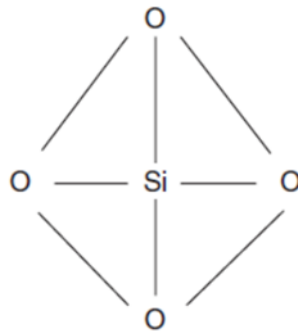


Figure 11: the basic tetrahedral structure of glass fibre Source (Gowayed, 2014).

The glass fibre bonds are randomly oriented causing the fibre to be isotropic or pseudo-isotropic. They exhibit useful properties such as hardness, transparency, and resistance to fire and chemical attack. On the contrary, moisture (water adsorption) can lead to reduction in strength. Moreover, stability and inertness are desirable fibre properties as well as strengthened flexibility (Mallick, 1997). They may have high-strength but the stiffness is limited, thus the specific stiffness is low. It is interesting to note that E-glass gets easily corroded in alkaline environment (concrete), and their mechanical properties decay rapidly above 400°C-500°C due to melting.

### 2.6.2 Carbon fibres

Carbon fibres are known since their development by Thomas Edison in 1870 and they have evolved constantly for the past 60 years (Hearle, 2001) (Gowayed, 2014). Nowadays, carbon fibres are gaining importance due to their good mechanical properties and thermal stability (Table 4). Carbon can be found in nature in many forms such as diamond, graphite, and ash. These are made from pure carbon atoms with different atomic arrangements. In particular, diamonds are made from covalent 3D bonds between carbon atoms while, graphite and carbon fibres are made from sheets of covalent-bonded carbon atoms, connected to each other via a weak secondary bond.

**Table 4:** mechanical properties of some carbon fibres. Source (Hearle, 2001).

<b>Precursor type</b>	<b>Product name</b>	<b>Young's modulus [GPa]</b>	<b>Tensile strength [GPa]</b>	<b>Strain to failure [%]</b>
PAN	T300	230	3.53	1.5
	T1000	294	7.06	2.0
	M55J	540	3.92	0.7
	IM7	276	5.30	1.8
Pitch	KCF200	42	0.85	2.1
	Thornel P25	140	1.40	1.0
	Thornel P75	500	2.00	0.4
	Thornel P120	820	2.20	0.2

Carbon fibres can be manufactured by controlled pyrolysis and cyclization of certain organic fibre precursors. It can be made from three types of polymer precursors: polyacrylonitrile (PAN) fibre, rayon fibre, and precursor mesophase pitch (MPP). The first is a synthetic fibre while, the third is produced from the destructive distillation of coal. It is interesting to note that rayon was one of the first precursors used to make carbon fibres. But during this conversion only 25% of the fibre mass is maintained and thus carbon fibres manufactured from Rayon precursors are very expensive (Hollaway, 1993) (Chand, 2000).

Another precursor named Polyacrylonitrile (PAN) fibre, is more economical with a conversion yield of around 50–55%. Moreover, carbon fibres made from a PAN precursor generally have higher strength when compared to fibres made from other precursors (Niroumand, 2009). This is due to the lack of surface defects, which act as stress concentrators, thereby reducing tensile strength. Another commonly used precursor is the Pitch precursor, which is a product of petroleum refining. But because of the irregular surfaces of the fibre, their tensile and compressive strengths are reduced (Hearle, 2001). Nowadays, carbon fibres are made from both a PAN and a Pitch precursor, while rayon precursors are used in less than 1% of the carbon fibres production (MIL-HDBK-17-5, 2002) (Gowayed, 2014).

There are several processes for converting a PAN precursor into a carbon fibre. The precursor-to-carbon-fibre conversion process consists of a sequence of procedures (shown in Figure 12):

- Stabilization
- carbonization
- graphitization
- surface treatment
- application of sizing and spooling.

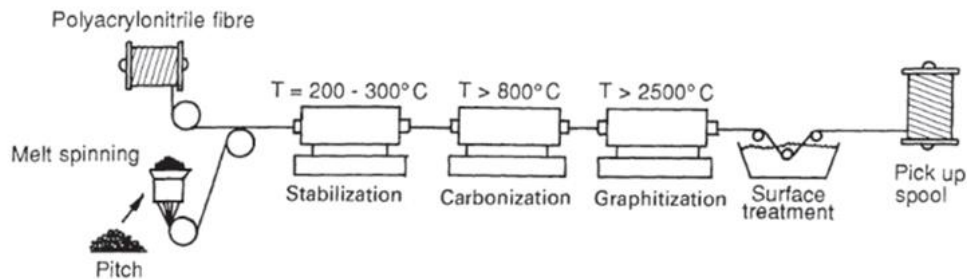


Figure 12: Manufacturing process of carbon fibre. Source (Hollaway, 1993).

Stabilization is performed at temperatures  $< 400^{\circ}\text{C}$  in various atmospheres to reach a dimensional stability. This phase is called the infusible step. During this step, the fibre is held under tension to improve molecular orientation, which increases fibre modulus and strength. Carbonization is carried out at temperatures from  $800$  to  $1200^{\circ}\text{C}$  in an inert atmosphere. The fibre is held under tension also during this process. In this step, polymer backbones are converted at higher temperature into ribbons of continuous carbon hexagonal rings. During the heating period, majority of elements other than carbon are removed and carbon crystallites are preferably orientated along the fibre length. Graphitization is an additional process and is performed at temperatures higher than  $2000^{\circ}\text{C}$  in an inert environment. In this process, the level of impurities decrease, the size of the carbon crystallites and the orientation of the fibre crystallites improves. Finally, the fibre passes through the surface treatment chamber to incentivise fibre adhesion. The crystalline size, crystal orientation, fibre porosity and impurity are major factors influencing the final physical properties of the filament. During the surface treatment process, various materials can be applied to the surface of

carbonized/graphitized fibre. These materials will control the interaction between the fibres and the matrix in composite materials. The coating is applied to fibre yarns to improve their handling characteristics in further textile forming operations. At the end, the fibre is spooled on a carrier tube to form a stable package.

Carbon fibre filaments are made typically with a diameter ranging from 5 to 8  $\mu\text{m}$ , and are combined into tows containing 5000 and 12000 filaments. The tows can be twisted into yarns and woven into fabrics. Hybrid fabrics, are also commercially available which contain either glass and carbon fibres (or aramid and carbon fibres).

Carbon fibres are characterized by low thermal expansion coefficients with respect to both glass and aramid fibres. Carbon fibre is an anisotropic material. Its transverse modulus are lower by an order of magnitude when compared to its longitudinal modulus. Carbon fibre material has very high fatigue and creep resistance. Its tensile strength decreases with increasing modulus, and thus its strain at rupture will also be much lower. As, this material is brittle, it should be carefully used in joints and connections which are places of high-stress concentration.

The modulus of elasticity of carbon fibres rises exponentially throughout the temperature range during heat treatment, as shown in Figure 13.

This is due to the increase in the crystallinity of the fibre which leads to a decrease in the amorphous characters. On the contrary, tensile strength increases in value to a maximum at about  $1600^{\circ}\text{C}$  and then falls to a constant value with further increase in value. Three distinct types of carbon fibres have been identified from the heat treatment temperatures. They can be classified as:

- Type 1: the stiffest carbon fibre, and thus requires the highest heat treatment temperature.
- Type 2: the strongest carbon fibre, and thus has been carbonised at the temperature that gives the greatest tensile strength.
- Type 3: the cheapest carbon fibre. The stiffness is lower than the previous types but has good strength. This type requires the lowest heat treatment temperature.

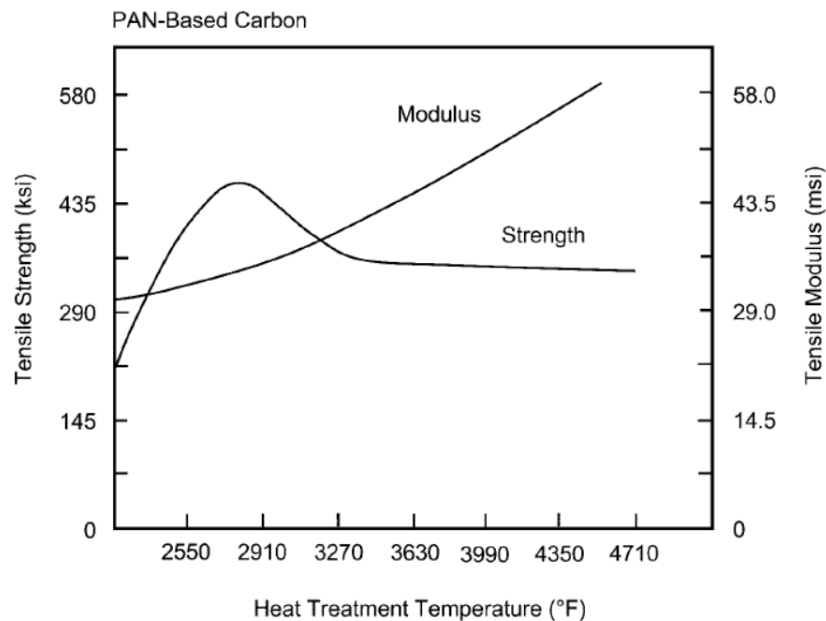


Figure 13: effect of heat treatment temperature compared to tensile strength and modulus of elasticity. Source (Campbell, 2010).

Carbon fibres are currently used for aerospace and space applications. They are also being considered for use in the construction sector. Its cost is comparable to glass fibre. Carbon fibres may be used together with a polymer or a cement matrix.

### 2.6.3 Aramid fibres

Aramid fibres are synthetic organic fibres in the aromatic polyamide family, which have a high-degree of crystallinity. They are distinguished from other commercial man-made synthetic fibres by their organic chemical composition of fully aromatic polyamides (aramids). The molecular chains are aligned and made rigid by means of aromatic rings linked by hydrogen bridges (Gowayed, 2014). This combination explains their very high strength. Their chemical structure is indicated in Figure 14.

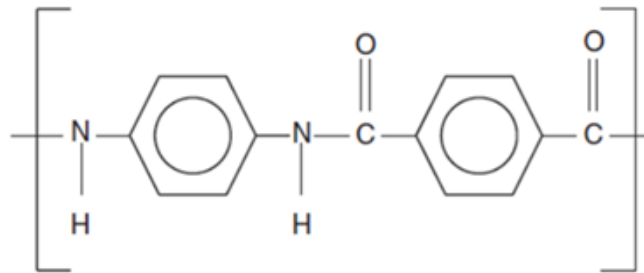


Figure 14: the chemical structure of Kevlar®. Source (Gowayed, 2014).

They have found applications in the field of composite materials. Different grades of stiffness are generally available starting from one with modulus of elasticity in the range of 60 GPa, to those in the range of 130 GPa. The higher modulus fibres are the one that is most frequently used in polymer composites (Hollaway, 1993).

The fibres are typically produced by an extrusion, and spinning process. A solution of the polymer in a suitable solvent at temperatures between  $-50^{\circ}\text{C}$  and  $-80^{\circ}\text{C}$  is extruded into a hot cylinder, which is at  $200^{\circ}\text{C}$ . This causes the solvent to evaporate and the resulting fibre is wound onto a bobbin. Liquid crystalline polymer solutions show a unique behaviour under shear. This aspect opened up new prospects for fibre manufacturing and processing. As the solution pass through a spinneret (orifice), the randomly oriented domains of the fibres, become fully oriented in the direction of the shear and emerge with near perfect molecular orientation. The fibres are then subjected to stretching and drawing process, to increase its strength and stiffness properties.

Aramid fibres are anisotropic material. Thus its transverse and shear modulus are an order of magnitude less than those in the longitudinal direction. The fibres may also have difficulty to achieve a mechanical or chemical link with the resin.

Aramid fibres were developed for demanding industrial and advanced-technology applications, and are produced to meet a broad range of end uses. There are various types of aramid fibres available on the market such as Kevlar®, which is produced in several versions by Du Pont in the USA and Northern Ireland, Twaron, which is made by Enka in the Netherlands, and Technora (eurofibers, 2017), which is manufactured by Teijin in Japan (Du Pont, 2017) (Bin Kabir & Ferdous, 2012). The mechanical properties of aramid fibres are shown in Table 5.

**Table 5:** mechanical properties of some carbon fibres. Source (Gowayed, 2014).

	<b>KEVLAR®29</b>	<b>KEVLAR®49</b>
Tensile modulus [GPa]	70.5	112.4
Poisson's ratio	-	0.36
Strength [GPa]	2.92	3
Strain to failure [%]	3.6	2.4
Density [g/cm <sup>3</sup> ]	1.44	1.44
Thermal conductivity [W/m <sup>2</sup> K]	0.04	0.04
Coefficient of thermal expansion [ $\times 10^{-6}/^{\circ}\text{K}$ ]	-4	-4.9

In Table 6 an overview on the main mechanical properties of glass, carbon, and aramid fibres is shown.

**Table 6:** typical mechanical properties for glass, aramid, and carbon fibres. Source (Hollaway, 1993).

<b>Material</b>	<b>Fibre</b>	<b>Elastic modulus</b> [GPa]	<b>Tensile strength</b> [MPa]	<b>Ultimate strain</b> [%]	<b>Density</b> [g/cm <sup>2</sup> ]	<b>Max temperature</b> [°C]
<b>Glass</b>	<b>E</b>	72.4	2400	3.5	2.55	250
	<b>A</b>	72.4	3030	3.5	2.50	250
	<b>S-2</b>	88.0	4600	5.7	2.47	250
<b>Aramid</b>	<b>49</b>	125	2760	2.4	1.44	180
	<b>29</b>	83	2750	4.0	1.44	180
<b>Teijin</b>	<b>Technora</b>	70	3000	4.4	1.39	-
<b>Carbon</b>	<b>XAS HS</b>	235	3800	1.64	1.79	600
<b>Grafil</b>	<b>HS</b>	235	3450	1.64	1.79	600
	<b>IM-S</b>	290	3100	1.64	1.76	600
	<b>HM-S6K</b>	370	2750	1.64	1.86	600
<b>Toray</b>	<b>T-300</b>	230	3530	1.5	1.77	600
	<b>M-46-J</b>	450	4100	2.4	1.82	600

## **2.7 Brief history of polymers and composites used in construction industry**

Bakelite was the first synthetic polymer and was first made in 1909. This material takes its name from its inventor Leo Baekeland who was an American chemist. From a chemical perspective Bakelite is a phenol formaldehyde resin produced when phenol (carbolic acid) and the gas formaldehyde are combined in the presence of a catalyst. If the reaction is allowed to proceed to completion, a dark brown substance of little use is produced. Baekeland discovered that, if the reaction is controlled by closing it before completion a material can be created which could flow and hence could be poured into moulds. If these were then heated and when appropriate pressure is applied a heavy solid plastic material is formed. This material is used nowadays in specific engineering applications. From this innovative invention, it is now possible to adapt polymers and to create new ones that can be designed for specific use (Holloway, 2003).

The history of the use of polymers and composites in the construction industry began during the Second World War, when rapid progress was made with the manufacture of the first radomes to house electronic radar equipment. Many aircraft components in this period, were also made using GFRP (Holloway, 2003).

It is possible to divide the history of composite materials into four different generations (Rawal, 2001) (Srivastava & Hoda, 2016).

### **2.7.1 First generation (1930s-1940s)**

The first generation was dedicated to Glass Fibre Reinforced Composites.

While solid-state scientists focused on the relation between structure and properties, industrial researchers were more concerned on the relations between functions and properties.

In 1932, Owens in the USA started the production of glass fibres. In 1935, they merged with Corning to form Owens-Corning Fibres with the sole purpose of starting a mass production of these fibres (OwensCorning, 1999). In 1939, in Europe Balzaretto Modigliani (Italy) obtained the rights for the Owens' patent, and transferred them to Saint-Gobain. At the same time, chemical companies were conducting research on new polymers. Phenolic, urea, and aniline-formaldehyde

resins were developed in the early 1930s, together with the unsaturated polyester resins patented in 1936 which then dominated the field of composites. In 1938, P. Castan (in Switzerland) received the first patent for epoxy resins, and soon authorised the patent to Ciba.

The mix of polymers with various additives (for example with chargers, fillers, and plasticity agents) were already a tradition in chemical industries.

The increasing importance of these innovative materials (polymers) in industry was evident with the establishment of the Society of the Plastics Industry in 1937 (Council®, 2012-2017), followed by the Society of Plastics Engineers in 1941 (Schulman, 2017). The creation of these scientific societies, showed an increasing interest on a topic that connects people from different universities and companies to exchange information about the latest discoveries (Figure 15).

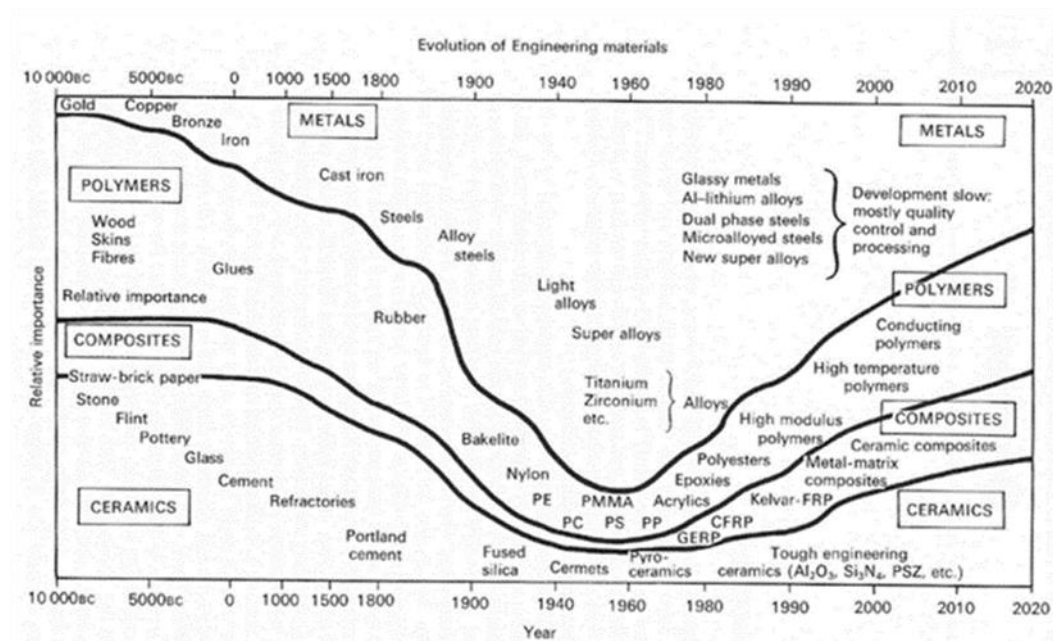


Figure 15: Schematic diagram showing the relative importance of ceramics, composites, polymers and metals, in mechanical and civil engineering as a function of time (The time scale is nonlinear). Source: (Ashby, 1987).

In 1940s, technicians and engineers had to find a best solution to add fibres to the system. The problem was that the fibres should be distributed throughout the matrix and should not be clustered together. The initial trials consisted in applying a high-pressure to the early resins and to allow them to cure. But, this resulted in

some problems. The high-pressure easily damaged the glass fibres. To solve this problem, in 1940, Pittsburgh Plate Glass developed low-pressure allyl polyester resins, and in 1942, Marco Chemical Company in Linden (New Jersey), was hired to investigate other similar low-pressure curing resins. In the same year, the first fiberglass laminates made from PPG CR-38 and CR-39 resins were produced (Rosato, 1982).

The earliest applications of GFRP products were in the marine industry (Selvaraju & Ilaiyave, 2011). In the early 1940s, GFRP boats were manufactured to replace traditional wooden and metal boats. GFRP boats which were very light, were not subject to rotting or rusting, as their predecessors, and they were easy to maintain. It is interesting to know that, in 1944 the Allied forces arrived at Normandy with ships made of GFRP components. In 1942, fiberglass-melamine or asbestos-melamine composite boards were used in the U.S. Navy for replacing all the electrical terminal boards on their ships thus improving their electrical insulation properties. Nowadays, fiberglass continues to be used in major parts of boats and ships.

In 1943, at the Wright-Patterson Air Force Base, projects were launched for building structural aircraft components using composite materials. This resulted in the first plane with a GFRP fuselage that was flown on the base a year later. In the same year, another significant advancement was the development of tooling processes for GFRP components by Republic Aviation Corporation. The capability to cut and model special parts to sizes established in design phase, allowed to reduce wastage and added greater flexibility to the manufacturing of complex components. In addition, pre-impregnated glass fibre sheets in a partially cured resin, made the production of the components easier. This was done by placing the fibres on a plastic film in a predetermined position. Resin was then added which was then pressed and finally partially cured. It was thus possible to produce flexible sheets of a precursor material. By pressure and heat, these sheets could be then cut into the desired size or shape, which are then superimposed, and then consolidated into a single piece.

Glass Fibre Reinforced Plastics dominate the market, and nowadays, comprise about 90% of the composite market (Palucka & Bensaude-Vincent, 2002).

### 2.7.2 Second generation (1950s-1960s)

In the 1950s, GFRP technology spread rapidly. In this year in France, a new Saint-Gobain plant was opened in Chambéry for the production of glass fibres. From 1957, they were known for producing composite helicopter blades for the Alouette II.

During this period demands for new type of fibres started to come from military space programs. This prompted the research of new high-modulus fibres. The combination of the world geopolitical situation and materials research created the need for having a general notion about composites materials.

In the 1960s, laboratory developments along with major world events to prompted the use of new stronger forms of reinforcement fibres. Graphite (carbon) fibres were produced using rayon as the starting compound. Texaco announced Boron fibres of high stiffness and strength that they had developed. Carbon and Boron fibres were developed almost at the same time. But during the 1960's, carbon fibres were widely accepted due to its superior processing capabilities and its lower cost (Rawal, 2001).

In 1961, in Japan, A. Shindo developed high-strength graphite fibres by replacing previously used rayon precursors with using polyacrylonitrile. (Dresselhaus, et al., 1988). Graphite fibres are just now used in polymer matrices. The use of graphite as reinforcement with metal matrices were initially not possible, because of the reactivity of carbon with aluminium and magnesium. It was thus necessary to invent air-stable coatings for carbon fibres which prevent the reaction between carbon and the metal in order to make graphite-aluminium and graphite-magnesium composites a reality.

Eventhough the strength of boron fibres were higher than that of carbon fibres, they found applications only in military applications where there high cost was not an issue. Boron had to be laid down on a tungsten wire that was used as a substrate. This resulted in these fibres to be expensive. This also resulted in filaments which could not be folded in with a small radius. Boron-epoxy rudders were installed on F-4 jet made by General Dynamics, for the first time in 1969. Boron also reacts with metal matrix above 600°C. Hence, coatings have to be provided before boron-reinforced MMCs become viable (Rawal, 2001).

In 1971, DuPont commercially introduced Kevlar, a fibre based on an aramid compound (belong to the nylon family of polymers), which was developed by

Stephanie Kwolek in 1964 (Kabir & Ferdous, 2012). The key structural features of aramid materials are its aromatic rings (benzene rings) linked by amide groups. Stephanie Kwolek began working on petroleum-based condensation polymers, and tried to develop stiffer and stronger fibres.

Aramid fibres can be used for the manufacture of bulletproof vests and helmets for soldiers. By applying a slight variation to the amide group positions between the aromatic rings, results in Nomex which is a fire-resistant fibre that is blended with Kevlar to produce protective equipment and tools for firefighters.

The general notion of “composites materials”, with the use of a variety of fibres and matrices, emerged first in the 1960s. A composite material is a combination of two or more heterogeneous phases, irrespective of their nature and origin. Their design led scientists to focus on the interface between the phases as the mechanical properties of heterogeneous structures depend on the quality of interfaces between the components. For this reason it was necessary to develop additive substances that support fibre and matrix chemical bonds. In this way, composite materials lead to a new direction on high-resistance materials research in which chemists also plays an important role (Palucka & Bensaude-Vincent, 2002).

### **2.7.3 Third generation (1970s-1980s)**

During the 1960s, developments in space and aircraft technologies had lead to extensive research on composites. But, during the 1970s with the decrease in the requirements from space and military sectors, new applications were found in sports and automobile markets (Miracle & Donaldson, 2001).

Since 1970s, carbon fibres were used extensively, for replacing the wooden tennis rackets (graphite) and the steel shafts of the golf clubs.

Aerospace engineers began to design re-usable spacecraft such as the Soviet MIR space station, the Skylab, and the Space Shuttle, (Dark III, 2008). All these structures were subjected to extreme and repeated temperature changes. This requires optimization of the metal-matrix composites (MMCs), which was investigated with the start of space challenges. These MMCs have the properties of high-strength and high-temperature resistance combined with a low coefficient of thermal expansion (CTE). This was necessary to ensure that the material will not undergo excessive expansion and contraction during the normal thermal cycles. In the mid-1970s, new fibres such as silicon carbide (SiC) were developed.

Moreover, coatings for carbon and boron fibres nowadays made them available as possible additives for metallic matrices (Miracle & Donaldson, 2001).

A wide variety of MMCs have been employed in spacecraft applications during the mid-1990s. For example, carbon-reinforced copper was used in the combustion chamber of rockets; SiC-reinforced copper was used for manufacturing rocket nozzles; Al<sub>2</sub>O<sub>3</sub>-reinforced aluminium was used in the production of fuselages and SiC-reinforced aluminium was employed for wings and blades. However, the cost of producing MMCs were very high and this limited their use in other sectors. MMCs were also used for making lightweight and high strength bicycle frames for some mountain bikes (Miracle & Donaldson, 2001).

For the production of ceramic matrix composites (CMCs) was necessary to develop high-temperature reinforcing fibres, such as silicon carbide. This was essential because the fibres with low melting point will be easily destroyed by the high processing temperatures required for ceramic sintering. The development of Nicalon™ SiC fibres, by Yajima in 1976 was thus an important milestone (Yajima, et al., 1976).

Alumina is the ceramic typically used for artificial hip prostheses. By adding fibres of silicon carbide to alumina matrices, the toughness of the implant can be increased by as much as 50% SiC-reinforced alumina is also used in long-lasting cutting tools, wood and metal.

Graphite fibres in a carbon matrix gave life to another important class of CMCs: the carbon-carbon composites characterised by an excellent heat resistance and toughness. These properties allowed them to be used as brakes on aircraft.

At the end, the innovation costs were reasonable as these plastic materials have opened new avenues for research. Plastic materials can always be moulded irrespective of fibres. Respect to metals, they can be shaped in the process of hardening the resin. Metals manufacturing and shaping the material are two successive operations, whereas in the case of composites they unite to form a single process (Palucka & Bensaude-Vincent, 2002).

#### **2.7.4 Fourth generation (1990s)**

The last generation started during the 1990s, when both industrial and academic researchers began to extend the composite model from a macroscopic

level to the molecular level. This resulted in two types of materials:

- hybrid materials
- Nanocomposites (towards the nanoscale)

Hybrid materials contains a mix of organic and inorganic components at the molecular scale. Historically the study of bio-mineralization has focused the attention of material scientists on the possibilities of such hybrid structures. A new design strategy was thus born and is known as biomimetism (Rawal, 2001).

Mollusk shells, bones, wood, and many other materials are made by living organisms associated with inorganic and organic components. Biological macromolecules form an intimate mix or composite of proteins and mineral phases at all level of composition, starting from the nanoscale up to the macroscopic scale. For instance, nacre is a kind of sandwich material made of layers of calcium carbonate crystal with alternate organic layers of proteins. In bones, collagen protein fibres form the matrix phase, which is reinforced with small, rod-like crystals of hydroxyapatite about 5x5x5 nm in size. Hydroxyapatite is an inorganic, calcium phosphate-based crystal with the formula  $\text{Ca}_{10}(\text{HPO}_4)_6(\text{OH})_2$ . This is a naturally available model of a reinforcing phase of small dimensions when compared to the matrix. MMCs and CMCs frequently mimic this design, with small particles of ceramic SiC used as a reinforcement in aluminium, or small particles of zirconia in alumina.

In the design of hybrid materials, the main objective is to mimic nature's process i.e., to get a spontaneous association of molecules into stable structures. Molecular self-assembly is a common standard process in biological systems. In order to perform such molecular self-assembly materials scientists have to overcome thermodynamic issues associated with the combination of molecules (Zhang, 2003). They rely on all sorts of non-covalent interactions - such as hydrogen bonds, or van der Waals interactions to link molecular surfaces into aggregates. In nature proteins are used as templates to manufacture stable structures while material scientists rely on inorganic porous matrices to insert organic molecules or enzymes.

Remarkably, hybridization techniques are not limited to polymers alone, but can be extended to cements and materials used for electronics or medical uses. Hybridization intensifies the need for multidisciplinary cooperation: molecular biologists, chemists, chemical engineers, mechanical engineers, electronic

engineers and physicists have to collaborate. Thus, hybrid materials constitute a composite field of research requiring the transfer of knowledge across various disciplines. For instance, they use the skills in intercalation processes of a by the solid-state chemist as well as the synthetic skills of the polymer chemist, their experience in the design of composites and multiphase systems using polymer blends, copolymers, and liquid crystal polymers. Scientists from various specialties have to learn the techniques of other disciplines instead of defending their own areas.

Nanocomposites are on a very small scale. Since micro-synthesis was successfully used for making computer components, materials scientists have aimed to go beyond the microscale and to build up materials atom by atom (that is at the nanoscale which is less than 100 nanometres) in order to make complex materials that can function as devices or micro machines (Hou & Jiang, 2009). Again, biological systems provided the inspiration. Lot of money and effort has been spent on nanocomposites. However, one major problem lies in the impossible extrapolation from the micro to the nanoscale. At the latter, quantum effects become the norm (Palucka & Bensaude-Vincent, 2002).

## **2.8 Composites for engineering applications**

Advanced composites have obtained significant use both in North America and Europe where the applications were mainly focused on space industry, on structures or components in extreme corrosive environments, on structures which are difficult to access for an inspection, and in advanced structures such as for radar transparency (in addition to conventional structures).

A number of studies in the past (i.e. (Salama, 1984) and (Burgoyne, 1998)) have investigated the possibility of reducing the weight by using composites in different parts of offshore structures and bridge stays. It is expected that in bridges composite materials will make significant progress in the coming years. In particular, composite materials can be used for walkways, gratings, handrails and cable trays (mainly pultrusion), pipework and vessels for all aqueous systems (mainly filament wound), and panels for separating operating areas and for use in accommodation modules (sandwich and other fiat laminates).

In the late 1970s, the construction of prototype footbridges in North America and Europe has started. The first known GFRP highway bridge was built in 1981 at Ginzi (Bulgaria), by using the hand lay-up technique. The main reason for the development of this highway bridge was to provide a lightweight military bridge,

which could be easily moved. In the same year, the concept of a “Bridge Enclosure” won a prize in the Civil Engineering Innovative Competition (Hollaway, 1993). In October 1982, the Miyun Bridge in Beijing, China (another prototype GFRP bridge structure), was completed (Karbhari & Zhao, 2000).

The use of FRP Eliminates the corrosion problems in metals which are caused by harsh environment. Nowadays, many universities and research institutes across the world are investigating the use of advanced composites for bridge construction and repair. Many reinforced concrete bridges have suffered from chronic corrosion due to de-icing salts. This problem is particularly felt in USA. To counter the problem over 200000 tonnes of epoxy-coated steel rebars have been used in bridge decks since 1987, but these have degraded (Hollaway, 2003) (Li, et al., 2002). GFRP rebars surpass the strength and fatigue properties of steel bars. These rebars can be manufactured by the pultrusion process and investigations are going on to see if they can be used as a replacement material for steel (Russo & Silvestri, 2008). Other features of these kind of rebars are its low weight (although it is not generally a problem for the reinforced concrete) and economy (i.e., the cost of GFRP rebars is about the same as for epoxy-coated steel rebars). In addition, as GFRP possesses excellent electrical insulation properties, it would be ideal for use at airports to help solve radar interference with electrical or magnetic fields.

Considerable research on the use of fibre reinforced polymer strands called Polystal to post-tension concrete beams has been undertaken in recent decades. This technique has been used to construct footbridges in Germany, for example. The first known example was a small-prestressed concrete footbridge built in Dusseldorf, Germany. In 1986, a continuous two-span highway bridge structure (Die Bruck Ulenbergstrasse) was erected in Dusseldorf. The slab was post-tensioned with 59 Polystal prestressing tendons, each made up from 19 GFRP rods with a nominal diameter of 7.5m (Hollaway, 1993). Another footbridge was constructed at Marien Flede in Berlin. In this case, external Polystal tendons were used as prestressing cables.

Aramid fibres, and AFRP, have been used for prestressing, bracing, and in particular for the anchoring of oil drilling platforms (Burgoyne, 1987) (Dolan, 1990). In bridge engineering CFRP was used for cables in case of cable-stayed and suspension bridges. More recently, CFRP materials were used as prestressing tendons. An 80 m long prestressed bridge, with a partial reinforcement of CFRP

tendons was constructed in Ludwigshafen in 1991 (Ryngier & Zdanowicz, 2015).

A large number of composites and polymers are also used in geotechnical applications such as for:

- soil anchoring;
- ground anchors;
- soil nailing;
- friction anchoring;
- reinforced soil;
- soil reinforcement techniques;
- reinforced soil rafts;
- embankment slope reinforcement.

After an extensive literature research it is possible to note that, for what concerns the applications of composite materials in construction field, the first applications were on concrete structures, with particular attention on concrete bridges. This because bridges have a strategic importance.

Only in a recent years (with respect to applications on concrete structures), researches on different kind of application were conducted. Particularly interesting for this dissertation are the applications on masonry structure, with a great attention for historical masonry buildings.

## **Chapter 3**

# **Using high performance materials for strengthening interventions: a literature review**

The aim of this chapter is to review the strengthening techniques and systems used for masonry structures, and experiences learned from previous works. During the last few decades, many testing campaigns on traditional and modern materials have been performed.

In the second part of this chapter, a series of real case studies are presented, in order to show the effectiveness of modern strengthening technique. The aim is also to highlight strengths and limitations, and to find possible gaps on their application in structural engineering, in particular on historical masonry structures.

### **3.1 Background**

Architectural heritage mainly consists of masonry structures, which are typically spread out over regions characterised by high seismic vulnerability (Aiello & Conte, 2009). Consequently, historical constructions (such as monuments, historic buildings, bridges, etc.) require ad hoc interventions, for mitigating any possible damage under earthquakes. The improvement of the

safety level of masonry buildings, in particular if they are historical masonry construction, is a complex task. Knowledge related to the complexity of the geometry, the variability in the material properties of different components used, and the different building techniques employed during the construction, is essential to design an efficient retrofitting strategy. But, sometimes data pertaining to the building's history, the structural modifications carried out in the past, possible damages suffered, and their related problems may not be always available. In some structures there may be strict restrictions regarding inspection which will not allow to obtain the required information. Even though the non-destructive tests cannot give a complete overview of the material and structural properties, the high costs involved in carrying such tests will again make the evaluation a complex task (Betti & Vignoli, 2008) (Lourenço, 2005) (Mallardo, et al., 2008) (Boothby, 2003).

The importance of structural interventions for repairing and strengthening architectural heritage is gaining demand. The guidelines for the regulation of strengthening interventions have already been stated in Chapter 1. One of the important requirement specified in the guidelines is that the intervention should not have an adverse effect on the character of the monument. The intervention must be reversible, especially when the technique applied was not been already consolidated over the years (Triantafillou & Fardis, 1997).

A wide variety of techniques can be considered for strengthening and repairing of masonry structures (Triantafillou & Fardis, 1997) (Triantafillou, 1998). Many ancient structures might have suffered from the accumulated effects of inadequate construction techniques and materials, overload, ground settlement, temperature variation (seasonal variation), impact and explosive loading (Buchan & Chen, 2007), traffic vibration, natural events like earthquake or wind, etc. In addition to these factors, change in usage of these structures and more stringent seismic design requirements might result in many of these ancient structures to become unsafe and thus need adequate retrofitting.

Traditional as well as modern techniques can be employed for retrofitting. The traditional techniques use the materials and building processes which were originally employed in the construction process. Conversely, the modern techniques provide more efficient solutions by employing innovative materials and technologies (Modena, et al., 2011).

Traditional interventions consist fundamentally in positioning alongside of an existing building of new elements (made with steel or reinforced concrete) that replace/reduce the loads acting on the original structure. This can be implemented by inserting elements that are more rigid and resistant. This also produce an increase in the loads and may also result in a change in the behaviour of the original structure. However, use of light materials like FRP which are light does not add any significant increase in vertical load but at the same time can provide significant increase in lateral stiffness (Briccoli Bati & Rovero, 2009) (Sivaraja, et al., 2013).

Initially, high performance materials were used for strengthening reinforced concrete structures. However, these are now analytically and experimentally studied for masonry structures in the last few years. There are numerous studies on this topic which focus on strengthening of vaults, which have an important role in many ancient buildings (see section 3.5.3).

High performance materials have numerous advantages in building construction such as (Kendall, 2007) (Sivaraja, et al., 2013) (Sen, 2003):

- they can be fabricated offsite,
- mobilization costs are lower and repairs can be made faster,
- the modular construction reduces the mass,
- higher durability,
- ability to produce complex shapes,
- higher thermal insulation and lack of cold bridging,
- the low weight allows a faster and simple installation,
- it is also less dangerous with respect to traditional confining techniques.

## 3.2 Strengthening actions

The effects of an intervention can be classified as follows:

- **Confinement:** prevents deformation. The confinement techniques can be applied to single elements, by reducing the lateral strain and thus improving the mechanical properties of masonry (local confining). It can also be provided to the structure as a whole, limiting the deformations at floor level for example, for reaching a monolithically

seismic behaviour, and thus avoiding the out-of-plane failure mechanism (Global confining).

- **Reinforcement:** incorporating a resisting element, with better mechanical properties and by properly connecting it to the base structure results in an overall increase in strength and stiffness.
- **Enlargement:** widening the resisting section by adding new material. The material employed generally has similar mechanical properties as the original structure. The improvement is due to a better stress distribution over a larger resisting area.
- **Material substitution** consists of removing and replacing the damaged parts of a structure. The materials employed during the reconstruction (to be effective) have to be similar to the original ones or possess better mechanical properties.
- **Structural substitution** consists in creating new load bearing structure with new (modern) materials, without the dismantling the original structure. This technique is used to maintain the external features of an existing building with insufficient capacity.
- **Tying** consists in linking together different elements or different parts of a single element. In global tying, steel bars are the most diffuse devices. In alternative, a wider variety of technologies was to be found in local tying.
- **Propping:** the structure is maintained by providing additional support elements. It can be applied both for damaged and intact structures which has to be strengthened. Propping provided can be lateral (strutting) or can be vertical.
- **Anchoring:** it is done to fix an element (or a part of a structure) to a rigid element/structure. The most diffuse form is anchoring to rock and soil. This action is employed to improve the stability of a structure and to avoid its collapse in case of critical events like earthquake.
- **Prestressing/Precompression:** this changes the stress field in a structure (or in an element) by applying adequate external loads.
- **Isolation:** vibrations and seismic forces are absorbed by means of external devices, which are usually placed between the foundation and the structure.
- **Soil stabilization:** this is focussed on soil underneath the structure and is aimed to improve its bearing capacity.

- **Improvement:** consists of a general improvement of the resisting sections characteristics and is not due to any of the methods.

### 3.3 Repairing and strengthening techniques

It is possible to repair and/or strengthen masonry structures with an extensive variety of practical applications that are continuously evolving. The most representative and widely used methods are listed below.

#### 3.3.1 Injection

This method aims to improve the characteristics of the resisting section. This technique is usually applied for strengthening or repairing walls with voids inside or has incoherence of the filling material, and also in cases where there are visible cracks (Corradi, et al., 2002).

This technique consists in injecting mortar or a fluid resin through holes that was previously drilled in the outer surface of the wall. The aim is to fill existing cavities and internal voids, and seal possible cracks. Injection increases the continuity of the masonry and hence its mechanical properties. This technique is normally used in stone-masonry structures.

**Examples of practical cases:** bell-tower of Monza (Italy) (Modena, et al., 2002).

#### 3.3.2 Local reconstruction named “cuci-scuci”

Material substitution technique consists in removing and replacing of damaged parts of a structure. The materials used in the reconstruction may be similar to the original ones, or possess better mechanical properties. It is one of the first techniques applied to restoration. Figure 16 shows systematically the procedure of doing this.

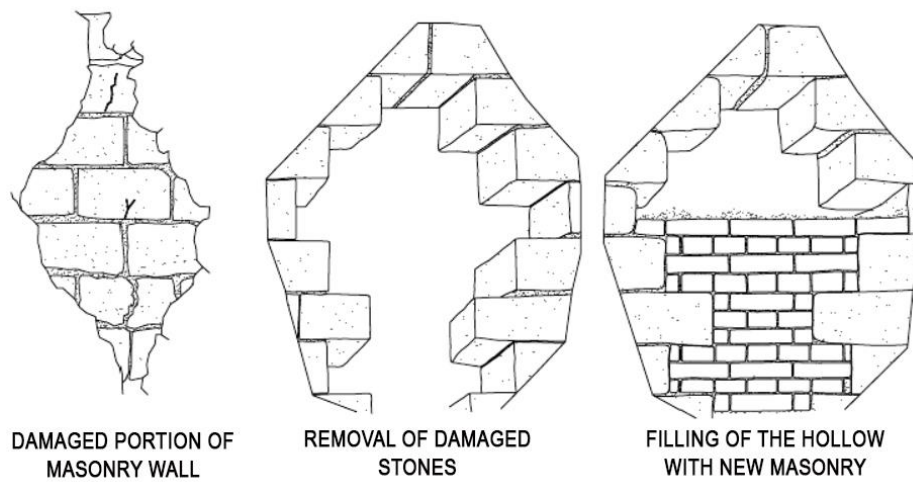


Figure 16: step in “cuci-scuci” strengthening intervention.



Figure 17: example of “cuci-scuci” intervention. Source (Modena, et al., 2011).

This technique is usually applied on walls with severe but localised cracks or highly deteriorated parts (Figure 17).

The main objective of this method is to preserve the mechanical efficiency and recuperate the continuity in a masonry structure.

### **3.3.3 External or internal reinforcement**

This strengthening effect is obtained using a reinforcement. This technique could be applied by the use of high performance materials (i.e. FRP, steel, etc.) on the external or internal sides of the wall, locally (i.e. strips), or to the whole surface of the structure (i.e. grid reinforcement). The connection with masonry is obtained with the use of epoxy resins or mortar. An effective use of this technique requires a certain regularity in the masonry surface. In arches and vaults, the reinforcement could be applied between the extrados and an additional masonry layer.

This technique is usually applied both on old and new masonry structures that require protection against earthquakes or, in general, higher mechanical properties. It is commonly used in arches and vaults suffering from cracks associated to intense compressive stress. The aim of this strengthening intervention is obtain an increase of ductility and a more resistant structure, by adding a material that can resist tension.

### **3.3.4 Stitching and local tying**

The strengthening effect is obtained using ties. This technique consists of binding together different elements or different parts of a single element. Steel bars are widely used for global tying.

Stitching is usually applied on masonry elements which require higher cohesion and mechanical characteristics without a visible modification, or on parts of an element or of a structure with poor connection, which has the risk of partial failure. Tying is one of the best techniques for protecting the arches. It consists into the integration of the ties between springers. It reduces the lateral thrust to the piers.

The aim is the increment of the mechanical properties, ductility of the element, and the development of a micro-continuity in the structure. The consequence is the improvement of monolithic behaviour, and strength.

### **3.3.5 Repointing and reinforced repointing**

This technique consists in a partial removal and substitution of deteriorated joint mortar with new mortar with better mechanical properties and durability. Reinforced repointing is suitable for masonry walls with regular horizontal joints

and consists in laying reinforcement bars in the mortar matrix. It is usually applied in combination with other interventions. In Figure 18 step-by-step for performing this method is illustrated.



Figure 18: **repointing technique**, phases of intervention: placing of the rebars (a) and of the anchors (b); view of a joints after repointing (before the injection of the pins' holes) (c); final view (d). Source (Valluzzi, et al., 2005).

The main objective of this method is to increase the compressive and shear strength in small thickness masonry and are more effective for the reduction of deformation. Reinforced repointing has also a confining effect on the walls, and helps in transmitting loads from brick to steel.

### 3.3.6 Tie bars

This technique is based on tying. Steel bars were anchored with plates or other devices to the structure. They work in tension. They have different practical applications and are used to provide a monolithic action of different elements. This technique is usually applied on masonry structures with poor interconnection between intersecting walls, arches or vaults.

The aim of this technique is to improve the overall structural behaviour by ensuring seismic cooperation between structural elements (Branco & Guerreiro, 2011).

**Examples of practical cases:** bell-tower of S. Giustina (Padova, Italy) (Figure 19).

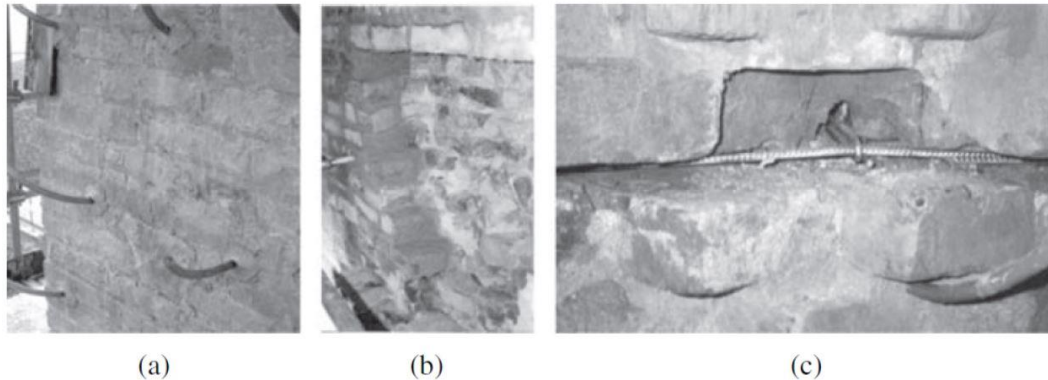


Figure 19: the interventions on S. Giustina (PD, Italy) bell-tower: injections (a), partial rebuilding ('cuci-scuci) (b), insertion of bar (c). Source (Modena & Valluzzi, 2008).

### 3.3.7 Structural and element substitution

In this method, a new structure is created to substitute the old one which is kept just to provide the required aesthetics. The element substitution, instead, consists in the overall substitution of the structural element under examination. The materials and technologies used can be similar to the original part or can be a new material with enhanced characteristics.

Structural substitution is usually applied for masonry structures and for elements which appears to be in good condition, but are not able to resist any loads. Element substitution is usually applied for elements which are damaged or are not capable to take loads.

The aim of this kind of interventions is to recover the functionality of a structure by maintaining its historical and cultural value, but modifying an erroneous design or its seismic response.

**Examples of practical cases:** "Mole Antonelliana" (Torino, Italy), and Tarazona Cathedral, Spain are relevant application examples of this technique (Roca, et al., 2008).

### **3.3.8 Dismantling and remounting**

Dismantling and remounting is a technique based in which an element is dismantled, repaired and then substituted back to the structure. This is adopted if the component cannot be replaced with another material.

As in the previous method, here the aim is to recover the functionality of the structure while maintaining its historical and cultural values.

### **3.3.9 Continuous and discrete confinement (jacketing)**

The jacketing technique is performed by preventing deformation. This technique can be applied to single elements (local form), for counteracting the lateral strain and thus improving its mechanical properties. This technique can be extended to the whole structure, (global confining), for limiting deformations at floor level to provide a monolithic seismic response, and avoid any out-of-plane failure mechanisms as an example (Triantafillou & Fardis, 1997).

This technique can improve the behaviour of elements which are subjected to large compressive force, excessive lateral deformations and for structures which are formed by weakly connected parts. Piers carrying large compressive force, multi-leaf masonry walls which are not connected between the different layers are typical examples of such cases.

The aim is to obtain a continuous confinement, thus improving the masonry strength and providing a monolithic behaviour for weakly connected elements. In the case of discrete confinement, a local confinement is provided where needed. This can help for example in enhancing the compressive strength of piers.

Jacketing with steel-reinforced shotcrete or cast-in-situ concrete is one of the most commonly used techniques since the nineties (Triantafillou, 1998) for aseismic strengthening of masonry buildings. This technique is effective in increasing the strength, stiffness, and ductility of unreinforced masonry buildings. But, it also have a number of disadvantages: the (usually) heavy concrete jackets add considerable mass to the structure thereby modifying the dynamic characteristics of the structure, (which can increase seismic forces). The thickness of these jackets may affect the aesthetics (as in the case of historic masonry building facades) and/or reduce the free space of the structure. It is also labour intensive, resulting in major obstruction of occupancy in the areas near the masonry walls to be strengthened.

### **3.3.10 Reinforced concrete and masonry edge-beams**

The strengthening actions that are important in reinforced concrete and masonry edge-beams are confinement and tying. This techniques is implemented by casting a ring of reinforced concrete beam in the thickness of the existing masonry wall at floor level. The connection between floor beams and existing walls are critical in this case. This tying effect can also be produced by providing a reinforced masonry edge-beam ring.

Thus, the aim of this method is to provide a stiffer monolithic seismic response of the whole structure by avoiding out-of-plane mechanisms thereby using its available strength more efficiently.

### **3.3.11 Enlargement**

This method is based on enlarging the resisting section by adding new materials. Usually the mechanical properties of the new material will be similar to that of the original section. The enhanced load carrying capability is thus due to the stress being carried/redistributed over a larger area.

Enlargement technique is usually applied for masonry elements which are in good conditions but are subjected to high stress fields.

### **3.3.12 Buttressing, suspension and strutting**

Buttressing, suspension and strutting are different methods of propping a part of the structure using additional elements. This technique can be applied to damaged or intact structures, which require higher strength or stiffness (Figures 20-21).

Buttressing technique use massive elements made of concrete or masonry to prop a structure on a side. Buttresses resists to lateral forces and deformations with their weight. Strutting technique instead, employ elements designed to resist to compressive loads, to support the structure. Struts can work in both vertical and inclined directions.

The aim of buttressing technique is to carry horizontal forces and thus prevents failure mechanisms related to lateral deformations. In suspension technique, the aims are stabilize and discharge the original structure. This is

accomplished by providing lateral struts to increase the lateral stiffness. Vertical struts are also used if there is excessive vertical loads.

Primarily these methods are applied for structures having low resistance to lateral forces or motion (arches or vaults). It can also be applied for structures requiring supports or are in the risk of collapse.



Figure 20: propping intervention of lateral wall of church of Onna (AQ). Source (Modena, et al., 2011).



Figure 21: shoring of facade with cables and wooden frames (Chiesa di S. Marco, L'Aquila). Source (Modena, et al., 2011).

### 3.3.13 Frictional contact, post-tension, and pre-compression

Frictional contact technique provides compressive stresses perpendicular to the contact surfaces of the confining elements. The main usual applications of frictional contact are on structures that present loose parts or elements.

Applying pre-compression changes the stress field in the structure and can be used for preventing the formation of tension cracks or for closing previously formed cracks. With respect to other methods, external post-tensioning with steel ties combines efficiency, simplicity and reversibility. This method can also use the frictional force generated across different members to provide a better connection. However, post-tensioning with steel ties presents several practical difficulties in protecting the strands against corrosion and other detrimental effects. Sometimes, they are difficult to handle at the site because of their considerable weight.

To overcome durability problems, designers have to select pre-stressing elements with large diameters, affecting the aesthetics of the building. As an alternative to the steel ties, FRP materials can be used. They offer excellent physical and mechanical properties and are characterized by their lightweight and resistance to corrosion. This type of elements can be applied to historical structures in a reversible manner, in the form of external tendons. It can be chosen in such a way as to resemble the external surface of the structure thereby maintaining the aesthetics of the structure (Triantafillou & Fardis, 1997).

**Examples of practical cases:** the Rotunda and the San Andreas domes in Thessaloniki, Greece. The Martinego rampart of the Old Castle in Corfu, Greece. Torre di Pisa. The domes of St. Ignatius of Loyola in Spain and the St. Charles Basilica in Rome. The external walls of the Santa Maria degli Angeli, Basilica in Assisi (Cavalagli & Gusella, 2015) (Triantafillou & Fardis, 1997).

### 3.3.14 Anchoring

Anchoring technique consists in fastening an element or a part of a structure, to a stronger solid part. The most widespread form is anchoring to rock and soil.

An important application of this method is to improve the stability of load bearing structures. It can also control excessive deformations which can lead to collapse during a seismic event.

### 3.3.15 Direct intervention on foundations

The foundations can be strengthened by widening/enlarging, connecting the different blocks, repairing and reinforcing the original foundation with the technologies discussed above.

The final aim is to improve the load distribution and to have better mechanical properties for the foundation material.

The usual applications are on damaged or poorly dimensioned foundations, or on foundations, which are poorly connected to the structure and where the load distribution is not proper.

### 3.3.16 Interventions on soil beneath foundation

Interventions on soil beneath foundation are focussed improving the bearing capacity.

It is possible to choose different techniques such as:

- **Micro-piling:** concrete piles grouted into steel hollow tubes can be drilled below the existing foundation to a soil layer with better characteristics.
- **Jet-grouting:** this technique is similar to micro piling. The concrete is directly grouted with high pressure in a borehole drilled in the soil, for improving the mechanical characteristics of the soil underneath.
- **Wooden-pile driving:** the piles are driven into the soil for compacting and consolidating the soil underneath.

This method is usually applied on foundations located on poorly consolidated soil to avoid any possible settlement of the structure. The aim is thus to transfer load to soil layers, which now possess better mechanical characteristics.

### 3.3.17 Seismic isolation

Isolation technique consists in absorbing the seismic forces and vibrations using external devices usually placed between the foundation, and the superstructure. There are different materials used for isolation and a few are as follows:

- elastomeric materials (steel plates in an elastomeric matrix)
- elastomeric materials reinforced with a lead core

- combination of elastomeric materials and frictional plates of steel bronze
- frictional plates of very low frictional coefficient coupled with neoprene rubber or steel springs
- assemblies of spiral springs coupled with viscous dampers
- frictional plates with very low frictional coefficient coupled with different types of dissipative tools (piezoelectric, electrostrictive and magnetostrictive materials, memory shape alloys, viscous, electrorheological and magnetorheological fluids).

The aim of this technique is to absorb the seismic vibration and prevent the superstructure from damaging. The usual applications of seismic isolation technique are on buildings of primary importance, which should be functional even after earthquakes such as hospitals (Branco & Guerreiro, 2011).

### **3.4 Repairing and strengthening systems**

When a repair technique is proposed, it is necessary to study it more deeply from both analytical and experimental perspective. It is not only important to know about the best method for application, its effectiveness is also a critical parameter. When the structure under investigation is an ancient masonry structure, then, no general strengthening method exists, due to the lack of similar raw materials and construction techniques. Before the retrofitting, necessary investigations and laboratory tests should always be carried out. In general, the following procedure is followed (Corradi, et al., 2015):

- accurate geometrical survey of the structure's morphology
- characterization of the constituent materials (brick and mortar in case of masonry structures)
- survey of the physical and mechanical decay
- crack pattern survey.

As discussed in Section 3.3, it is possible to choose different strengthening systems, which are characterized by a different matrix type, fibre properties, and application techniques.

A first classification could be carried out between:

- Externally Bonded Reinforcement (EBR)

- Near surface mounted reinforcement (NSM)
- Mechanically Fastened (MF)

### **3.4.1 Externally bonded reinforcement**

In this kind of reinforcement system, different types of composites such as unidirectional or bidirectional fibre sheets, textiles, laminates, etc. are used. Unidirectional FRP sheets are widely used for practical applications. It was the first commercially available externally bonded reinforcement material in for structural applications (Capozucca & Ricci, 2016).

The first step to be performed prior to the application of this strengthening technique is the surface preparations. This phase is extremely important as the adhesion of the fabric with the structure is dependent on this step. The masonry surface should be properly cleaned, any imperfections should be eliminated and chemical contamination if any should be removed. Now, the surface can be filled with a high-strength putty (usually epoxy resin based), in order to make it as plane as possible. It is essential that, when FRP is applied on masonry surface, it must be completely dry and clean. Once the composite is fixed, non-destructive tests can be performed to evaluate the quality of work and to check the effectiveness of the applied. The choice of the matrix (mortar) for the reinforcement is very difficult because it is necessary to ensure an adequate durability. The matrix should be compatible with the existing masonry in terms of its chemical, physical, and mechanical properties.

In case of the application of EBR technique to existing masonry structures, it is better to use an inorganic matrix as an alternative to organic matrices due to the following reasons (Corradi, et al., 2015):

- it allows a higher degree of perspiration through the reinforcement material;
- it can be applied on wet masonry substrate;
- it neither require specialised skills nor any special equipment.
- it does not produce toxic gases;
- it protects the reinforcement (fibres) due to its high fire resistance and thus guarantees good performance in case of fire;
- it is easy to handle and can be applied to curved surfaces. This characteristic makes it especially useful in arched structures (vaults,

domes etc.). It can also be applied on masonry structures with irregular surfaces.

### 3.4.2 Near surface mounted reinforcement

This technique consists in placing FRP rebars or laminates into grooves, which are previously cut in the tension region of the element that need to be reinforced. This method is relatively simple and greatly improve the bond of the mounted FRP reinforcements, thus utilising the material more effectively. This method could be a valid alternative to EBR with FRP sheets or laminates (Corradi, et al., 2015) (Konthesingha, et al., 2013).

The application of NSM-FRP elements on existing masonry structures can enhance the shear and flexural strength of deficient structural elements. NSM method does not require any surface preparation work. It also can be installed in a shorter time compared to traditional FRP sheets placement. This advantage has made this method quite attractive to designers (Konthesingha, et al., 2013).

### 3.4.3 Mechanically fastened FRP-system

The mechanically fastened FRP-system (MF-FRP system) consists of pre-cured FRP laminates with enhanced longitudinal bearing strength. They are attached to substrates by means of mechanical steel anchors.

A crucial point to emphasise is that, only information on the behaviour of MF-FRP systems on concrete elements are currently available. Connections is nowadays limited to results obtained from applications of the MF-FRP system on concrete elements (Ascione, et al., 2009) (Figures 22-23).

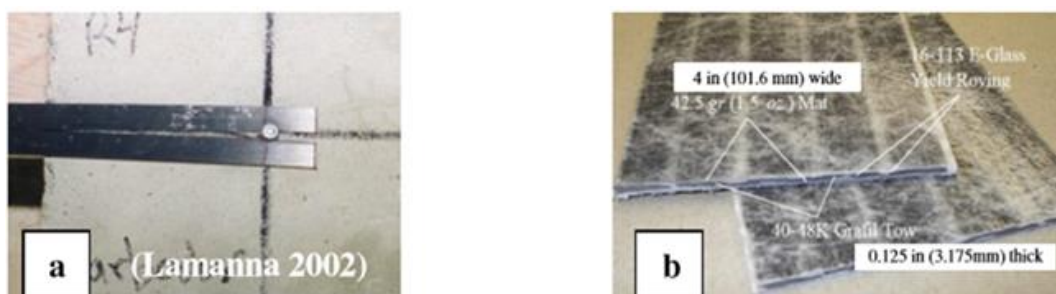


Figure 22: a) splitting failure for EB-FRP laminates; b) laminates used for MF-FRP systems. Source (Ascione, et al., 2009).

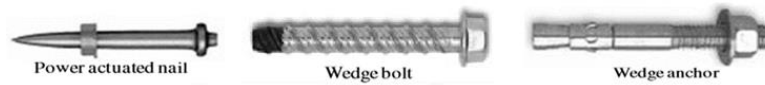


Figure 23: fasteners used for MF-FRP systems. Source (Ascione, et al., 2009).

Another classification of FRP systems suitable for external strengthening of structures can be as follows:

- **Pre-cured systems** are directly bonded to the structural member to be strengthened. They are manufactured in various shapes through pultrusion or lamination processes.
- **Wet lay-up systems** are impregnated to the support with resin in situ. Fibres can be placed in one or more directions, as FRP sheets or fabrics (Sciolti, et al., 2010) (Figure 24).
- **Prepreg systems** are pre-impregnated at the manufacturing plant with partially polymerized resin. They may be bonded to the member to be strengthened with (or without) the use of additional resins. They can also be produced with unidirectional or multidirectional fibre sheets or fabrics.

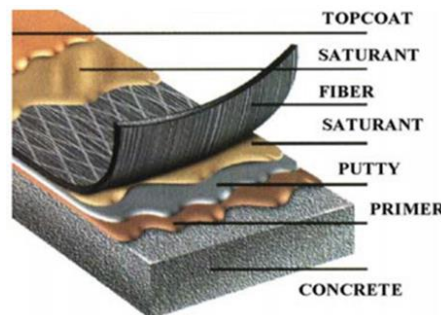


Figure 24: wet lay up system. Source (CNR-DT 200/2004, 2004).

### 3.5 Interventions on masonry buildings using FRP

The use of composite materials, especially carbon fibres in construction industry have been developed in Italy since the middle of 90's. In a time span of just a decade, their application has incredibly spread, in particular their use for retrofitting of historical buildings (Credali, 2009). Moreover, traditional confinement techniques can be too invasive, in particular when it is necessary to

safeguard the historical value of architectural heritage. In such cases, properties like reversibility, compatibility and sustainability can be crucial points in choosing appropriate strengthening technique (D'Ambra, et al., 2009).

Among the past applications of these interventions, the renovation of the Corte Benedettina in Legnaro (Italy) using this technology is significant as this was the first such application on a large scale in an historical building. There was a widespread use of these techniques in the construction sector in the past years. An important contribution which helped the use of composite materials came from universities and specialised labs' research groups. These studies allowed for the examination of different issues related to the application of these techniques and provided their solution in a simple and effective way (Tumialan, et al., 2003).

The document of **CNR DT200/2004** (CNR-DT 200/2004, 2004), is the result of an exceptional collaboration between universities and specialised companies and represents a summary of work completed till then. It gives the guidelines for the application of composite materials in the construction sector, and promotes the use such technologies.

### **3.5.1 Improvement of Connections to Activate Box Behaviour**

One of the most important aspects to take into consideration for strengthening existing masonry buildings is the lack of good connections between structural elements. It is necessary to improve the connections between horizontal and vertical elements, to enable the structure to activate a good global behaviour (Modena, et al., 2011) (Tomaževič & Weiss, 1994) (Tomaževic & Lutman, 1996).

This could be achieved by using traditional techniques like inserting ties, providing confining rings, and adding tie beams at the top. The tie beams should be preferably made of reinforced masonry or steel. It is better to avoid reinforced concrete beams in cases where the walls are not sufficient to bear the additional loads in uniform way, such as in case of multi-leaf masonry type. The connection between horizontal and vertical members are important to provide an efficient distribution of lateral loads. In any case, an effective connection is fundamental to counteract the walls' overturning. In case of wooden floors, fasteners anchored on to the exterior side of walls ensures proper connection. On the contrary, is better to avoid the insertion of tie beams in the masonry thickness at intermediate floor, due to their damaging effects on perimeter walls. In addition, they cause a non-

uniform distribution load among masonry leaves. They could cause hammering effects on the external walls.

In addition, injections may be avoided in most cases. During execution, this technique can severely damage the masonry elements, which are in already damaged or weakened.

A valid alternative for providing the box action is by using composite materials. In this section some case studies in Italy which used this technique is given (ElGawady, et al., 2005).

**Palazzo Bufalini (Città di castello (PG), Italy).** Few years ago, a structural strengthening intervention on a building of particular historical interest (XV century), was realised. The project concerns the consolidation of wall panels and decks. The consolidation was performed using composite materials such as sheets of glass and carbon fibres pre-impregnated. The strengthening intervention for creating the enchainment of the horizontal elements was performed (in both directions), by gluing ribbons of high-strength carbon fibres on the facing wall, which was already cleaned and levelled. In this case, carbon fibres of 0.165mm thickness in a double layer of 250mm width were used. This effect can also be reproduced by using equivalent area in steel (Fe360), corresponding a rod of 30mm diameter (Celestini, 2009).

**Villa Monticelli (Ponte Rio di Perugia (PG), Italy).** This is an architectural complex of great historical and cultural interest located in the outskirts of Perugia. This structure was retrofitted in 2000, and concerns the improvement of the masonry's perimeter connection who does not have an adequate connection system of the wall's panels. The main building dates back to the XIV century, and was considerably damaged by the 1997 earthquake. The structure was retrofitted with strips of carbon fibres by using prepreg system. Strips of 20cm width were employed for the confinement of interior wall facing (Celestini, 2009).

In a work of Borri e Castori (Borri & Castori, 2009) were shown the results of experimental tests for monitoring the application of FRP on masonry structures, especially at two properties of the composite: the adhesion resistance bond to tensile forces perpendicular or tangential to the reinforcement fibres. Moreover, the increasing use of steel fibre composites embedded in a cementitious matrix (SRG) for structural strengthening, has led to a considerable interest on the durability of this new type of composite materials in harsh environments. In this

work are also presented the results relating to an experimental campaign on a series of fibre samples of steel subject to artificial or natural aging processes.

A masonry building damaged by the Italian earthquake of September 1997 (located in Forcatura, near Perugia (PG), Italy) was retrofitted by wrapping with CFRP sheets in two levels in the horizontal direction (Figure 25).

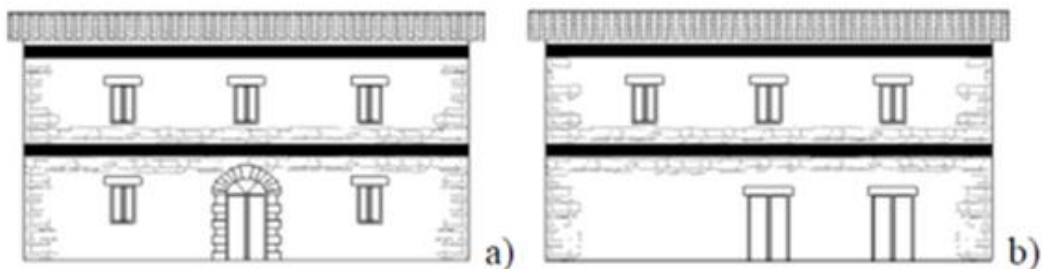


Figure 25: a), b) the north and west elevation of the masonry building, and position of CFRP wrapping interventions. Source (Borri & Castori, 2009).

The horizontal sheets, placed at floors levels, have a width of 300mm and are placed over a layer of cement mortar of about 10mm thickness.

In this work (Borri, et al., 2009) the design and implementation of the SRG reinforcement system was carried based on static and dynamic analysis of the building. The final design consisted of two levels of horizontal SRG wrapping and three levels of vertical wrapping to take flexure (Figure 26).

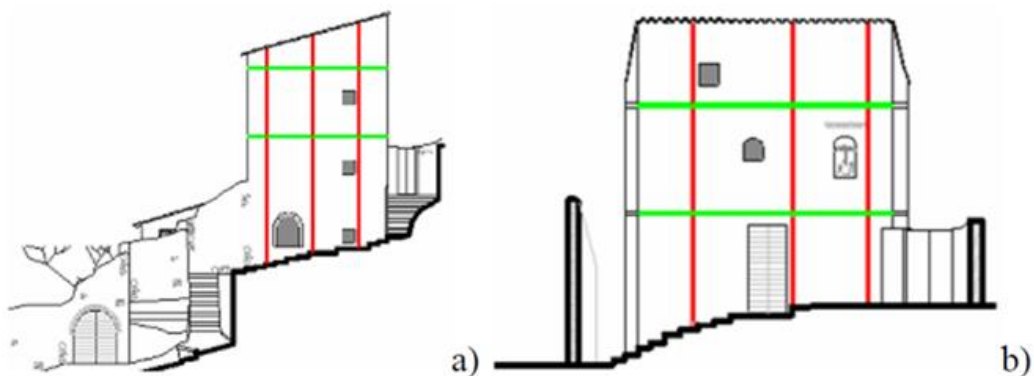


Figure 26: a), b) east and north elevation of the masonry building with horizontal and vertical SRG reinforcement. Source (Borri & Castori, 2009).

### **3.5.2 Increase of Strength and Compactness of Walls**

Several techniques to increase the strength and the compactness of walls are available, such as “cuci-scuci”, injection or insertion of possible ties “diatoni”, or concrete jackets (see section 3.3).

One of the first works on the use of non-metallic reinforcements for strengthening masonry walls was carried out by Croci et al. in 1987. In this work, shear wall specimens were tested with reinforcements in vertical and inclined directions. Low modulus polypropylene braids were used for this test (this material does not fall in the class of high-strength FRP composites). This was the start for many further works. Triantafillou (Triantafillou, 1998) reports some significant works carried between 1987 to 1997 on improving the strength using non-metallic materials.

In recent years, various techniques based on the use of high performance materials for improving the seismic resistance of masonry building were studied. Borri et.al (Borri, et al., 2009), performed experiments on masonry walls reinforced by high-resistance metal strands placed directly on a cement matrix (SRG). This method can be used for strengthening masonry joints.

The wall panels were subjected to diagonal compression tests (Figure 27), in order to evaluate some properties like strength, shear stiffness, and ductility. In addition, the failure modes of unreinforced and reinforced panels where the reinforcements were provided in different configurations were also studied. The study has shown significant improvement in strength and shear stiffness (Kalali & Kabir, 2012).



Figure 27: diagonal compression tests. Source (Borri, et al., 2009).

Among the different uses of CFRP materials, it is of considerable interest the wrapping of wall panels subjected to compression load. Calderoni et al. (Calderoni, et al., 2009) have conducted experiments on 21 pillars of tuff masonry with pozzolanic mortar. This is the historical and contemporary masonry style in Naples between the middle of the XV century and XX century. The influence of radius of curvature of rounding of the edges, the type of fabric, and the number of the reinforcing layers were studied (Aiello, et al., 2007). The aim of this kind of works is to provide a further contribution to the experimental data currently available, and investigate, in particular, the effectiveness of the reinforcement.

The experimental results show that the wrapping made with FRP significantly changes the mechanical behaviour of the masonry, resulting in both an increase in resistance and a change in the failure mechanism from brittle to ductile (an extremely ductile behaviour). The change in resistance is highly dependent on the extension of the wrapped section of the pillar. The effectiveness of the reinforcement was smaller with increase in the cross sectional dimensions of the structure. Furthermore, it was found that the increase in resistance is also strongly influenced by the texture of the masonry. There is an increment of benefit when the masonry is poor.

In the case of **Chiesa di S. Maria, o Collegiata Pazzaglia (Montone (PG), Italy)**, the aim of the intervention was to confine the apse and to contain the

pressures arising from the static situation. The structure was retrofitted by applying a CFRP double wrap at two levels. It was applied on the outside of the wall, along the whole perimeter of the apse. (Celestini, 2009).

Regarding the **Ex convento SS. Trinità (Macchia dei Frati, Orvieto (TN), Italy)**, the structural reinforcement intervention was applied for both the floors and the dividing walls. The outside walls, with poor connection system, have been joined solid by using a single layer of 30cm steel fibre strips (SRP). The strengthening intervention was carried out below the roof level. (Celestini, 2009).

**Corte Benedettina di Legnaro ((PD), Italy)**, is one of the first examples of structural strengthening and restoration of historic buildings in Italy. The strengthening system was realised by means of a kerb. This is a widespread strengthening solution. The project involved the creation of two kerbs (made by CFRP), placed on the roof. (Figure 28a). The kerbs were obtained laminating the two side of the wall (internal and external facade), and connecting the two reinforcement laminates, placed at  $\pm 45^\circ$  (Figure 28b) (Credali, 2009).

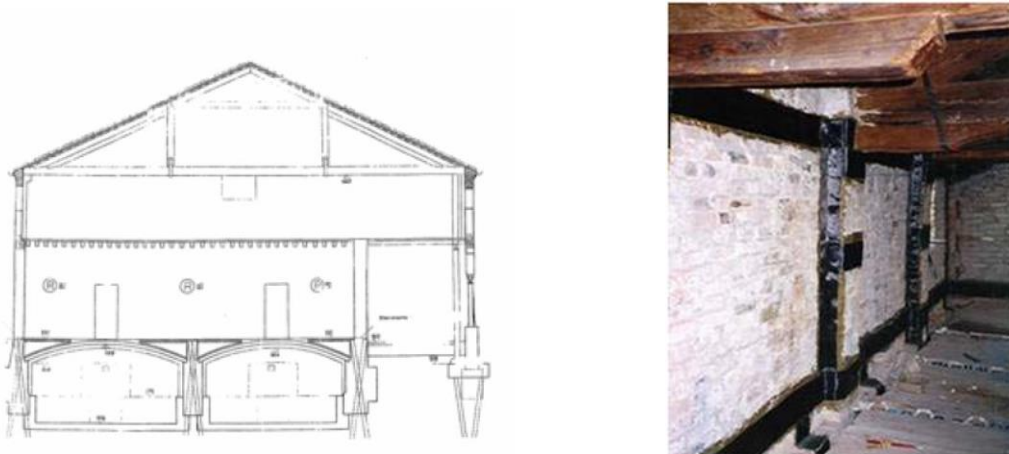


Figure 28: a) kerbs realised with carbon fibres placed up to the roof and the ceiling, and b) horizontal and vertical kerbs placed on internal and external walls. Source (Credali, 2009).

Another example of the application of FRP on masonry structure is on **Villa Bertani (Reggio Emilia (RE), Italy)**. The structure had suffered significant damage from the earthquake in 1996. Internal and external CFRP curb (Figure 29), (placed on the floor of the roof level) have been replaced with concrete's curb

in the frame of an earlier project. During the strengthening works, after the installation of the first hoops, the building underwent a series of seismic shocks caused by the earthquake in 2000. However, there was no further damage reported despite the unhealthy condition of masonry at that time (Credali, 2009).

In the case of **Grand Hotel di Alassio (Savona (SV), Italy)**, significant retrofitting works were adopted. The masonry external façade showed significant. In this case, hoops and bracing with carbon fibre strips were applied externally and internally (Figure 30). The brick's drilling operation for the connectors application was performed, in well-defined points, before the mortar injection. In this way, a lattice structure on the two sides of the façade was obtained (Credali, 2009).

In **Chiesa di S. Maria in Sovana (Sovana, Grosseto (GR), Italy)**, the external hoops of the building (realised with tuff blocks) has forced the tuff milling, for a thickness of about 10cm, in the areas in which the carbon reinforcements had to be applied. The recovery of the part of the milled tuff has been realised with elements of the same material, so that the reinforcement, embedded in the wall, did not cause aesthetic problems (Credali, 2009).



Figure 29: horizontal and vertical CFRP kerbs on internal and external walls. Source (Credali, 2009).



Figure 30: restoration intervention realised on the masonry external façade. Source (Credali, 2009).

Another significant retrofitting work was carried in a **Library in the Basilica of S. Antonio da Padova (Italy)** (Figure 31). Here hybrid reinforced carbon-aramid fibre systems were employed, because of better energy dissipation capabilities. In addition, the reinforcing sheets were applied on both sides of the masonry, and were connected by means of ARDFIX connectors, forming a reticular structure (Credali, 2009).

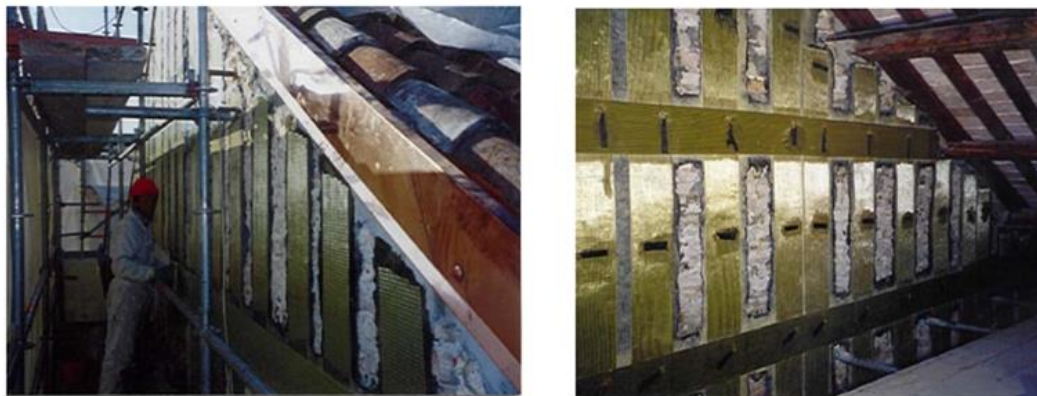


Figure 31: strengthening intervention with hybrid reinforced carbon-aramid fibres systems. Source (Credali, 2009).

In the past decade, there have been many studies involving the use of advanced composite material for reinforcing masonry walls. Performance tests on concrete masonry reinforced with a fiberglass/polyester-styrene composite and on solid clay masonry reinforced with a fiberglass/epoxy material shown how these

FRP systems may be effective in strengthening masonry walls both in case of in-plane and in out-of-plane bending (Christensen, et al., 1996).

In another study (Papanicolaou, et al., 2011) , externally bonded grids were used for increasing the load-carrying and deformation capability of unreinforced masonry (URM) walls subjected to cyclic loads which induced in-plane flexure combined with axial force, out-of-plane flexure, and in-plane shear with axial force. The experimental study was performed on two groups of medium-scale, single-wythe walls consisting of perforated fired clay bricks, or solid stone blocks. The parameters considered were the number of reinforcement layers (one or two layers, placed on internal/external sides), the type of mesh (open mesh structures comprising carbon, glass or basalt fibres and polypropylene or polyester), the matrix (mortars with different chemical compositions or epoxy resin) and, the compressive stress applied to specimens subjected to in-plane loading. This study have shown that the use of externally bonded grids is a promising alternative to traditional techniques for upgrading existing masonry structures.

### **3.5.3 Strengthening of arches and vaults**

Arches and vaults in historic buildings represent one of the most important parts that are damaged during earthquakes. Strengthening methods can be applied using the traditional techniques of tie-rods that compensate the thrust applied on bearing walls. Adding buttresses or reinforced transverse vertical diaphragms are also effective. Jacketing the extrados using concrete (with or without reinforcement), must be avoided (Modena, et al., 2011).

Composite materials, such as FRP (Valluzzi, et al., 2001) or SRP/SRG, is well suited for the recovery of structures. FRPs have high potential for such specific applications, in comparison with heavier materials such as steel and concrete, for the reinforcement of transverse diaphragms (Credali, 2009).

In bibliography experimental and numerical studies conducted on the behaviour of vaults and arches strengthened at the extrados or intrados with FRP strips or laminated, are available. Masonry vaults strengthened by different FRPs (mainly glass or carbon) have been tested. All the results have shown enhancement in strength and ductility of the strengthened vaults, the influence in the ultimate strength of the width of the strips, and of the bond between the laminate and the masonry (Valluzzi, et al., 2001).

Numerical investigations (FEM analysis) are also referred to the interfacial behaviour of masonry-FRP (Briccoli Bati & Rovero, 2008) (Borri, et al., 2009) (Basilio, et al., 2004), because the delamination is the reason of a brittle and premature failure at the interface. The delamination can affect the effectiveness of the strengthening strategies adopted. In order to properly consider the local behaviour in the numerical modelling of the vaults, the bond performance analysis has been also extended to curved substrate (Shrive, 2006) (Aiello & Conte, 2009) (Aiello & Sciolti, 2009).

Some researches have conducted numerical investigations on semi-circular vaults to study the influence of CFRP reinforcement to extrados (Aiello & Conte, 2009) (Borri, et al., 2009).

The results show that the effectiveness of FRP reinforcement increase in the diameter of vault. The effectiveness was found seems to increase only when the thickness is limited. This work highlights the worthlessness (for this point of view) of the FRP reinforcement for vaults with an important thickness.

Basilio et al. (Basilio, et al., 2004) worked on semi-circular unstrengthen and reinforced masonry arches. They were numerically modelled to evaluate the effectiveness of different CFRP strengthening proposed. The results obtained in the two cases (with or without reinforcement) are compared. At the end, the paper presents results and conclusions regarding the optimal strengthening of masonry arches.

Mahini et al. performed nonlinear finite element analysis on a historical building located in Yazd, Iran to study its response and failure mechanisms when subjected to lateral loads. The influence of CFRP sheets on the seismic performance of vault was also investigated (also include the results from the analysis) (Mahini, et al., 2007).

Briccoli et al. (Briccoli Bati & Rovero, 2009), conducted experiments on models of masonry arches reinforced by CFRP strips. Here, CFRP strips of different width was bonded to the intrados. The aim of the study was to evaluate the impact of different reinforcement configurations on the strength of masonry arches. It was found that the kinematic ductility decreases with increase in the width of strip in the strip width, highlighting the stiffening action produced by increasing of the reinforcement (Caratelli, et al., 2009) (Briccoli Bati & Rovero, 2008) (Foraboschi, 2004).

Borri et al. in 2009 (Borri, et al., 2009) performed experiments on a new form of composite material wherein fine steel cords are embedded in either an epoxy (SRP) or cementitious matrix (SRG) for strengthening masonry arches. Their use reduces the installation and material costs, and induces the increasing of ductility, in particular way when a cementitious matrix was employed. In this way, the use of these “new” materials should become extremely interesting in the restoration of masonry arches in historical building. The influence of the fibres used (steel and carbon), the matrix (epoxy and cementitious), their placement (intrados and extrados) and the boundary conditions are investigated in the laboratory by using scaled models.

Some typical works where FRP was used for strengthening of domes, vaults and arches are given below:

**Cattedrale di Città di Castello ((PG), Italy).** The strengthening work consists of a consolidation of masonry domes of the apse and transept. The CFRP size, based on to deformation state, was identified at the modelling stage. This issue leads to design of a double frame oriented according to meridians and parallels. The strengthening project of the dome, at the intersection between nave and transept, consists of a replacement of the metallic hoop, without the need of removing the pre-existing one (Celestini, 2009).

After a consolidation phase was visible an increase of the transmission rate of the waves on the masonry surface. This confirm an increment of the overall homogeneity of the masonry. The Laboratory SGM srl Perugia has conducted the testing and monitoring of the CFRP used.

**Villa Monticelli (Ponte Rio di Perugia (PG), Italy).** Here the vaults were strengthened with strips of pre-impregnated carbon fibres. (Celestini, 2009).

**Palazzo Magherini Graziani (San Giustino, Perugia (PG), Italy)** is one of the most important noble palace among those in the urban fabric of Città di Castello. It was subjected to extensive retrofitting works. The strengthening intervention in CFRP regard the vaults placed at the noble floor. These vaults which were made of bricks were strengthened using carbon sheets on the extrados. The intrados were not changed as some of them were painted while others were covered with stucco of great value (Celestini, 2009).

**Ex convento SS. Trinità (Macchia dei Frati, Orvieto, Italy).** The vaults have been reinforced by CFRP strips. The external walls had poor connection.

The improvement of monolithic behaviour has been made using steel fibre strips (SRP) (Celestini, 2009).

**Palazzo Reale (Milano, Italy).** The masonry vaults of this structure was strengthened using GFRP sheets on the extrados and by placing aramid bars on the lateral masonry walls for anchoring the extremities of the GFRP sheets (Celestini, 2009).

**Basilica di S. Francesco (Assisi, Italy).** The Italian earthquake of 1997 called for an urgent strengthening of the tympanum and of the vaults to prevent their collapse, for preventing the global collapse (Figure 32). The inner surface of the vaults were covered with frescoes, thus making any strengthening method on this surface impossible. Consequently, it was impossible to recover the deformations and to re-establish an adequate curvature and autonomous bearing capacity. Many studies, researches and mathematical models were performed to choose an efficient solution. Finally, it was decided to provide small ribs on the extrados. Figure 33 shows the strengthened structure (Crocì, 2000).



Figure 32: cracks and deformation in the vaults with relative displacement till 30cm.  
Source (Crocì, 2000).



Figure 33: the new ribs, made of a central timber nucleus and external aramid fibres. In the background, the steel belt to anchor the base of the arches which sustain the roof is visible. Source (Croci, 2000).

These ribs are made up of AFRP embedded in epoxy resins and a central timber nucleus. Aramid material is very light, very strong (the tensile strength of the fibre with resins is about  $14\,000\text{kg}\cdot\text{cm}^2$ ) and less stiff than steel (the elasticity modulus is  $1\,200\,000$  for aramid fibres and  $600\,000\text{kg}\cdot\text{cm}^2$  for steel). As clear from several tests they provide good ductility. The ribs were constructed in situ. With this method it was easy to follow the deformed shape of the vault. The width of the ribs was constant (8cm), while the height have an average value of 20cm, but is varied according to the deformation. This because the extrados of the ribs follows the original ideal surface of the not deformed vaults.

Another interesting application of this type of hybrid composite materials can be appreciated in the monumental complex of **Scuderie della Venaria Reale (Torino, Italy)** (Credali, 2002). A wide vaulted surface, with a span of 12m, was retrofitted to be used as a museum. The loads on the masonry structure had caused a stress states of traction no longer tolerable. For this reason, it was decided to combine traditional intervention methods with modern technique, such as composite materials.

The strengthening intervention, after upgrading of tie rods placed on the extrados, consists in the application of hybrid unidirectional carbon-aramid fibre sheets. They are placed in geometrically and statically adequate positions, for graduating the reinforcement in the most loaded areas.

One single layer in the two areas characterized by lower radius of curvature, and two layers in the central area (higher radius of curvature) are used. The reinforcement scheme is shown in Figure 34.

The reinforcement (placed at the intrados), consists of two sheets of composite material (width of 20cm). The overlapping in the central area was realised. The sheets were placed, after preparation of the masonry surface, using the two-component epoxy resins for laminating.

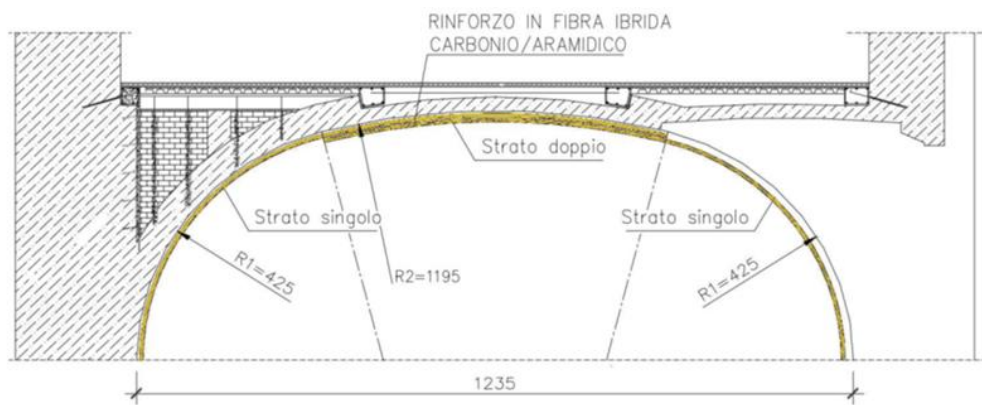


Figure 34: Complesso di Venaria Reale (TO) – Strengthening intervention with strips placed to the intrados and extrados of the vaults. Source (Credali, 2002).

### 3.5.4 Strengthening and stiffening of floors

During earthquakes, floors play an important role by redistributing the loads from the out of plane walls to the in plane walls. Previous studies have shown that floors should never be substituted as this might cause further damage and can lead to collapse. Before retrofitting existing floors the effect of increase in mass and

stiffness due to the strengthening strategies should be studied. Also, connections between floors and the surrounding walls have to be ensured for redistribution of loads (Parisi & Piazza, 2002) (Modena, et al., 2011).

A simple way to strengthen old wooden floors is by adding another layer of wooden planks. But, this method will not help in redistributing the lateral loads. Double planking is another popular method wherein planks are arranged in orthogonal or at an angle and is connected using tongue and groove joints or using nails or screws.

Metallic belts, FRP strips and metallic tie beam bracing can also be used to stiffen the floor and the wall-floor connection (Corradi, et al., 2006). FRP strips can be arranged in a crossed pattern underneath the wooden floors. A layer of reinforced concrete can also be used, but must be studied carefully as this procedure causes an increase in dead load.

### **3.5.5 Confinement of masonry columns**

Wrapping the columns by FRP sheets or laminates is one of the modern technique for strengthening columns. They were introduced in the last decade as an effective alternative for wood and steel ties (Corradi, et al., 2007) (Sivaraja, et al., 2013).

Since ancient times, different kind of methods were used to reinforce compressed elements (Alecci, et al., 2009). Different materials were used for this. Traditionally, masonry columns were confined by using reinforced concrete (or steel) jacketing (D'Ambra, et al., 2009), or iron bands are used, still hot or with special devices for example, for producing a self-stress state into the compressed elements. These system were effective in preventing the brittle failure due to compressive loads, seismic forces and creep effects. These materials were then replaced by FRP.

There are many benefits of using FRP to confine concrete or masonry elements. Using FRP will not result in an increase in the area of the members thus maintaing the functionality of the structure. FRP is also light, so it does not add any extra dead load. FRP can also be applied very easily thus saving significant time. Numerous researches were performed on this topic for studying the benefits of FRP interventions on both in plane and out-of-plane behaviour of masonry walls (ElGawady, et al., 2005) (Marcari, et al., 2007).

In both **Villa Reale in Monza (Milano, Italy)** (ResinProget, 2012) and **Real Albergo dei Poveri a Napoli (Italy)** (Olympus, 2016) masonry walls were confined (Figure 35). In the first case columns were strengthened with structural plaster and a series of hoops of aramid fabric. While in the second case, aramid fabric was applied by using connectors to improve the confinement efficiency.



Figure 35: strengthening intervention with FRP in Villa Reale in Monza (sx), and Real Albergo dei Poveri a Napoli (dx). Source (Olympus, 2016) and (ResinProget, 2012).

A review of state of the art literatures shows that only few studies were carried regarding the application of FRP to increase the axial strength and deformation capacity of masonry columns (D'Ambra, et al., 2009) (Aiello, et al., 2007) (Corradi, et al., 2007). These studies have shown that as the traditional methods add a significant amount of dead load to the structure which lead to an increase in earthquake loads, they are not suitable for seismic strengthening. The increase in dead load can also result in an unsafe foundation and consequently lead to strengthening foundations also.

As FRP has poor resistance to cutting, FRP confinement in columns with sharp corners (polygonal sections) have shown premature breakage of fibres (Borri & Corradi, 2009). However, this problem can be solved by using curved steel sections at these edges. Another viable alternative is to use new material such as SRG (Steel Reinforced grouts) and SRP (Steel Reinforced Polymers). It was also found that using cement mortars to connect metal fabric to masonry columns resulted in some issues related to the flexural stiffness of metallic fibres which does not allow (for columns with reduced cross-sections) to mobilise the tensile strength of metal fibres when the columns are compressed.

On the other hand, if epoxy resin is employed to connect the fibres to the surfaces of the columns a small increment of the reinforcement thicknesses (less than 1 cm) was observed but, was found to be more effective in bonding the fibres to masonry. Also, no premature detachment of metallic fibres at the edges of the masonry columns were observed in this case.

Several experimental researches on concrete, brick masonry, and tuff masonry test specimens are based on the evaluation of the effective cooperation of an FRP wrap, and on the estimation of the ultimate strength of the structure. Masonry pillars in particular, are structural elements largely diffused in historical buildings. They constitute a significant portion of the world's architectural heritage (Calderoni, et al., 2009).

Another work shows the results of an experiments with 18 scaled columns of square cross-sections (tuff and clay brick masonry) subjected to uniaxial compressive load (D'Ambra, et al., 2009). Three different confinement schemes (uniaxial glass FRP laminates (GFRP), uniaxial carbon FRP (CFRP) laminates and uniaxial basalt FRP (BFRP) laminates) were experimentally analysed for evaluating and comparing the effectiveness of the proposed strengthening techniques.

In some countries like Canada, FRP's are used for both new constructions and rehabilitation (Shrive, et al., 2001). In research projects on masonry, the wrapping of damaged columns with CFRP sheets to restore/increase strength, is one of the major topics investigated. The experimental program conducted by Shrive and co-workers, consists in axially load each column until cracking in the masonry was observed. At this point, the columns were then wrapped with CFRP sheets (over their full height), and re-tested until failure occurred. The aim of the work was to damage the columns until a stage that should be considered in need to be repaired but not replaced. To reach this goal, the columns were instrumented with displacement transducers (one at each corner) placed approximately at one third of the column height, and centred about at mid height. All projects show considerable promise for their respective applications. FRP's therefore ensure an additional option for structural engineers when considering these types of applications.

In the study by Krevaikas et al. (Krevaikas & Triantafillou, 2005), 42 specimens of masonry columns were subjected to uniaxial compressive tests. The effects of the curvature radius at the corners, aspect ratio of cross-section, the

number of layers and the type of fibres (CFRP and GFRP) were studied. It was seen that, the FRP-confined masonry behaves in similar way to FRP-confined concrete. The confinement increases the load-bearing capacity and the deformability of the masonry almost linearly with the average confining stress. (Also include the effects of increasing the number of layers, curvature aspect ratio).

Alecci et al. (Alecci, et al., 2009), studied the theoretical formulations available from the past literature and in CNR-DT 200/2004 (CNR-DT 200/2004, 2004). The reliability of these formulations were also investigated. Show the results and inferences from these studies.

### **3.6 Numerical investigations on the possible use of aramid fibres for a permanent strengthening intervention on the Fossano belfry**

Nowadays, the use of aramid fibres in structural engineering field is rather limited due to uncertainties about their long-term behaviour, and durability. In this section, a possible implementation for strengthening masonry structures are discussed. The intervention proposed here refers to a particular monument called the Fossano belfry tower, a system that has suffered over the years from significant structural problems. In recent years, the structure was equipped with metal rods. This retrofitting method is temporary and invasive, from an aesthetic point of view intervention. The aim of this solution was to prevent the cracks from enlarging and to improve the overall structural behaviour in view of future seismic actions and vibrations induced by vehicular traffic. In this section, an alternative solution based on the employment of high performance materials (AFRP) will also be investigated. The proposed solution will be an alternative method which will be less invasive with respect to the widely used techniques for protecting buildings of historic significance.

Part of the work described in this Chapter has also been presented at 16<sup>th</sup> International Brick and Block Masonry Conference (Pinotti, et al., 2016).

#### **3.6.1 The Fossano belfry description**

The Fossano Cathedral in Cuneo (province, Italy) is dedicated to San Giovenale, patron of the city. Quarini designed the church in 1771. The belfry is earlier, contemporary with the previous building. The Cathedral that replaces the

previous XIII century building has a stately brick facade and follows the typical Piedmonte's and neoclassical style.

The bell tower (Figure 36), under investigation, has a square base and a height of 35 m. It is made of masonry walls with an average thickness of 1.5m. The octagonal bell tower has masonry tower of a thickness of 0.5m and is 46m tall. Originally the stairs were placed within the thickness of its perimeter walls.

The earthquake of 1887 caused a series of cracks. After this event, a particularly effective consolidation intervention was carried out, as core drilling, has shown. The internal passages in the walls were partially closed, and the stairs were completely replaced with a series of wooden ramps located inside the tower (Figure 36).



Figure 36: the Fossano belfry; wood ramps located inside the tower.

Moreover, reinforcing metal rods of diameter of 6 cm were provided at three levels of 14, 21 and 32 meters of height. The bell tower presents a cracking map that highlights widespread lesions, which trace a vertical trend. On the outside, the reinforcing metal rods are covered by plaster.

From a preliminary surface inspection, the masonry walls of the belfry seems to be in a good condition. But, the core drillings have shown a non-homogenous masonry, located within the outer layers of the perimeter walls.

After the experimental campaign, the results confirmed serious concerns about the stability of the monument. The last safety operation works were performed subsequent to further opening of vertical cracks which were visible inside the monument in 2012. The retrofitting operation included steel tie-rods placed both inside and outside the bell tower in eleven levels from the ground. (Figure 37). Moreover, a vertical steel structure was also added, which puts in tension the internal cerclage by means of diagonal elements.



Figure 37: the belfry of the Fossano Cathedral with the strengthening intervention.

A complete and detailed survey to estimate the cracks carried out in recent years, together with core drilling, and a structural identification of the structures was performed. This allowed for calibrating a FE model.

### 3.6.2 Finite Element (FE) model calibration

A FE model of the bell tower was created using the material properties collected from experimental tests, in addition to the original documentation (Figure 38). The belfry was the subject of previous studies (Ceravolo, et al.,

2014), and has resulted in calibrated/updated finite element model. The bell tower behaviour was investigated through dynamic tests. The calibration of FE models, through experimental data, is a well-known procedure in the field of numerical simulation (i.e. (Boscatto, et al., 2015) (Zanotti Fragonara, et al., 2017)).

In particular, the approach followed can be described in through these phases:

- generation of a reference geometrical and a mechanical model
- designing the test
- on-site testing
- signal pre-processing
- structural identification.

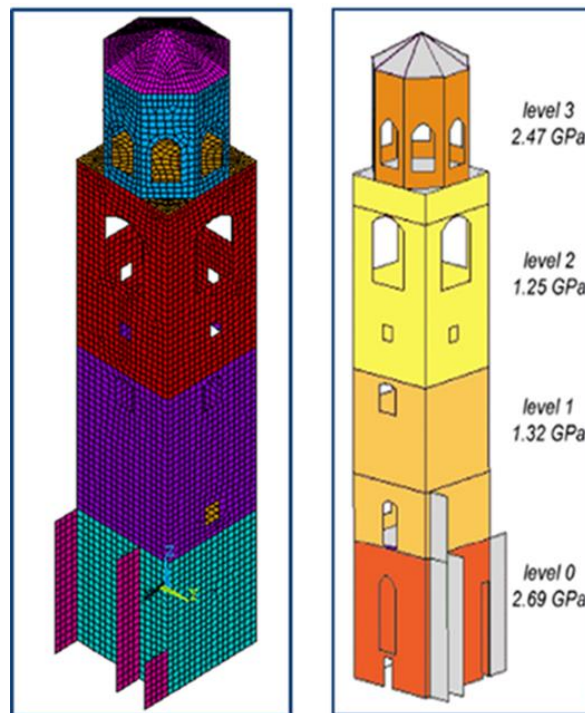


Figure 38: the FE model: subdivision in macroelements, and updated values of the elastic moduli. Source (Ceravolo, et al., 2014).

The FE model is composed of about 7500 elements and 15000 nodes. The mechanical relationships between the bell tower and the adjacent church should be carefully evaluated. For this reason, special elements or springs were introduced and calibrated into the model for simulating the interaction between

the two adjacent bodies. To simulate the weak connection state between belfry and church, a fictitious material was assigned to that portion (elastic modulus of 500 MPa). As shown in Figure 38 the FE model was subdivided into macroelements with different materials, in order to take into account the spatial distribution of mass and stiffness. Uniform elastic moduli were initially chosen for all the elements. The model updating procedure was performed using a finite element program and MATLAB, and employing an algorithm that investigates the minimum of a cost function, by varying the parameters associated with the macroelements within a predetermined range. The adopted stochastic subspace procedure estimated 11 natural modes (range 1.28-9.65 Hz). The first two ones (1.28 Hz and 1.34 Hz) were the bending modes in the two horizontal directions, while the third showed torsional characteristics (3.28 Hz). Within the above mentioned, frequency range, a few extracted modes were characterised by mutual movements of the four walls. Also local wall modes were detected at low frequencies, a condition that is associated with poor connections between walls and indicate a vulnerable condition. Table 7 shows the updated material properties.

**Table 7:** materials properties after model-updating. Source (Ceravolo, et al., 2014).

<b>MATERIAL</b>	<b>ELEMENT</b>	<b>E [MPa]</b>	<b>v [-]</b>
1	Masonry-level 0	2690	0.3
2	Masonry-level 1	1320	0.3
3	Masonry-level 2	1250	0.3
4	Masonry-level 3	2470	0.3
5	Walls-x direction	500	0.3
5	Walls-y direction	500	0.3

### 3.6.3 The AFRP strengthening intervention

In this study, different approaches to model AFRP reinforcement are investigated. This can be modelled in two different ways: through shell elements, overlapping to the masonry mesh, or through truss elements. Advantages of shell elements include the possibility to take into account the orthotropic behaviour of the reinforcement material, and a realistic distribution of FRP materials over the

masonry. As expected, preliminary analysis has shown that for a global model of the structure (as the Fossano belfry), the results does not depend on the orthotropic behaviour of the reinforcement. Considering also the difficulties of matching the masonry mesh with the overlapping elements, it was chosen to employ truss elements such as LINK 180, for modelling the Kevlar® reinforcement of the bell tower. An advantage of these elements is the possibility to consider a tension-only behaviour, which better simulates the real behaviour of the reinforcement which are not effective in compression. The proposed and modelled intervention consists in the application of vertical and horizontal strips. The vertical strips were located at the corners of the bell tower, while the horizontal ones were placed mainly at the base of openings (windows). Three different models were generated and are shown in Figure 39, with three, five and seven orders of horizontal strips. Moreover, different types of Kevlar® were considered. They are characterised by different values of the elastic modulus (70, 140 and 160 GPa). Finally, a parametric analysis was performed to obtain an efficient the more performing configurations, by varying the ratio between the areas of the vertical and horizontal reinforcement.

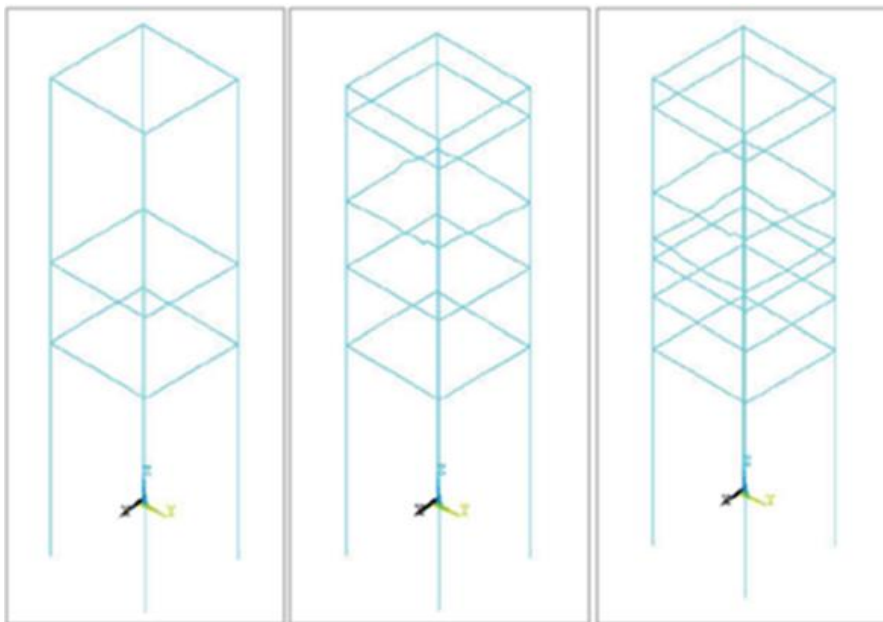


Figure 39: different position of the Kevlar® reinforcements investigated.

### 3.6.4 Analysis and results

Pushover analyses were carried out in both the horizontal directions by varying the following parameters of the reinforcement:

- elastic modulus
- number and arrangement of the fabrics
- size.

For modelling masonry an orthotropic material was adopted, together with a maximum stress failure criterion. It is characterised by different values of strength in tension, compression and shear. In addition, a brittle behaviour in tension was simulated, considering higher values of the stiffness reduction factor. Instead, a linear elastic behaviour was assumed for the reinforcement material with tension-only capability (no stiffness in compression) for the truss elements. The pushover curves of the reinforced structure with AFRP (elastic modulus of 70 GPa) are shown in Figure 40.

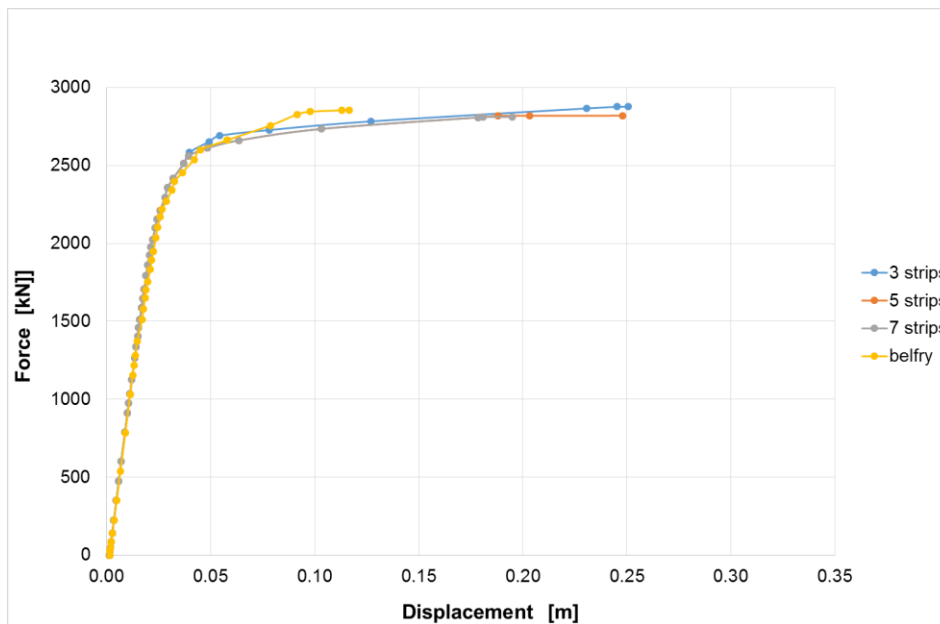


Figure 40: pushover curves, in x direction (Kevlar® 29 with  $E = 70\text{GPa}$ ).

The results compare three different positions of the reinforcement strips, with the belfry in its original condition (without reinforcement). Figure 41 shows the results with AFRP reinforcement having an elastic modulus of 160GPa.

An increase in ductility is attained for all reinforcement types and configurations investigated. The ultimate displacement of the original structure (without reinforcement) was about 12 cm while in case of reinforced bell tower it was 20 to 30 cm (an increment of about 70 to 150%).

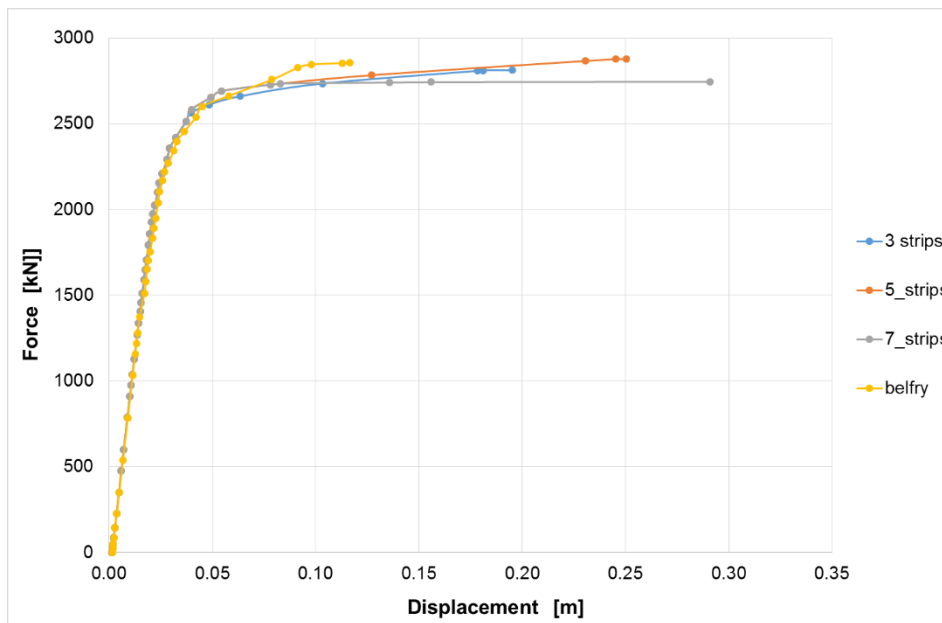


Figure 41: pushover curves, in x direction (Kevlar® 49 with  $E = 160$  GPa).

The best performance in terms of ultimate displacement is obtained for the model with reinforcement arranged in seven layers with the stiffest AFRP. Interesting improvements in terms of strength are not observed, because the ultimate horizontal force was more or less same for the unreinforced belfry and for the different configurations of reinforcement. In these analyses, the same area was provided for both horizontal and vertical reinforcement stripes.

Another parametric study was performed by varying the ratio between the areas of the vertical and horizontal reinforcement. Figures 43-44 shows the results for maximum displacement with the ratio between the areas of the strips. Three different values for the vertical and horizontal reinforcement, (considering the same ratio between the two), were also analysed and the results are shown.

Generally, a good performance in terms of ultimate displacement was obtained for similar values of the area of vertical and horizontal reinforcement strips. It corresponds to a ratio of  $0.8 \div 1.2$ . The maximum values for the ultimate displacements are obtained with horizontal and vertical reinforcement of 1000

mm<sup>2</sup> and 800 mm<sup>2</sup> area respectively and for large dimensions of the horizontal reinforcement with respect to the vertical one.

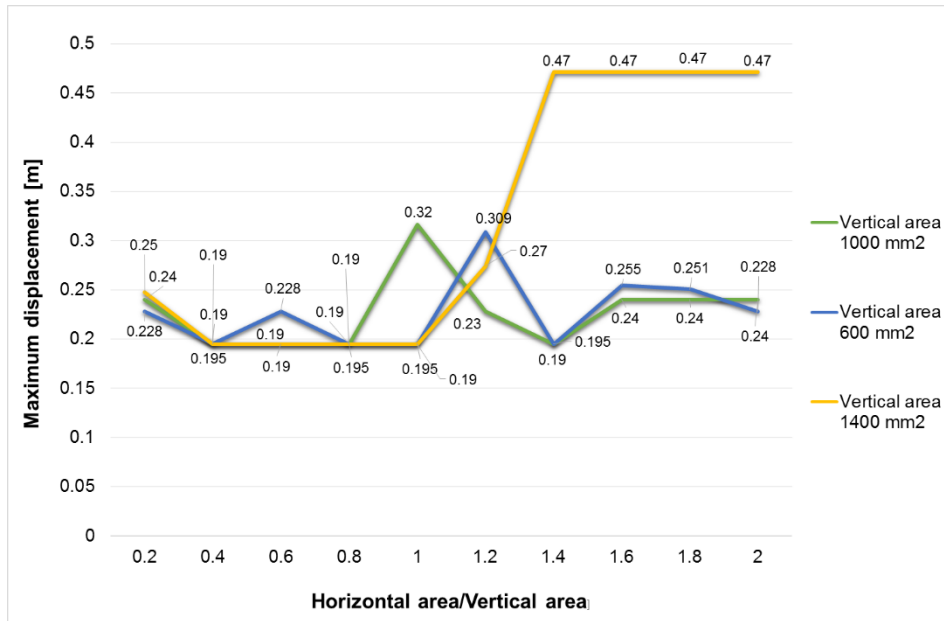


Figure 42: maximum displacement vs. ratio between the areas of the horizontal and vertical stripes.

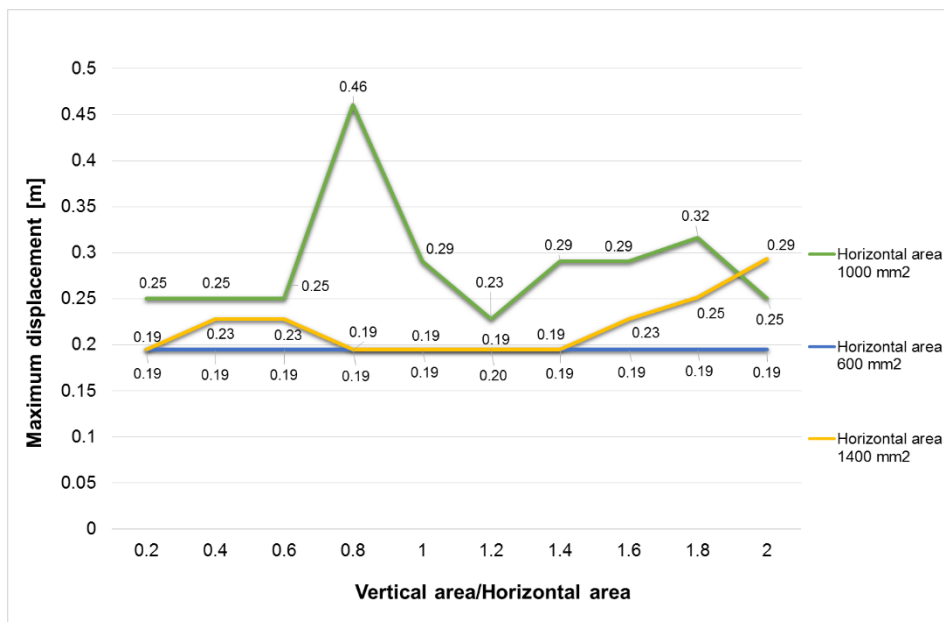


Figure 43: maximum displacement vs. ratio between the areas of the vertical and horizontal stripes.

As expected, the horizontal reinforcement appeared more effective when compared to the vertical. Figure 44 shows the damage evolution in the masonry structure. Grey areas represent those in which the failure index is higher than one which indicates that it has failed. Yellow and red indicates failure index to be close to one. It is possible to observe that damage starts under the window near the top of the bell tower (probably due to stress concentrations), and follows a path in the direction of the nearby lower windows.

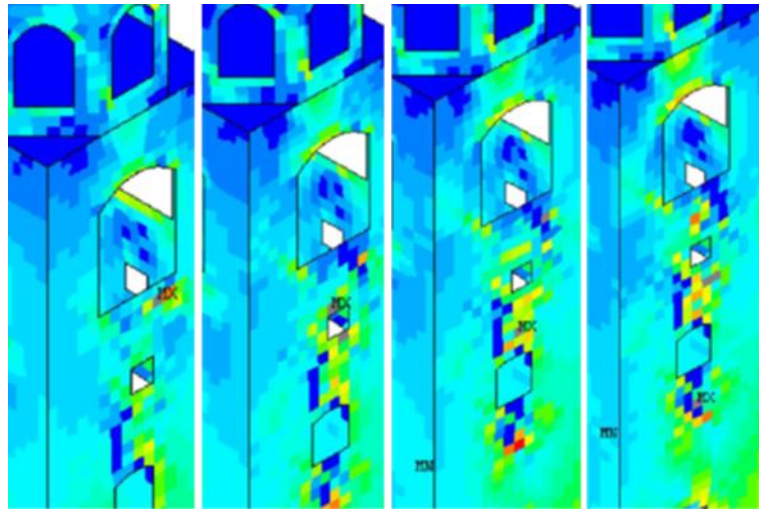


Figure 44: contour plots of the failure index for some load steps.

### 3.6.5 Comparison with traditional strengthening techniques

Pushover analyses of the Fossano belfry model for different types of traditional interventions were performed, in another work (Manno, 2013). The traditional interventions previously investigated were grout injection, an auxiliary steel structure, and a reinforced concrete layer. The results are compared with those obtained in the present study and also with the unreinforced bell tower. Figure 45 shows the comparison of various cases.

The results indicate a significant increase in the ultimate displacement relative to the proposed intervention that results to about 150% higher than with the use of the use traditional techniques. This indicates a significant increment in the ductility, which indicates a good performance against horizontal actions (seismic load, i.e.). Instead, the maximum horizontal acceleration results significantly higher in the analyses of the structure reinforced with traditional technique.

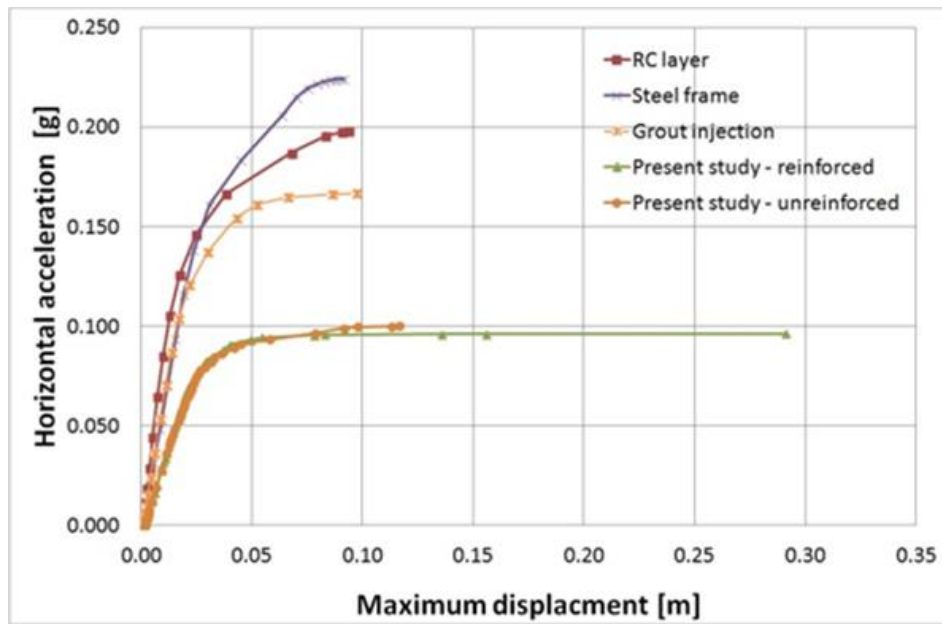


Figure 45: pushover curves relative to the unreinforced structure, the proposed intervention and the adoption of traditional techniques.

## Chapter 4

# A prototype-testing machine for the dynamic characterization of high performance materials

FRPs are commonly used for structural repair and strengthening interventions, and exhibit high potential for applications to existing buildings, including heritage constructions. For years, uncertainties connected with the long-term behaviour and durability of FRPs materials have often made the designers reluctant to use them in structural engineering applications.

In this Chapter, an innovative and alternative method for measuring the damping, and the nonlinear behaviour of high-strength fibre materials is described. In particular, Kevlar® 29 (para aramid), silicon carbide (SiC) and carbon fibres were tested. The method used is based on resonant response characterization of a spring-mass system excited by a sine-wave forcing term. It is applied as a vertical force to the suspended mass. The damping is obtained from the measured resonance quality factor  $Q$ , and the non-linearity index is obtained through the evaluation of the “backbone curve”. To evaluate low damping values, special attention has been taken for ensure that the energy dispersions are much smaller with comparison to the energy dispersions due to the material damping of the tested sample.

The non-linearity index is obtained from the resonance profile variations as a function of the forcing term amplitude. This index could be used for damage detection, or Structural Health Monitoring applications.

Part of the work described in this Chapter has also been published in *Experimental Mechanics* (Ceravolo, et al., 2017).

## 4.1 Introduction

High performance fibre materials have recently received growing attention because they are versatile materials, and can be used in different ways and for different applications (see previous chapters). More applications regard force transmission (e.g. fibres in composites materials), signal transmission (El Abdi, et al., 2008), and protection and coating (e.g. textile tissue), and much more. In any cases, fibres are always subject during use to deformation and vibrations. This occurs both if they are embedded in a matrix or not. Therefore, is very important to study the dynamic behaviour of the fibres with particular attention to their damping characteristics. They influence the dynamic response, and consequently their efficiency (Nciri, et al., 2017) (Pambaguan & Mervel, 1996) (Grouvea, et al., 2008).

The research field of high-strength low damping fibres is of the utter interest for structural engineering, with high potential for significant advancements in the some specific areas, including the seismic protection and monitoring of cultural heritage. Structural engineers are typically interested to obtaining information about the mechanical damping in high-strength fibres in order to evaluate some features such as:

- energy absorption capability
- clarify the effects of weaving on their behaviour
- to evaluate the use non-destructive tests for evaluating their characteristics (including the damping and the non-linear behaviour), also for damage assessment purposes.

In this work, the tests were conducted by using a multifilament tow of parallel fibres. Several techniques for testing the damping behaviour of composite materials are described in earlier studies, and can be found after investigation of the available literature (Ochola, et al., 2004). Instead, research on free-standing fibres are less common. For this reason, is not easy to find data in the open

literature on dynamic characteristics of free-standing fibres. These data, could be very useful for the evaluation of the ageing, damage, or also for the dynamic behaviour of composite materials. It is frequent that standard equipment used for the evaluation of the mechanical and dynamical properties are unsuitable for the investigation of thin fibres and yarns.

A universal testing machine for an accurate dynamic characterization of thin fibres (with diameter in the order of 10  $\mu\text{m}$ ) and/or a small yarn does not exist (Więcek, 2014). Different is in for composite materials (Botelho, et al., 2006) (Cerny, et al., 2000) (El-Mahdy & Gadelrab, 2000) (Nagasankar, et al., 2014) (Berthelot & Sefrani, 2004). The main difficulties are related to the sample' geometry constrains, with particular attention to its handling and clamping. This research work suggests a possible approach to the problem.

Experimental methods currently used, and potentially applicable for the evaluation of the dynamic moduli and damping of composite materials, include:

- the free vibration technique (impulse technique),
- the rotating-beam deflection,
- the forced vibration response,
- the resonance technique,
- the continuous wave or pulse propagation technique (Botelho, et al., 2006), (Wei & Kukureka, 2000) (Černý, et al., 2000).

A popular and simple test is the impulse technique. It can be used to measuring natural frequencies and loss factors, for example (Nagasankar, et al., 2014). The input is provided through an instrumented impact hammer, and the response is usually captured by an accelerometer or visualised by means of a high-speed camera (Valtorta, et al., 2005) (Rice, et al., 2014), and read by means of an acquisition card (Berthelot & Sefrani, 2004). Different authors such as Suarez et al. (Suarez, et al., 1984), Suarez and Gibson (Suarez & Gibson, 1984) and Crane and Gillespie (Crane & Gillespie, 1991) propose as first the impulse technique for the characterisation of composites materials, but these studies have not been subsequently applied to fibres. The requirement of high sensitivity of the vibration amplitude sensor is a great obstacle that arises due to geometrical reasons towards the application of the impulse technique to high stiffness fibres. In another work, Di Carlo and Williams (Di Carlo & Williams, 1980) tested the damping properties of boron and SiC fibres with a free-decay technique. They employed a capacitive sensor in which the fibre was part of the capacitor. Despite

the limited dimensions of the fibre, they obtained usable results. In any cases, this method cannot be applied to non-conductive materials.

In Dynamic Mechanical Analysis (DMA) resonance techniques consist of exciting a mechanical system at its eigen frequency and in the measurement of the motion for extracting the damping parameters (Wielage, et al., 2003). DMA are often used for various applications, including the evaluation of viscoelastic behaviour of composite materials (Więcek, 2014), during temperature changes (Nagasankar, et al., 2014). Another kind of studies are conducted by Gibson et al. (Suarez, et al., 1984) (Gibson & Plunkett, 1977) (Gibson, et al., 1982). They measured the longitudinal damping of a fibre, which held in tension by fixing its upper end (hanging it down vertically) and fixing a mass on its lower end. The measurement requires this configuration, because it is necessary to reach a suitable initial longitudinal tensioning of the fibre that, in turn, influences the outcome of the measurement.

The work described in this Chapter could be included in the category of resonant techniques. The final aim is the implementation of a method for the dynamic characterization of free-standing, high-strength, and low-damping fibre materials, such as para-aramids (Kevlar®-29), silicon carbide (SiC) and carbon, and the investigation of a possible weak non-linear behaviour. Driving the fibre sample with a low intensity dynamic excitation force, and subsequently recording the response (displacement expressed in terms of frequency and amplitude) leads to obtain the dynamic characterisation of the fibre. The elastic modulus is obtained as derivative of the resonant frequency, the damping as derivative of the quality factor  $Q$ , and the non-linearity factor is obtained from the backbone analysis of resonance response distortions as a function of the excitation amplitude.

The main problem in measuring very small damping values in high-strength low-damping fibre materials is the need to use equipment where the energy dispersions are much smaller than dispersions in the fibre (very low). This requires a careful selection of all components, including the sample holder, the measurement system and the exciter.

A dedicated testing machine was developed to overcome the above described issues. The machine consists of a spring-mass resonator (section 4.3), where the spring is the fibre (or fibre bundle) under test, and the suspended mass is designed to conveniently preload the fibres. A web of thin “tie-rods” (made by nylon fibre,

section 4.4) constrains the mass to the single vertical degree of freedom, in order to keep low dissipation. A high sensitivity non-contact optical position detector was adopted for the same low dissipation reason, to measure the vertical displacements. Measurements are taken at resonance frequency, as the system is excited by a low dissipation home-made non-contact voice-coil transducer.

In this Chapter, the prototype-testing machine is described, the principle of operation of the testing apparatus, and the design parameters are after discussed.

## **4.2 Prototype-testing machine description**

The prototype-testing machine, object of this work, was developed in cooperation with the Metrology Laboratory of the Department of Electronics and Telecommunications of Politecnico di Torino. In Figure 46 are shown the real prototype, and a schematic model. It consists of a portal with an upper beam, a half meter long piece of 40x40 mm square section aluminium, resting on two cylindrical aluminium columns tall 0.95 m. From the centre of the upper beam, the fibre specimen is hanging, holding the mass attached at the bottom. The mass disposes only of a vertical degree of freedom as five of the six degrees of freedom are constrained by means of a containment structure realised by fibre tie-rods. All components of the prototype are assembled by using a cyano-acrylic super-glue. It makes easy to changing configurations, allows a quick positioning, and the necessary assembly stiffness.

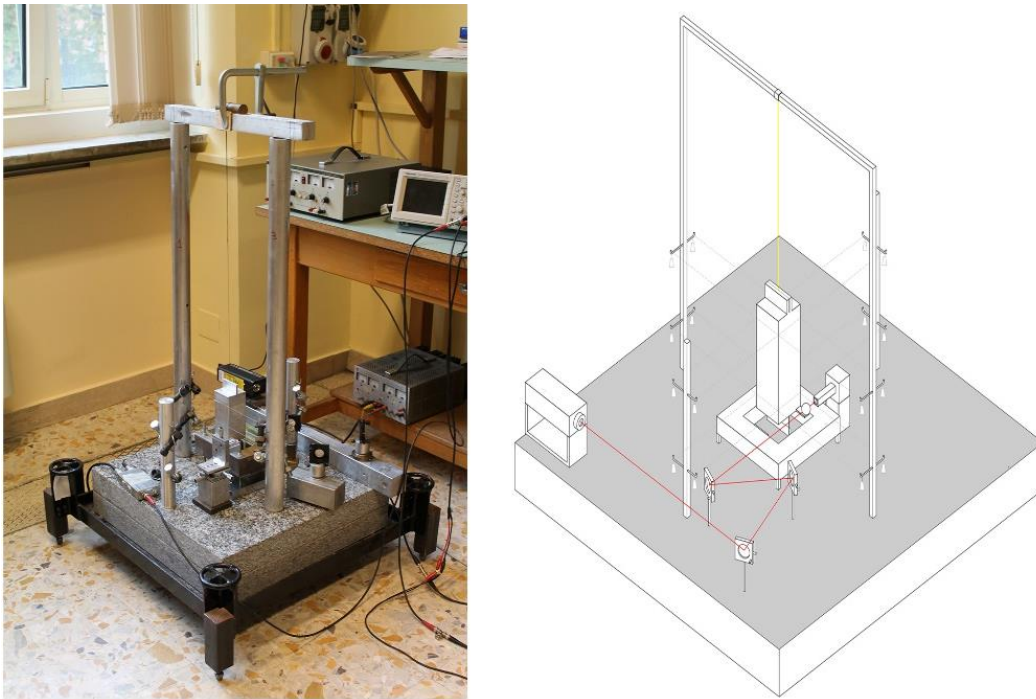


Figure 46: real prototype testing machine, and a schematic model.

The hanging mass of the resonator system is a 1.375 kg aluminium block. It cannot be considered the best choice because of the relatively high acoustic power dissipation during vibrations resulting from its low density. On the contrary, it was practical to use in the laboratory due to its square section shape suited to the need, and sufficient for a prototype. Similar general considerations can be made for the aluminium used for the portal (upper beam and the two columns).

The mass is chosen to make the biasing DC stretch of the sample (pretension) a suitable fraction of its tensile strength. In this way, the resonant measurements can be carried out without fully unloading it up to an excitation level that is suitable for the non-linear behaviour evaluation of the material under investigation.

The columns are glued on a massive 0.6x0.6x0.145 m square granite basement. Moreover, two cylindrical aluminium poles (which hold the constraining fibre harness) the optical circuit, and the electromagnetic circuit (voice-coil), are glued on the basement are appropriately positioned around the suspended mass, and consequently the fibre specimens. The confinement structure

is realised with nylon tie-rod (diameter of 0.2 mm), as shown in Figure 47 and after detailed in Figure 51 and 53 (Sections 4.3 and 4.4).

The detection of the vertical displacement was realised by means of an optical system (Figure 47). It is composed of an 8 mm ball lens and a split detector, which had a sensitivity of about 50 mV/ $\mu\text{m}$  after amplification of the differential signal. The light source was a 10mW HeNe laser, which was suitably attenuated to avoid detector damage where the laser power was highly focused by the very fast-ball lens. Some care was needed during alignment to obtain the aforementioned sensitivity, but the light attenuation, limited the sensitivity that could be reached. For positioning the detector in the focus of the ball lens, it is necessary using of a XYZ translation stage. The ball lens was attached to the hanging mass and moved with it, and consequently displacing the point at which the laser focuses.

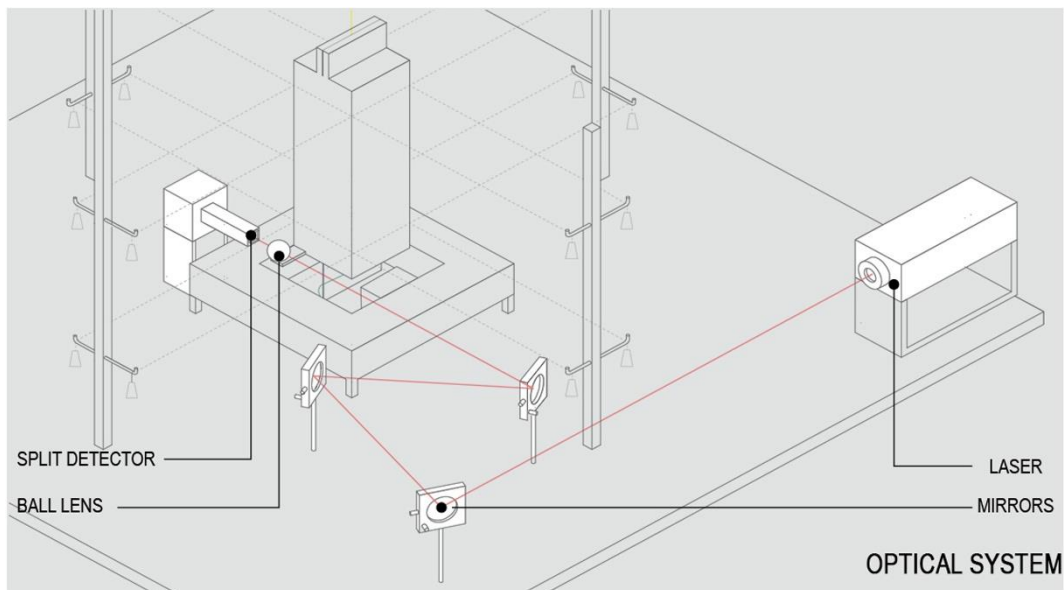


Figure 47: schematic representation of the optical system.

The voice coil actuator (60 N/A) consists of a 50x50x12.5 mm NdFeB permanent magnet, driving a homemade magnetic circuit (1 Tesla) realized with an L-shaped laminated transformer type silicon loaded iron and a fiberglass PCB type card fixed vertically below the suspended mass (Figures 48-49). It has a single 0.5 mm Copper wire glued horizontally to its lower edge. The sample

length was adapted for positioning the conductor in the middle of the 8 mm air gap of the magnetic circuit to position the wire in the centre of the magnet.

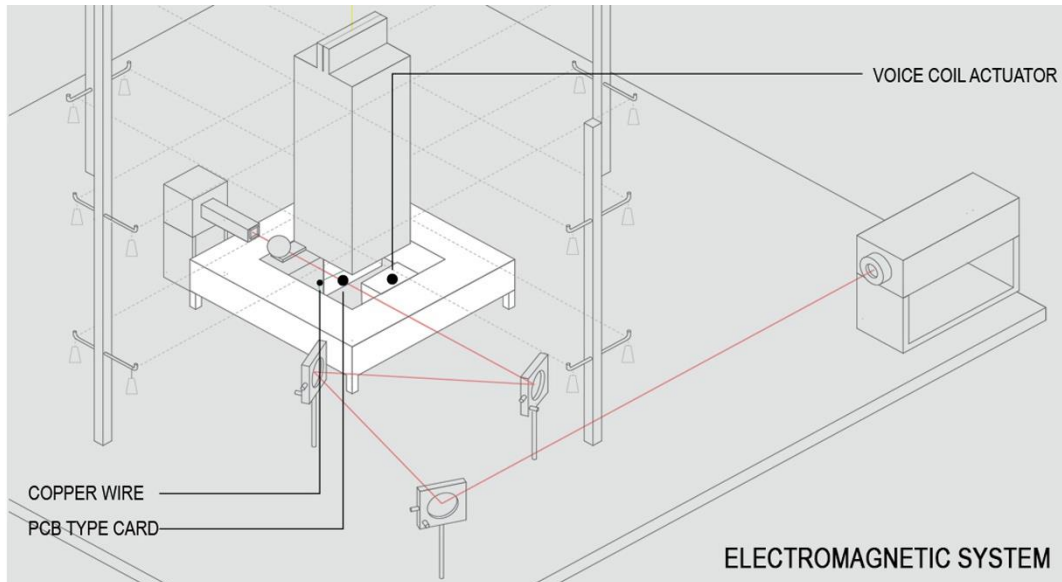


Figure 48: schematic representation of the electromagnetic system.



Figure 49: the homemade magnetic circuit.

The observed electronic noise was under 1 mV (20 nm) without averaging, which is well below the environmental mechanical/seismic noise that instead varied significantly throughout the day on the non-damped table. It is in all cases

being the most important noise source. Averaging helped to reduce its effects, and was adopted in adequate amounts when taking measurements.

The prototype-testing machine realised may be used for free-decay and forced tests. In the free-decay tests, the ring-down of vertical oscillations is observed by the detector, and digitally recorded after A/D conversion. In the forced tests, sine wave excitation is provided through the voice coil by a function generator. The amplitude and phase of the induced vertical oscillation sine wave are measured with an oscilloscope or an AC digital voltmeter. The sine wave source, a function generator, (AGILENT 3320 A, 50  $\Omega$  output) reaches, at 1  $\mu$ Hz, 1  $\mu$ Hz resolution in the range of interest. Given the 50 Ohm output resistance of the generator, the short circuit output current of 200 mA peak-to-peak delivered at the maximum peak-to-peak amplitude of 10 V is within the specified linear range. Nevertheless, a check on distortion was run for safety before deciding to load directly the generator with the low resistance voice coil.

### **4.3 The resonant spring-mass approach**

During the tests for the evaluation of the mechanical properties of fibres or yarn via a spring-mass approach (both static and dynamic tests), all single fibres of the sample are subjected to the same tension at all times. The preload imposed selecting a suspended mass it is very important, because may be used for the selection of the operating point on the stress-strain curve. In addition, the suspended mass guarantees that the fibres in the bundle never unload during an oscillation cycle. In case of weak nonlinearities, the damping values obtained from a single unwoven bundle are expected to be representative of the single fibre behaviour. Highly accurate information of the relevant material properties can be obtained directly from such measurements. No deconvolution is necessary and the experimental conditions are well defined.

The resonance frequency is the parameter used for the suspension stiffness, and consequently the elastic modulus  $E$  of the material. However, it is possible only if both the number and the diameter of the fibres are known. To evaluate the resonant frequency with high accuracy is necessary introducing an appropriate containment structure, for reducing the system disturbances. In this work, the movement of the mass was reduced to a single vertical degree of freedom by means of a confinement structure (realised by means of a web of fibre called “tie-rods”) that minimizing their contributions to both resonance frequency and losses.

The principles of operation of the confinement structure of the prototype-testing machine developed are described in detail because they are a fundamental aspect of the proposed approach. The basic idea is to take advantage of the cosine law to minimize the stretching imposed on the tie-rods, when a mass oscillates along the vertical direction. The tie-rods are fixed to the mass horizontally (Figure 50), to constrain lateral displacements, but to allow only the vertical ones.

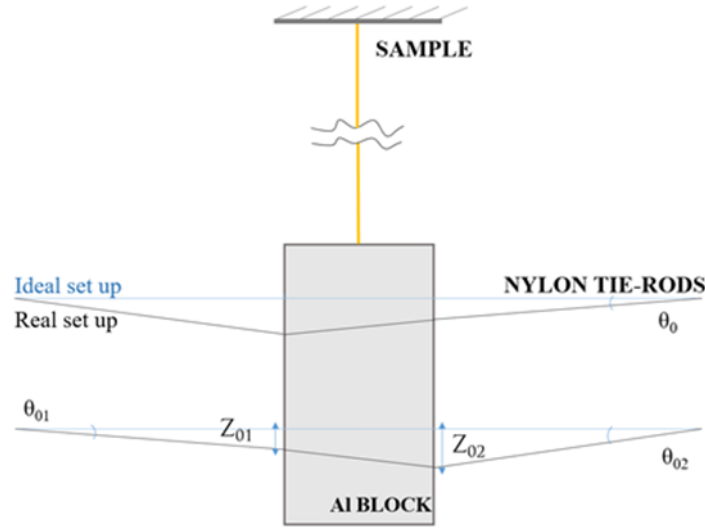


Figure 50: Schematic arrangement of tie-rods, with attachment errors.

A useful additional stiffness  $k_{tz}$  is introduced by the application of the  $n$  tie-rods to vertical oscillations. However, the additional stiffness is reduced in such a scheme, by the strain  $\epsilon_{t0}$  produced in the tie-rods due to pre-tension when they are horizontal, plus half the square of their inclination angle  $\vartheta$ . This relation is expressed by the following equation (1). It can be easily obtained from the analysis of the schematic representation show in Figure 50

$$k_{tz} \approx nk_t \left( \frac{1}{2} \theta^2 + \epsilon_{t0} \right) \quad (1)$$

The lateral stiffness to horizontal movements of the mass is given by  $nk_t/2$  for each orthogonal direction. Careful alignment, suitable choice of material and the imposed tension play the key role in the optimisation of the confinement structure's performance. The lateral stiffness must be high. In this

way, the pendulum mode frequency is much higher compared to the vertical spring-mass mode frequency of interest for this work. Instead, the vertical stiffness contribution from the confinement structure must be low, in order to minimize the effect on resonance frequency and damping. As discussed below, it is easier to guarantee this condition for a multifilament bundle than for a single fibre. For the same reason, measurements on the single fibres should be avoided in the first phase of development.

The practical realization and the mechanism chosen to fix the tie-rods' tension of the confinement structure in the prototype-testing machine is shown in Figure 51. The mechanism is constituted by sixteen 0.13 kg bolts, suspended at each end of a tie-rod beyond a pulley fixed on a post similar to the Atwood machine. Once all pulleys are carefully placed on the table at the same height and the tie-rods glued to the mass only after all components are at rest, the residual long term creep in the tested fibres can produce meaningful values of the angle  $\theta$  in equation (1). It is possible to expect to remain below a couple of milliradians. As a result, the contribution to the stiffness is unimportant as compared to the effect of strain. In a similar way, negligible effect on stiffness, and consequently on the resonance frequency, are expected to be caused by small dynamic variation of  $\theta$ . This is valid only if the non-linearity, introduced by the tie-rods, is counterbalanced with the assessment of the non-linearity of the tested sample.

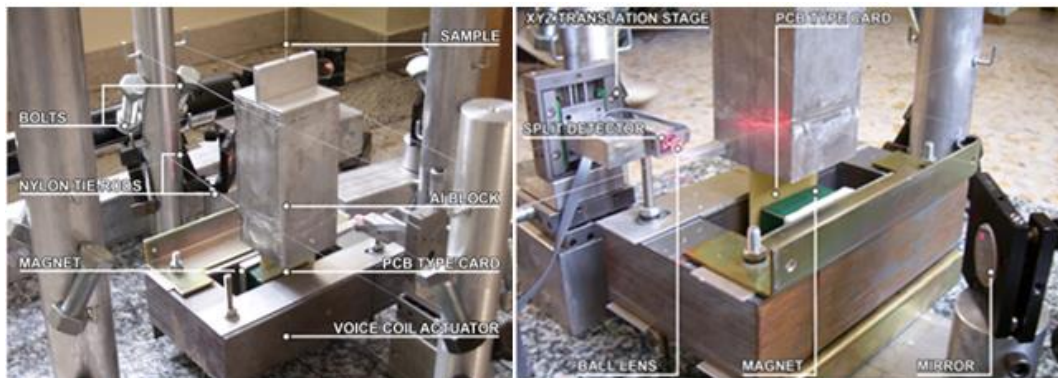


Figure 51: Significant components in the prototype machine.

It is worth to underline that, during the mass's oscillation, the maximum value of the dynamic angle  $\theta$  in equation (1) is evaluated as a ratio between the oscillation amplitude and the tie-rods' length. For some fibres, this condition can require a minimum length for the tie-rods and/or impose limits on the excitation level when the constraints on the confinement structure disturbance are critical.

The oscillation amplitude itself should be fixed at a fraction (e.g. 20%) of the static pretension imposed by the weight of the suspended mass, in order to guarantee that unloading does not occur. This level could reach approximately the 20% of the fibre strength. This value corresponds to the maximum admissible strain, of which the amplitude is limited within a few percent. It is typically about  $10^{-3}$  for high strength fibres, which suggests rms strains below  $10^{-4}$  for the oscillation term. The strain variation entails for the suspended mass an rms amplitude with values ranging from below  $10\ \mu\text{m}$  to above  $100\ \mu\text{m}$ , for samples of a few centimetres and a couple of meters, respectively. It depends very much on the length of the fibre sample under testing. This, in turn, calls for high sensitivity of the vibration detector that was designed to provide a sensitivity, which was well below a micrometre. To overcome these issues, and the requirement for low disturbance, which suggested the use of a non-contact detector, an optical position sensor was employed. Interferometry was excluded due to the limited analogue range, which it grants and the quiet mechanical environment that it necessitates. A focused light approach was used, as illustrated in the following, which yields a sensitivity below  $10\ \text{nm}$  in the sine-wave mode without narrow-banding.

The methods chosen for non-contact excitation and detection are shown schematically in Figure 52. A voice coil (also observable in Figure 48) introduces the vertical forcing tension term. A ball lens glued to the suspended mass focuses a laser beam onto a split detector that is used for detecting the position. These elements should be taken into account for the minimization of disturbances that could be otherwise introduced by both functions.

The resonance frequencies expected are low enough for high-strength low-damping fibres because of their stiffness. In fact, the resonance angular frequency  $\omega_0$  may be expressed in the following form (eq. 2)

$$\omega_0 = \sqrt{\frac{g}{L\varepsilon_M}} = \frac{\omega_p}{\sqrt{\varepsilon_M}} \quad (2)$$

where  $\omega_p$  is the free pendulum frequency and  $\varepsilon_M$  is the fibre strain under the static pre-tension. It is induced by the weight of the suspended mass.

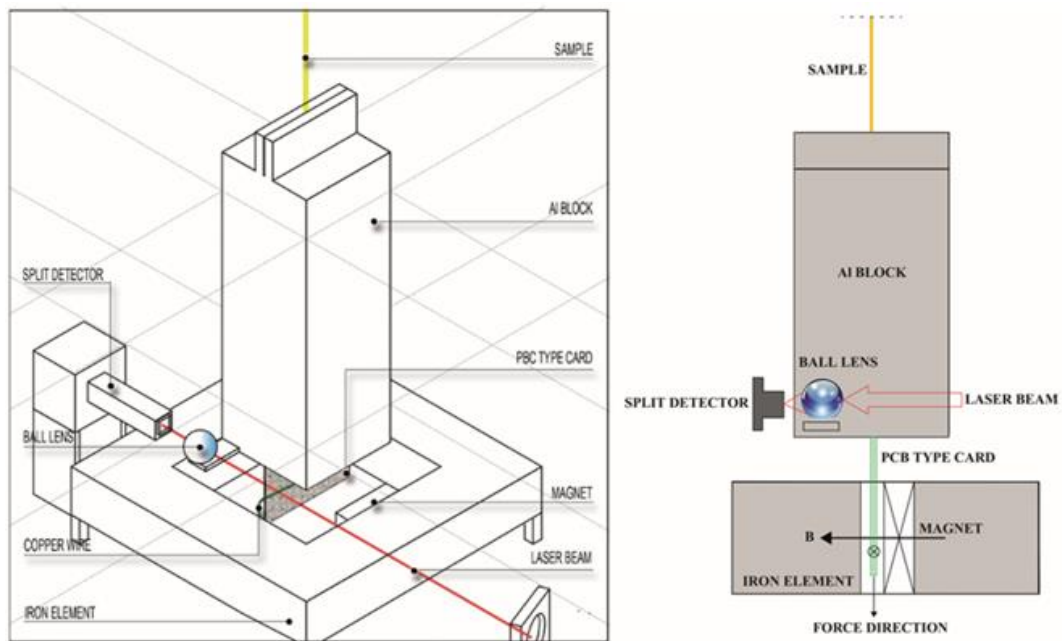


Figure 52: non-contact excitation and detection.

The expected values, previously mentioned, for L&M ranging from 50  $\mu\text{m}$  to 1 mm for samples between a few centimetres and a couple of meters. Consequently, the expected resonance frequency may range between 10 Hz and 100 Hz that is actually, what was measured for samples of various lengths.

Many experiments were made with fibre lengths ranging from 40 mm and 2 m before the prototype testing-machine was designed and built with its final setup.

#### 4.4 The containment structure and its effects

The aim of the containment structure is to constrain the suspended mass along the vertical axis, and consequently the fibre sample will be vertical (Figure 53). The containment structure is designed for maximizing containment and minimizing undesired effects. These errors could significantly alter the measurement of mechanical characteristics of the fibre material under investigation. For these reasons, an analysis to suggest the design and choice of the material to be used for the tie-rods, and to determine how well the containment structure must be realised is presented here.

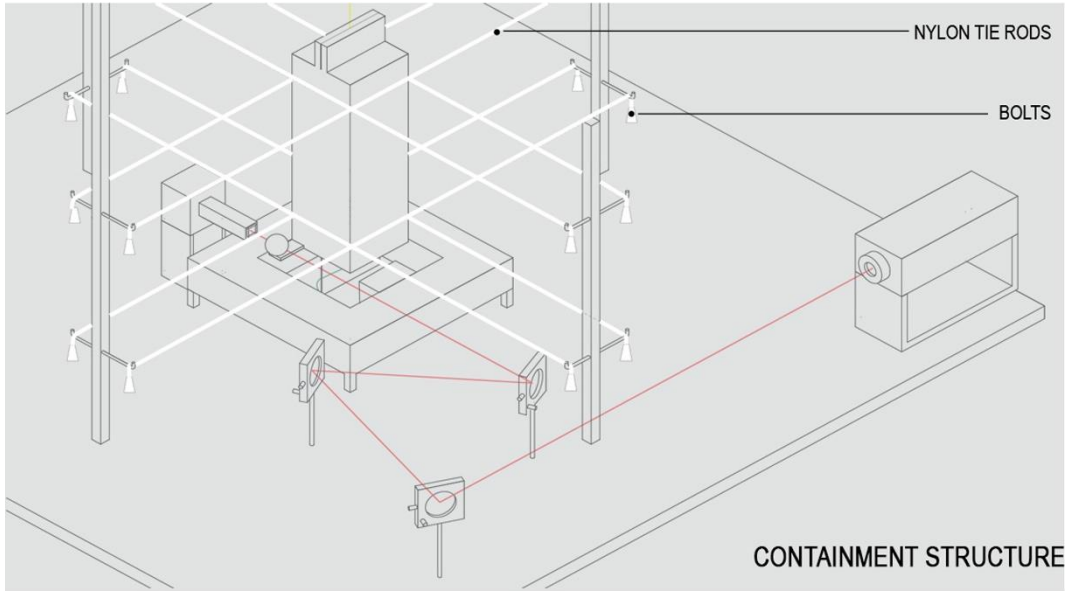


Figure 53: schematic representation of the containment structure.

In this analysis based on the schematic representation of Figure 50, a well-defined equal pre-tension is assumed to be applied to all tie-rods. It is produced by means of the application of bolts, weight of 0.13 kg each, that provide a tension of 1.3 N. The generated pre-strain  $\varepsilon_{t_0}$  of the tie-rods depends on their stiffness  $k_t$ . The stiffness is a function of the length and diameter of the tie-rods. At this contribution, an oscillating term  $\varepsilon_{r-rms}$  is added during operation (and during oscillation), because of tie-rod's length changes imposed by geometry. It is difficult to put the tie-rods in a perfectly horizontal setting. It is therefore possible than an approximation could be introduced. It occurs despite the applied tension, because the mechanism that keeps the tension constant is not fast enough to track oscillations.

The fibre's stiffness is evaluated from the Young modulus  $E_f$  of the sample material under investigation. For evaluating it, the important contribution is given by the angular frequency  $\omega_z$  for vertical oscillations,

$$\omega_z = \sqrt{\frac{k_f + k_{tz}}{M}} \quad (3)$$

Its fractional variation induced by the tie-rods containment structure may be written as

$$\frac{\Delta\omega_z}{\omega_z} = \frac{n k_t}{2 k_f} \varepsilon_{t0} \quad (4)$$

when taking into account the tie-rod's stiffness (eq. (1)) and considering its contribution to the vertical stiffness, the contribution is mainly given by their pre-tension. To obtain an accuracy better than 0.1% of the stiffness, it is possible seen from equation (4) that the elastic modulus of the tie-rods must be 10 times smaller respect to the sample material, for a pre-strain of  $3 \times 10^{-4}$ . The tie-rods used in this prototype-testing machine have roughly the same diameter and one-fourth the length of the sample under investigation. For this reason, the material chosen for the tie-rods was Nylon. Its Young modulus is about 6 GPa, respect to 80 GPa that is expected for the elastic modulus of a para-aramid material, for example. The tie-rods' length and diameter were chosen to be 0.17 m and 0.18 mm, respectively. According to equation (4), it is worth pointing out that, as previously affirmed, it would be easier to minimise the effects on confinement structure in the measurement of vertical stiffness testing multifilament fibres than single fibre. Indeed, the tie-rod's stiffness is proportional to the number of fibres and this imposes the use of single fibres as tie-rods. Variations in temperature can be minimised as Nylon thermal expansion coefficient is  $7.2 \cdot 10^{-5}/\text{K}$ ; in this case, even an excursion of 14 K would only produce an increment of 0.1% on the static strain  $\varepsilon_{t0}$ . The Nylon confinement structure, as explained in equation (4), increases its resonance frequency by 0.2%. It was deemed acceptable, and temperature variations are therefore expected to affect the sixth decimal, which is insignificant.

It is important to pay attention to the non-linear contribution introduced by equation (1), the oscillating part of  $\theta$  angle that has to be added to the static angle. The additional contribution introduces a third order coefficient to the system stiffness, which does not belong to the sample of fibres under testing. Consequently, it represents an error contribution into the evaluation of the non-linearity of the sample. All tested fibres showed a softening non-linearity (a negative third order coefficient; on the other hand, this dynamic contribution was positive (hardening non-linearity)). This result supports our confidence in the capability to measure the non-linear behaviour of high-strength fibres.

## 4.5 Quality Factor limitations

The quality factor  $Q$  is used for the characterization of the resonator and its losses, as is a common practice in measurements of forced oscillation. The quality factor is experimentally obtained as the ratio between the resonance frequency  $\nu$  and full 3 dB width  $\Delta\nu$  of the amplitude response to excitation:

$$Q = \nu / \Delta\nu \quad (5)$$

It is usually measured as the frequency difference between the two  $\pm 45^\circ$  phase shift points on both side of the resonance frequency. The quality factor is strictly linked to the damping ratio  $\zeta$ , (it is inversely proportional), and can be expressed through the following relation

$$Q = 1 / 2\zeta \quad (6)$$

The quality factor can also be written as

$$Q = \omega_n \frac{W}{P_d} = 2\pi \frac{W}{W_d} \quad (7)$$

where  $P_d$  is the average dissipated power,  $W$  is the energy stored in the resonator and  $W_d$  is the energy lost during each cycle.

Many sources of mechanical energy dissipation contribute to the limitation of  $Q$  in a spring-mass system. The aim of this section is to analyse all sources and their contributions, in order to evaluate how well the measured quality factor represents the intrinsic one of the fibre sample. The contributions taken into consideration in this work are:

- the energy dissipation in the tie-rods of the confinement structure ( $Q_t$ )
- the acoustic radiation ( $Q_a$ ),
- the dissipation in the equipment producing the forcing term in the forced oscillation technique ( $Q_e$ ).

The measured quality factor can be evaluated as the combination of  $Q$  limitations. Each limitation can be ascribed to one of these mechanisms, appearing as the measured value if the represented power losses were the only

contribution to system dissipation. The limitations taken into consideration and their combination can be expressed through the following equation

$$\frac{1}{Q} = \frac{1}{Q_f} + \frac{1}{Q_t} + \frac{1}{Q_a} + \frac{1}{Q_e} \quad (8)$$

The comparison between tie-rods' contribution and the dissipation in the fibre samples could be done because both are generated by the same mechanism. Indeed, during the oscillation of the spring-mass system, the change in strain varies periodically in both tie-rods and fibres under test. In this way, the energy stored in the system is converted backward and forward between kinetic energy stored in the mass and elastic energy stored in the fibres. As a result, a part of the converted energy is lost into heat process. The lost power is proportional to the one converted by the damping ratio  $\zeta$ . In the same way, the energy  $W_d$  is dissipated in a full cycle. However, the elastic energy stored at any time in a stretched string can be expressed as

$$W = \frac{1}{2} E A l \varepsilon^2 \quad (9)$$

The ratio between one-cycle dissipation in the 16 tie-rods ( $W_{dt}$ ) and in the fibres under test ( $W_{df}$ ), may be written as

$$\frac{W_{dt}}{W_{df}} = 16 \frac{\zeta_t E_t A_t a \varepsilon_{trms}^2}{\zeta_f E_f A_f L \varepsilon_{frms}^2} \quad (10)$$

The actual values of the final setup, namely  $E_t/E_f \approx 0.1$ ,  $A_t/A_f \approx 1$ ,  $a/L \approx 0.25$ , and  $\zeta_t \approx 0.02$  are separately measured with the same machine. By introducing these values in equation (10) it appears clear how, due to a dissipation error in the confinement structure smaller than 0.5%, in the measurement of  $Q_f$  (for the extreme case of  $Q_f \approx 10^3$ ), the dynamic rms strain ratio between tie-rods and fibre bundle must be smaller than 0.014. This condition is satisfied if the tie-rods are perfectly horizontal, as in that case

$$\varepsilon_{trms} = \frac{1}{2} \varepsilon_{frms}^2 \left( \frac{L}{a} \right)^2 \quad (11)$$

It imposes an easy  $\varepsilon_{frms} < 1.4 \cdot 10^{-3}$  to reach the desired limit in the error of the quality factor. On the contrary, it is difficult to achieve such a limit if the tie-rods are not perfectly horizontal, but inclined by angle  $\theta_0$ . In this second case:

$$\frac{\varepsilon_{trms}}{\varepsilon_{frms}} = \theta_0 \frac{L}{a} \quad (12)$$

And, consequently, it must be  $\theta_0 < 3.5 \cdot 10^{-3}$ . It means that the maximum acceptable vertical misalignment is 0.5 mm. To conclude, great attention should be put into containment structure setup, in order to obtain a configuration where the dissipation in the tie-rods do not affect excessively  $Q_f$  measurement.

The next contribution to power loss during oscillation, taken into consideration, is the acoustic radiation from the upper and lower faces of the vibrating mass. It is considered as a sound wave propagates away from them. Since in that case the amplitudes of oscillation and the velocities are very small, the power of the acoustic radiation may be calculated by the following equation

$$P_{d,a} = 2\rho_0 c S u_{rms}^2 \sigma_{rad} \quad (13)$$

in which  $\rho_0$  is the air density,  $c$  the speed of sound,  $S$  the front surface of the vibrating body,  $u_{rms}$  the rms velocity of the radiating surfaces, and finally  $\sigma_{rad}$  the radiation efficiency. It depends on the frequency and on radiator shape and is considered to be as small as 0.01 for this specific case, mainly because of the low 20 Hz frequency (Allard & Champoux, 1992) (Dahl, et al., 1987) (Larko & Cotoni, 2007).

In this method, the radiated acoustic power is proportional to the square of rms displacement, and the same is for the stored energy. It means that the system Q limitation introduced by this mechanism is independent of the oscillation amplitude. This limit is about  $10^4$  in the experimental testing machine, which implies an error of -10% if  $Q_f$  is on the order of 1000. The reduction of S, can be obtained by using a slimmer and denser mass. This alternative should introduce a simple improvement. An example could be the use of a longer and lighter tungsten mass. In this way is possible to reach a reduction by a factor of 10 of the cross section S, and guarantee also an error below 1% on  $Q_f$ . About power dissipation in the excitation circuit, the physical mechanism is Joule heating. In fact, the vibration induced e.m.f. dissipates power on the output resistance of the

electrical circuit which drives a current into the actuator voice coil, namely the negligible conductor resistance and the relevant  $50 \Omega$  output resistance  $R_0$  of the signal generator. Such dissipated electrical power can be written as

$$P_{de} = \frac{B^2 l^2 u_{rms}^2}{R_0} \quad (14)$$

where  $B$  is the magnetic induction in the magnet gap and  $l$  is the length of the exposed Copper wire. To evaluate how much this effect influences the measured quality factor, the power dissipation in the excitation circuit must be compared with the input power required to maintain oscillation ( $P_{in}=P_d$ ). The input power is given by:

$$P_{in} = B l I_{rms} u_{rms} \quad (15)$$

where  $I_{rms}$  is the rms current driven into the voice coil, and since

$$u_{rms} = \omega_n Q \frac{B l I_{rms}}{k_f} \quad (16)$$

by considering that  $P_{in}/P_{de} = Q_e/Q$  it can be easily seen that

$$Q_e = \frac{R_0 \sqrt{kM}}{B^2 l^2} \quad (17)$$

In the last equation, the term  $\sqrt{kM}$  represents the characteristic mechanical impedance of the resonator. A simple calculation of this  $Q$  limitation yields  $Q_e \approx 4 \cdot 10^5$  for the prototype-testing machine that means that the error introduced by this mechanism in the evaluation of  $Q_f$  is about -0.2% in the case of a fibre with  $Q_f = 1000$ . Clearly, a dramatic improvement could be readily introduced by adopting a current source with high output impedance to drive the current into the voice coil, instead of the signal generator at hand. A simple improvement can be made by interfacing the signal generator to the voice coil via a suitable driver stage that could be a series resistor.



## **Chapter 5**

# **Experimental investigation on high-strength fibres and results**

This Chapter presents the experimental investigation and the results obtained with the prototype testing machine in its final setup configuration. The experimental investigation consisted in the dynamic characterization of high-strength fibres, by means of simple non-destructive non-linearity tests (forced tests). The results could be used in the near future as an alternative to traditional methods currently used for assessing damage, defects and malfunctions in high-strength fibres and elements (Mininni, et al., 2016).

During the forced tests, the fibres sample was excited by means of a sinusoidal low intensity force, and the response, in term of strain as a function of frequency and input amplitude, was recorded. The results are used to evaluate, the damping from the quality factor measurement, and finally the non-linearity index by means of the analysis of the “backbone curve”, function of the resonant frequency and input amplitude.

The idea is to associate weak non-linearity of the material, as detected in the dynamic response to forced tests, as an indicator used in safety and lifecycle assessment. For the high-strength tested materials, the cubic stiffness coefficient  $\chi$

of an equivalent Duffing oscillator was chosen for representing an indicator of weak nonlinear behaviour.

Samples of high-strength material, such as carbon, para-aramid (Kevlar® 29), and silicon carbide (SiC), were tested initially in pristine condition. In a second phase, Kevlar® 29 samples were subjected to UV rays and tested (Chapter 6).

Part of the work described in this chapter has also been published in *Experimental Mechanics* (Ceravolo, et al., 2017).

## **5.1 Experimental investigation on pristine samples**

The dynamic response of a system can be analysed in different ways. Forced oscillations at resonance tests were carried out on pristine high-strength material, and in a second phase on damaged Kevlar® 29 fibres (Chapter 6).

To perform dynamic tests, it was necessary to realise a vibrating system, and the prototype-testing machine was previously described in Chapter 4. The suspended 1.375 kg aluminium block had the role of the mass in a mass-spring resonator. Such mass is designed to keep the sample in tension, usually a few percent of its tensile strength. In this way, the resonant measurements may be carried out without fully unloading the sample under investigation.

### 5.1.1 Samples investigated

As previously mentioned in the introduction, three different materials were investigated: SiC, Kevlar® 29, and carbon. Their main characteristics are shortly listed hereinafter in Table 8.



Figure 54: the SiC (Type S) sample tested.

The SiC (Type S) specimen tested (Figure 54), had a length of 0.66 m and consisted of 500 parallel single fibres with a diameter of 14  $\mu\text{m}$  each, and consequently, a cross sectional area of 0.0565  $\text{mm}^2$ . His colour is black, typical for ceramic materials. The elastic modulus of the fibre was about 270 GPa and the linear density was about 3000  $\text{kg/m}^3$ .



Figure 55: Kevlar® 29 sample tested.

The Kevlar® 29 samples tested was provided from S.I.G.I.T. *snc* company (S.I.G.I.T., 2015), making high-tech materials for the glass-industry. It is a para-aramid material, realised with filaments of DuPont production with 100% purity. The yarn is yellow, and is manufactured in the form of continuous filament (Figure 55). In other words, various filaments of infinite theoretical length form it, with a diameters ranging from 10  $\mu\text{m}$  to 15  $\mu\text{m}$ , positioned one

beside the other until obtaining the desired thread count (2500 dTex, in this case).

For what concerns the Kevlar® 29 specimen tested, it had a length of 0.66 m. It was a rope consisted of about 2000 single fibres with a diameter of 12  $\mu\text{m}$  each and the cross-sectional area is of 0.174  $\text{mm}^2$ . The elastic modulus of the sample was about 80 GPa, whilst the linear density was about 1440  $\text{kg/m}^3$ .



Figure 56: carbon sample tested.

The third specimen tested was carbon (Figure 56). Carbon fibers tested were a bundle of about 6000 PAN precursor 7.2  $\mu\text{m}$  PX35 fibers by Zoltek<sup>TM</sup>, taken from a tow of 50000. The yarn had a length of 0.66 m. Consequently, the cross sectional area was of 0.244  $\text{mm}^2$ . The Elasticity modulus of the fibre was about 240 GPa and the linear density was about 3000  $\text{kg/m}^3$ .

Its colour is also black. Carbon fibres are very brittle, and consequently very difficult to handle.

**Table 8:** Recap of the main features of samples tested.

	<b>SiC</b>	<b>Kevlar® 29</b>	<b>Carbon</b>
Length [m]	0.66	0.66	0.66
Number of fibres	500	2000	6000
Diameter [ $\mu\text{m}$ ]	14	12	7.2
Cross section area [ $\text{mm}^2$ ]	0.0565	0.1736	0.2443
Elastic modulus [GPa]	270	80	240

### 5.1.2 Test procedure of forced tests

In order to find possible non-linearity, a testing campaign with harmonic forced excitation tests was performed. The sine wave excitation was provided through the voice coil by a function generator. The amplitude and phase of the induced vertical oscillation sine wave are measured with an oscilloscope or a vector voltmeter. The sine wave source (AGILENT 3320 A, 50  $\Omega$  output) reaches, at 1 $\mu\text{Hz}$ , 1 $\mu\text{Hz}$  resolution.

The frequency range investigated was about of  $\pm 0.200$  Hz around the resonance frequency of the system. Because of the long time-constants

determined by high Q values at low frequencies, the sweep-sine approach was avoided in favour of measuring the steady-state response with discrete steps of 5 or 10 mHz in relation to material sample under test, while keeping the force constant. Then the test was repeated with different levels of the driving force, regulated by adjusting the current driven into the voice coil by the function generator, in steps of 1 V (or 0.5 V) from 0.5 V to 10 V (from 40 mA to 200 mA) peak-to-peak, corresponding to a maximum rms force range of about 3.5 mN and 0.35 mN steps.

Once the input voltage interval was defined, changing the frequency of the driving force (via the function generator) it was possible to record the values of the output voltage, from which the displacement can be determined by using the detector sensitivity measured for each curve in DC during photodiode calibration (the testing machine sensitivity).

In this way it is possible to draw, point by point, the frequency-strain curve, useful for the subsequent nonlinear characterization.

In Figures 57-62, the results of the strain evaluated from values recorded are shown for the three different samples of high-strength materials (Section 5.1.1). Moreover, Tables 9-11 show the input amplitude investigated and the corresponding strain evaluated at a precise frequency value.

The testing machine sensitivity measured is 150 mV/ $\mu\text{m}$  for silicon carbide sample, 70 mV/ $\mu\text{m}$  for pristine Kevlar® 29 sample, and 150 mV/ $\mu\text{m}$ , for carbon sample, respectively.

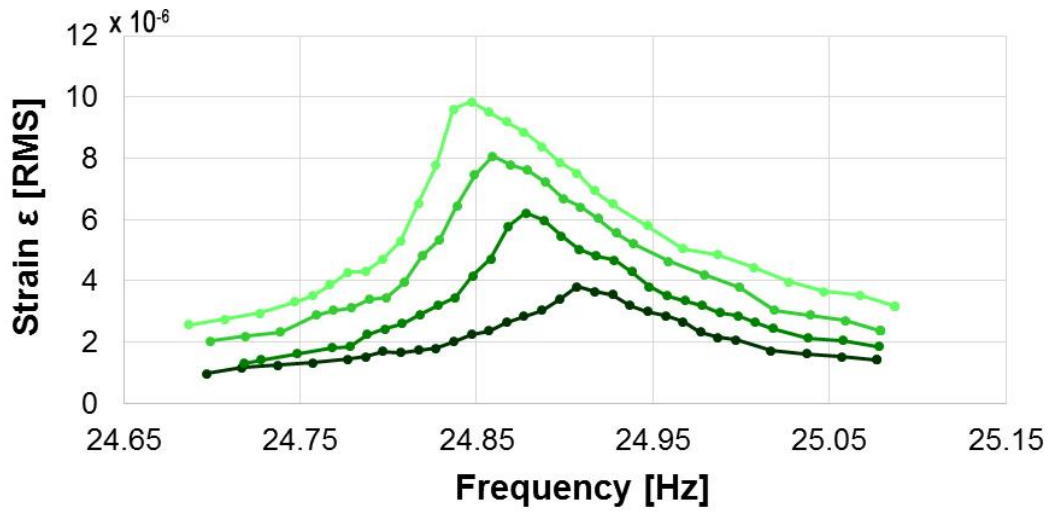


Figure 57: **Silicon Carbide:** values of frequency response recorded around resonance for increasing levels of driving force.

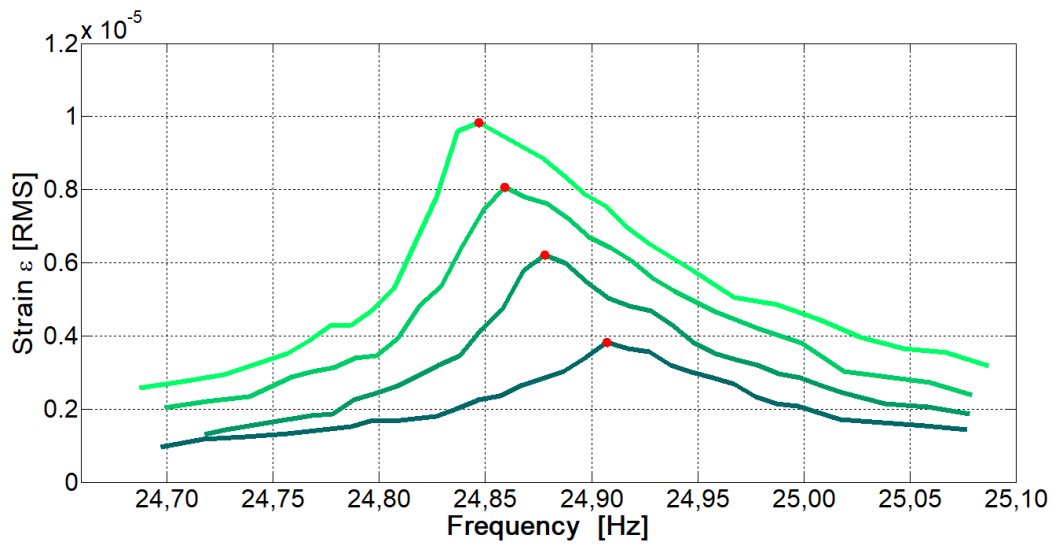


Figure 58: **Silicon Carbide:** frequency response measured around resonance for increasing levels of driving force. The maximum value is indicated by red dot.

**Table 9: SiC:** strain values calculated from the numerical data acquired during the forced tests.

0.5 [V]		1.0 [V]		1.5 [V]		2.0 [V]	
Freq. [Hz]	$\epsilon$ [RMS]	Freq. [Hz]	$\epsilon$ [RMS]	Freq. [Hz]	V [RMS]	Freq. [Hz]	$\epsilon$ [RMS]
24.697	0.965E-6	24.718	1.313 E-6	24.699	2.040 E-6	24.687	2.567 E-6
24.717	1.164 E-6	24.728	1.433 E-6	24.719	2.199 E-6	24.707	2.756 E-6
24.737	1.244 E-6	24.748	1.632 E-6	24.739	2.338 E-6	24.727	2.935 E-6
24.757	1.333 E-6	24.768	1.811 E-6	24.759	2.886 E-6	24.747	3.323 E-6
24.777	1.453 E-6	24.778	1.861 E-6	24.769	3.035 E-6	24.757	3.512 E-6
24.787	1.522 E-6	24.788	2.249 E-6	24.779	3.124 E-6	24.767	3.871 E-6
24.797	1.701 E-6	24.798	2.428 E-6	24.789	3.403 E-6	24.777	4.279 E-6
24.807	1.672 E-6	24.808	2.617 E-6	24.799	3.463 E-6	24.787	4.308 E-6
24.817	1.731 E-6	24.818	2.896 E-6	24.809	3.940 E-6	24.797	4.716 E-6
24.827	1.801 E-6	24.828	3.204 E-6	24.819	4.826 E-6	24.807	5.294 E-6
24.837	2.020 E-6	24.838	3.453 E-6	24.829	5.343 E-6	24.817	6.537 E-6
24.847	2.259 E-6	24.848	4.159 E-6	24.839	6.448 E-6	24.827	7.781 E-6
24.857	2.368 E-6	24.858	4.726 E-6	24.849	7.453 E-6	24.837	9.602 E-6
24.867	2.647 E-6	24.868	5.791 E-6	24.859	8.070 E-6	24.847	9.841 E-6
24.877	2.836 E-6	24.878	6.209 E-6	24.869	7.791 E-6	24.857	9.502 E-6
24.887	3.035 E-6	24.888	5.980 E-6	24.879	7.612 E-6	24.867	9.194 E-6
24.897	3.403 E-6	24.898	5.463 E-6	24.889	7.214 E-6	24.877	8.866 E-6
24.907	3.821 E-6	24.908	5.025 E-6	24.899	6.697 E-6	24.887	8.388 E-6
24.917	3.662 E-6	24.918	4.816 E-6	24.909	6.418 E-6	24.897	7.881 E-6
24.927	3.562 E-6	24.928	4.687 E-6	24.919	6.050 E-6	24.907	7.522 E-6
24.937	3.194 E-6	24.938	4.308 E-6	24.929	5.562 E-6	24.917	6.955 E-6
24.947	3.005 E-6	24.948	3.821 E-6	24.939	5.214 E-6	24.927	6.507 E-6
24.957	2.856 E-6	24.958	3.512 E-6	24.959	4.637 E-6	24.947	5.811 E-6
24.967	2.677 E-6	24.968	3.353 E-6	24.979	4.199 E-6	24.967	5.055 E-6
24.977	2.338 E-6	24.978	3.194 E-6	24.999	3.801 E-6	24.987	4.856 E-6
24.987	2.149 E-6	24.988	2.965 E-6	25.019	3.035 E-6	25.007	4.448 E-6
24.997	2.070 E-6	24.998	2.856 E-6	25.039	2.886 E-6	25.027	3.960 E-6
25.017	1.711 E-6	25.008	2.647 E-6	25.059	2.716 E-6	25.047	3.662 E-6
25.037	1.632 E-6	25.018	2.448 E-6	25.079	2.378 E-6	25.067	3.542 E-6

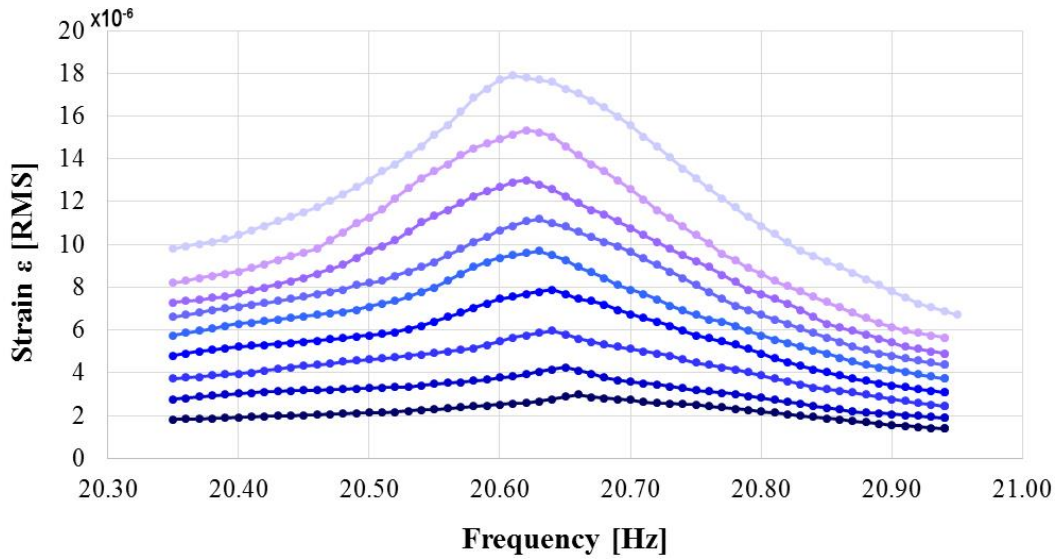


Figure 59: **Kevlar® 29**: values of frequency response recorded around resonance for increasing levels of driving force.

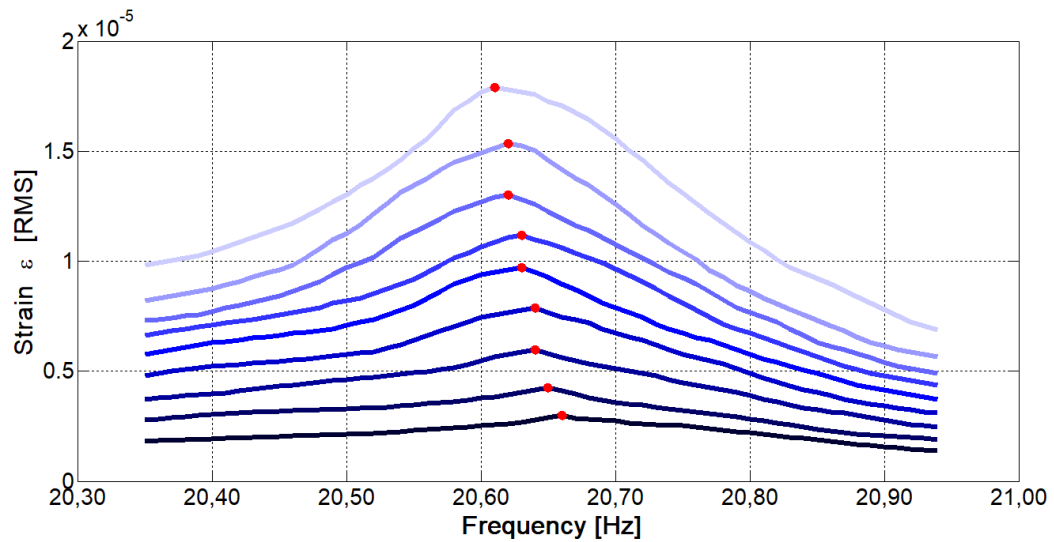


Figure 60: **Kevlar® 29**: frequency response measured around resonance for increasing levels of driving force. The maximum value is indicated by red dot.

**Table 10: Kevlar® 29:** strain values calculated from the numerical data acquired during the forced tests.

2.0 [V]		3.0 [V]		4.0 [V]		5.0 [V]	
Freq.	$\varepsilon$	Freq.	$\varepsilon$	Freq.	E	Freq.	$\varepsilon$
[Hz]	[RMS]	[Hz]	[RMS]	[Hz]	[RMS]	[Hz]	[RMS]
20.35	1.812E-6	20.35	2.772 E-6	20.35	3.731 E-6	20.35	4.797 E-6
20.36	1.834 E-6	20.36	2.814 E-6	20.36	3.774 E-6	20.36	4.904 E-6
20.37	1.855 E-6	20.37	2.900 E-6	20.37	3.817 E-6	20.37	5.011 E-6
20.38	1.876 E-6	20.38	2.942 E-6	20.38	3.881 E-6	20.38	5.075 E-6
20.39	1.898 E-6	20.39	2.985 E-6	20.39	3.923 E-6	20.39	5.160 E-6
20.40	1.919 E-6	20.40	3.028 E-6	20.40	3.966 E-6	20.40	5.224 E-6
20.41	1.940 E-6	20.41	3.070 E-6	20.41	4.009 E-6	20.41	5.267 E-6
20.42	1.962 E-6	20.42	3.113 E-6	20.42	4.115 E-6	20.42	5.309 E-6
20.43	1.983 E-6	20.43	3.134 E-6	20.43	4.179 E-6	20.43	5.352 E-6
20.44	2.004 E-6	20.44	3.156 E-6	20.44	4.264 E-6	20.44	5.394 E-6
20.45	2.026 E-6	20.45	3.177 E-6	20.45	4.328 E-6	20.45	5.437 E-6
20.46	2.047 E-6	20.46	3.198 E-6	20.46	4.371 E-6	20.46	5.501 E-6
20.47	2.068 E-6	20.47	3.220 E-6	20.47	4.435 E-6	20.47	5.565 E-6
20.48	2.090 E-6	20.48	3.241 E-6	20.48	4.520 E-6	20.48	5.629 E-6
20.49	2.111 E-6	20.49	3.262 E-6	20.49	4.584 E-6	20.49	5.693 E-6
20.50	2.132 E-6	20.50	3.284 E-6	20.50	4.627 E-6	20.50	5.757 E-6
20.51	2.154 E-6	20.51	3.305 E-6	20.51	4.670 E-6	20.51	5.821 E-6
20.52	2.175 E-6	20.52	3.326 E-6	20.52	4.733 E-6	20.52	5.885 E-6
20.53	2.217 E-6	20.53	3.348 E-6	20.53	4.797 E-6	20.53	6.055 E-6
20.54	2.260 E-6	20.54	3.412 E-6	20.54	4.861 E-6	20.54	6.183 E-6
20.55	2.303 E-6	20.55	3.475 E-6	20.55	4.925 E-6	20.55	6.397 E-6
20.56	2.345 E-6	20.56	3.539 E-6	20.56	4.989 E-6	20.56	6.610 E-6
20.57	2.388 E-6	20.57	3.561 E-6	20.57	5.075 E-6	20.57	6.823 E-6
20.58	2.431 E-6	20.58	3.625 E-6	20.58	5.160 E-6	20.58	7.036 E-6
20.59	2.473 E-6	20.59	3.689 E-6	20.59	5.288 E-6	20.59	7.249 E-6
20.60	2.516 E-6	20.60	3.774 E-6	20.60	5.480 E-6	20.60	7.463 E-6
20.61	2.559 E-6	20.61	3.838 E-6	20.61	5.650 E-6	20.61	7.569 E-6
20.61	2.601 E-6	20.61	3.945 E-6	20.61	5.757 E-6	20.61	7.676 E-6
20.63	2.665 E-6	20.63	4.051 E-6	20.63	5.864 E-6	20.63	7.783 E-6

---

20.64	2.772 E-6	20.64	4.158 E-6	20.64	5.970 E-6	20.64	7.889 E-6
20.65	2.878 E-6	20.65	4.264 E-6	20.65	5.800 E-6	20.65	7.676 E-6
20.66	2.985 E-6	20.66	4.115 E-6	20.66	5.608 E-6	20.66	7.463 E-6
20.67	2.857 E-6	20.67	3.966 E-6	20.67	5.458 E-6	20.67	7.356 E-6
20.68	2.814 E-6	20.68	3.795 E-6	20.68	5.330 E-6	20.68	7.186 E-6
20.69	2.772 E-6	20.69	3.667 E-6	20.69	5.224 E-6	20.69	6.930 E-6
20.70	2.729 E-6	20.70	3.582 E-6	20.70	5.117 E-6	20.70	6.738 E-6
20.71	2.644 E-6	20.71	3.518 E-6	20.71	5.011 E-6	20.71	6.567 E-6
20.72	2.601 E-6	20.72	3.454 E-6	20.72	4.904 E-6	20.72	6.397 E-6
20.73	2.559 E-6	20.73	3.369 E-6	20.73	4.797 E-6	20.73	6.183 E-6
20.74	2.537 E-6	20.74	3.284 E-6	20.74	4.627 E-6	20.74	5.970 E-6
20.75	2.516 E-6	20.75	3.198 E-6	20.75	4.478 E-6	20.75	5.757 E-6
20.76	2.452 E-6	20.76	3.134 E-6	20.76	4.371 E-6	20.76	5.629 E-6
20.77	2.388 E-6	20.77	3.070 E-6	20.77	4.264 E-6	20.77	5.480 E-6
20.78	2.324 E-6	20.78	3.006 E-6	20.78	4.158 E-6	20.78	5.330 E-6
20.79	2.260 E-6	20.79	2.921 E-6	20.79	4.030 E-6	20.79	5.117 E-6
20.80	2.196 E-6	20.80	2.836 E-6	20.80	3.881 E-6	20.80	4.904 E-6
20.81	2.132 E-6	20.81	2.751 E-6	20.81	3.731 E-6	20.81	4.691 E-6
20.82	2.068 E-6	20.82	2.644 E-6	20.82	3.603 E-6	20.82	4.499 E-6
20.83	2.004 E-6	20.83	2.559 E-6	20.83	3.454 E-6	20.83	4.328 E-6
20.84	1.940 E-6	20.84	2.452 E-6	20.84	3.305 E-6	20.84	4.158 E-6
20.85	1.876 E-6	20.85	2.367 E-6	20.85	3.241 E-6	20.85	4.030 E-6
20.86	1.812 E-6	20.86	2.281 E-6	20.86	3.156 E-6	20.86	3.881 E-6
20.87	1.748 E-6	20.87	2.196 E-6	20.87	3.092 E-6	20.87	3.731 E-6
20.88	1.684 E-6	20.88	2.154 E-6	20.88	2.985 E-6	20.88	3.625 E-6
20.89	1.620 E-6	20.89	2.111 E-6	20.89	2.878 E-6	20.89	3.518 E-6
20.90	1.557 E-6	20.90	2.068 E-6	20.90	2.772 E-6	20.90	3.412 E-6
20.91	1.514 E-6	20.91	2.026 E-6	20.91	2.687 E-6	20.91	3.326 E-6
20.92	1.471 E-6	20.92	1.983 E-6	20.92	2.580 E-6	20.92	3.241 E-6
20.93	1.429 E-6	20.93	1.940 E-6	20.93	2.516 E-6	20.93	3.156 E-6
20.94	1.386 E-6	20.94	1.898 E-6	20.94	2.452 E-6	20.94	3.092 E-6

---

6.0 [V]		7.0 [V]		8.0 [V]		9.0 [V]		10.0 [V]	
Freq. [Hz]	$\varepsilon$ [RMS]								
20.35	5.76E-6	20.35	6.61E-6	20.35	7.29E-6	20.35	8.21E-6	20.35	9.81E-6
20.36	5.86E-6	20.36	6.72E-6	20.36	7.36E-6	20.36	8.32E-6	20.36	9.92E-6
20.37	5.97E-6	20.37	6.82E-6	20.37	7.42E-6	20.37	8.42E-6	20.37	10.02E-6
20.38	6.08E-6	20.38	6.93E-6	20.38	7.51E-6	20.38	8.53E-6	20.38	10.13E-6
20.39	6.18E-6	20.39	7.02E-6	20.39	7.57E-6	20.39	8.63E-6	20.39	10.24E-6
20.40	6.29E-6	20.40	7.10E-6	20.40	7.72E-6	20.40	8.74E-6	20.40	10.45E-6
20.41	6.35E-6	20.41	7.19E-6	20.41	7.87E-6	20.41	8.91E-6	20.41	10.66E-6
20.42	6.42E-6	20.42	7.27E-6	20.42	7.99E-6	20.42	9.08E-6	20.42	10.87E-6
20.43	6.50E-6	20.43	7.36E-6	20.43	8.14E-6	20.43	9.27E-6	20.43	11.09E-6
20.44	6.57E-6	20.44	7.46E-6	20.44	8.29E-6	20.44	9.45E-6	20.44	11.30E-6
20.45	6.63E-6	20.45	7.57E-6	20.45	8.42E-6	20.45	9.62E-6	20.45	11.51E-6
20.46	6.72E-6	20.46	7.68E-6	20.46	8.64E-6	20.46	9.81E-6	20.46	11.73E-6
20.47	6.78E-6	20.47	7.78E-6	20.47	8.85E-6	20.47	10.19E-6	20.47	12.05E-6
20.48	6.84E-6	20.48	7.89E-6	20.48	9.06E-6	20.48	10.58E-6	20.48	12.37E-6
20.49	6.93E-6	20.49	8.10E-6	20.49	9.38E-6	20.49	10.98E-6	20.49	12.69E-6
20.50	7.08E-6	20.50	8.21E-6	20.50	9.70E-6	20.50	11.26E-6	20.50	13.01E-6
20.51	7.23E-6	20.51	8.32E-6	20.51	9.92E-6	20.51	11.64E-6	20.51	13.43E-6
20.52	7.36E-6	20.52	8.53E-6	20.52	10.19E-6	20.52	12.15E-6	20.52	13.75E-6
20.53	7.57E-6	20.53	8.74E-6	20.53	10.59E-6	20.53	12.63E-6	20.53	14.18E-6
20.54	7.78E-6	20.54	8.96E-6	20.54	11.05E-6	20.54	13.11E-6	20.54	14.61E-6
20.55	7.80E-6	20.55	9.17E-6	20.55	11.34E-6	20.55	13.43E-6	20.55	15.14E-6
20.56	8.32E-6	20.56	9.49E-6	20.56	11.62E-6	20.56	13.73E-6	20.56	15.56E-6
20.57	8.64E-6	20.57	9.81E-6	20.57	11.94E-6	20.57	14.18E-6	20.57	16.21E-6
20.58	8.95E-6	20.58	10.13E-6	20.58	12.26E-6	20.58	14.49E-6	20.58	16.84E-6
20.59	9.17E-6	20.59	10.34E-6	20.59	12.47E-6	20.59	14.71E-6	20.59	17.27E-6
20.60	9.38E-6	20.60	10.66E-6	20.60	12.69E-6	20.60	14.96E-6	20.60	17.69E-6
20.61	9.49E-6	20.61	10.87E-6	20.61	12.90E-6	20.61	15.14E-6	20.61	17.91E-6

---

20.62	9.59E-6	20.62	11.09E-6	20.62	13.01E-6	20.62	15.35E-6	20.62	17.80E-6
20.63	9.70E-6	20.63	11.19E-6	20.63	12.79E-6	20.63	15.25E-6	20.63	17.69E-6
20.64	9.49E-6	20.64	10.98E-6	20.64	12.58E-6	20.64	15.03E-6	20.64	17.59E-6
20.65	9.26E-6	20.65	10.83E-6	20.65	12.26E-6	20.65	14.61E-6	20.65	17.27E-6
20.66	8.95E-6	20.66	10.59E-6	20.66	11.94E-6	20.66	14.18E-6	20.66	17.06E-6
20.67	8.69E-6	20.67	10.34E-6	20.67	11.62E-6	20.67	13.75E-6	20.67	16.74E-6
20.68	8.42E-6	20.68	10.13E-6	20.68	11.41E-6	20.68	13.43E-6	20.68	16.42E-6
20.69	8.10E-6	20.69	9.92E-6	20.69	11.09E-6	20.69	13.01E-6	20.69	15.99E-6
20.70	7.89E-6	20.70	9.64E-6	20.70	10.77E-6	20.70	12.58E-6	20.70	15.57E-6
20.71	7.68E-6	20.71	9.34E-6	20.71	10.45E-6	20.71	12.11E-6	20.71	15.03E-6
20.72	7.44E-6	20.72	9.06E-6	20.72	10.13E-6	20.72	11.62E-6	20.72	14.61E-6
20.73	7.14E-6	20.73	8.74E-6	20.73	9.81E-6	20.73	11.24E-6	20.73	14.07E-6
20.74	6.91E-6	20.74	8.42E-6	20.74	9.51E-6	20.74	10.83E-6	20.74	13.54E-6
20.75	6.72E-6	20.75	8.10E-6	20.75	9.23E-6	20.75	10.45E-6	20.75	13.09E-6
20.76	6.50E-6	20.76	7.78E-6	20.76	8.96E-6	20.76	10.06E-6	20.76	12.62E-6
20.77	6.39E-6	20.77	7.46E-6	20.77	8.59E-6	20.77	9.55E-6	20.77	12.15E-6
20.78	6.18E-6	20.78	7.14E-6	20.78	8.25E-6	20.78	9.26E-6	20.78	11.73E-6
20.79	5.97E-6	20.79	6.93E-6	20.79	7.89E-6	20.79	8.89E-6	20.79	11.30E-6
20.80	5.76E-6	20.80	6.72E-6	20.80	7.68E-6	20.80	8.64E-6	20.80	10.87E-6
20.81	5.54E-6	20.81	6.50E-6	20.81	7.46E-6	20.81	8.32E-6	20.81	10.49E-6
20.82	5.39E-6	20.82	6.29E-6	20.82	7.25E-6	20.82	8.06E-6	20.82	10.08E-6
20.83	5.22E-6	20.83	6.08E-6	20.83	6.93E-6	20.83	7.80E-6	20.83	9.70E-6
20.84	5.05E-6	20.84	5.86E-6	20.84	6.61E-6	20.84	7.57E-6	20.84	9.47E-6
20.85	4.90E-6	20.85	5.65E-6	20.85	6.29E-6	20.85	7.31E-6	20.85	9.21E-6
20.86	4.71E-6	20.86	5.44E-6	20.86	6.12E-6	20.86	7.06E-6	20.86	8.95E-6
20.87	4.54E-6	20.87	5.22E-6	20.87	5.97E-6	20.87	6.82E-6	20.87	8.68E-6
20.88	4.37E-6	20.88	5.07E-6	20.88	5.80E-6	20.88	6.57E-6	20.88	8.38E-6
20.89	4.26E-6	20.89	4.90E-6	20.89	5.61E-6	20.89	6.31E-6	20.89	8.10E-6
20.90	4.16E-6	20.90	4.78E-6	20.90	5.42E-6	20.90	6.14E-6	20.90	7.80E-6
20.91	4.05E-6	20.91	4.69E-6	20.91	5.22E-6	20.91	5.97E-6	20.91	7.53E-6

---

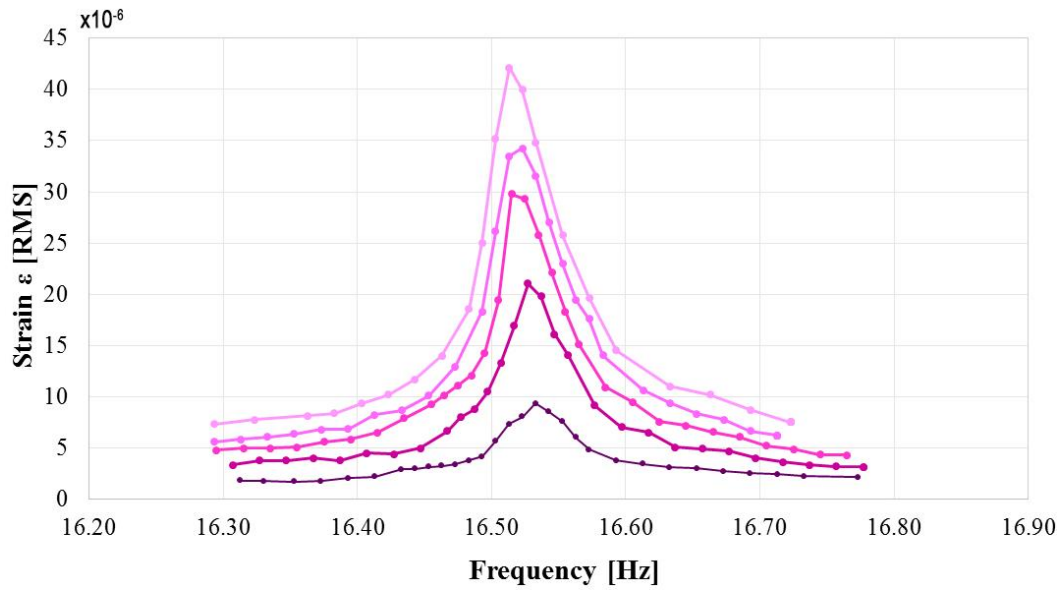


Figure 61: **Carbon:** values of frequency response recorded around resonance for increasing levels of driving force.

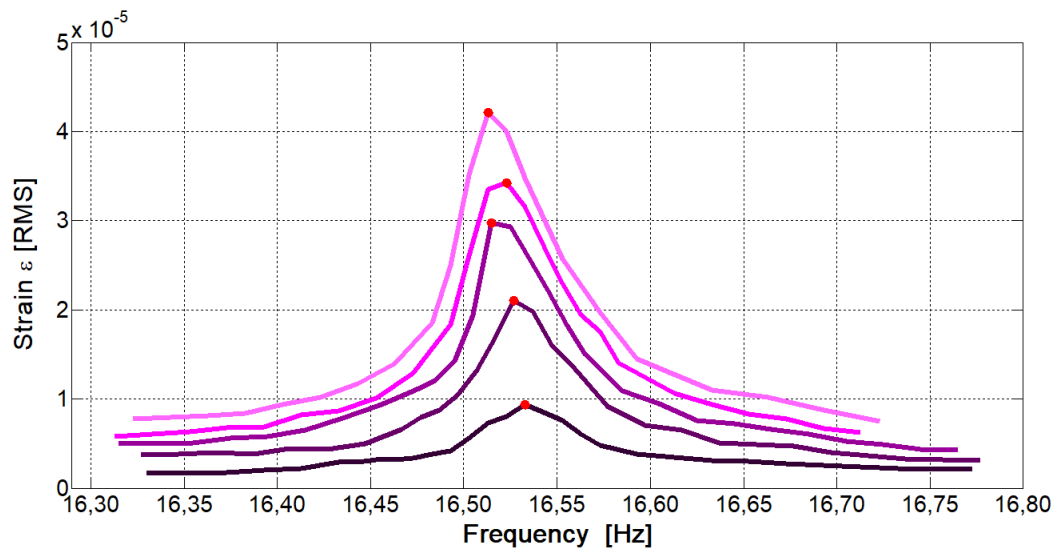


Figure 62: **Carbon:** frequency response measured around resonance for increasing levels of driving force. The maximum value is indicated by red dot.

**Table 11: Carbon:** strain values calculated from the numerical data acquired during the forced tests.

1.0 [V]		3.0 [V]		5.0 [V]		7.0 [V]		9.0 [V]	
Freq.	$\epsilon$								
[Hz]	[RMS]								
16.31	1.821E-6	16.31	3.343E-6	16.30	4.776E-6	16.29	5.612E-6	16.29	7.313E-6
16.33	1.731E-6	16.33	3.761E-6	16.32	4.955E-6	16.31	5.821E-6	16.32	7.731E-6
16.35	1.701E-6	16.35	3.791E-6	16.34	4.985E-6	16.33	6.090E-6	16.36	8.119E-6
16.37	1.761E-6	16.37	4.030E-6	16.36	5.045E-6	16.35	6.358E-6	16.38	8.358E-6
16.39	2.060E-6	16.39	3.791E-6	16.38	5.612E-6	16.37	6.776E-6	16.40	9.343E-6
16.41	2.209E-6	16.41	4.478E-6	16.40	5.821E-6	16.39	6.836E-6	16.42	10.179E-6
16.43	2.925E-6	16.43	4.388E-6	16.42	6.507E-6	16.41	8.239E-6	16.44	11.701E-6
16.44	2.955E-6	16.45	4.955E-6	16.44	7.881E-6	16.43	8.657E-6	16.46	14.000E-6
16.45	3.164E-6	16.47	6.627E-6	16.46	9.254E-6	16.45	10.119E-6	16.48	18.567E-6
16.46	3.224E-6	16.48	7.970E-6	16.47	10.149E-6	16.47	12.925E-6	16.49	25.045E-6
16.47	3.403E-6	16.49	8.776E-6	16.48	11.104E-6	16.49	18.328E-6	16.50	35.164E-6
16.48	3.791E-6	16.50	10.478E-6	16.49	12.060E-6	16.50	26.119E-6	16.51	42.119E-6
16.49	4.149E-6	16.51	13.254E-6	16.50	14.269E-6	16.51	33.493E-6	16.52	39.970E-6
16.50	5.642E-6	16.52	16.925E-6	16.51	19.403E-6	16.52	34.239E-6	16.53	34.806E-6
16.51	7.313E-6	16.53	21.045E-6	16.52	29.791E-6	16.53	31.582E-6	16.55	25.731E-6
16.52	8.030E-6	16.54	19.791E-6	16.53	29.284E-6	16.54	27.075E-6	16.57	19.672E-6
16.53	9.343E-6	16.55	16.090E-6	16.54	25.791E-6	16.55	22.955E-6	16.59	14.507E-6
16.54	8.507E-6	16.56	14.060E-6	16.55	22.090E-6	16.56	19.433E-6	16.63	11.015E-6
16.55	7.552E-6	16.58	9.164E-6	16.56	18.328E-6	16.57	17.582E-6	16.66	10.179E-6
16.56	6.030E-6	16.60	7.045E-6	16.57	15.075E-6	16.58	14.030E-6	16.69	8.716E-6
16.57	4.836E-6	16.62	6.507E-6	16.59	10.925E-6	16.61	10.657E-6	16.72	7.522E-6

From the experimental results previously reported in Figures 57-62, a weak nonlinear behaviour of the response was evident. Increasing the input voltage, the peak of the curves indicates that the resonance frequency tends to shift towards lower values of frequency.

### **Survey on nonlinear system identification in structural dynamics**

System identification is a method of estimating the mathematical model of a system from input and output measurements. System identification methodologies can be employed to a broad range of applications like industrial processes, control systems, economic data, biology and the life sciences, medicine, social systems and many more.

The most common approaches in system identification assume a linear relationship between input and output. Modal identification is the most common and widely applied approach in the structural engineering field. It entails estimating the modal parameters of the investigated structure on the basis of vibration data collected.

Most systems encountered in the real world are nonlinear to some extent, and in many practical applications nonlinear models are required to achieve an acceptable prediction accuracy.

One of the most recent and comprehensive classifications and reviews on nonlinear identification methodologies is proposed by Kerschen (Noël & Kerschen, 2017) (Kerschen, et al., 2006). He suggests to consider the identification of nonlinear structural models as a three-step process:

- detection
- characterization
- parameter estimation

The focus of his literature review is on the classification of parameter estimation methods. They may fall into seven categories:

- linearization methods
- time-domain methods
- frequency-domain methods
- time-frequency domain methods
- modal methods
- black-box modelling
- numerical modal updating

### *Linearization method*

These methods consist in linearizing the nonlinear dynamic behaviour of a structure around its operating point. Linearization bring to two main issues. Firstly, the linearized models are essentially valid for a unique set of excitation parameters, preventing them from being interpolated (i.e. used to predict the structural response at lower forcing levels). Second, they fail to predict intrinsically nonlinear phenomena, including harmonics, jumps or modal interactions. However, using linear system identification to model nonlinear structures has persisted to be a popular solution. The reason for this is probably the understanding and widespread use of linear techniques (Pintelon and Schoukens 2001) (Ewins 2000) (Maia and Silva 1997) (Ljung, 1999). In addition, most standardised design and certification procedures followed in industry are based on linear structural models.

Schoukens and co-workers provide a solid theoretical framework to derive the best possible linear model of a nonlinear system, in a least-squares optimally sense. Another frequency-domain linearization method applicable to random data was introduced in 2009 by Grange et al. (Grange, et al., 2009). In this paper, the nonlinear dynamics of break squeal was studied by seeking a linear model which synthesises at best the measured power spectral density of the nonlinear system output. Recently, Wang followed a similar reasoning to propose the equivalent dynamic stiffness mapping technique (Wang & Zheng, 2016).

Finally, some authors have considered the use of time-varying models as a linearization tools, suggesting that, by analysing nonlinear vibrations over small portions of time, linear system identification may reasonably well apply. In addition, Sracic and Allen (Sracic & Allen, 2011) pursued that idea by fitting linear time-periodic models to transient data recorded in response to slight perturbations superposed to sustained periodic excitations. The method was originally demonstrated using single-degree-of-freedom systems, but its application to multiple degrees of freedom followed in 2014 (M.W.Sracic, 2014).

### *Time-domain method*

The time-domain identification of nonlinear structural models exclusively relies on processing time series. Three major identification techniques were distinguished, namely:

- RFS: restoring force surface method

- NARMAX: nonlinear autoregressive moving average with exogenous inputs modelling
- TNSI: time-domain nonlinear subspace identification method

In a NARMAX technique, the system is modelled in terms of a nonlinear functional expansion of lagged input, output and prediction errors. The functional description of an actual system can be very complex and the explicit form of this functional is usually unknown. Therefore, the practical modelling of real signal must be based upon a chosen set of the unknown functions. The input–output model is a means of describing the dynamics of a system. Furthermore, an important question regarding the model is how to relate this information in some straightforward way that will provide an adequate approximation to a wide class of the systems with a reasonable computational cost. In general terms, it is admitted that apply the NARMAX framework to large-scale structures is a difficult to endeavour, as it suffers from a rapid explosion in the number of parameters, even in the case of systems with reasonable dimension (Chen, et al., 2007) (Peng, et al., 2011).

The RFS method constitutes one of the earliest identification methodologies (Masri & Caughey, 2010). It has continued to attract attention during the past decade. Parameter estimation based on the RFS method is commonly restricted to systems with a few degrees of freedom. It consists in the direct fitting of Newton’s second law. However, the method can still be exploited to visualise qualitatively nonlinear restoring forces in complex structures.

Applications of the RFS method to identification of nonlinear stiffness mechanisms have been numerous. In a work of Saad et al. (Saad, et al. 2006), the prediction capabilities of a nonlinear restoring force model of two elastomer specimens were compared to rheological equations based on traction-compression and shear test data. Complex damping nonlinearities have equally been addressed in the technical literature (Worden, et al. 2009) (Ceravolo, Erlicher and Zanotti Fragonara 2013) (Xu, He and Dyke 2015).

Nonlinear subspace methods, originally proposed in the control literature (Lacy and Bernstein 2005), were first applied to mechanical systems by Marchisiello & Garibaldi in 2008 (Marchesiello and Garibaldi 2008). The time-domain nonlinear subspace identification (TNSI) method represents a major advance across the field. TNSI is a nonlinear generalisation of the classical time-domain linear subspace identification algorithms (VanOverschee and DeMoor

1996). The implementation of this method builds on robust numerical tools, such as the QR and singular value decompositions, yielding superior accuracy compared to competing approaches like the NIFO (Adams & Allemang, 1999) and the conditioned reverse path (CRP) technique (Richards and Singh 1998), which will be introduced in the subsection dedicated to frequency-domain methods.

#### *Frequency-domain methods*

The frequency domain methods use to process a wider type of data than in the time-domain. They can take the form of Fourier spectra, frequency response and transmissibility functions, or power spectra densities.

Three methods were surveyed as promising frequency-domain approaches:

- NIFO, the nonlinear identification through feedback of the outputs (Richards & Singh, 1998)
- CRP, the conditioned reverse path methods (Richards & Singh, 1998)
- Volterra series (Schetzen 1980).

NIFO method is based on a compact formulation referred to as nonlinear identification through feedback of the outputs. The data associated with the spatial configuration of the nonlinearities provide additional information that is needed to simultaneously identify the linear and nonlinear parts of the system. Adams and Allemang (Adams & Allemang, 1999) introduced the frequency domain nonlinear identification in the form of a method that decouples the linear and nonlinear dynamics of a system and estimates the linear and nonlinear components in one computational step.

CRP method is based on the construction of a hierarchy of uncorrelated response components in the frequency domain. If excitations are applied at each response location, parameter estimation is completed by solving an algebraic system for each frequency, by using the reverse path method. However, when the number of excitations is smaller than the number of response locations and non-linearities are far from the locations of the excitations, the reverse path method cannot be directly applied (Garibaldi 2003).

Another traditional way of addressing system identification in the frequency domain is the use of functional series, and in particular of the Volterra series

(Schetzen, 1980). In short the output can be considered a nonlinear convolution of the input where nonlinear behaviours are captured by high order kernels (Friston, et al., 2000). The common limit of Volterra identification of high-dimensional systems is the very high number of parameters to be estimated. Volterra series have also constituted the basis of the new concept of nonlinear output frequency response functions developed during the last 10 years or so by Billings and co-workers (Lang & Billings, 2005) (Peng, et al., 2007). This method found application in linear (Peng, et al., 2007) and nonlinear (Peng, et al., 2008) system identification.

#### *Time-frequency methods*

Because nonlinear oscillations are intrinsically frequency-energy dependent, time–frequency transformations generally offer useful insight into the dynamics of nonlinear systems. Well-established methods, such as the wavelet and Hilbert transforms, have continued to be used during the last 10 years as nonlinear system identification tools, and, particularly, in the identification of backbone curves, (Heller, et al., 2009) (Demarie, et al., 2010). In addition, two new techniques for the decomposition of multicomponent signals emerged during this period:

- EMD, the empirical mode decomposition (Norden Huang, et al., 1998)
- HVD, Hilbert vibration decomposition (Feldman, 2006) (Feldman, 2007).
- TFIE, time-frequency instantaneous estimator (Spina, et al., 1996) (Ceravolo, et al., 2013).

The idea of EMD is to decompose the original signal into a sum of elemental components, the intrinsic mode functions (IMFs). The extraction process, termed sifting process, relies on a spline approximation of the lower and upper envelopes of the signal based on its extrema (Kerschen, et al., 2008).

HVD method is a distinct approach to the decomposition of a vibration signal into a series of mono-component signals. HVD is based on the assumptions that the original signal is formed of a superposition of quasi-harmonic functions, and that the envelopes of each vibration component differ.

The HVD method was applied for the identification of nonlinear systems with two degrees of freedom (Feldman, 2007), but has not yet been applied to larger-scale structures. It found different applications in structural dynamics

(Gendelman, et al., 2008) and the analysis of linear (Bertha & Golinval, 2014) and nonlinear (Feldman, 2014) time-varying systems.

The EMD and HVD methods have limitations and have to be used with great attention (Braun & Feldman, 2011) (Huang, et al., 2012). Despite everything, they represent important additions to the nonlinear structural dynamist's toolbox.

TFIE is a method recently proposed able to cope with non-linear and hysteretic systems where the parameter identification can be carried out minimising a residual signal in the time-frequency domain using any time-frequency transform. This allows to the estimation of instantaneous optimal estimator of the model.

### *Modal methods*

Modal features (natural frequencies, damping ratios and mode shapes), form the basis of classical linear design strategies in engineering dynamics. They provide an effective and intuitive way to study the structural behaviour around resonances, which is one of the main limiting factors as for integrity and certification (Ewins, 2006). On the contrary, nonlinear modal identification is a quite recent research field, as confirmed by the very few related methods surveyed in 2006 (Kerschen, et al., 2006). Nowadays it is a very active area of investigation that has showed important progress during the last decade. These progresses have been accompanied by the emergence of efficient algorithms, to carry out theoretical nonlinear modal analysis (Renson, et al., 2016).

The popularity of modal analysis stems from its great generality. Modal parameters can describe the behaviour of a system for any input type and any range of the input.

A couple of example of nonlinear modal method are

- CONCERTO method
- NLRDM method

The COde for Nonlinear identifiCation from mEasured Response To vibratiOn (CONCERTO), proposed by Carrella et al. (Carrella & Ewins, 2011) identifies an isolated nonlinear resonance based on stepped-sine data. Since CONCERTO relies on a single-harmonic assumption, it adopts a linearized view of nonlinear modal identification, and yields equivalent natural frequencies and damping ratios which vary with the amplitude of motion.

Unlike CONCERTO, the nonlinear resonant decay method (NLRDM) can perform multiple-mode identification by introducing nonlinear coupling terms in an otherwise linear modal-space model of the tested structure. This method was recognised as one of the most promising nonlinear modal identification approaches in the early 2000s (Kerschen, et al., 2006). If no further developments of the theoretical foundations of NLRDM were brought during the last 10 years, the method was successfully validated using structures of increasing complexity, namely a two-degree-of-freedom system with free play (Yang, et al., 2006), a single-bay panel structure (Platten, et al., 2009), a wing with two stores connected by means of nonlinear pylons (Platten, et al., 2009), a geometrically nonlinear joined-wing structure, and a complete transport aircraft (Fuellekrug & Goege, 2012).

#### *Black-box method*

The aforementioned nonlinear system identification methodologies are essentially based on the selection of a model structure based on available prior knowledge, and processing data to estimate its parameters. Accessing prior knowledge, can however be very difficult in many cases owing to the highly individualistic nature of real nonlinearities. This makes very difficult the specification of an accurate, physically-motivated model in terms of macroscopic nonlinear stiffness and damping lumped elements. The nonlinear black-box situation is much more difficult. The main reason is that nothing is excluded, and a very rich spectrum of possible model descriptions must be handled.

Recently, a new black-box model structure based on a state-space representation of measured data was proposed (Paduart, et al., 2010). It builds on nonlinear model terms constructed as a multivariate polynomial combination of the state and input variables. This approach proved successful in the identification of very diverse nonlinear systems, including a magnetorheological damper (Paduart, et al., 2010), a wet-clutch device (Widanage, et al., 2011), and a Li-Ion battery (Relan, et al., 2015). However, as usual in black-box identification, it suffers from a combinatorial increase in the number of parameters because of the multivariate nature of the representation.

#### *Model updating method*

Techniques to detect damage in civil structures using vibrational data have been under development for about two decades, and are currently a topic of widespread interest in the international community (Wu & Abe, 2003).

Numerical models have to be compared with experimental data and subsequently updated to improve their reliability.

Nonlinear modal updating method should be used for different applications. Evaluating degradation in the capacity of a structure requires construction of an updated nonlinear finite element (FE) model. In each structures, it is necessary to distinguish between the various types of damage to have a true understanding of the condition of the structure, and this may only be possible through proper updating of a nonlinear FE model. Each model updating technique has its assumptions and applicable range. Over the lifetime of a structure, it is possible that these assumptions may not hold at all times. It is possible to apply a linear or nonlinear model updating as required.

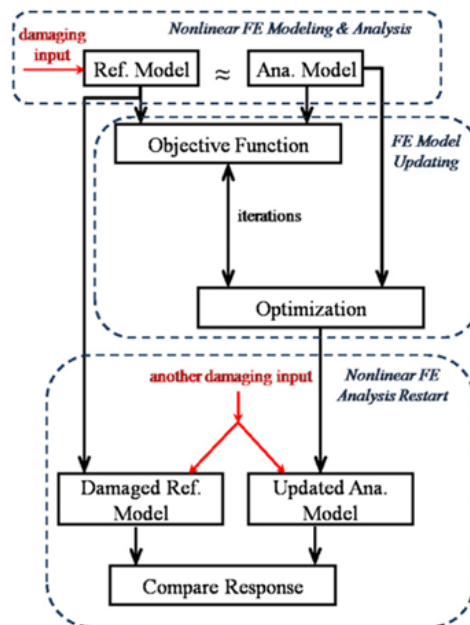


Figure 63: flowchart of the general numerical procedure. Source (Song, et al., 2013).

As shown in Figure 63, the entire procedure consists of three stages. In the first stage (i.e., nonlinear FE modelling and analysis), both reference and analytical models were built using the same material parameters (no damage), and then the damage was imposed to the reference model by enforcing a damaging loading condition. Then, the modal information of both models was fed into the objective function block, which was the beginning of the second stage. In the second stage (i.e., FE model updating), the discrepancies between the damaged reference model and the analytical model were compared in the scores of the objective function values. The analytical model was updated using a chosen

optimization program with iterative evaluations of the objective function value. The final stage (i.e., nonlinear FE analysis restart) was designed to check the efficacy of the updated model. By applying a new damaging input (a load case resulting in damage of the structure) to both the damaged reference model and the updated analytical model, the obtained responses were compared (Song, et al., 2013).

### **Dynamic parameter estimation**

Given the simplicity of the case and the materials under investigation, the non-linearity was considered enclosed in a cubic nonlinear coefficient. This solution seems to well apply to the described case.

To try to quantify this non-linearity, the following expression, which take into account it, was applied. The following expression defines the dynamics of a system excited by a harmonic force and characterized by a cubic non-linearity (Kalmar-Nagy & Balachandran, 2011):

$$\ddot{u} + 2\varepsilon\zeta\dot{u} + \omega_n^2u + \varepsilon\chi u^3 = F \cos(\Omega t) \quad (18)$$

where  $\zeta$  is the damping,  $\chi$  represents the coefficient of cubic non-linearity,  $\omega_n$  is the natural angular frequency of the linear system, and  $\Omega$  is the excitation frequency.

Equation (18) describes, the motion of a damped nonlinear oscillator having a more complicated behaviour compared to the simple harmonic motion. In physical terms, the equation (18) models a mass-spring system, whose spring stiffness does not exactly follow the Hooke's law. Our interest is on the cubic stiffness coefficient  $\chi$  (cubic non-linearity index), which controls the nonlinear part of the restoring force.

Respect to the linear behaviour, the amplitude of the response into the nonlinear one can varying depending on the material investigated. If  $\chi$  is negative, the material shows a softening behaviour, if is equal to zero represents a linear behaviour, and finally if is positive the material shows a hardening behaviour. In the following Figure 64 are shown an explanation of the response curves to varying the cubic stiffness coefficient  $\gamma$ , which was called  $\chi$  in this dissertation.

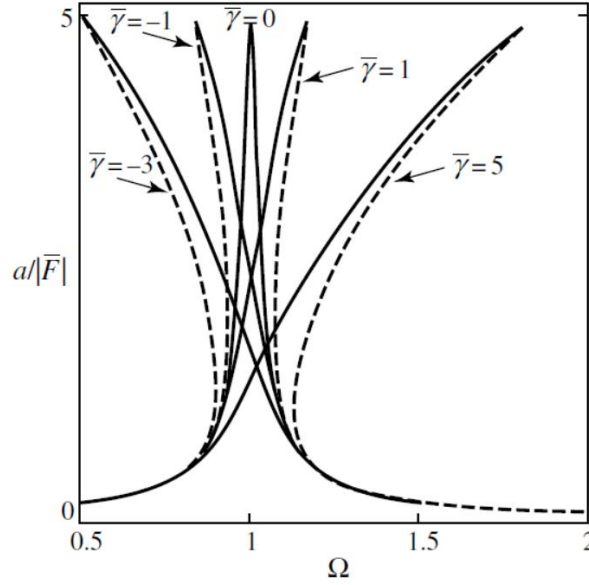


Figure 64: amplitude-response curves for a varying strength of nonlinearities  $\gamma$ .  
Source (Kalmar-Nagy & Balachandran, 2011).

### 5.1.3 Nonlinear identification of the backbone curve

In order to define the dynamics of a system characterized by cubic non-linearity excited by a harmonic force, the following expression found in the open literature, which represents the Duffing oscillator equation was exploited:

$$m\ddot{x} + c\dot{x} + kx + \chi x^3 = F \quad (19)$$

where  $F$  is the external sinusoidal forcing term,  $m$  the mass of the system,  $c$  the linear viscous damping term, and  $\chi$  the cubic stiffness coefficient, respectively.

In order to identify the nonlinear material behaviour, the Krylov-Bogoliubov method was used to determine the variation of the first nonlinear resonance frequency of a Duffing oscillator of equation 19. It was characterized by a nonlinear force-displacement relationship (Kalmar-Nagy & Balachandran, 2011) (Nayfeh & Mook, 1995).

The distortion in frequency  $f$  was quantified as:

$$f = f_n \left[ 1 + \frac{3\chi}{8k} a^2 \right] \quad (20)$$

where  $a$  is the amplitude of the response,  $k$  is the linear stiffness,  $f_n$  is the natural frequency and  $\chi$  is the cubic stiffness coefficient.

Equation 20 was used to identify the so-called backbone curve of the nonlinear response, as a red line in Figures 65-67 highlights it. The red dots indicate the maximum amplitude values, corresponding to the resonance frequency at different amplitudes of the external exciting force. The amplitude response of a nonlinear system is generally multivalued, as opposed to a linear system. The results presented below show a softening behavior (negative value of cubic stiffness parameter, because the response curve deviates toward lower frequencies).

This approach confirmed the high sensitivity of this new prototype-testing machine for the dynamic characterization of high-strength materials, with regard to low levels of non-linearity. Indeed, the nonlinear effects in the measurements were provided only by very small intrinsic nonlinear levels in the materials.

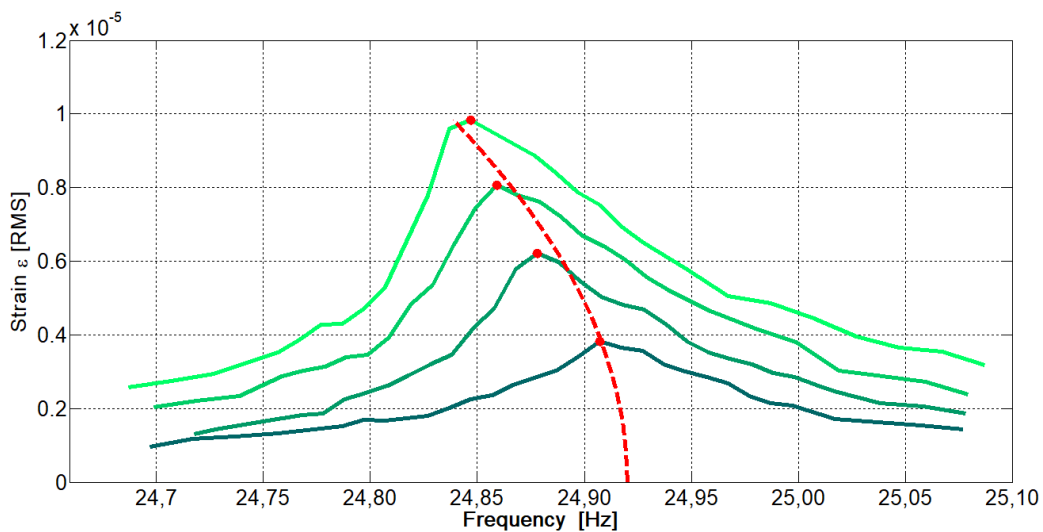


Figure 65: **Silicon Carbide**: frequency response measured around resonance for increasing levels of driving force. The red dots highlight the maximum of the response curve and the dashed red line is the estimated backbone response curve.

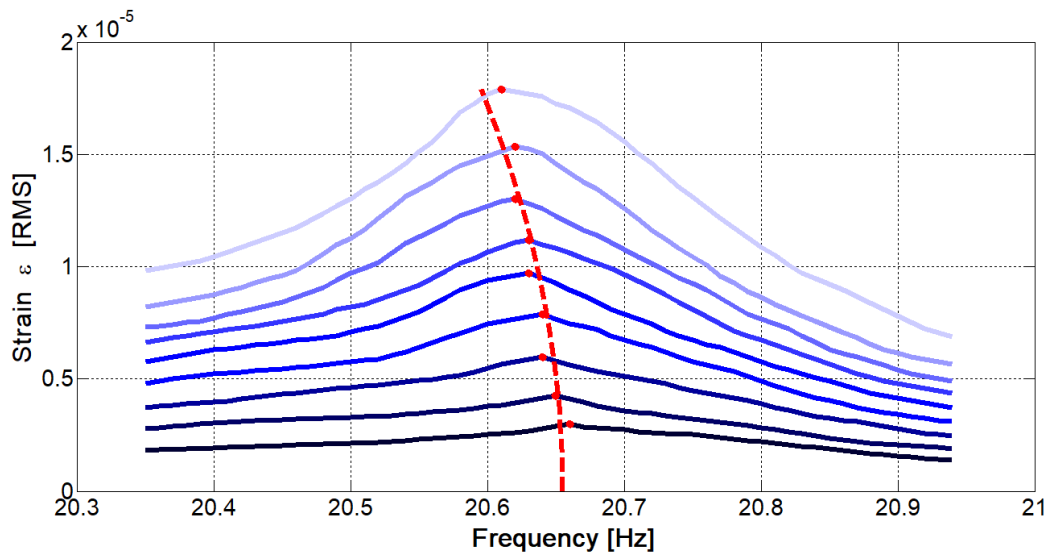


Figure 66: **Kevlar® 29**: frequency response measured around resonance for increasing levels of driving force. The red dots highlight the maximum of the response curve and the dashed red line is the estimated backbone response curve.

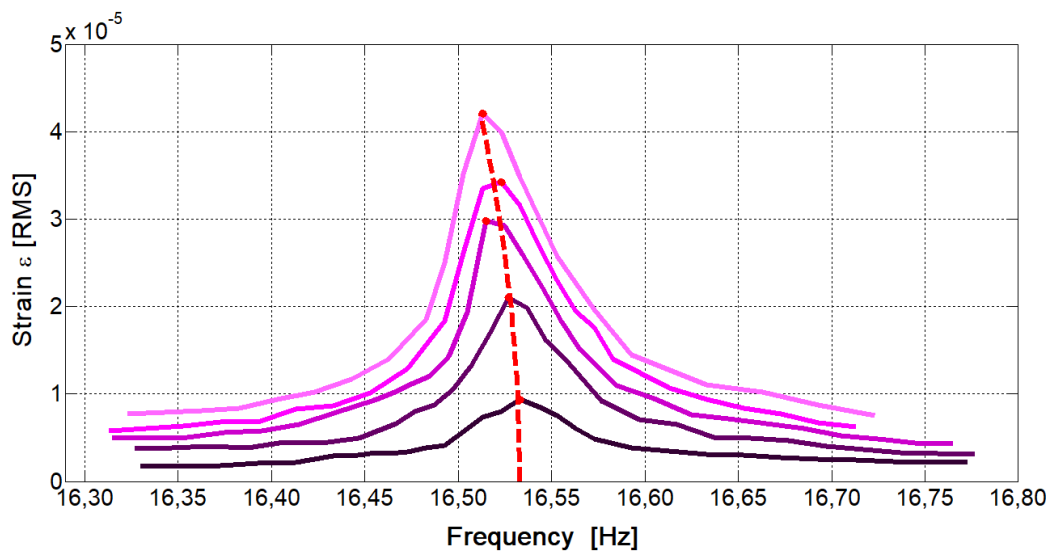


Figure 67: **Carbon**: frequency response measured around resonance for increasing levels of driving force. The red dots highlight the maximum of the response curve and the dashed red line is the estimated backbone response curve.

The cubic stiffness coefficient obtained in these cases are equal to  $\chi = -2.21 \cdot 10^{12} \text{ N/m}^3$  for silicon carbide sample,  $-4.03 \cdot 10^{11} \text{ N/m}^3$  for Kevlar® 29 sample in pristine condition, and  $-2.08 \cdot 10^{10} \text{ N/m}^3$  for carbon sample.

#### 5.1.4 Dissipation properties and quality factor: experimental evaluation

In physics and engineering the quality factor ( $Q$ ) is a dimensionless parameter that describes how under-damped an oscillator or resonator is, and characterizes a resonator's bandwidth relative to its centre frequency. Higher  $Q$  indicates a lower rate of energy loss relative to the stored energy of the resonator. Resonators with high quality factors have low damping so that they ring or vibrate longer.

In the context of resonators, there are two common definitions for  $Q$ , which are not necessarily equivalent. They become approximately equivalent as  $Q$  becomes larger, meaning the resonator becomes less damped. One of these definitions is the frequency-to-bandwidth ratio of the resonator:

$$Q = \frac{f_r}{\Delta_f} = \frac{\omega_r}{\Delta_\omega} \quad (21)$$

where  $f_r$  is the resonant frequency,  $\Delta_f$  is the resonance width or full width at half maximum (the bandwidth over which the power of vibration is greater than half the power at the resonant frequency),  $\omega_r = 2\pi f_r$  is the angular resonant frequency, and finally  $\Delta_\omega$  is the angular half-power bandwidth.

The other common definition for the quality factor is the ratio of the energy stored in the oscillating resonator to the energy dissipated per cycle by damping processes:

$$Q = 2\pi \frac{\text{Energy stored}}{\text{Energy dissipated per cycle}} = 2\pi f_r \frac{\text{Energy stored}}{\text{Power loss}} \quad (22)$$

where in electrical systems, the stored energy is the sum of energies stored in lossless inductors and capacitors, while the lost energy is the sum of the energies dissipated in resistors per cycle. In mechanical systems, the stored energy is the maximum possible stored energy, or the total energy (the sum of the potential and kinetic energies at some point in time, for example). The lost energy is the work

done by an external conservative force per cycle, for maintaining the amplitude. The description of how were calculated the energy stored and the power loss was previously explained in detail in chapter 4, section 4.5.

In addition, similar to the dynamic amplification factor  $R_d$ , the quality factor can be considered as the ratio between the displacement at resonance ( $u_r$ ) and the one due to a statically applied force ( $u_{st}$ ):

$$Q = \frac{u_r}{u_{st}} \quad (23)$$

The  $Q$  factor results to be an important parameter in the study of vibrating systems, and for the dynamic characterization of materials. It is a measure of the energy loss of an oscillating system and consequently a measure of the damping. The damping is therefore function of the  $Q$  factor by means of the relation below:

$$Q = \frac{1}{2\zeta} \quad (24)$$

No such comparison could be performed for the  $Q$  values and the non-linearity of the three materials, as no data were found in the open literature. The quality factors were measured in a number of different ways, besides the inverse of the 3 dB relative frequency width of the resonance. Approaches using the phase slope in frequency of the stress to strain transfer function, the 1/e quenching time after cutting the excitation, and the enhancement factor of the strain in resonance were also applied, all yielding pretty much the same values for  $Q$ .

However, the first is certainly the most accurate. Values of 74 for para-aramid, 360 for SiC, and 475 for carbon fibers were asymptotically obtained at low excitation levels, where the asymmetry of the resonance profiles due to non-linearity is less pronounced. These values of  $Q$  correspond to a damping of 0.68% for Kevlar® 29, 0.14% for SiC, and 0.11% for carbon fibres.

**Table 12:** main Q and damping values, estimated using the half-power bandwidth method, was computed for the 5 V response, for Kevlar® 29 and carbon, and for 1V response for SiC, respectively.

<b>MATERIAL</b>	<b>Q</b>	<b>DAMPING</b>
Kevlar® 29	74	0.0068
SiC	360	0.0014
Carbon	475	0.0011



## **Chapter 6**

# **Experimental investigation and results on damaged Kevlar® 29 samples**

In Chapter 5 the experimental investigation and the results performed on three different high-strength materials were presented. The experimental investigation consisted into the dynamic characterization of high-strength fibres, by means of simple non-destructive non-linearity tests. Subsequently, three para-aramid samples of Kevlar® 29 were subjected to UV rays to different time, and tested.

In this chapter the results of this second experimental campaign were presented. The demonstrated sensitivity to UV rays of these kind of high-strength materials, in terms of decreased stiffness and potential relaxation, may be a discriminating factor when choosing the type of material to be employed for the confinement interventions on concrete or masonry columns, or vaults in historic buildings.

The idea has been to use the demonstrated existence of weak nonlinearities (through a non-linearity index) (Chapter 5), which may be detected in the forced dynamic response of the specimen, as indicators for safety and lifecycle assessment of high-performance fibres. The results could be applied, as a possible alternative, in Structural Health Monitoring (SHM) or damage detection

application. Particularly interesting is the application to monitoring existing high-strength materials reinforcements. These reinforcements are applied to buildings of particular historical and artistic interest, which more than others are in need of monitoring and protection.

Part of the work described in this Chapter has also been published in *Composite Structures* (Ceravolo, et al., 2018)

## **6.1 Effects of UV exposure on high-strength materials: background**

High-strength materials are currently employed as a reinforcing material for buildings. In this situation, they are permanently subjected to external factors (environmental factors), which had the ability to degrade these materials depending on the exposure to different elements, and the exposure time to these elements over the life of the system. The material should be chosen, and designed based on these considerations, in order to maximise the benefits of this reinforcement technique (Granata & Parvin, 2001). In the specific area of structural engineering and retrofitting, problems arising from the structural performance of polymeric materials after long-term exposure to the agents render the end-users still cautious when and where to apply them (Oliveira & Creus, 2004).

Systems using high-strength materials can be suitable for every need taken advantage of the possibility to have different FRP configurations, material properties, and installations. To ensure that high-strength materials will be used effectively and widely in a common practice, the engineers should evaluate all aspects of the project, including the structures location. In particular, when high-strength materials used in reinforcement technique, were externally bonded to structures they are exposed to ultraviolet (UV) rays, and consequently to UV degradation. UV rays have the ability to degrade the resin matrix, in which the fibres were embedded, and can even degrade the fibres themselves after sufficient exposure.

The UV rays are one part in the solar spectrum, and their wavelengths contained in the sunlight are measured from 200 nm to 400 nm. UV rays are dangerous for any polymer, on which the corrosion process caused by the oxygen in the atom state would be accelerated because of the presence of the UV ray, resulting in a weight loss and deterioration (HuangGu, 2005).

In other works, available into open literature (Silva, 2007) (Silva & Biscaia, 2008) (Wang, et al., 2012) (Cai, et al., 2014) (Micelli & Nanni, 2004), the strength of the filaments before and after the UV exposure was tested, in order to evaluate the strength decrement function of the time exposition.

The author in a work (HuangGu, 2005) asserts that short time exposure to the UV ray does not damage the Kevlar® fibres. However, prolonged exposure to the UV ray will cause strength decrease. The main bonds into the Kevlar® fibre are C–O and N–H, and the corresponding wavelengths of their bond energy are 340 and 306 nm, respectively. Consequently, the required wavelength to break the N–H bond is 306 nm. After the UV exposure, micro cracks on the fibre surface appear. Aging studies on Kevlar® were also conducted by Arrieta et al. (Arrieta, et al., 2011).

Another work (Said, et al., 2006) reports the changes into mechanical behaviour in the cases of pre and post-exposure to UV rays of four commercial high-strength fibres (Zylon® HM, Vectran® T-97, Kevlar® 49, Spectra® 1000). The experimental campaign was conducted by using a weatherometer with a Xenon lamp, emitting UV rays at 340 nm at an irradiance of  $1.1 \text{ W/m}^2$  (Figure 68). The results indicate that exposing high-strength fibres in continuous yarn form to UV could cause serious loss strength of the fibres, with the exception of Spectra® fibres.



Figure 68: weatherometer with a Xenon lamp, emitting UV rays at 340 nm at an irradiance of  $1.1 \text{ W/m}^2$  used in an experimental tests. Source (Said, et al., 2006).

Previous studies have reported results on UV degradation of thick ropes. The objective of this research was to study high-strength fibres in single continuous yarn form, and to quantify their strength loss with UV exposure. This work further explains that Kevlar® is self-screening. Its light stability depends on the thickness of the exposed item. Very thin Kevlar® 49 fabric, if directly exposed to very high intensity sunlight for an extended period, will lose about half its tensile strength within few days. In thicker element, such as a half-inch diameter rope, the outer layer protects the majority of the rope and strength loss is minimised (Said, et al., 2006).

The aim of the work presented in this Chapter is to identify, assess and quantify the changes in the fibre material response when exposed to UV light on the basis of several parameters taken into consideration such as the resonant frequency of the spring-mass system, the Q-factor, and a non-linearity index. These results could be used as damage indicators for safety and lifecycle assessment of high-strength materials.

## **6.2 Experimental investigation on damaged Kevlar® 29 samples**

After that the tests on undamaged para-aramid sample of Kevlar® 29 were carried out (Chapter 5), it was decided to damage it. The effect that the damage could have on the behaviour of the fibres will then be evaluated by repeating the forced tests and comparing the results obtained with those already reported for the undamaged sample.

The type of procedure chosen to cause the damage is a prolonged exposure to UV rays. UV rays attack many of the natural and synthetic polymers. This problem is known as UV degradation, and is more common in products constantly exposed to sunlight. In particular, a continuous and prolonged exposure results to be more harmful than an intermittent one, because the dangerousness of the attack depends on the extent and the degree of exposure. The polymers that possess UV-absorption groups, such as aromatic rings (aramid and para-aramid), can be sensitive to the effect of ultraviolet radiation, and often should be protected from the deleterious effects that could have the sunlight. The damage caused by UV effects on this type of materials, which are visible after a long time exposure, can be evaluated by means of accelerated exposure testing.

In order to carry out this kind of test, a UV lamp for industrial applications (OSRAM Ultra-Vitalux®) was chosen (OSRAM, 2017) (Figure 69).

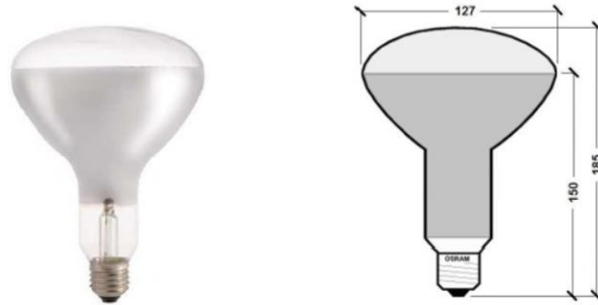


Figure 69: geometrical details of a UV lamp chosen to cause the damage on Kevlar®29 samples. Source (OSRAM, 2017).

The radiation's composition of this lamp is similar to the radiation mixture of natural sunlight, in an alpine environment. It emits a mixed light, generated from a tungsten filament in high-pressure conditions. In addition, the special mushroom shape, with internal reflector, ensures the passage of a high UVA and UVB fraction, while it tends to absorb the most harmful UVC radiation. In Table 13, the main technical characteristics of the UV lamp are listed.

**Table 13:** Technical details of an OSRAM Ultra-Vitalux®. Source (OSRAM, 2017).

<b>ELECTRICAL DATA</b>	
Nominal power [W]	300
Nominal voltage [V]	230
<b>PHOTOMETRIC DATA</b>	
UVA emission [W] (after 1 hour of operation)	13.6
UVB emission [W] (after 1 hour of operation)	3
<b>GEOMETRIC SIZE</b>	
Diameter [mm]	127
Length [mm]	185

Figure 70, shows also the relative spectral power distribution provided by the datasheet.

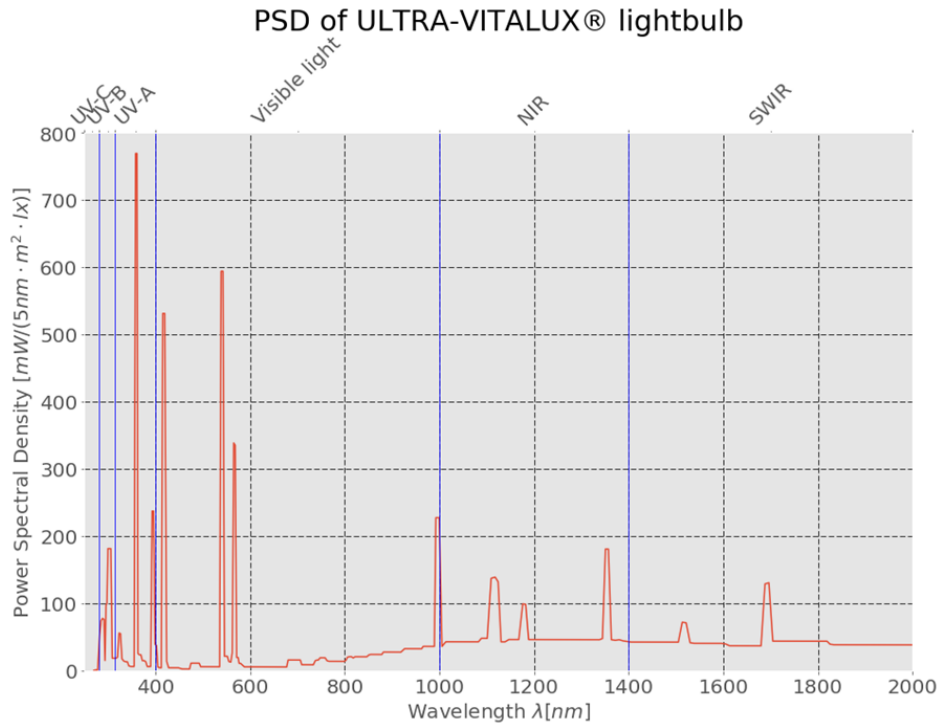


Figure 70: power spectra distribution of Ultra-Vitalux® lightbulb subdivided for the different components of the electromagnetic spectrum. Source (OSRAM, 2017).

It can be noted that the ultraviolet radiation is the portion of the electromagnetic spectrum, in which the wavelength ranges from 100 to 400 nm. It corresponds to the part immediately lower than the human eye visible light, and just over to X-rays.

The UV radiation is further divided into three different wavelength bands:

- UVA, wavelength ranges from 315 to 400 nm
- UVB, wavelength ranges from 280 to 315 nm
- UVC, wavelength ranges from 100 to 280 nm

The graph in Figure 70 clearly shows as the greater peaks are in correspondence of the spectrum's portion that identifies the UVA radiation, or however for wavelengths not particularly high.

If compared to the solar spectrum, the emission spectrum of the UV lamps is constituted by discrete lines, which taking a greater entity for some critical values of wavelength. The material exhibits a high absorption of radiation in these points. This fact explains the particular effectiveness of this kind of lamps in the various industrial processes in which it is used.

The peaks related to the UV lamp's spectrum that exceed the trend of the solar spectrum, are those relating to UVA and UVB fractions. These radiations are those most harmful for the material under investigation in this work. Consequently, is easy to see the effectiveness of the chosen lamp in order to damage the samples under investigation. Since most of the UVA emission is in that bright line, its power content can be taken to be roughly equal to the UVA total flux specification of 13.6 W given in Table 13, which is then used here to figure out the total radiation dose per hour of exposure.

At this point, the chosen lamp for damaging the sample was mounted on a support, specially realised with recycled materials. The experiment was conducted into the Metrology Laboratory of the Department of Electronics of the Politecnico di Torino (Figure 71).

A sheet metal cylinder ( $\varnothing 13$  cm) was used to focus the most part of the light toward the fibre sample. It is necessary to ensure the presence of an open space below the cylinder to ensure a natural air recirculation during the test.



Figure 71: the experimental setup used to focus the light flux onto fibre samples.

It is here assumed that the guiding efficiency for UV of the steel cylinder shown in Figure 71 be rather good, so that most of the flux would flood the target down below. Once a week, the sample was turned upside down to produce as uniform as possible a damage. A flux of roughly  $1 \text{ kW/m}^2$  is then assumed on the fibre samples, which means about  $6 \text{ mW/m}$  on a single  $12 \text{ }\mu\text{m}$  diameter fibre, considering an average screen effect of 50 % (Burgoyne, 1993). The total UVA dose on 1 m of a single fibre would then be about 20 J per hour of exposure. Obviously these evaluations are not very precise, but they can surely be taken as a reasonable indication of what can be expected in real-life exposure, given the fact that average sunlight UVA flux values are also quite uncertain in real life. Since the UVA fraction of sunlight reaching the Earth is approximately 5% and a typical clear sky total irradiance is about half a  $\text{kW/m}^2$  at its peak, it can be safely stated that the used UVA flux was roughly 40 times the real-life average cumulative exposure that fibres may have to face in operation.

Three samples (extracted from the same bundle) underwent three different cycles of continued exposure, where the first was 792 hours, the second 1272, and the third 2040 hours, respectively. Such times of accelerated test roughly correspond to 8, 13, and 20 years of exposure to sunlight in temperate latitudes, considering 8 hours per day of sunlight.

As outlined in the introduction, once the process of damage of the Kevlar® 29 fibres were completed, harmonic tests have been repeated, as previously on the undamaged fibres. The aim of this work was to assess any changes in the material's behaviour, based on parameters taken into consideration such as resonance frequency, quality factor, and non-linearity index.

### 6.2.1 Forced testing on the sample damaged for 792 hours



Forced tests on damaged Kevlar® 29 sample (792 hours, 33 days), shows in Figure 72, were performed in order to investigate any change in the nonlinear behaviour of the material compared to the undamaged case.

As already mentioned, the voltage values of output are recorded. After, it is possible to calculate the rms strain value

Figure 72: damaged Kevlar® 29 sample (792 hours)

by using a conversion factor evaluated during the calibration of the photodiode (measurement sensitivity  $S=70 \text{ mV}/\mu$ , in this case).

The frequency interval taken into consideration has an amplitude of 0.590 Hz, roughly centred on the resonance frequency of the system. Moreover, the step increment of the excitation frequency is always equal to 0.010 Hz.

In the following Table 14 are reported the strain values calculated from the numerical data acquired during the forced tests.

**Table 14:** strain values calculated from the numerical data acquired during the forced tests.

2.0 [V]		3.0 [V]		4.0 [V]		5.0 [V]	
Freq.	$\epsilon$	Freq.	$\epsilon$	Freq.	$\epsilon$	Freq.	$\epsilon$
[Hz]	[RMS]	[Hz]	[RMS]	[Hz]	[RMS]	[Hz]	[RMS]
20.42	1.399E-6	20.42	2.425E-6	20.42	3.172E-6	20.42	4.104E-6
20.43	1.437E-6	20.43	2.519E-6	20.43	3.265E-6	20.43	4.160E-6
20.44	1.493E-6	20.44	2.612E-6	20.44	3.358E-6	20.44	4.216E-6
20.45	1.586E-6	20.45	2.668E-6	20.45	3.451E-6	20.45	4.291E-6
20.46	1.679E-6	20.46	2.705E-6	20.46	3.545E-6	20.46	4.384E-6
20.47	1.772E-6	20.47	2.761E-6	20.47	3.638E-6	20.47	4.478E-6
20.48	1.866E-6	20.48	2.799E-6	20.48	3.731E-6	20.48	4.571E-6
20.49	1.959E-6	20.49	2.892E-6	20.49	3.862E-6	20.49	4.664E-6
20.50	2.052E-6	20.50	2.985E-6	20.50	3.993E-6	20.50	4.757E-6
20.51	2.108E-6	20.51	3.041E-6	20.51	4.104E-6	20.51	4.851E-6
20.52	2.164E-6	20.52	3.078E-6	20.52	4.198E-6	20.52	5.000E-6
20.53	2.239E-6	20.53	3.172E-6	20.53	4.291E-6	20.53	5.149E-6
20.54	2.295E-6	20.54	3.265E-6	20.54	4.384E-6	20.54	5.317E-6
20.55	2.351E-6	20.55	3.358E-6	20.55	4.534E-6	20.55	5.504E-6
20.56	2.425E-6	20.56	3.489E-6	20.56	4.683E-6	20.56	5.690E-6
20.57	2.481E-6	20.57	3.619E-6	20.57	4.851E-6	20.57	5.877E-6
20.58	2.537E-6	20.58	3.731E-6	20.58	5.037E-6	20.58	6.101E-6

20.59	2.612E-6	20.59	3.787E-6	20.59	5.224E-6	20.59	6.325E-6
20.60	2.668E-6	20.60	3.843E-6	20.60	5.410E-6	20.60	6.530E-6
20.61	2.724E-6	20.61	3.918E-6	20.61	5.597E-6	20.61	6.940E-6
20.62	2.799E-6	20.62	4.049E-6	20.62	5.784E-6	20.62	7.351E-6
20.63	2.929E-6	20.63	4.179E-6	20.63	5.970E-6	20.63	7.743E-6
20.64	3.060E-6	20.64	4.291E-6	20.64	6.287E-6	20.64	7.966E-6
20.65	3.172E-6	20.65	4.478E-6	20.65	6.623E-6	20.65	8.209E-6
20.66	3.265E-6	20.66	4.664E-6	20.66	6.903E-6	20.66	8.545E-6
20.67	3.358E-6	20.67	4.851E-6	20.67	7.183E-6	20.67	8.862E-6
20.68	3.451E-6	20.68	5.037E-6	20.68	7.463E-6	20.68	9.235E-6
20.69	3.545E-6	20.69	5.224E-6	20.69	7.743E-6	20.69	9.515E-6
20.70	3.638E-6	20.70	5.410E-6	20.70	7.873E-6	20.70	9.701E-6
20.71	3.825E-6	20.71	5.690E-6	20.71	7.985E-6	20.71	9.795E-6
20.72	3.918E-6	20.72	5.970E-6	20.72	8.116E-6	20.72	9.888E-6
20.73	4.011E-6	20.73	6.063E-6	20.73	8.209E-6	20.73	9.981E-6
20.74	4.104E-6	20.74	6.157E-6	20.74	8.302E-6	20.74	10.075E-6
20.75	4.291E-6	20.75	6.250E-6	20.75	8.209E-6	20.75	9.888E-6
20.76	4.478E-6	20.76	6.063E-6	20.76	8.116E-6	20.76	9.701E-6
20.77	4.384E-6	20.77	5.877E-6	20.77	7.929E-6	20.77	9.515E-6
20.78	4.198E-6	20.78	5.690E-6	20.78	7.743E-6	20.78	9.235E-6
20.79	4.011E-6	20.79	5.597E-6	20.79	7.556E-6	20.79	8.955E-6
20.80	3.825E-6	20.80	5.410E-6	20.80	7.276E-6	20.80	8.675E-6
20.81	3.638E-6	20.81	5.317E-6	20.81	6.996E-6	20.81	8.396E-6
20.82	3.582E-6	20.82	5.224E-6	20.82	6.754E-6	20.82	8.116E-6
20.83	3.545E-6	20.83	5.037E-6	20.83	6.530E-6	20.83	7.836E-6
20.84	3.433E-6	20.84	4.851E-6	20.84	6.343E-6	20.84	7.556E-6
20.85	3.302E-6	20.85	4.664E-6	20.85	6.157E-6	20.85	7.276E-6
20.86	3.172E-6	20.86	4.515E-6	20.86	5.896E-6	20.86	7.015E-6
20.87	3.060E-6	20.87	4.384E-6	20.87	5.653E-6	20.87	6.772E-6
20.88	2.929E-6	20.88	4.235E-6	20.88	5.410E-6	20.88	6.530E-6

20.89	2.799E-6	20.89	4.104E-6	20.89	5.224E-6	20.89	6.269E-6
20.90	2.817E-6	20.90	3.862E-6	20.90	5.037E-6	20.90	6.026E-6
20.91	2.668E-6	20.91	3.638E-6	20.91	4.851E-6	20.91	5.784E-6
20.92	2.519E-6	20.92	3.507E-6	20.92	4.664E-6	20.92	5.597E-6
20.93	2.425E-6	20.93	3.377E-6	20.93	4.478E-6	20.93	5.410E-6
20.94	2.332E-6	20.94	3.265E-6	20.94	4.291E-6	20.94	5.224E-6
20.95	2.239E-6	20.95	3.097E-6	20.95	4.160E-6	20.95	5.075E-6
20.96	2.164E-6	20.96	2.948E-6	20.96	4.049E-6	20.96	4.907E-6
20.97	2.108E-6	20.97	2.799E-6	20.97	3.918E-6	20.97	4.757E-6
20.98	2.052E-6	20.98	2.649E-6	20.98	3.769E-6	20.98	4.590E-6
20.99	1.940E-6	20.99	2.537E-6	20.99	3.619E-6	20.99	4.422E-6
21.00	1.810E-6	21.00	2.425E-6	21.00	3.489E-6	21.00	4.272E-6
21.01	1.679E-6	21.01	2.332E-6	21.01	3.358E-6	21.01	4.104E-6

6.0 [V]		7.0 [V]		8.0 [V]		9.0 [V]		10.0 [V]	
Freq. [Hz]	$\epsilon$ [RMS]	Freq. [Hz]	$\epsilon$ [RMS]	Freq. [Hz]	E [RMS]	Freq. [Hz]	$\epsilon$ [RMS]	Freq. [Hz]	$\epsilon$ [RMS]
20.42	5.13E-6	20.42	6.06E-6	20.42	7.28E-6	20.42	8.39E-6	20.42	9.33E-6
20.43	5.22E-6	20.43	6.16E-6	20.43	7.43E-6	20.43	8.55E-6	20.43	9.61E-6
20.44	5.32E-6	20.44	6.25E-6	20.44	7.58E-6	20.44	8.69E-6	20.44	9.89E-6
20.45	5.41E-6	20.45	6.39E-6	20.45	7.74E-6	20.45	8.86E-6	20.45	1.17E-6
20.46	5.50E-6	20.46	6.55E-6	20.46	7.84E-6	20.46	8.99E-6	20.46	10.45E-6
20.47	5.63E-6	20.47	6.72E-6	20.47	7.93E-6	20.47	9.12E-6	20.47	10.67E-6
20.48	5.78E-6	20.48	6.85E-6	20.48	8.02E-6	20.48	9.24E-6	20.48	10.91E-6
20.49	5.88E-6	20.49	6.98E-6	20.49	8.25E-6	20.49	9.52E-6	20.49	11.04E-6
20.50	5.97E-6	20.50	7.09E-6	20.50	8.49E-6	20.50	9.79E-6	20.50	11.28E-6
20.51	6.06E-6	20.51	7.24E-6	20.51	8.68E-6	20.51	10.08E-6	20.51	11.53E-6
20.52	6.21E-6	20.52	7.39E-6	20.52	8.92E-6	20.52	10.39E-6	20.52	11.75E-6
20.53	6.53E-6	20.53	7.56E-6	20.53	9.16E-6	20.53	10.71E-6	20.53	12.13E-6
20.54	6.72E-6	20.54	7.79E-6	20.54	9.42E-6	20.54	11.01E-6	20.54	12.41E-6
20.55	6.96E-6	20.55	8.04E-6	20.55	9.89E-6	20.55	11.44E-6	20.55	12.69E-6
20.56	7.11E-6	20.56	8.30E-6	20.56	10.35E-6	20.56	11.88E-6	20.56	13.15E-6

20.57	7.37E-6	20.57	8.71E-6	20.57	10.82E-6	20.57	12.31E-6	20.57	13.62E-6
20.58	7.74E-6	20.58	9.12E-6	20.58	11.31E-6	20.58	12.82E-6	20.58	14.27E-6
20.59	7.98E-6	20.59	9.56E-6	20.59	11.81E-6	20.59	13.30E-6	20.59	15.02E-6
20.60	8.23E-6	20.60	9.94E-6	20.60	12.31E-6	20.60	13.81E-6	20.60	15.67E-6
20.61	8.49E-6	20.61	10.35E-6	20.61	12.69E-6	20.61	14.40E-6	20.61	16.51E-6
20.62	8.95E-6	20.62	10.82E-6	20.62	13.06E-6	20.62	15.02E-6	20.62	17.35E-6
20.63	9.33E-6	20.63	11.29E-6	20.63	13.38E-6	20.63	15.58E-6	20.63	17.91E-6
20.64	9.70E-6	20.64	11.75E-6	20.64	13.81E-6	20.64	16.04E-6	20.64	18.32E-6
20.65	9.98E-6	20.65	12.16E-6	20.65	14.27E-6	20.65	16.60E-6	20.65	18.77E-6
20.66	10.21E-6	20.66	12.59E-6	20.66	14.46E-6	20.66	17.16E-6	20.66	19.22E-6
20.67	10.54E-6	20.67	12.97E-6	20.67	14.74E-6	20.67	17.54E-6	20.67	19.49E-6
20.68	10.91E-6	20.68	13.25E-6	20.68	15.11E-6	20.68	17.82E-6	20.68	19.40E-6
20.69	11.19E-6	20.69	13.43E-6	20.69	15.29E-6	20.69	18.01E-6	20.69	19.22E-6
20.70	11.47E-6	20.70	13.53E-6	20.70	15.58E-6	20.70	17.91E-6	20.70	19.03E-6
20.71	11.66E-6	20.71	13.71E-6	20.71	15.76E-6	20.71	17.72E-6	20.71	18.75E-6
20.72	11.75E-6	20.72	13.62E-6	20.72	15.67E-6	20.72	17.35E-6	20.72	18.47E-6
20.73	11.57E-6	20.73	13.43E-6	20.73	15.48E-6	20.73	17.16E-6	20.73	18.09E-6
20.74	11.38E-6	20.74	13.34E-6	20.74	15.11E-6	20.74	16.79E-6	20.74	17.82E-6
20.75	11.19E-6	20.75	13.06E-6	20.75	14.83E-6	20.75	16.42E-6	20.75	17.44E-6
20.76	10.91E-6	20.76	12.78E-6	20.76	14.49E-6	20.76	15.95E-6	20.76	17.16E-6
20.77	10.63E-6	20.77	12.50E-6	20.77	14.18E-6	20.77	15.48E-6	20.77	16.79E-6
20.78	10.37E-6	20.78	12.22E-6	20.78	13.77E-6	20.78	15.02E-6	20.78	16.32E-6
20.79	10.13E-6	20.79	11.94E-6	20.79	13.34E-6	20.79	14.65E-6	20.79	15.95E-6
20.80	9.89E-6	20.80	11.57E-6	20.80	12.95E-6	20.80	14.14E-6	20.80	15.58E-6
20.81	9.42E-6	20.81	11.19E-6	20.81	12.54E-6	20.81	13.77E-6	20.81	15.17E-6
20.82	9.09E-6	20.82	10.82E-6	20.82	12.13E-6	20.82	13.34E-6	20.82	14.77E-6
20.83	8.86E-6	20.83	10.50E-6	20.83	11.73E-6	20.83	12.98E-6	20.83	14.36E-6
20.84	8.58E-6	20.84	10.21E-6	20.84	11.32E-6	20.84	12.65E-6	20.84	13.99E-6
20.85	8.30E-6	20.85	9.89E-6	20.85	10.91E-6	20.85	12.31E-6	20.85	13.56E-6
20.86	8.02E-6	20.86	9.52E-6	20.86	10.45E-6	20.86	11.94E-6	20.86	13.15E-6
20.87	7.89E-6	20.87	9.14E-6	20.87	10.17E-6	20.87	11.57E-6	20.87	12.72E-6
20.88	7.52E-6	20.88	8.77E-6	20.88	9.89E-6	20.88	11.19E-6	20.88	12.27E-6
20.89	7.27E-6	20.89	8.62E-6	20.89	9.55E-6	20.89	10.82E-6	20.89	11.85E-6
20.90	6.99E-6	20.90	8.27E-6	20.90	9.22E-6	20.90	10.45E-6	20.90	11.47E-6
20.91	6.72E-6	20.91	8.12E-6	20.91	8.86E-6	20.91	10.07E-6	20.91	11.04E-6

20.92	6.44E-6	20.92	7.74E-6	20.92	8.58E-6	20.92	9.81E-6	20.92	10.63E-6
20.93	6.27E-6	20.93	7.37E-6	20.93	8.30E-6	20.93	9.57E-6	20.93	10.35E-6
20.94	6.12E-6	20.94	7.18E-6	20.94	8.02E-6	20.94	9.33E-6	20.94	10.07E-6
20.95	5.97E-6	20.95	6.99E-6	20.95	7.76E-6	20.95	9.05E-6	20.95	9.79E-6
20.96	5.78E-6	20.96	6.75E-6	20.96	7.52E-6	20.96	8.77E-6	20.96	9.55E-6
20.97	5.59E-6	20.97	6.53E-6	20.97	7.28E-6	20.97	8.49E-6	20.97	9.33E-6
20.98	5.41E-6	20.98	6.34E-6	20.98	7.11E-6	20.98	8.28E-6	20.98	9.05E-6
20.99	5.28E-6	20.99	6.16E-6	20.99	6.94E-6	20.99	8.06E-6	20.99	8.82E-6
21.00	5.17E-6	21.00	5.97E-6	21.00	6.77E-6	21.00	7.79E-6	21.00	8.62E-6

As can be noted from the acquired numerical data, there is an increment of the resonant frequency compared to that obtained for the original Kevlar® 29 sample. The values ranging from 20.76 Hz, for the first curve relating to 2 V, to 20.67 Hz for the last one, relating to 10 V.

Using the acquired numerical data, it is possible build the curves shown in Figure 73, for different levels of input.

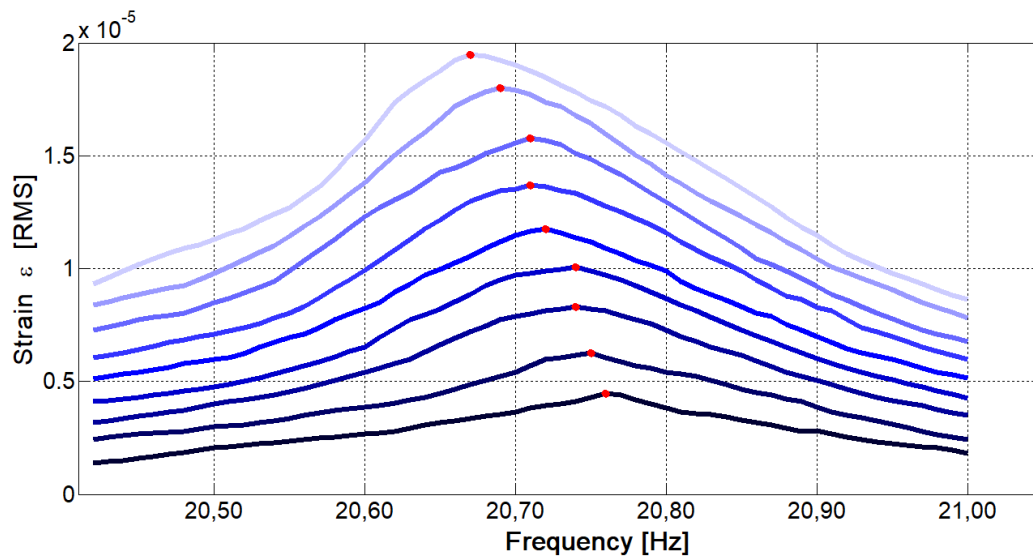


Figure 73: Sample exposed 792 hours: frequency response measured around resonance for increasing levels of driving force. The excitation range is 2 V – 10 V.

According to the graph shown in Figure 73, also in this case there is a nonlinear behaviour of the response. It is clear because increasing the voltage input, the peak of the curves indicates that the resonance frequency tends to shift towards values of the frequency lower.

For quantifying this non-linearity, was again used a backbone curve, which represent the best approximation of the trend points, corresponding to the various peaks of the curves.

By referring to the numerical data acquired for this sample, in Figure 74 is shown the backbone curve obtained. In this way is possible to quantify the nonlinear behaviour of the material under investigation.

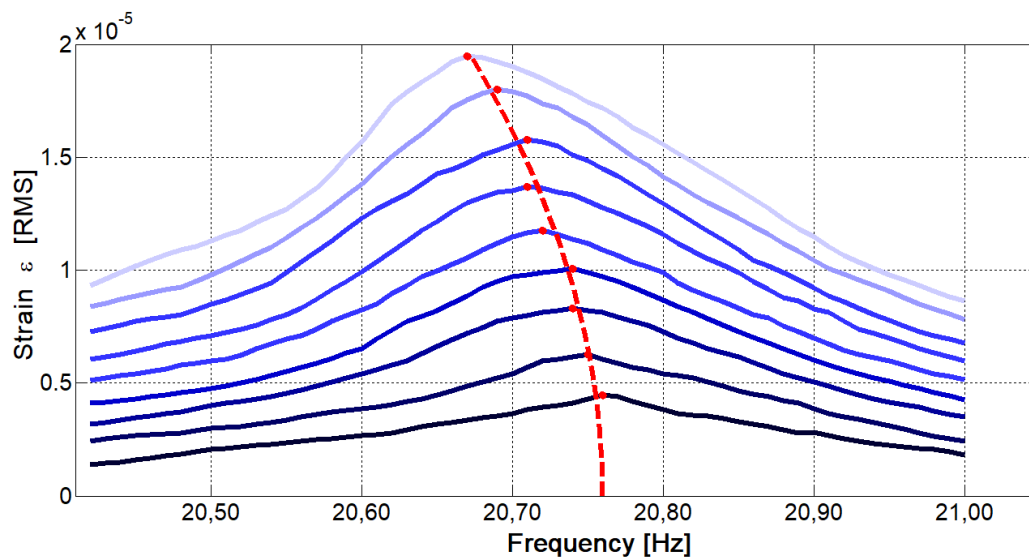


Figure 74: sample exposed 792 hours: frequency response measured around resonance for increasing levels of driving force. The excitation range is 2 V – 10 V. The red dots highlight the maximum of the response curve and the dashed red line is the estimated backbone response curve.

The cubic stiffness coefficient obtained in this case is equal to  $\chi = -5.028 \cdot 10^{11} \text{ N/m}^3$ .

Finally, the value of the  $\zeta$  damping of the system was calculated applying the half-power bandwidth method, and was computed for the 5 V response and was estimated at 0.58% ( $Q= 86$ ).

## 6.2.2 Forced testing on the sample damaged for 1272 hours



Figure 75: damaged Kevlar® 29 sample (1272 hours)

The second sample investigated is a Kevlar® 29 material exposed for 53 days (1272 hours) to UV rays (Figure 75). A set of forced tests was performed, and in this case, the measurement's sensitivity evaluated is equal to 90 mV/ $\mu$ .

The frequencies range taken into account during the tests has an amplitude of 0.600 Hz, centred roughly on the resonance frequency of the system. Moreover, the increment step of the frequency was chosen equal to 0.010 Hz.

In the following Table 15 are reported the strain values calculated from the numerical data acquired during the forced tests.

**Table 15:** strain values calculated from the numerical data acquired during the forced tests.

2.0 [V]		3.0 [V]		4.0 [V]		5.0 [V]	
Freq. [Hz]	$\epsilon$ [RMS]	Freq. [Hz]	$\epsilon$ [RMS]	Freq. [Hz]	$\epsilon$ [RMS]	Freq. [Hz]	$\epsilon$ [RMS]
19.53	1.57E-6	19.53	2.24E-6	19.53	2.98E-6	19.53	3.81E-6
19.54	1.62E-6	19.54	2.32E-6	19.54	3.07E-6	19.54	3.93E-6
19.55	1.69E-6	19.55	2.41E-6	19.55	3.15E-6	19.55	4.03E-6
19.56	1.74E-6	19.56	2.49E-6	19.56	3.23E-6	19.56	4.15E-6
19.57	1.79E-6	19.57	2.57E-6	19.57	3.35E-6	19.57	4.26E-6
19.58	1.84E-6	19.58	2.65E-6	19.58	3.47E-6	19.58	4.36E-6
19.59	1.91E-6	19.59	2.74E-6	19.59	3.56E-6	19.59	4.48E-6
19.60	1.96E-6	19.60	2.79E-6	19.60	3.65E-6	19.60	4.64E-6
19.61	2.02E-6	19.61	2.84E-6	19.61	3.73E-6	19.61	4.81E-6
19.62	2.07E-6	19.62	2.90E-6	19.62	3.81E-6	19.62	4.96E-6
19.63	2.12E-6	19.63	2.98E-6	19.63	3.95E-6	19.63	5.17E-6

---

19.64	2.17E-6	19.64	3.07E-6	19.64	4.08E-6	19.64	5.37E-6
19.65	2.24E-6	19.65	3.15E-6	19.65	4.23E-6	19.65	5.56E-6
19.66	2.32E-6	19.66	3.23E-6	19.66	4.39E-6	19.66	5.80E-6
19.67	2.41E-6	19.67	3.32E-6	19.67	4.56E-6	19.67	6.05E-6
19.68	2.48E-6	19.68	3.40E-6	19.68	4.73E-6	19.68	6.30E-6
19.69	2.57E-6	19.69	3.53E-6	19.69	4.89E-6	19.69	6.60E-6
19.70	2.65E-6	19.70	3.66E-6	19.70	5.06E-6	19.70	6.89E-6
19.71	2.74E-6	19.71	3.81E-6	19.71	5.22E-6	19.71	7.21E-6
19.72	2.82E-6	19.72	3.98E-6	19.72	5.56E-6	19.72	7.55E-6
19.73	2.90E-6	19.73	4.15E-6	19.73	5.89E-6	19.73	7.88E-6
19.74	2.98E-6	19.74	4.31E-6	19.74	6.22E-6	19.74	8.21E-6
19.75	3.10E-6	19.75	4.51E-6	19.75	6.50E-6	19.75	8.57E-6
19.76	3.22E-6	19.76	4.71E-6	19.76	6.78E-6	19.76	8.94E-6
19.77	3.32E-6	19.77	4.89E-6	19.77	7.05E-6	19.77	9.28E-6
19.78	3.45E-6	19.78	5.17E-6	19.78	7.33E-6	19.78	9.67E-6
19.79	3.58E-6	19.79	5.47E-6	19.79	7.63E-6	19.79	10.03E-6
19.80	3.73E-6	19.80	5.72E-6	19.80	8.01E-6	19.80	10.28E-6
19.81	3.89E-6	19.81	5.88E-6	19.81	8.37E-6	19.81	10.61E-6
19.82	4.06E-6	19.82	6.05E-6	19.82	8.71E-6	19.82	10.78E-6
19.83	4.31E-6	19.83	6.38E-6	19.83	8.87E-6	19.83	11.03E-6
19.84	4.48E-6	19.84	6.63E-6	19.84	9.12E-6	19.84	11.28E-6
19.85	4.64E-6	19.85	6.79E-6	19.85	9.29E-6	19.85	11.44E-6
19.86	4.89E-6	19.86	6.96E-6	19.86	9.37E-6	19.86	11.36E-6
19.87	5.14E-6	19.87	7.13E-6	19.87	9.20E-6	19.87	11.19E-6
19.88	4.98E-6	19.88	7.05E-6	19.88	9.04E-6	19.88	11.03E-6
19.89	4.81E-6	19.89	6.88E-6	19.89	8.87E-6	19.89	10.61E-6
19.90	4.64E-6	19.90	6.72E-6	19.90	8.71E-6	19.90	10.36E-6
19.91	4.54E-6	19.91	6.55E-6	19.91	8.54E-6	19.91	10.03E-6
19.92	4.43E-6	19.92	6.38E-6	19.92	8.37E-6	19.92	9.70E-6
19.93	4.33E-6	19.93	6.23E-6	19.93	8.14E-6	19.93	9.45E-6

19.94	4.23E-6	19.94	6.10E-6	19.94	7.93E-6	19.94	9.20E-6
19.95	4.06E-6	19.95	5.97E-6	19.95	7.71E-6	19.95	8.95E-6
19.96	3.93E-6	19.96	5.85E-6	19.96	7.53E-6	19.96	8.67E-6
19.97	3.79E-6	19.97	5.75E-6	19.97	7.33E-6	19.97	8.39E-6
19.98	3.66E-6	19.98	5.64E-6	19.98	7.13E-6	19.98	8.13E-6
19.99	3.53E-6	19.99	5.47E-6	19.99	6.88E-6	19.99	7.91E-6
20.00	3.40E-6	20.00	5.31E-6	20.00	6.63E-6	20.00	7.69E-6
20.01	3.33E-6	20.01	5.14E-6	20.01	6.38E-6	20.01	7.46E-6
20.02	3.28E-6	20.02	5.02E-6	20.02	6.07E-6	20.02	7.25E-6
20.03	3.32E-6	20.03	4.92E-6	20.03	5.94E-6	20.03	7.03E-6
20.04	3.18E-6	20.04	4.81E-6	20.04	5.80E-6	20.04	6.79E-6
20.05	3.12E-6	20.05	4.67E-6	20.05	5.62E-6	20.05	6.60E-6
20.06	3.07E-6	20.06	4.52E-6	20.06	5.42E-6	20.06	6.40E-6
20.07	2.97E-6	20.07	4.39E-6	20.07	5.22E-6	20.07	6.22E-6
20.08	2.85E-6	20.08	4.24E-6	20.08	5.08E-6	20.08	6.02E-6
20.09	2.74E-6	20.09	4.11E-6	20.09	4.94E-6	20.09	5.82E-6
20.10	2.65E-6	20.10	3.98E-6	20.10	4.81E-6	20.10	5.64E-6
20.11	2.57E-6	20.11	3.86E-6	20.11	4.67E-6	20.11	5.47E-6

6.0 [V]		7.0 [V]		8.0 [V]		9.0 [V]		10.0 [V]	
Freq.	$\epsilon$	Freq.	$\epsilon$	Freq.	$\epsilon$	Freq.	$\epsilon$	Freq.	$\epsilon$
[Hz]	[RMS]	[Hz]	[RMS]	[Hz]	[RMS]	[Hz]	[RMS]	[Hz]	[RMS]
19.53	4.64E-6	19.53	5.80E-6	19.53	6.79E-6	19.53	7.55E-6	19.53	9.04E-6
19.54	4.78E-6	19.54	5.94E-6	19.54	7.13E-6	19.54	7.76E-6	19.54	9.24E-6
19.55	4.91E-6	19.55	6.07E-6	19.55	7.29E-6	19.55	7.98E-6	19.55	9.45E-6
19.56	5.06E-6	19.56	6.22E-6	19.56	7.46E-6	19.56	8.21E-6	19.56	9.78E-6
19.57	5.22E-6	19.57	6.42E-6	19.57	7.63E-6	19.57	8.49E-6	19.57	10.03E-6
19.58	5.39E-6	19.58	6.62E-6	19.58	7.88E-6	19.58	8.77E-6	19.58	10.28E-6
19.59	5.56E-6	19.59	6.79E-6	19.59	8.13E-6	19.59	9.04E-6	19.59	10.65E-6
19.60	5.77E-6	19.60	7.07E-6	19.60	8.37E-6	19.60	9.40E-6	19.60	11.03E-6
19.61	5.99E-6	19.61	7.33E-6	19.61	8.71E-6	19.61	9.77E-6	19.61	11.61E-6

19.62	6.22E-6	19.62	7.63E-6	19.62	9.04E-6	19.62	10.19E-6	19.62	12.27E-6
19.63	6.47E-6	19.63	7.85E-6	19.63	9.37E-6	19.63	10.65E-6	19.63	12.69E-6
19.64	6.72E-6	19.64	8.19E-6	19.64	9.75E-6	19.64	11.09E-6	19.64	13.18E-6
19.65	6.97E-6	19.65	8.46E-6	19.65	10.13E-6	19.65	11.61E-6	19.65	13.59E-6
19.66	7.25E-6	19.66	8.79E-6	19.66	10.53E-6	19.66	12.24E-6	19.66	14.09E-6
19.67	7.53E-6	19.67	9.12E-6	19.67	11.08E-6	19.67	12.87E-6	19.67	14.84E-6
19.68	7.79E-6	19.68	9.45E-6	19.68	11.57E-6	19.68	13.52E-6	19.68	15.59E-6
19.69	8.16E-6	19.69	9.83E-6	19.69	12.11E-6	19.69	14.09E-6	19.69	16.58E-6
19.70	8.52E-6	19.70	10.23E-6	19.70	12.65E-6	19.70	14.68E-6	19.70	17.76E-6
19.71	8.87E-6	19.71	10.61E-6	19.71	13.20E-6	19.71	15.53E-6	19.71	18.24E-6
19.72	9.34E-6	19.72	11.14E-6	19.72	13.85E-6	19.72	15.84E-6	19.72	18.91E-6
19.73	9.80E-6	19.73	11.68E-6	19.73	14.43E-6	19.73	16.50E-6	19.73	19.24E-6
19.74	10.28E-6	19.74	12.19E-6	19.74	14.93E-6	19.74	17.16E-6	19.74	19.57E-6
19.75	10.69E-6	19.75	12.77E-6	19.75	15.42E-6	19.75	17.75E-6	19.75	19.90E-6
19.76	11.03E-6	19.76	13.35E-6	19.76	15.92E-6	19.76	18.08E-6	19.76	20.23E-6
19.77	11.53E-6	19.77	13.76E-6	19.77	16.34E-6	19.77	18.41E-6	19.77	20.56E-6
19.78	11.86E-6	19.78	14.09E-6	19.78	16.67E-6	19.78	18.66E-6	19.78	20.89E-6
19.79	12.11E-6	19.79	14.34E-6	19.79	16.92E-6	19.79	18.99E-6	19.79	20.81E-6
19.80	12.36E-6	19.80	14.68E-6	19.80	17.16E-6	19.80	18.74E-6	19.80	20.48E-6
19.81	12.52E-6	19.81	14.84E-6	19.81	16.99E-6	19.81	18.49E-6	19.81	20.15E-6
19.82	12.85E-6	19.82	15.01E-6	19.82	16.78E-6	19.82	18.24E-6	19.82	19.98E-6
19.83	13.10E-6	19.83	14.76E-6	19.83	16.58E-6	19.83	17.91E-6	19.83	19.49E-6
19.84	12.94E-6	19.84	14.51E-6	19.84	16.42E-6	19.84	17.66E-6	19.84	19.15E-6
19.85	12.77E-6	19.85	14.26E-6	19.85	16.09E-6	19.85	17.25E-6	19.85	18.77E-6
19.86	12.60E-6	19.86	14.01E-6	19.86	15.75E-6	19.86	16.83E-6	19.86	18.41E-6
19.87	12.35E-6	19.87	13.76E-6	19.87	15.42E-6	19.87	16.42E-6	19.87	18.01E-6
19.88	12.06E-6	19.88	13.52E-6	19.88	15.09E-6	19.88	16.02E-6	19.88	17.63E-6
19.89	11.76E-6	19.89	13.15E-6	19.89	14.76E-6	19.89	15.64E-6	19.89	17.25E-6
19.90	11.44E-6	19.90	12.79E-6	19.90	14.43E-6	19.90	15.26E-6	19.90	16.79E-6
19.91	11.16E-6	19.91	12.44E-6	19.91	14.09E-6	19.91	14.84E-6	19.91	16.37E-6
19.92	10.88E-6	19.92	12.16E-6	19.92	13.69E-6	19.92	14.43E-6	19.92	15.92E-6
19.93	10.61E-6	19.93	11.87E-6	19.93	13.32E-6	19.93	14.01E-6	19.93	15.51E-6
19.94	10.32E-6	19.94	11.61E-6	19.94	12.94E-6	19.94	13.77E-6	19.94	15.21E-6
19.95	10.02E-6	19.95	11.28E-6	19.95	12.70E-6	19.95	13.52E-6	19.95	14.68E-6
19.96	9.70E-6	19.96	10.95E-6	19.96	12.32E-6	19.96	13.27E-6	19.96	14.26E-6

19.97	9.42E-6	19.97	10.61E-6	19.97	12.02E-6	19.97	12.97E-6	19.97	13.85E-6
19.98	9.14E-6	19.98	10.33E-6	19.98	11.74E-6	19.98	12.67E-6	19.98	13.43E-6
19.99	8.87E-6	19.99	10.05E-6	19.99	11.41E-6	19.99	12.35E-6	19.99	13.10E-6
20.00	8.66E-6	20.00	9.78E-6	20.00	11.11E-6	20.00	12.07E-6	20.00	12.77E-6
20.01	8.44E-6	20.01	9.54E-6	20.01	10.85E-6	20.01	11.79E-6	20.01	12.44E-6
20.02	8.21E-6	20.02	9.29E-6	20.02	10.56E-6	20.02	11.53E-6	20.02	12.07E-6
20.03	7.99E-6	20.03	9.04E-6	20.03	10.28E-6	20.03	11.24E-6	20.03	11.74E-6
20.04	7.78E-6	20.04	8.76E-6	20.04	9.98E-6	20.04	10.96E-6	20.04	11.36E-6
20.05	7.55E-6	20.05	8.47E-6	20.05	9.67E-6	20.05	10.69E-6	20.05	11.11E-6
20.06	7.25E-6	20.06	8.21E-6	20.06	9.37E-6	20.06	10.45E-6	20.06	10.86E-6
20.07	6.95E-6	20.07	8.01E-6	20.07	9.12E-6	20.07	10.19E-6	20.07	10.69E-6
20.08	6.79E-6	20.08	7.81E-6	20.08	8.87E-6	20.08	9.95E-6	20.08	10.36E-6
20.09	6.55E-6	20.09	7.63E-6	20.09	8.62E-6	20.09	9.70E-6	20.09	10.12E-6
20.10	6.47E-6	20.10	7.49E-6	20.10	8.43E-6	20.10	9.45E-6	20.10	9.87E-6
20.11	6.39E-6	20.11	7.36E-6	20.11	8.23E-6	20.11	9.20E-6	20.11	9.67E-6

Using the acquired numerical data, it is possible to build the curves shown in Figure 76, for different levels of input.

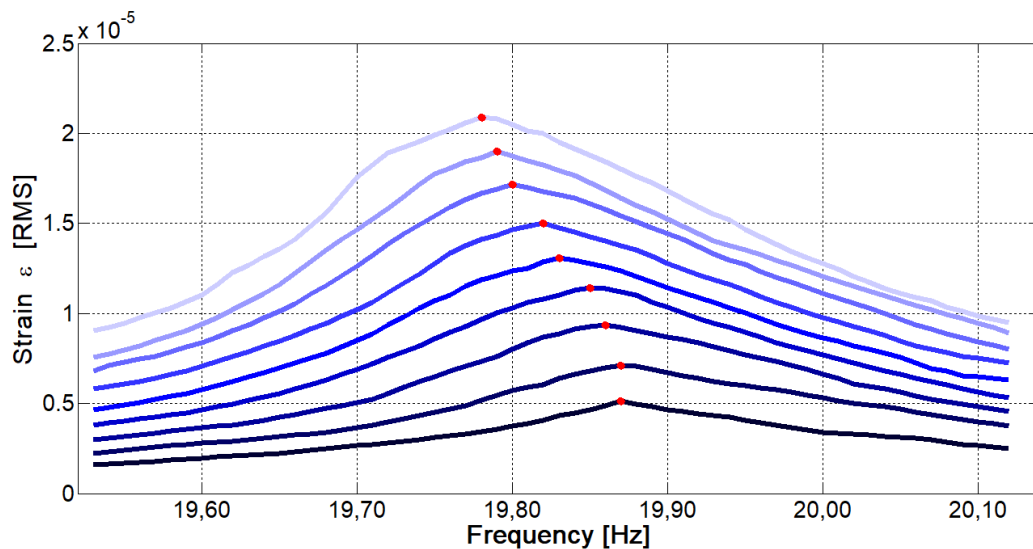


Figure 76: sample exposed 1272 hours: frequency response measured around resonance for increasing levels of driving force. The excitation range is 2 V – 10 V.

As can be noted from the acquired numerical data, there is an increment of the resonant frequency compared to that obtained for the first level of damaging of the Kevlar® 29 sample. The values ranges from 19.87 Hz, for the first curve relating to 2 V, to 19.78 Hz for the last one, relating to 10 V.

By referring to the numerical data acquired for this second sample, in Figure 77 is shown the backbone curve obtained. In this way is also possible to quantify the nonlinear behaviour of the material under investigation.

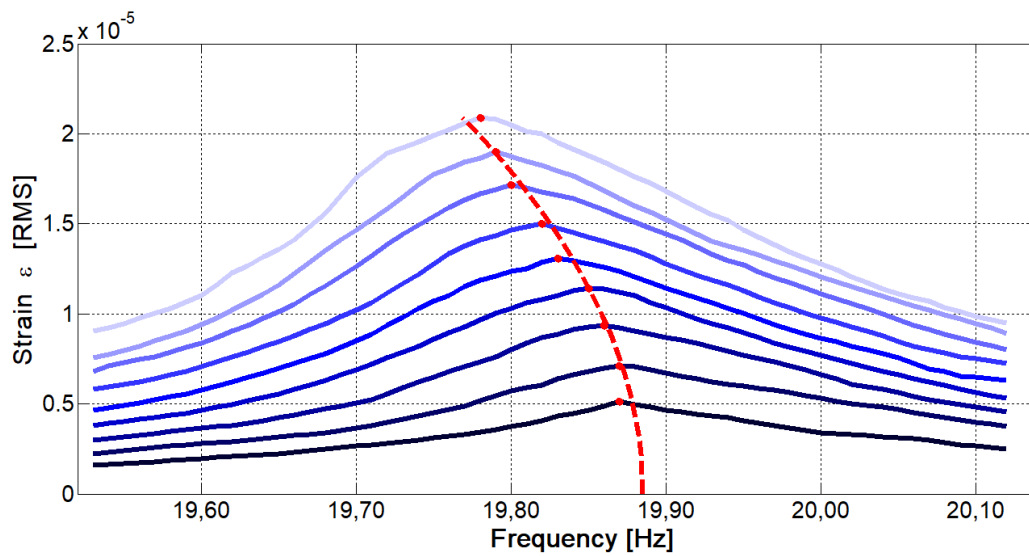


Figure 77: sample exposed 1272 hours: frequency response measured around resonance for increasing levels of driving force. The excitation range is 2 V – 10 V. The red dots highlight the maximum of the response curve and the dashed red line is the estimated backbone response curve.

The cubic stiffness coefficient obtained in this case is equal to  $\chi = -5.567 \cdot 10^{11} \text{ N/m}^3$ .

Finally, the value of the  $\zeta$  damping of the system was calculated applying the half-power bandwidth method, and was computed for the 5 V response, and was estimated at 0.66% ( $Q= 76$ ).

### 6.2.3 Forced testing on the sample damaged for 2040 hours



Figure 78: damaged Kevlar® 29 sample (2040 hours)

The third sample investigated is a para-aramid material exposed for 85 days (2040 hours) to UV rays (Figure 78). A set of forced tests was performed, and in this case, the measurement's sensitivity evaluated is equal to 100 mV/ $\mu$ .

The frequency range taken into account during the tests has an amplitude of 0.66 Hz, centred roughly on the resonance frequency of the system. Moreover, the increment step of the frequency was chosen equal to 0.010 Hz.

In the following Table 16 are reported the strain values calculated from the numerical data acquired during the forced tests.

**Table 16:** strain values calculated from the numerical data acquired during the forced tests.

2.0 [V]		3.0 [V]		4.0 [V]		5.0 [V]	
Freq. [Hz]	$\epsilon$ [RMS]	Freq. [Hz]	$\epsilon$ [RMS]	Freq. [Hz]	$\epsilon$ [RMS]	Freq. [Hz]	$\epsilon$ [RMS]
19.61	0.52E-6	19.61	1.34E-6	19.61	2.09E-6	19.61	3.13E-6
19.62	0.59E-6	19.62	1.42E-6	19.62	2.24E-6	19.62	3.28E-6
19.63	0.67E-6	19.63	1.49E-6	19.63	2.39E-6	19.63	3.43E-6
19.64	0.75E-6	19.64	1.57E-6	19.64	2.54E-6	19.64	3.58E-6
19.65	0.82E-6	19.65	1.64E-6	19.65	2.69E-6	19.65	3.73E-6
19.66	0.89E-6	19.66	1.72E-6	19.66	2.84E-6	19.66	3.88E-6
19.67	0.97E-6	19.67	1.87E-6	19.67	2.99E-6	19.67	4.03E-6
19.68	1.05E-6	19.68	2.02E-6	19.68	3.13E-6	19.68	4.18E-6

19.69	1.12E-6	19.69	2.16E-6	19.69	3.28E-6	19.69	4.33E-6
19.70	1.19E-6	19.70	2.24E-6	19.70	3.43E-6	19.70	4.48E-6
19.71	1.27E-6	19.71	2.39E-6	19.71	3.58E-6	19.71	4.63E-6
19.72	1.34E-6	19.72	2.46E-6	19.72	3.73E-6	19.72	4.78E-6
19.73	1.42E-6	19.73	2.61E-6	19.73	3.88E-6	19.73	4.93E-6
19.74	1.57E-6	19.74	2.76E-6	19.74	4.03E-6	19.74	5.08E-6
19.75	1.72E-6	19.75	2.84E-6	19.75	4.21E-6	19.75	5.22E-6
19.76	1.87E-6	19.76	2.91E-6	19.76	4.36E-6	19.76	5.37E-6
19.77	2.02E-6	19.77	2.98E-6	19.77	4.51E-6	19.77	5.67E-6
19.78	2.16E-6	19.78	3.13E-6	19.78	4.66E-6	19.78	5.97E-6
19.79	2.31E-6	19.79	3.21E-6	19.79	4.81E-6	19.79	6.27E-6
19.80	2.43E-6	19.80	3.36E-6	19.80	4.95E-6	19.80	6.57E-6
19.81	2.51E-6	19.81	3.51E-6	19.81	5.18E-6	19.81	6.87E-6
19.82	2.57E-6	19.82	3.66E-6	19.82	5.40E-6	19.82	7.16E-6
19.83	2.64E-6	19.83	3.81E-6	19.83	5.66E-6	19.83	7.46E-6
19.84	2.73E-6	19.84	4.03E-6	19.84	5.89E-6	19.84	7.76E-6
19.85	2.81E-6	19.85	4.25E-6	19.85	6.12E-6	19.85	8.21E-6
19.86	2.97E-6	19.86	4.48E-6	19.86	6.37E-6	19.86	8.51E-6
19.87	3.13E-6	19.87	4.70E-6	19.87	6.79E-6	19.87	8.81E-6
19.88	3.21E-6	19.88	4.93E-6	19.88	7.16E-6	19.88	9.10E-6
19.89	3.28E-6	19.89	5.15E-6	19.89	7.34E-6	19.89	9.40E-6
19.90	3.52E-6	19.90	5.37E-6	19.90	7.69E-6	19.90	9.70E-6
19.91	3.76E-6	19.91	5.59E-6	19.91	7.98E-6	19.91	10.00E-6
19.92	3.93E-6	19.92	5.82E-6	19.92	8.36E-6	19.92	10.31E-6
19.93	4.10E-6	19.93	6.04E-6	19.93	8.66E-6	19.93	10.64E-6
19.94	4.22E-6	19.94	6.27E-6	19.94	8.84E-6	19.94	10.94E-6
19.95	4.36E-6	19.95	6.49E-6	19.95	9.03E-6	19.95	11.19E-6
19.96	4.46E-6	19.96	6.64E-6	19.96	9.13E-6	19.96	11.31E-6
19.97	4.55E-6	19.97	6.910E-6	19.97	9.224E-6	19.97	11.48E-6
19.98	4.70E-6	19.98	7.060E-6	19.98	9.403E-6	19.98	11.40E-6

---

19.99	4.85E-6	19.99	7.164E-6	19.99	9.522E-6	19.99	11.37E-6
20.00	4.93E-6	20.00	7.343E-6	20.00	9.478E-6	20.00	11.21E-6
20.01	5.08E-6	20.01	7.299E-6	20.01	9.299E-6	20.01	11.05E-6
20.02	5.03E-6	20.02	7.194E-6	20.02	9.104E-6	20.02	10.84E-6
20.03	4.97E-6	20.03	7.090E-6	20.03	9.030E-6	20.03	10.63E-6
20.04	4.85E-6	20.04	6.940E-6	20.04	8.881E-6	20.04	10.46E-6
20.05	4.70E-6	20.05	6.866E-6	20.05	8.627E-6	20.05	10.29E-6
20.06	4.59E-6	20.06	6.612E-6	20.06	8.418E-6	20.06	10.08E-6
20.07	4.55E-6	20.07	6.493E-6	20.07	8.179E-6	20.07	9.77E-6
20.08	4.43E-6	20.08	6.343E-6	20.08	8.000E-6	20.08	9.48E-6
20.09	4.33E-6	20.09	6.194E-6	20.09	7.731E-6	20.09	9.18E-6
20.10	4.21E-6	20.10	6.045E-6	20.10	7.463E-6	20.10	8.88E-6
20.11	4.07E-6	20.11	5.896E-6	20.11	7.179E-6	20.11	8.58E-6
20.12	3.95E-6	20.12	5.672E-6	20.12	6.910E-6	20.12	8.28E-6
20.13	3.85E-6	20.13	5.522E-6	20.13	6.642E-6	20.13	7.98E-6
20.14	3.69E-6	20.14	5.224E-6	20.14	6.463E-6	20.14	7.76E-6
20.15	3.52E-6	20.15	5.075E-6	20.15	6.269E-6	20.15	7.46E-6
20.16	3.36E-6	20.16	4.925E-6	20.16	6.045E-6	20.16	7.16E-6
20.17	3.19E-6	20.17	4.627E-6	20.17	5.821E-6	20.17	6.87E-6
20.18	3.06E-6	20.18	4.328E-6	20.18	5.597E-6	20.18	6.72E-6
20.19	2.93E-6	20.19	4.104E-6	20.19	5.224E-6	20.19	6.42E-6
20.20	2.76E-6	20.20	3.881E-6	20.20	5.000E-6	20.20	6.12E-6
20.21	2.61E-6	20.21	3.582E-6	20.21	4.776E-6	20.21	5.97E-6
20.22	2.46E-6	20.22	3.433E-6	20.22	4.552E-6	20.22	5.67E-6
20.23	2.31E-6	20.23	3.284E-6	20.23	4.328E-6	20.23	5.37E-6
20.24	2.16E-6	20.24	3.134E-6	20.24	4.104E-6	20.24	5.08E-6
20.25	2.02E-6	20.25	2.985E-6	20.25	3.881E-6	20.25	4.77E-6
20.26	1.87E-6	20.26	2.836E-6	20.26	3.657E-6	20.26	4.48E-6
20.27	1.716E-6	20.27	2.687E-6	20.27	3.433E-6	20.27	4.179E-6

---

6.0 [V]		7.0 [V]		8.0 [V]		9.0 [V]		10.0 [V]	
Freq.	$\epsilon$	Freq.	$\epsilon$	Freq.	E	Freq.	$\epsilon$	Freq.	$\epsilon$
[Hz]	[RMS]	[Hz]	[RMS]	[Hz]	[RMS]	[Hz]	[RMS]	[Hz]	[RMS]
19.61	4.33E-6	19.61	4.93E-6	19.61	5.79E-6	19.61	6.81E-6	19.61	8.28E-6
19.62	4.45E-6	19.62	5.08E-6	19.62	5.97E-6	19.62	6.98E-6	19.62	8.51E-6
19.63	4.58E-6	19.63	5.22E-6	19.63	6.15E-6	19.63	7.16E-6	19.63	8.73E-6
19.64	4.70E-6	19.64	5.37E-6	19.64	6.34E-6	19.64	7.39E-6	19.64	9.03E-6
19.65	4.81E-6	19.65	5.52E-6	19.65	6.54E-6	19.65	7.59E-6	19.65	9.37E-6
19.66	4.89E-6	19.66	5.67E-6	19.66	6.73E-6	19.66	7.85E-6	19.66	9.73E-6
19.67	4.98E-6	19.67	5.82E-6	19.67	6.93E-6	19.67	8.13E-6	19.67	10.12E-6
19.68	5.15E-6	19.68	5.97E-6	19.68	7.12E-6	19.68	8.43E-6	19.68	10.51E-6
19.69	5.31E-6	19.69	6.12E-6	19.69	7.31E-6	19.69	8.70E-6	19.69	10.87E-6
19.70	5.49E-6	19.70	6.27E-6	19.70	7.54E-6	19.70	9.02E-6	19.70	11.34E-6
19.71	5.66E-6	19.71	6.57E-6	19.71	7.85E-6	19.71	9.37E-6	19.71	11.82E-6
19.72	5.82E-6	19.72	6.87E-6	19.72	8.18E-6	19.72	9.67E-6	19.72	12.31E-6
19.73	6.04E-6	19.73	7.16E-6	19.73	8.43E-6	19.73	10.15E-6	19.73	12.76E-6
19.74	6.27E-6	19.74	7.31E-6	19.74	8.88E-6	19.74	10.58E-6	19.74	13.22E-6
19.75	6.49E-6	19.75	7.61E-6	19.75	9.29E-6	19.75	11.16E-6	19.75	14.06E-6
19.76	6.72E-6	19.76	7.91E-6	19.76	9.70E-6	19.76	11.72E-6	19.76	14.89E-6
19.77	6.97E-6	19.77	8.21E-6	19.77	10.15E-6	19.77	12.29E-6	19.77	15.52E-6
19.78	7.22E-6	19.78	8.66E-6	19.78	10.59E-6	19.78	12.89E-6	19.78	16.34E-6
19.79	7.54E-6	19.79	9.10E-6	19.79	11.10E-6	19.79	13.54E-6	19.79	16.97E-6
19.80	7.73E-6	19.80	9.40E-6	19.80	11.61E-6	19.80	14.15E-6	19.80	17.69E-6
19.81	8.15E-6	19.81	9.85E-6	19.81	12.16E-6	19.81	14.84E-6	19.81	18.40E-6
19.82	8.48E-6	19.82	10.29E-6	19.82	12.69E-6	19.82	15.66E-6	19.82	19.15E-6
19.83	8.88E-6	19.83	10.75E-6	19.83	13.33E-6	19.83	16.21E-6	19.83	19.63E-6
19.84	9.28E-6	19.84	11.19E-6	19.84	14.06E-6	19.84	16.94E-6	19.84	20.12E-6
19.85	9.78E-6	19.85	11.64E-6	19.85	14.55E-6	19.85	17.34E-6	19.85	20.39E-6
19.86	10.36E-6	19.86	12.09E-6	19.86	15.15E-6	19.86	17.88E-6	19.86	20.52E-6
19.87	10.75E-6	19.87	12.66E-6	19.87	15.57E-6	19.87	18.16E-6	19.87	20.72E-6
19.88	11.18E-6	19.88	13.22E-6	19.88	15.81E-6	19.88	18.33E-6	19.88	20.58E-6
19.89	11.64E-6	19.89	13.73E-6	19.89	16.05E-6	19.89	18.42E-6	19.89	20.52E-6
19.90	12.09E-6	19.90	14.18E-6	19.90	16.42E-6	19.90	18.28E-6	19.90	20.34E-6
19.91	12.34E-6	19.91	14.59E-6	19.91	16.64E-6	19.91	18.21E-6	19.91	20.07E-6

---

19.92	12.66E-6	19.92	14.78E-6	19.92	16.94E-6	19.92	17.94E-6	19.92	19.70E-6
19.93	13.06E-6	19.93	15.00E-6	19.93	16.76E-6	19.93	17.70E-6	19.93	19.37E-6
19.94	13.13E-6	19.94	15.19E-6	19.94	16.64E-6	19.94	17.45E-6	19.94	19.13E-6
19.95	13.36E-6	19.95	15.15E-6	19.95	16.33E-6	19.95	17.21E-6	19.95	18.81E-6
19.96	13.28E-6	19.96	15.10E-6	19.96	16.15E-6	19.96	16.84E-6	19.96	18.39E-6
19.97	13.21E-6	19.97	14.89E-6	19.97	15.85E-6	19.97	16.49E-6	19.97	18.03E-6
19.98	13.16E-6	19.98	14.70E-6	19.98	15.57E-6	19.98	16.05E-6	19.98	17.54E-6
19.99	12.84E-6	19.99	14.48E-6	19.99	15.19E-6	19.99	15.67E-6	19.99	17.25E-6
20.00	12.61E-6	20.00	14.25E-6	20.00	14.78E-6	20.00	15.37E-6	20.00	16.78E-6
20.01	12.46E-6	20.01	13.92E-6	20.01	14.40E-6	20.01	14.98E-6	20.01	16.29E-6
20.02	12.24E-6	20.02	13.61E-6	20.02	14.10E-6	20.02	14.63E-6	20.02	15.91E-6
20.03	11.84E-6	20.03	13.31E-6	20.03	13.73E-6	20.03	14.29E-6	20.03	15.48E-6
20.04	11.58E-6	20.04	13.01E-6	20.04	13.43E-6	20.04	13.95E-6	20.04	15.19E-6
20.05	11.31E-6	20.05	12.72E-6	20.05	13.13E-6	20.05	13.61E-6	20.05	14.68E-6
20.06	11.02E-6	20.06	12.27E-6	20.06	12.69E-6	20.06	13.22E-6	20.06	14.36E-6
20.07	10.72E-6	20.07	11.94E-6	20.07	13.39E-6	20.07	12.89E-6	20.07	13.93E-6
20.08	10.37E-6	20.08	11.64E-6	20.08	12.09E-6	20.08	12.57E-6	20.08	13.54E-6
20.09	10.07E-6	20.09	11.34E-6	20.09	11.75E-6	20.09	12.24E-6	20.09	13.22E-6
20.10	9.82E-6	20.10	11.04E-6	20.10	11.45E-6	20.10	11.91E-6	20.10	12.91E-6
20.11	9.55E-6	20.11	10.75E-6	20.11	11.15E-6	20.11	11.67E-6	20.11	12.58E-6
20.12	9.28E-6	20.12	10.45E-6	20.12	10.89E-6	20.12	11.36E-6	20.12	12.33E-6
20.13	9.03E-6	20.13	10.15E-6	20.13	10.59E-6	20.13	11.04E-6	20.13	11.98E-6
20.14	8.76E-6	20.14	9.85E-6	20.14	10.29E-6	20.14	10.75E-6	20.14	11.63E-6
20.15	8.51E-6	20.15	9.55E-6	20.15	10.00E-6	20.15	10.45E-6	20.15	11.34E-6
20.16	8.25E-6	20.16	9.25E-6	20.16	9.70E-6	20.16	10.15E-6	20.16	11.07E-6
20.17	7.91E-6	20.17	8.95E-6	20.17	9.40E-6	20.17	9.85E-6	20.17	10.81E-6
20.18	7.61E-6	20.18	8.66E-6	20.18	9.10E-6	20.18	9.55E-6	20.18	10.57E-6
20.19	7.31E-6	20.19	8.36E-6	20.19	8.81E-6	20.19	9.25E-6	20.19	10.24E-6
20.20	7.01E-6	20.20	8.06E-6	20.20	8.51E-6	20.20	8.95E-6	20.20	9.98E-6
20.21	6.72E-6	20.21	7.76E-6	20.21	8.21E-6	20.21	8.81E-6	20.21	9.73E-6
20.22	6.42E-6	20.22	7.46E-6	20.22	7.91E-6	20.22	8.51E-6	20.22	9.54E-6
20.23	6.12E-6	20.23	7.16E-6	20.23	7.61E-6	20.23	8.36E-6	20.23	9.34E-6
20.24	5.82E-6	20.24	6.87E-6	20.24	7.31E-6	20.24	8.06E-6	20.24	9.21E-6
20.25	5.52E-6	20.25	6.57E-6	20.25	7.16E-6	20.25	7.91E-6	20.25	8.91E-6

20.26	5.37E-6	20.26	6.42E-6	20.26	6.87E-6	20.26	7.76E-6	20.26	8.67E-6
20.27	5.07E-6	20.27	6.27E-6	20.27	6.72E-6	20.27	7.61E-6	20.27	8.43E-6

Using the acquired numerical data, it is possible to build the curves shown in Figure 79, for different levels of input.

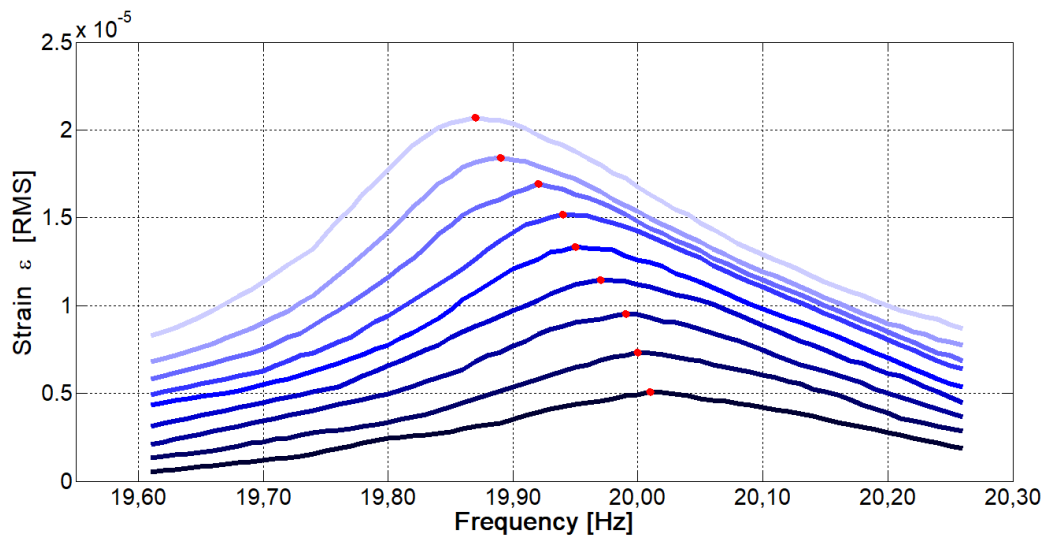


Figure 79: sample exposed 2040 hours: frequency response measured around resonance for increasing levels of driving force. The excitation range is 2 V – 10 V.

As can be noted from the acquired numerical data, there is an increment of the resonant frequency compared to that obtained for the second level of damaging of the para-aramid sample. The values range from 20.01 Hz, for the first curve relating to 2 V, to 19.87 Hz for the last one, relating to 10 V.

By referring to the numerical data acquired for this second sample, in Figure 80 is shown the backbone curve obtained, and the relative value of  $\chi$  cubic stiffness coefficient. In this way it is also possible to quantify the nonlinear behaviour of the material under investigation.

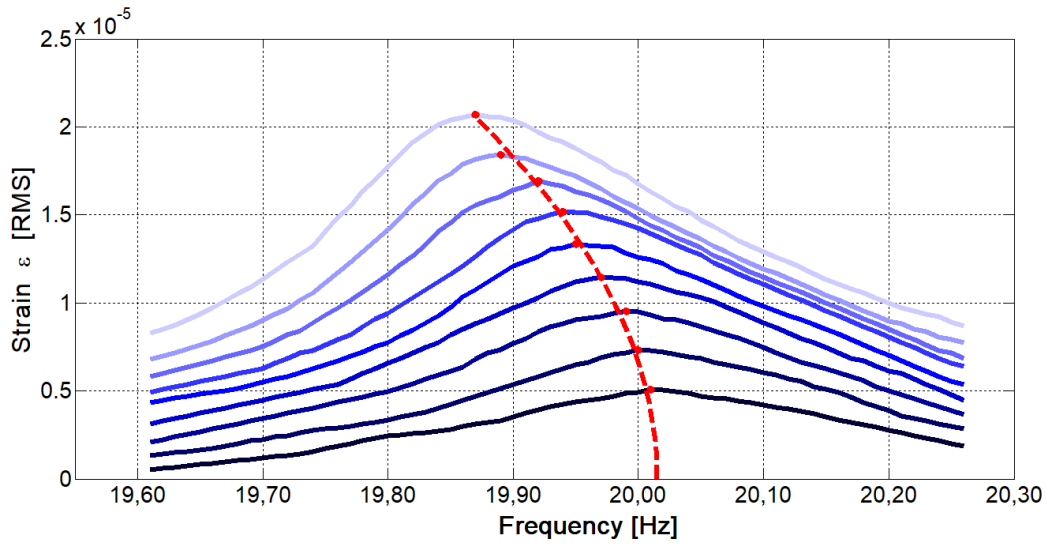


Figure 80: sample exposed 2040 hours: frequency response measured around resonance for increasing levels of driving force. The excitation range is 2 V – 10 V. The red dots highlight the maximum of the response curve and the dashed red line is the estimated backbone response curve.

The cubic stiffness coefficient obtained in this case is equal to  $\chi = -7.221 \cdot 10^{11} \text{ N/m}^3$ .

Finally, the value of the  $\zeta$  damping of the system was calculated applying the half-power bandwidth method, and was computed for the 5 V response and was estimated at 0.69% ( $Q=73$ ).

Alternatively, the resonant frequency distortion can be quantified by the nonlinear backbone curve connecting peak amplitudes  $a_p$  of the various resonance curves at different excitation levels. The frequency  $f(a_p)$  at which the peak occurs can be approximated using perturbation analysis (Worden & Tomlinson, 2001) as

$$f(a_p) = f_0 \sqrt{1 + \frac{3k_3}{4k} a_p^2} \quad (25)$$

where  $f_0$  is the frequency of the underlying resonance frequency.

In order to identify a **material-specific device-independent parameter**, the backbone curves represented here in terms of the deformation strain  $\varepsilon$ , with a dimensionless coefficient:

$$X = \frac{3}{4}L^2k_3k \quad (26)$$

where  $k_3$  in the cubic stiffness coefficient,  $k$  the linear stiffness term, and  $L$  the sample length.

The non-linearity index rewritten in this way is dimensionless and suitable to characterize material non-linearity. Its rms value, indicated just as  $\varepsilon$ , will be used for consistency. Equation 25 is then rewritten as

$$f(a_p) = f_0(1 + X\varepsilon^2) \quad (27)$$

The common engineering unit  $\mu\varepsilon$  will be adopted, usually indicated as “micro-strain” ( $1 \mu\varepsilon = 1 \mu\text{m}/\text{m}$ ). Equation 27 was used to identify  $X$  from the backbone curve.

The coefficient  $X$  of Equation 27 was estimated for each sample by fitting the theoretical parabolic shape of the backbone curve onto the family of resonance curves. The dots mark the peaks of response curves and the dashed red line is the best estimated backbone curve. The coefficient  $X$  was obtained by peak frequencies and peak strains of various pairs of curves in Equation 28, and combining results in an uncertainty weighted average.

$$\frac{f_1 - f_2}{f_2} = X(\varepsilon_1^2 - \varepsilon_2^2) \quad (28)$$

In Equation 28, indexes 1 and 2 identify parameters of the two curves of the pair used in the calculation. Absolute uncertainty was evaluated for  $X$  to be less than  $1 \cdot 10^{-6}$  for all families of curves by computing the standards deviation of such values and dividing it by the square root of the used number of pairs. This means for the most damaged sample a relative uncertainty of roughly 5%, aligned to what evaluated for the other quantities. However, in this case, it turns out to be more than adequate to support clear evidence of the effects of UV exposure because  $X$  was increased in the process by almost a factor of four.

The best values obtained for the coefficient  $X$  are  $-5.6 \cdot 10^{-6}$ ,  $-1.08 \cdot 10^{-5}$ ,  $-1.41 \cdot 10^{-5}$ , and  $-1.81 \cdot 10^{-5}$  per square micro strain respectively for 0, 792, 1272, and 2040 hours of exposure to UV radiation.

The progressive increase in non-linearity is represented in Figure 81, where a linear increase of the coefficient  $X$  versus exposure time can be clearly observed.

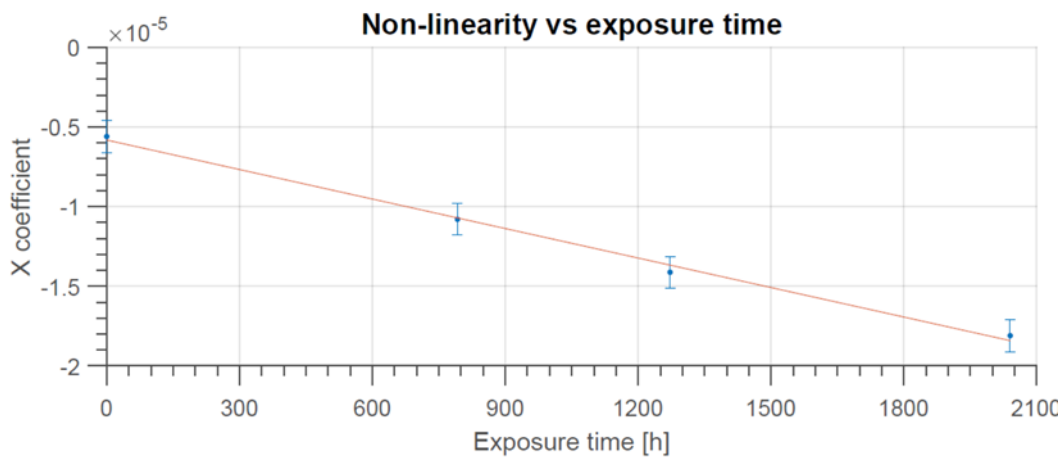


Figure 81: variations of measured nonlinear coefficient  $X$  with respect to UV exposure time.

The slope of the non-linearity coefficient change versus exposition to UVA radiation time in hours can be evaluated from this plot to be about  $-6.1 \cdot 10^{-9}/\text{h}$  at the used irradiation level of  $1 \text{ kW}/\text{m}^2$ . This is equivalent to about  $-0.3 \cdot 10^{-9}/\text{J}$  of incident UV energy on 1 m of a single  $12 \mu\text{m}$  fibre, according to the dose evaluation given in section 6.2. Whether the damage per Joule depends on radiation level remains to be determined. What can be safely stated here is that unambiguous detection of UV damage can be assessed with this method at the present level of uncertainty after about 150 h of continuous exposure to  $1 \text{ kW}/\text{m}^2$  UVA radiation, because that is the time that it takes in these conditions for  $X$  to increase more than the uncertainty. This is equivalent to about 2 years of normal environmental UV exposure at mid latitudes if damage is independent of intensity. The question whether this is true deserves more experimentation.

How changes in the nonlinear coefficient are physically related with fibre deterioration, and whether reduced fibre strength can be reliably evaluated by measurements of non-linearity with the low excitation method illustrate here, are

questions that most certainly deserve further attention, but the possibility of developing this approach into a field applicable non-destructive method appears unquestionably attractive.

#### 6.2.4 Comparison of the results obtained

Tests were carried out on different Kevlar® 29 yarn samples extracted from the same bundle. Yarns consist of roughly 1500 fibres, 12  $\mu\text{m}$  in diameter, judging from the specified 2500 dTex number provided by the manufacturer, which yields a total cross-sectional area of 0.174  $\text{mm}^2$  for the bundle. This value is used to convert voice coil force into applied stress, for which a maximum rms value of about 20 kPa is obtained. Four samples were cut to equal length, for a free length in operation in the test machine of 665 mm. Uncertainty on the latter was estimated to be about  $\pm 1$  mm. One of the samples was not exposed to UV and served as a reference. The other three were exposed to radiation as detailed in this chapter. The yarn is pale yellow when new, but takes on an increasingly “burnt” colour after exposure to UV radiation.

The resonance frequency of about 20 Hz of all samples returns a tensile modulus of 70 GPa by using the mentioned values for length and cross section, quite in line with typical data which can be found in the literature. Sample-to-sample variations are below 5% and must be considered meaningless due to lack of information on actual fibre count and diameter.

The damping coefficient  $\zeta$  (estimated with the half-power bandwidth method) appeared to vary for all samples with the excitation level, increasing from below 0.005 (Q above 100) at the 4 kPa rms (2 V), to below 0.006 (Q above 80) at the 20 kPa rms (10 V). However, for low excitation, values obtained with this approach are quite strongly affected by the judgement on where the zero is positioned in the curve, and for high-excitation by detector saturation.

Uncertainty must therefore be taken conservatively to be at least of the order of a few percent, and higher at low excitation. A correction can be applied to account for detector non-linearity, which seems to suggest smaller dependence of damping on excitation level than is shown in Figure 82. This is not reported here as quality factor at the end didn't turn out to change significantly with UV exposure and was finally discarded as a useful indicator for UV damage in para-aramid fibres.

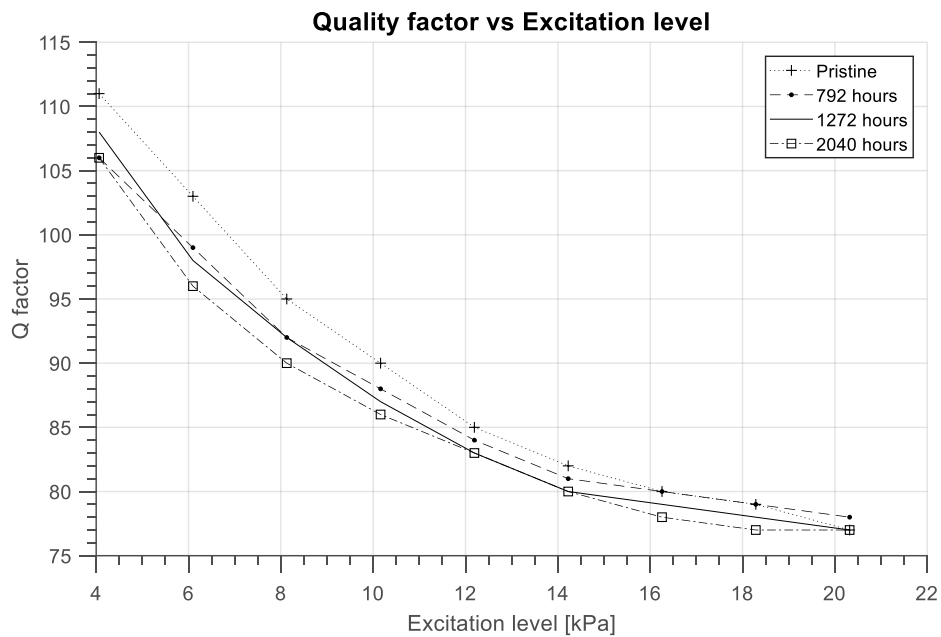


Figure 82: measured variations of Q-factor versus drive level for different exposure times to UV.

In Figure 82 variations with excitation level of measured quality factor  $Q$  are shown for all four samples. It can be noticed that the curves show similar magnitude and behaviour. Because of the uncertainty in the  $Q$  factor determination, the slight decrease in the  $Q$  values that might be inferred by these curves does not appear to be significant.

It may be useful to point out here that the peak tension developed on resonance in the sample for the maximum excitation stress of 20 kPa rms (10 V), as obtained by multiplying it by the  $Q$  factor, can be inferred to be about 2.2 MPa. This is less than 3% of the preloading given by the weight of the oscillating mass at rest (which guarantees the sample is never fully unloaded), and less than 0.1% of the ultimate strength of the material (which proves the ability of the adopted approach to monitor damage without overstressing the sample).

In Table 17, are contained the results of the forced tests obtained in terms of frequency, non-linearity index, and quality factor (for the 5 V response), both for the case of original Kevlar® sample, that for the three level of damaging.

**Table 17:** results recap

<b>PRISTINE SAMPLE</b>	
Resonance frequency [Hz]	From 20.61 to 20.66
Non-linearity index $\chi$ [N/m <sup>3</sup> ]	-4.0282E+11
Non-linearity index $X$ [-]	-5.6E-6
Quality factor	74
<b>DAMAGED SAMPLE FOR 792 HOURS (33 days)</b>	
Resonance frequency [Hz]	From 20.67 to 20.76
Non-linearity index $\chi$ [N/m <sup>3</sup> ]	-5.0280E+11
Non-linearity index $X$ [-]	-1.08E-5
Quality factor	86
<b>Damaged sample for 1272 hours (53 days)</b>	
Resonance frequency [Hz]	From 19.78 to 19.87
Non-linearity index $\chi$ [N/m <sup>3</sup> ]	-5.5670E+11
Non-linearity index $X$ [-]	-1.41E-5
Quality factor	76
<b>Damaged sample for 2040 hours (85 days)</b>	
Resonance frequency [Hz]	From 19.87 to 20.01
Non-linearity index $\chi$ [N/m <sup>3</sup> ]	-7.2209E+11
Non-linearity index $X$ [-]	-1.81E-5
Quality factor	73

The non-linearity index was used to characterize non-linearity of the material under investigation. It was evaluated with the method of fitting a parabolic backbone curve, connecting the maxima, to the family of resonance profiles taken at different excitation levels (from 2 V to 10 V).

The experimental results showed that  $X$  is sensitive to cumulated UVA radiation, increasing linearly with the latter. Its measured variations after quite normal amount of irradiation, in fact, greatly exceed the uncertainty with which it is evaluated with the proposed method. This is undoubtedly due to a weak nonlinear response of the material. All other source of non-linearity have been

duly considered, modelled and quantified as negligible in Chapter 4. Using this parameter to assess cumulated damage occurred in Kevlar® 29 fibres from exposure to environmental UVA radiation should therefore be considered seriously.

The other characteristics considered do not show the same clear and easily identified sensitivity, and should therefore be discarded as damage detectors. Specifically, the tensile modulus does not seem to suffer noticeably from UV irradiation, although the increasing non-linearity suggests a possible decrease in ultimate strength. How exactly the two may be physically related to radiation appears to deserve further study at the light of results presented here.

Therefore, this result is confirming our initial hypothesis that this parameter may be used as a valuable and trustworthy index of damage in case of material evaluation, for applications in Structural Health Monitoring (SHM) field. With the uncertainty level demonstrated in this work, a couple of years of deployment in normal outdoors would already show a measurable increase in non-linearity, which would imply a decrease in ultimate strength. Clearly, more sensitive methods might be devised, allowing even earlier warning of UV damage.



## **Chapter 7**

# **A new concept for a tie element with self-diagnosis properties**

As stated in the introductory sections, this research was developed in the field of “Advanced Structural Materials for Applications to Cultural Heritage”. In particular, this work is focused on high-performance materials for applications aimed to structural and seismic protection of cultural heritage. For this reason, the final aim of the whole research was to define a self-diagnosis strategy for high-strength fibres, yarns and ties in view of efficient, non-invasive, and reversible interventions on cultural heritage buildings.

The work reported in the previous chapters has demonstrated a link between the exposure time to UV rays, and the dynamic behaviour of the material. This connection was evaluated by means of a non-linearity index. Exposure to UV rays was used to produce a damage because aramid materials, such as Kevlar®, are particularly sensitive to this factor. The prototype testing machine developed in this research (see chapter 4) has been conceived in order to be able to detect weak nonlinear behaviours, being consequently a very sensitive machine.

It was decided to use the distinctive characteristics of the testing machine to create a control system with self-diagnosis properties for applications to in-place reinforcement elements, which are in need of continuous (on line) monitoring. A natural application of this testing strategy could be on ties realised with HPM

materials, and those employed for the reinforcement of structural elements of building with particular historical and artistic relevance.

In this chapter, which constitutes the conclusive part of this work, a new concept of control system with self-diagnosis properties was described. This may result in possible applications of our prototype-testing machine to structural and seismic protection of cultural heritage, i.e. the final aim of this dissertation.

## 7.1 Structural Health Monitoring

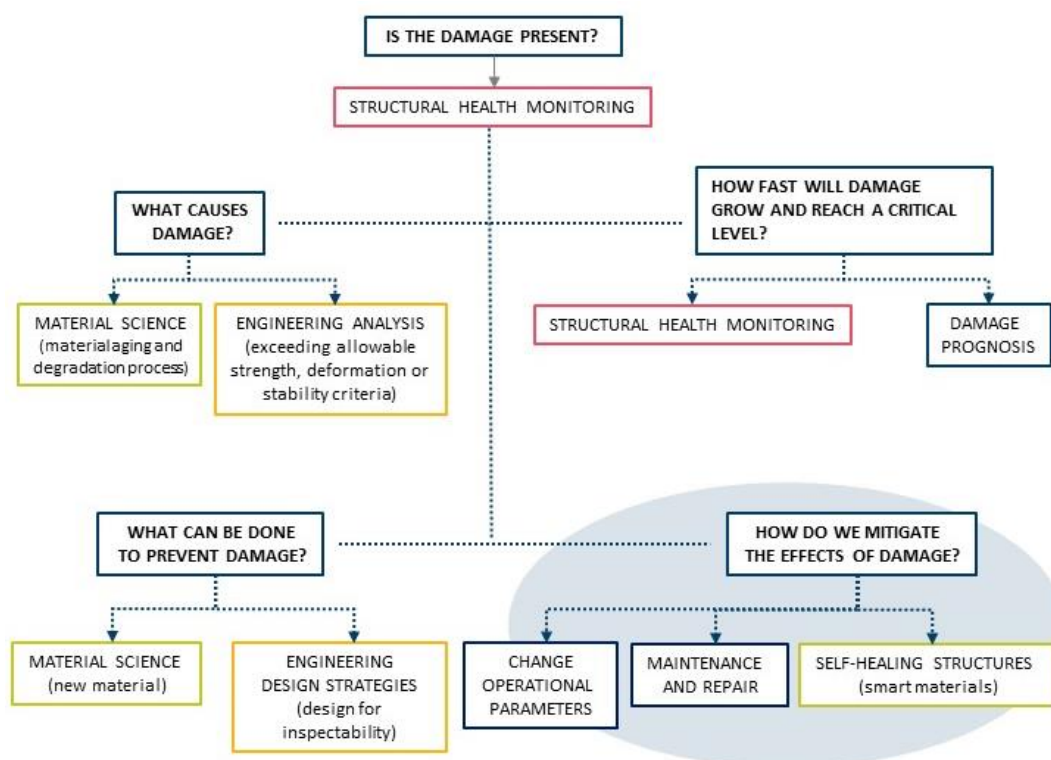


Figure 83: typical Structural Health Monitoring strategy..

According to Worden (Farrar & Worden, 2013), the damage will be defined as changes to the material and/or geometric properties of a structural or mechanical system, including changes to the boundary conditions and system connectivity, which adversely affect current or future performance of that system (Figure 83).

Implicit in this definition of damage is a comparison between two different states of the system (i.e. stiffness, boundary and/or connectivity change).

All materials used in engineering systems have some inherent initial flaws. Under appropriate loading flaws will grow and coalesce to the point where they produce component level failure. Further loading may cause additional component failures that can lead to system-level failure. In some cases this evolution can occur over relatively long time scales (e.g. corrosion, fatigue crack growth). Instead, other cases cause this damage evolution to occur over relatively short time scales (e.g. earthquake loading, impact-related damage).

Must consider the length and time scales associated with damage initiation and evolution when developing a SHM system. SHM is the process of implementing a damage detection strategy for different field of application such as aerospace, civil and mechanical engineering infrastructure. This technique is very useful for “novel materials”, because the long-term degradation processes are not well understood.

The SHM process involves the observation of a system over time using periodically sampled dynamic response measurements from an array of sensors. The extraction of damage-sensitive features from these measurements. The statistical analysis of these features is then used to determine the current state of system health. SHM can make use of non-destructive evaluation techniques.

After extreme events, such as earthquakes or blast loading, SHM is used for rapid condition screening and aims to provide, in near real time, reliable information regarding the integrity of the structure (Farrar & Worden, 2013).

## **7.2 The concept of a tie with self-diagnosis properties**

There is a growing body of literature on non-destructive evaluation technique. The low cost system proposed in this work, could be realised by using the same components, devices, and principle of operation described in Chapter 4. The interesting aspect is that the testing machine developed is less invasive, very versatile (could be adapted to different situation), cheap, and, and removable with little effort.

The setup may be modified case-by-case, taking into account:

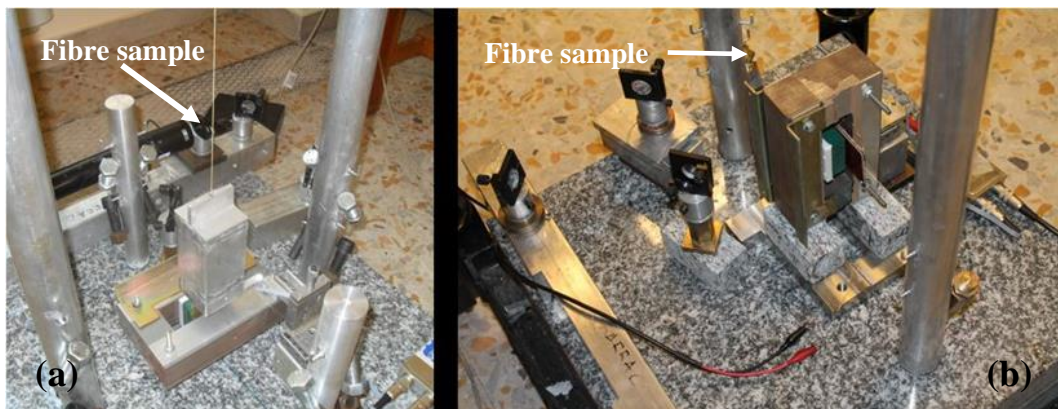
- the special needs,

- the structural reinforcing element to be monitored,
- the context in which the control system is placed.

The equipment that may be adapted case-by-case is composed by:

- a physical structure,
- a confinement structure,
- an optical system
- an electromagnetic system (the voice coil).

In Figure 84 are shown three different setup of the testing machine investigated, by using the same components and devices.



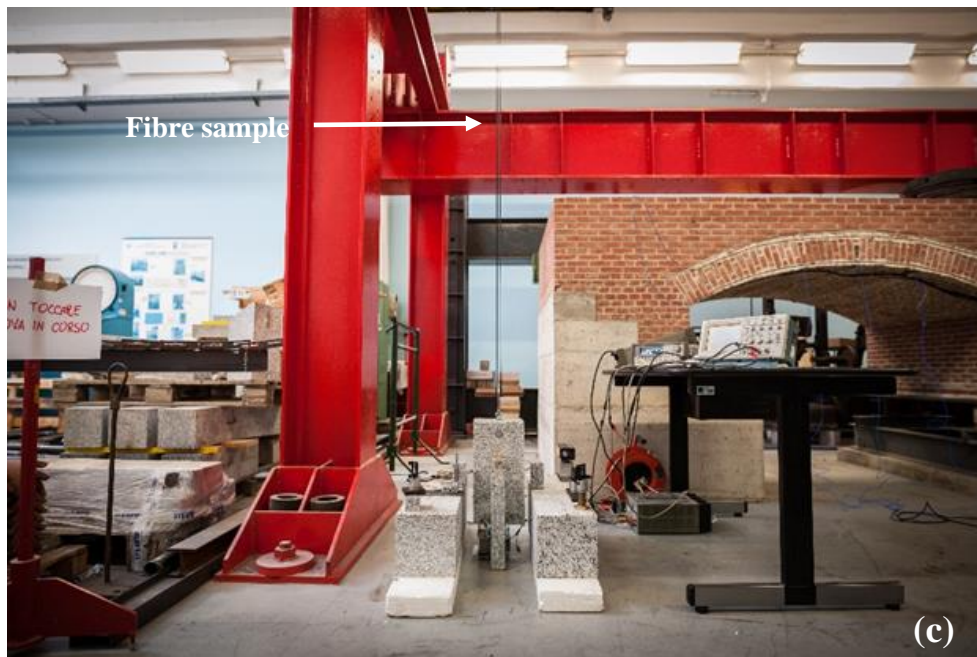


Figure 84: possible setup configurations investigated: a) vertical sample, and suspended mass of 1.345 kg, b) horizontal sample, and mass of 0.150 kg, c) vertical sample, and suspended mass of 45 kg.

In the following Figures 85-87 a possible alternative solution is shown of how this testing machine could be applied to ties employed for the reinforcement of masonry arches and vaults, as a system with self-diagnosis properties.

In the setup of the testing machine used in Chapters 5 and 6, the sample investigated was placed vertically with a suspended mass at one hand, which guaranteed the tensioned during the tests (Figure 85 a-b). A small ball lens was glued on a support attached to the suspended mass, through which it was possible an indirect reading of the sample displacement. In this new setup, the ball lens is applied to a mass placed in a middle span (Figure 85 c).

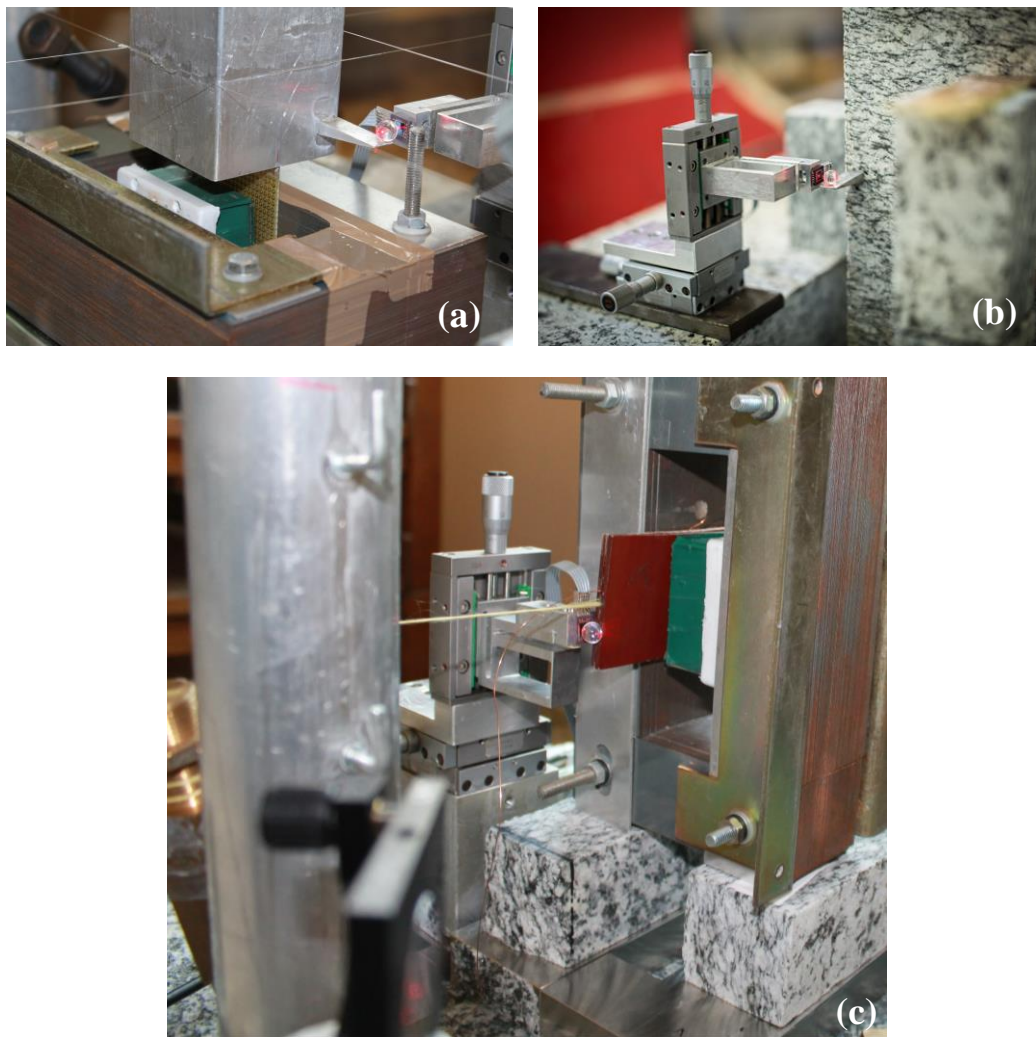


Figure 85: different setup investigated with different ball lens position.

The system shown in these figures is nothing more than an example of one possible application, not in scale. It was built in the Metrology Laboratory of the Electronic and Telecommunication Department of Politecnico di Torino.

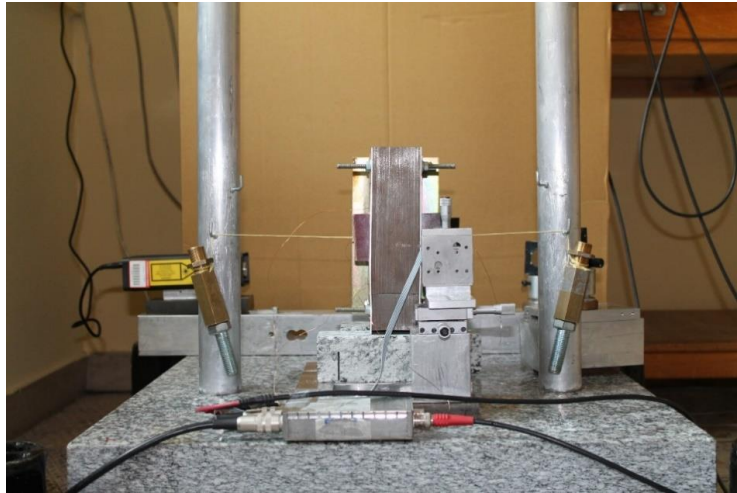


Figure 86: the concept of control and self-diagnosis system.

In this case, since it is applied to an existing reinforcing element, which is already tensioned, as in the case of a tie for example, the mass is positioned at mid-span, and does not apply a stress into the element. In any case, the measured displacement of the mass allows the study of the dynamic behaviour of the element under investigation.



Figure 87: the concept of the system for self-diagnosis: demonstrative sketch of a possible application.

Another type of possible application can be identified in a permanent strengthening intervention on the Fossano belfry, which was presented in Section 3.6.

The last safety measure works on this tower were actually put in place in 2012 after the vertical cracking pattern became evident. The structure was provisionally retrofitted when these cracks reached a critical state. Steel tie-rods were placed on the inside and outside of the bell tower at eleven different levels along the height (Figures 88-89).



Figure 88: the belfry of the Fossano Cathedral with the strengthening intervention.

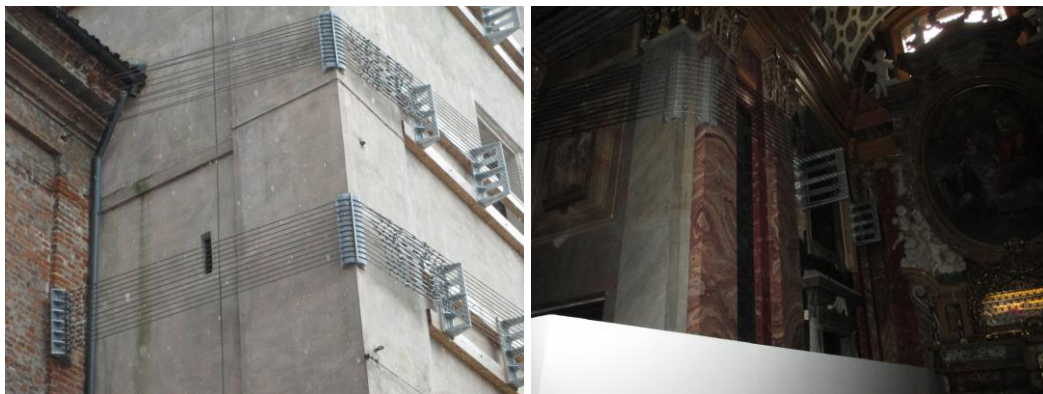


Figure 89: particular of the last safety measure works.

In Section 3.6.5, it was evidenced how a strengthening intervention with high-performance materials (AFRP strips or cables) can be a viable solution when compared to standard ones.

The proposed self-diagnosis system can be incorporated in cables made with high-performance materials (e.g. Kevlar®), which are placed inside or outside the belfry (in protected positions). This system can detect changes in the material properties which affect the dynamic properties of the structure, this representing an advantageous choice for provisional and/or reversible interventions. In fact, the minimally invasive self-diagnosis system presented in this chapter can constantly monitor the efficacy of the system, e.g. due to the possible relaxation phenomena.

In conclusion, this last chapter strives to emphasize how, with accurate and well-thought design, it is possible to realise a cheap control system, able to measure dynamic parameters by using a relatively low-cost equipment. Currently, the same measurements can be performed only in very controlled environments and would require very costly equipment. With this new concept, after the accomplishment of the full engineering process, it will be possible to conceive self-diagnosis systems and interventions that satisfy all the mentioned principles of conservation (see Chapter 1), with a view to producing real world applications to cultural heritage buildings.



# Conclusions

This dissertation concerns high resistance materials for application to seismic protection and monitoring of cultural heritage, with a special focus on historical masonry structures. In particular, the final aim of this research was to define a self-diagnosis strategy for fibres, yarns and ties in view of efficient, non-invasive, reversible and cheap intervention on cultural heritage buildings.

The first part of the this work illustrates the principles and realization of a prototype apparatus for fiber testing, capable of accurately measuring material  $Q$  values up to  $10^3$ . The presented results were obtained from three different types of high strength fibers, namely Kevlar® 29, Silicon Carbide and Carbon. Suggestions are also given for the improvement of the apparatus and for extending its accuracy. The proposed apparatus could be a critical tool in the study of mechanical dissipation mechanisms in materials with particularly low levels of intrinsic dissipation.

As a further step, it was explored the potential of a recently conceived optical test system for high-sensitivity dynamic measurements, for assessing damage caused by UV exposure of Kevlar® 29 samples. Various mechanical properties of the fibres were estimated and compared at different damage levels. The non-linearity index, identified resorting to the backbone curve, proved to be a more robust damage indicator with respect to damping.

The experimental findings led to propose a concept in which a prototype acts as a control system with self-diagnosis properties for fibres, yarns and ties. The proposed application of the new prototype-testing machine is precisely in the field of structural and seismic protection of cultural heritage. In addition, the dissertation emphasized how, with accurate and well-thought design, it is possible to measure these dynamic parameters using a relatively low-cost equipment,

compared to typical costs of dynamic testing machines. In the field of cultural heritage, in particular, the availability of low-cost sensing and actuation devices will be a key factor for conceiving non-invasive and reversible interventions with high resistance materials.

Future studies will investigate different definitions for the non-linearity index to be used for diagnosis purpose.

In addition, the prototype testing machine will be optimised for application to full-scale heritage structures. Further verifications on HPM are necessary, especially about their performances when are coupled with masonry and other traditional materials. Further research will be in turn required to develop and incorporate a control strategy, so as to exploit the self-diagnosis properties and transform the concept to reality.

# References

(FIB), F. I. d. B., 2001. *Externally bonded FRP reinforcement for RC structures*. Lausanne, Switzerland: Bulletin 14.

ACI Committee 440, 2001. *Guide for the design and construction of concrete reinforced with FRP bars*. Farmington Hills, Mich.: American Concrete Institute.

ACI Committee 440, 1996. *State of the art report on fiber reinforced plastic (FRP) reinforcement for concrete structures*. Farmington Hills, Mich.: American Concrete Institute.

Adams, D. & Allemang, R., 1999. A new derivation of the frequency response function matrix for vibrating non-linear systems. *Journal of Sound and Vibration*, 227(5), pp. 1083-1108.

Aiello, M. & Conte, C., 2009. *Seismic vulnerability of masonry curved elements*. Venezia, Associazione Italiana Compositi (AICO), pp. 1-8.

Aiello, M., Micelli, F. & Valente, L., 2005. *Circular masonry columns confined with FRP*. Lyon, France, Proceedings of the 3rd International Conference.

Aiello, M., Micelli, F. & Valente, L., 2007. Structural Upgrading of Masonry Columns by Using Composite Reinforcements. *Journal of Composites for Construction*, pp. 650-658.

Aiello, M. & Sciolti, M., 2009. *Elementi curvi in muratura rinforzati con nastri in FRP: analisi dell'aderenza*. Venezia, Associazione Italiana Compositi (AICO), pp. 18-25.

Aiello, M. & Sciolti, S., 2006. Bond analysis of masonry structures strengthened with CFRP sheets. *Construction and Building Materials*, pp. 90–100.

Alecci, V., Briccoli Bati, S. & G., R., 2009. *Confining compressed pillars with FRP composites*. Venezia, Associazione Italiana Compositi (AICO), pp. 26–33.

Alecci, V., Briccoli Bati, S. & Ranocchiali, G., 2009. *Confining compressed pillars with FRP composites*. Venezia, Associazione Italiana Compositi (AICO), pp. 26–33.

Allard, J. & Champoux, Y., 1992. New empirical equations for sound propagation in rigid frame fibrous materials. *The Journal of Acoustical Society of America*, pp. 3346–3353.

Amada, S. et al., 1997. The mechanical structures of bamboos in viewpoint of functionally gradient and composite materials. *Journal of Composite Materials*, pp. 800–819.

Arrieta, C., David, E., Dolez, P. & Vu-Khanh, T., 2011. Hydrolytic and photochemical aging studies of a Kevlar-PBI blend. *Polymer Degradation and Stability*, pp. 1411–1419.

Ascione, L., Feo, L. & Fraternali, F., 2005. Load carrying capacity of 2D FRP/strengthened masonry structures. *Composites Part B*, pp. 619–626.

Ascione, L., Napoli, A. & Realfonzo, R., 2009. *Strengthening of masonry with Mechanically Fastened FRP laminates*. Venezia, Associazione Italiana Compositi (AICO), pp. 43–50.

Bakis, C. et al., 2002. Fiber-Reinforced Polymer Composites for Construction: State-of-the-Art Review. *Journal of composites for construction*, pp. 73–83.

Baratta, A. & Corbi, O., 2007. Stress analysis of masonry vaults and static efficacy of FRP repairs. *International Journal of Solids and Structures*, pp. 8028–8056.

Barbieri, A., Borri, A., Corradi, M. & Di Tommaso, A., 2002. *Dynamic Behaviour of Masonry Vaults Repaired with FRP: Experimental Analysis*.

Basilio, I., Oliveira, D. & Lourenço, P., 2004. *Optimal FRP strengthening of masonry arches*. Amsterdam, pp. 1-10.

Beckmann, P. & Bowles, R., 2004. *Structural aspects of building conservation*. Oxford Elsevier.

Bednarz, L., Jasienko, J., Rutkowski, M. & Nowak, T., 2014. Strengthening and long-term monitoring of the structure of an historical church presbytery. *Engineering Structures*, pp. 62-75.

Benichou, N., Kodur, V., Green, M. & Bisby, L., 2010. Fire Performance of Fibre-Reinforced Polymer Systems Used for the Repair of Concrete Buildings. *Construction Technology Updates - CNRC*, pp. 1-6.

Berg, A., Bank, L., Oliva, M. & Russell, J., 2006. Construction and cost analysis of an FRP reinforced concrete bridge deck. *Construction and Building Materials*, pp. 515–526.

Bertha, M. & Golinval, J., 2014. *Identification of a time-varying beam using Hilbert Vibration Decomposition*. Orlando, FL, USA.

Berthelot, J. & Sefrani, Y., 2004. Damping analysis of unidirectional glass and Kevlar fibre composites. *Composites Science and Technology*, pp. 1261-1278.

Betti, M. & Vignoli, A., 2008. Modelling and analysis of a Romanesque church under earthquake loading: Assessment of seismic resistance. *Engineering Structures*, pp. 352-367.

Bin Kabir, R. & Ferdous, N., 2012. Kevlar-The Super Tough Fiber. *International Journal of Textile Science*, pp. 78-83.

Boothby, T., 2003. Analysis of masonry arches and vaults. *Progress in Structural Engineering and Materials*, pp. 246-256.

Borri, A., Casadei, P., Castori, G. & Ebaugh, S., 2007. *Research on composite strengthening of masonry arches*. Patras, Greece, Proceedings of the 8th International Symposium.

Borri, A., Casadei, P., Castori, G. & Hammond, J., 2009. Strengthening of Brick Masonry Arches with Externally Bonded Steel Reinforced Composites. *Journal of Composites for Construction*, pp. 468-475.

- Borri, A. & Castori, G., 2009. *Un contributo allo studio della durabilità dei rinforzi strutturali con materiali compositi*. Venezia, Associazione Italiana Compositi (AICO), pp. 99-107.
- Borri, A., Castori, G. & Corradi, M., 2009. *Una nuova tecnica di realizzazione di muratura armata con fibre metalliche*. Venezia, Associazione Italiana Compositi (AICO), pp. 108-115.
- Borri, A., Castori, G. & Paci, G., 2009. *Indagine numerica sull'efficacia dell'utilizzo di nastri in materiali compositi fibrorinforzati applicati su volte cilindriche*. Venezia, Associazione Italiana Compositi (AICO), pp. 116-123.
- Borri, A. & Corradi, M., 2009. *Confinamento di pilastri in muratura tramite compositi con fibre metalliche*. Venezia, Associazione Italiana Compositi (AICO), pp. 124-131.
- Borri, A., Corradi, M. & Vignoli, A., 2002. *New materials for strengthening and seismic upgrading interventions*. Prague, Czech Republic.
- Boscato, G., Russo, S., Ceravolo, R. & Zanotti Fragonara, L., 2015. Global Sensitivity-Based Model Updating for Heritage Structures. *Computer-Aided Civil and Infrastructure Engineering*, pp. 620-635.
- Botelho, E. et al., 2006. Damping behaviour of continuous fibre/metal composite materials by the free vibration method. *Composites: Part B*, pp. 255-263.
- Branco, M. & Guerreiro, L., 2011. Seismic rehabilitation of historical masonry buildings. *Engineering Structures*, pp. 1626-1634.
- Braun, S. & Feldman, M., 2011. Decomposition of non-stationary signals into varying time scales: Some aspects of the EMD and HVD methods. *Mechanical Systems and Signal Processing*, pp. 2608-2630.
- Briccoli Bati, S. & Rotunno, T., 2001. *Environmental durability of the bond between the CFRP composite materials and masonry structures*. Guimaraes, Portugal., Proceedings of the 3rd International Conference, pp. 1039–1046.
- Briccoli Bati, S. & Rovero, L., 2000. *Consolidation of masonry arches with carbon-fiber reinforced plastics*. Madrid, Spain.

Briccoli Bati, S. & Rovero, L., 2001. *Experimental validation of a proposed numerical model for the FRP consolidation of masonry arches*. Guimaraes, Portugal, Proc. of the 3rd Int. Conf., pp. 1057–1066.

Briccoli Bati, S. & Rovero, L., 2008. Towards a methodology for estimating strength and collapse mechanism in masonry arches strengthened with fibre reinforced polymer applied on external surfaces. *Materials and Structures*, pp. 1291–1306.

Briccoli Bati, S. & Rovero, L., 2009. *Experimental analysis on scale models of CFRP reinforced arches*. Venezia, Associazione Italiana Compositi (AICO), pp. 140-145.

Buchan, P. & Chen, J., 2007. Blast resistance of FRP composites and polymer strengthened concrete and masonry structures– A state-of-the-art review. *Composites: Part B*, pp. 509-522.

Bunton, D., 2002. Generic moves in PhD thesis introductions.. In: *Academic discourse*. London: Pearson Education Limited, pp. 57-75.

Burgoyne, C., 1987. Structural use of parafil ropes. *Construction & Buildings materials*, pp. 3-13.

Burgoyne, C., 1993. Parafil ropes for prestressing applications. *Fibre-Reinforced-Plastic Concr. Struct. Prop. Appl.*, pp. 333–351.

Burgoyne, C., 1998. *Advanced composites - the challenge to bridge designers*. Calgary, Alberta, Canada, Canadian Society for Civil Engineering, pp. 1-14.

Burgoyne, C. & Balafas, I., 2007. *Why is FRP not a financial success?*. Patras, Greece, pp. 7-18.

Burgoyne, C. J., 1991. *Parafil ropes - from development to application*. Cambridge.

Burley, E. & Rigden, S. R., 1997. *The use of life cycle costing in assessing alternative bridge design*. London, Municipal Engr., pp. 22-27.

Cai, G., Li, D., Fang, D. & Yu, W., 2014. A new apparatus to measure the effect of temperature and light on the bending fatigue properties of Kevlar 49 and PBO fibers. *Polymer Testing*, pp. 143-148.

- Calderoni, B., Cordasco, E., Lenza, P. & Pacella, G., 2009. *Indagine sperimentale su elementi compressi in muratura di tufo rinforzati con fibre di carbonio*. Venezia, Associazione Italiana Composito (AICO), pp. 153-160.
- Campbell, F., 2010. *Structural Composite Materials*. Materials Park, OHIO: ASM International.
- Capozucca, R. & Ricci, V., 2016. Bond of GFRP strips on modern and historic brickwork masonry. *Composite Structures*, pp. 540-555.
- Caprili, S., Mangini, F. & Salvatore, W., 2015. *Evaluation of structural safety and seismic vulnerability of historic studies and applications*. WIT Press, pp. 369-380.
- Caratelli, A., Ianniruberto, U. & Rinaldi, Z., 2009. *Experimental behaviour of masonry frames strengthened with composite sheets*. Venezia, Associazione Italiana Compositi (AICO), pp. 161-168.
- Cardoso, R., Lopes, M. & Bento, R., 2005. Seismic evaluation of old masonry buildings. Part I: Method description and application to a case-study. *Engineering Structures*, pp. 2024–2035.
- Carrella, A. & Ewins, D., 2011. Identifying and quantifying structural nonlinearities in engineering applications from measured frequency response functions. *Mechanical Systems and Signal Processing*, 25(3), pp. 1011-1027.
- Casareto, M., Oliveri, A., Romelli, A. & Lagomarsino, S., 2003. *Bond behavior of FRP laminates adhered to masonry*. Milano, Italy, Proceedings of the International Conference.
- Cavalagli, N. & Gusella, V., 2015. Dome of the Basilica of Santa Maria Degli Angeli in Assisi: Static and Dynamic Assessment. *International Journal of Architectural Heritage*, pp. 157-175.
- Cecchi, A., Milani, G. & Tralli, A., 2004. In-plane loaded CFRP reinforced masonry walls: mechanical characteristics by homogenisation procedures. *Composites Science and Technology*, pp. 2097–2112.
- Celestini, G., 2009. *Evoluzione della tecnologia dei rinforzi strutturali con materiali composite nel consolidamento e recupero del patrimonio monumentale e di edifici esistenti attraverso l'analisi di esperienze umbre. Ipotesi di sviluppo*. Venezia, Associazione Italiana Compositi (AICO), pp. 177-183.

Celestini, G., 2009. *Innovation on Advanced Composite Materials for Strengthening and Protection of Historical Masonry Structures*. Venezia, Associazione Italiana Compositi (AICO), pp. 184-191.

Ceravolo, R. et al., 2012. *Reconciling geometry and dynamics: model for oval domes*. Firenze

Ceravolo, R. et al., 2017. A New Testing Machine for the Dynamic Characterization of High Strength Low Damping Fiber Materials. *Experimental Mechanics*, pp. 65–74.

Ceravolo, R. et al., 2018. Measurement of weak non-linear response of Kevlar® fibre damaged by UV exposure. *Composite Structures*, pp. 807-813.

Ceravolo, R., Erlicher, S. & Zanotti Fragonara, L., 2013. Comparison of restoring force models for the identification of structures with hysteresis and degradation. *Journal of Sound and Vibration*, pp. 6982-6999.

Ceravolo, R. et al., 2014. Vibration-based monitoring and diagnosis of cultural heritage: a methodological discussion in three examples.. *International Journal of Architectural Heritage* , pp. 274-303.

Černý, M., Glogar, P. & Manocha, L., 2000. Resonant frequency study of tensile and shear elasticity moduli of carbon fibre reinforced composites (CFRC). *Carbon*, pp. 2139-2149.

Chand, S., 2000. Review Carbon fibers for composites. *Journal of Materials Science*, pp. 1303 – 1313.

Charter of Venice., 1964. *Decision and Resolution*. Venezia, pp. 25–31.

Chen, Q., Worden, K., Peng, P. & Leung, A., 2007. Genetic algorithm with an improved fitness function for (N)ARX modelling. *Mechanical Systems and Signal Processing*, pp. 994-1007.

Chopra, A., 1995. *Dynamics of structures*. Englewood Cliffs, New Jersey: Prentice Hall.

Chou, T., Kelly, A. & Okura, A., 1985. Fibre-reinforced metal matrix composites. *Composites*.

Christensen, B., Gilstrap, J. & Dolan, C., 1996. Composites Materials Reinforcement of Existing Masonry Walls. *Journal of Architectural Engineering*, pp. 63-70.

Circolare n°564., 1997. *Istruzioni generali per la redazione dei progetti di restauro nei beni architettonici di valore storico-artistico in zona sismica.*

CNR-DT 200/2004, 2004. Istruzioni per la Progettazione, l'Esecuzione ed il Controllo di Interventi di Consolidamento Statico mediante l'utilizzo di Compositi Fibrorinforzati. pp. 1-172.

Codice dei Beni Culturali e del Paesaggio, 2004. *Governo Italiano. Gazzetta Ufficiale*, 45. Governo Italiano.

Codispoti, R. et al., 2015. Mechanical performance of natural fiber-reinforced composites for the strengthening of masonry. *Composites Part B*, pp. 74-83.

CompositeBuild.com, 2014. *CompositeBuild.com*. [Online] Available at: <http://compositebuild.com/inform/why-use-composites/>

Composites, R., 2014. *Revolution Composites*. [Online] Available at: <http://www.revolutioncomposites.com/>

Consiglio superiore dei lavori pubblici, 2011. *Linee Guida per la valutazione e riduzione del rischio sismico del patrimonio culturale - allineamento alle nuove Norme tecniche per le costruzioni.*

Corradi, M., Borri, A., Osofero, A. & Castori, G., 2015. Strengthening of Historic Masonry Structures with Composite Materials. In: *Handbook of Research on Seismic Assessment and Rehabilitation of Historic Structures*. Hershey (PA), USA: IGI Global, pp. 257-292.

Corradi, M., Borri, A. & Vignoli, A., 2002. Strengthening techniques tested on masonry structures struck by the Umbria-Marche earthquake of 1997–1998. *Construction and Building Materials*, pp. 229-239.

Corradi, M., Grazini, A. & Borri, A., 2007. Confinement of brick masonry columns with CFRP materials. *Composites Science and Technology*, p. 1772–1783.

Corradi, M., Speranzini, E., Borri, A. & Vignoli, A., 2006. In-plane shear reinforcement of wood beam floors with FRP. *Composites: Part B*, pp. 310-319.

Corradi, S. et al., 2009. Composite Boat Hulls with Bamboo Natural Fibres. *International Journal Materials and Product Technology*, pp. 73-89.

Council®, A. C., 2012-2017. *Operation Clean Sweep®*. [Online] Available at: <https://opcleansweep.org/Overview/About-SPI.html>

Crane, R. & Gillespie, J., 1991. Characterization of the vibration damping loss factor of glass and graphite fiber composites. *Composite Science Technology*, pp. 355-375.

Credali, L., 2002. *Recupero strutturale di opere murarie nel Complesso della Basilica di S. Antonio–Padova e nel Complesso di Venaria Reale–Torino, mediante rinforzi ibridi: fibra di carbonio–fibra aramidica*. Ferrara, Associazione Italiana Compositi (AICO), pp. 1-11.

Credali, L., 2009. *L'impiego delle tecnologie FRP nel recupero strutturale di Edifici Storici*. Venezia, Associazione Italiana Compositi (AICO), pp. 208-223.

Croci, G., 2000. General methodology for the structural restoration of historic buildings: the cases of the Tower of Pisa and the Basilica of Assisi. *Journal of Cultural Heritage*, pp. 7-18.

Croci, G., Ayala, D., Asdia, P. & Palombini, F., 1987. *Analysis on shear walls reinforced with fibres*. Tokyo, Japan.

D'Ambra, C. et al., 2009. *Confinement of tuff and brick masonry columns with FRP laminates*. Venezia, Associazione Italiana Compositi (AICO), pp. 232-241.

Dahl, M., Rice, E. & Groesbeck, E., 1987. *Effects of fiber motion on the acoustic behaviour of an anisotropic, flexible fibrous material*. Indianapolis, Indiana.

Dark III, T., 2008. Reclaiming the Future: Space Advocacy and the idea of progress. In: *The Societal Impact of Spaceflight*. Washington, DC: National Aeronautics and Space Administration, pp. 555-572.

Das, S. & Nizam, E., 2014. Applications of Fibber Reinforced Polymer Composites (FRP) in Civil Engineering. *International Journal of Advanced Structures and Geotechnical Engineering*, pp. 299-309.

De Lorenzis, L., Dimitri, R. & La Tegola, A., 2007. Reduction of the lateral thrust of masonry arches and vaults with FRP composites. *Construction and Building Materials*, pp. 1415–1430.

De Lorenzis, L., Galati, N. & Ombres, L., 2004. *In-plane shear strengthening of natural masonry walls with NSM CFRP strips and FRCM overlay*. Padova, Italy, Proceedings of 4th International Sem., pp. 843–855.

De Lorenzis, L., Tinazzi, A. & Nanni, A., 2000. *Near Surface Mounted FRP Rods for Masonry Strengthening: Bond and Flexural Testing*. Venezia, Italy, proc. of the 2nd Nat. Symp.

Dell'Isola, A. J. & Kirk, S. J., 1981. *Life cycle costing for design professionals*. New York: McGraw-Hill.

Demarie, G., Ceravolo, R., Sabia, D. & Argoul, P., 2010. Experimental identification of beams with localized nonlinearities. *Journal of Vibration and Control*.

Di Carlo, J. & Williams, W., 1980. *Dynamic modulus and damping of boron, silicon carbide and alumina fibers*. Florida.

Dizhur, D., Griffith, M. & Ingham, J., 2014. Out-of-plane strengthening of unreinforced masonry walls using near surface mounted fibre reinforced polymer strips. *Engineering Structures*, pp. 330-343.

Dolan, C., 1990. Developments in Non-Metallic Prestressing Tendons. *Precast/Prestressed concrete institute*, pp. 80-88.

Dresselhaus, M. et al., 1988. *Graphite Fibers and Filaments*. Berlino: Springer-Verlag.

Du Pont, c., 2017. *Du Pont*. [Online] Available at: <http://www.dupont.com/products-and-services/fabrics-fibers-nonwovens/fibers/articles/kevlar-properties.html>

Duflou, J., Deng, Y., Van Acker, K. & Dewulf, W., 2012. Do fiber-reinforced polymer composites provide environmentally benign alternatives? A life-cycle-assessment-based study. *MRS Bulletin*, pp. 374-382.

Ehlen, M., 1997. Life-Cycle Costs of new construction materials. *Journal of Infrastructure systems*, pp. 129-133.

Ehlen, M., 1999. Life-Cycle Costs of fiber-reinforced-polymer bridge decks. *Journal of Materials in Civil Engineering*, pp. 224-230.

Ehsani M.R., S. H. A.-S. A., 1997. Shear behavior of URM retrofitted with FRP overlays.. *Journal of Composites for Construction ASCE*, pp. 17-25.

El Abdi, R. et al., 2008. New method for strength improvement of silica optical fibres. *Optics and Lasers in Engineering*, pp. 222-229.

El-Dakhkhni, W., Hamid, A., Hakam, Z. & Elgaaly, M., 2006. Hazard mitigation and strengthening of unreinforced masonry walls using composites. *Composite Structures*, pp. 458–477.

ElGawady, M., Lestuzzi, P. & Badoux, M., 2005. In-Plane Seismic Response of URM Walls Upgraded with FRP. *Journal of Composites for Construction*, pp. 524-535.

El-Mahdy, T. & Gadelrab, R., 2000. Free vibration of unidirectional fiber reinforcement composite rotor. *Journal of Sound and Vibration*, pp. 195-202.

eurofibers, 2017. *eurofibers, smart fiber solutions*. [Online] Available at: <http://eurofibers.com/technora/>

Ewins, D., 2000. *Modal Testing: Theory, Practice and Application*. Baldock, UK: Research Studies Press.

Ewins, D., 2006. *A future for experimental structural dynamics*. Leuven, Belgium.

Farrar, C. & Worden, K., 2013. *Structural Health Monitoring- A machine learning perspective*. John Wiley & Sons, Ltd.

Feilden, B., 2003. *Conservation of historic buildings*. Architectural Press.

Feldman, M., 2006. Time-varying vibration decomposition and analysis based on the Hilbert transform. *Journal of Sound and Vibration*, pp. 518-530.

Feldman, M., 2007. Considering high harmonics for identification of non-linear systems by Hilbert transform. *Mechanical Systems and Signal Processing*, pp. 943-958.

Feldman, M., 2007. Identification of weakly nonlinearities in multiple coupled oscillators. *Journal of Sound and Vibration*, pp. 357-370.

- Feldman, M., 2014. Hilbert transform methods for nonparametric identification of nonlinear time varying vibration systems. *Mechanical Systems and Signal Processing*, pp. 66-77.
- Foraboschi, P., 2001. Strength Assessment of Masonry Arch Retrofitted Using Composite Reinforcements. *Masonry International*, pp. 17-25.
- Foraboschi, P., 2004. Strengthening of Masonry Arches with Fiber-Reinforced Polymer Strips. *Journal of Composites for Construction*, pp. 191-202.
- Forsyth, M. et al., 2007. *Structures & construction in historic building conservation*. Blackwell Publishing Ltd.
- Foster, P., Gergely, J., Young, D. & McGinley, M., 2005. *Strengthening masonry buildings with FRP composites*. Edinburgh, UK., Proceedings of International Conference.
- Friston, K., Mechelli, A., Turner, R. & Price, C., 2000. Nonlinear Responses in fMRI: The Balloon Model, Volterra Kernels, and Other Hemodynamics. *NeuroImage*, pp. 466–477.
- Fuellekrug, U. & Goege, D., 2012. Identification of weak non-linearities within complex aerospace structures. *Aerospace Science and Technology*, 23(1), pp. 53-62.
- Garibaldi, L., 2003. Application of the conditioned reverse path method. *Mechanical Systems and Signal Processing*, pp. 227–235.
- Garmendia, L., San-José, J., García, D. & Larrinaga, P., 2011. Rehabilitation of masonry arches with compatible advanced composite material. *Construction and Building Materials*, pp. 4374–4385.
- Gendelman, O., Starosvetsky, Y. & Feldman, M., 2008. Attractors of harmonically forced linear oscillator with attached nonlinear energy sink I: Description of response regimes. *Nonlinear Dynamics*, pp. 31-46.
- Gibson, R. & Plunkett, R., 1977. A forced vibration technique for measurement of material damping. *Experimental Mechanics*, pp. 297-302.
- Gibson, R., Yau, A. & Riegner, D., 1982. An improved forced-vibration technique for measurements of material damping. *Experimental techniques*, pp. 10-14.

Gilstrap, J. & Dolan, C., 1998. Out-of-plane bending of FRP-reinforced masonry walls.. *Composites Science and Technology*, pp. 1277–1284.

Giuffrè, A., 1993. *Sicurezza e conservazione dei centri storici: il caso di Ortigia*. Bari, Italy: Laterza.

Gokarneshan, N. & Alagirusamy, R., 2009. Weaving of 3D fabrics: A critical appreciation of the developments. *Textile Progress*, pp. 1-58.

Gowayed, Y., 2014. High performance fibers and fabrics for civil engineering applications. In: *High Performance Textiles and Their Applications*. Cambridge, UK: Woodhead Publishing Limited in association with The Textile Institute Woodhead Publishing is an imprint of Elsevier, pp. 351-354.

Granata, P. & Parvin, A., 2001. An experimental study on Kevlar strengthening of beam–column connections. *Composite Structures*, pp. 163-171.

Grande, E., Imbimbo, M. & Sacco, E., 2008. *FRP-strengthening of masonry structures: Effect of debonding phenomenon..* London, UK, Taylor and Francis, pp. 1017-1023.

Grange, P., Clair, D., Baillet, L. & Fogli, M., 2009. Brake squeal analysis by coupling spectral linearization and modal identification methods. *Mechanical Systems and Signal Processing*, pp. 2575–2589.

Grouvea, W. et al., 2008. Delamination detection with fibre Bragg gratings based on dynamic behaviour. *Composites Science and Technology*, pp. 2418–2424.

Hamid, A., El-Dakhakhni, W., Hakam, Z. & Elgaaly, M., 2005. Behavior of Composite Unreinforced Masonry – Fiber-Reinforced Polymer Wall Assemblages Under In-Plane Loading. *ASCE Journal of Composites for Construction*, pp. 73–83.

Hamid, A., Mohmond, A. & El Magal, S., 1994. *Strengthening and Repair of Un-reinforced Masonry Structures: State-of-the-art*. London, Elsevier Applied Science, pp. 485-497.

Hamilton III, H. & Dolan, C., 2001. Flexural capacity of glass FRP strengthened concrete masonry walls. *Journal of Composites for Construction*, pp. 170-178.

- Hamoush, S. et al., 2001. Out-of-plane Strengthening of Masonry Walls with Reinforced Composites. *ASCE J. of Composites for Construction*, pp. 139–145.
- Haroun, M., Mosallam, A. & Allam, K., 2003. Cyclic In-Plane Shear of Concrete Masonry Walls Strengthened by FRP Laminates. *Journal of Engineering Mechanics*, pp. 562–573.
- Hastak, M. & Halpin, D., 2000. Assessment of life-cycle benefit-cost of composite in construction. *Journal of Composites for Construction*, pp. 103-111.
- Hearle, J., 2001. *High-Performance Fibres*. Boca Raton: Woodhead Publishing Limited.
- Heller, L., Foltête, E. & Piranda, J., 2009. Experimental identification of nonlinear dynamic properties of built-up structures. *Journal of Sound and Vibration*, pp. 183-196.
- Hollaway, L., 1993. *Polymer Composites for Civil and Structural Engineering*. New Delhi: Springer.
- Hollaway, L., 1994. *Handbook of polymer composites for engineers*. Cambridge, England: Wothead Publishing Limited.
- Hollaway, L., 2010. A review of the present and future utilisation of FRP composites in the civil infrastructure with reference to their important in-service properties. *Construction and Building Materials*, pp. 2419–2445.
- Hollaway, L. & Head, P., 2001. *Advanced polymer composites and polymers in the civil infrastructure*. Oxford: Elsevier.
- Hollaway, L., 2003. The evolution of and the way forward for advanced polymer composites in the civil infrastructure. *Construction and Building Materials*, pp. 365-378.
- Hou, X. & Jiang, L., 2009. Learning from Nature: Building Bio-Inspired Smart Nanochannels. *American Chemical Society Nano Publications*, pp. 3339–3342.
- HuangGu, 2005. Ultraviolet treatment on high performance filaments. *Materials and Design*, pp. 47–51.

Huang, Y., Yan, C. & Xu, Q., 2012. *On the difference between empirical modede composition and Hilbert vibration decomposition for earthquake motion records*. Lisbon,Portugal.

Hull, D. & Clyne, T., 1996. *An introduction to composite materials*. Cambridge, UK: Cambridge University Press.

ICOMOS, 2003. *Principles for the analysis, conservation and structural restoration of architectural heritage*, ICOMOS, Guidelines.

Ilg, P., Hoehne, C. & Guenther, E., 2016. High-performance materials in infrastructure: a review of applied life cycle costing and its drivers e the case of fiber-reinforced composites. *Journal of Cleaner Production*, pp. 926-945.

Janssen, J., 1991. *Mechanical properties of bamboo*. Amsterdam: Kluwer Academic.

Jones, R., 1998. *Mechanics Of Composite Materials*. USA: Taylor & Francis.

Jungwirth, D. & Windisch, A., 1995. *Tendons made of non-metallic materials, requirements and economic application*. Ghent, Belgium, pp. 35-40.

Kabir, R. & Ferdous, N., 2012. Kevlar-The Super Tough Fiber. *International Journal of Textile Science*, pp. 78-83.

Kalali, A. & Kabir, M., 2012. Experimental response of double-wythe masonry panels strengthened with glass fiber reinforced polymers subjected to diagonal compression tests. *Engineering Structures*, pp. 24-37.

Kalmar-Nagy, T. & Balachandran, B., 2011. Forced harmonic vibration of a Duffing oscillator with linear viscous damping. In: *The Duffing equation: nonlinear oscillators and their behaviour*. John Wiley & Sons..

Karbhari, V., 2007. *Durability of composites for civil structural applications*. Cambridge (UK): Woodhead Publishing in Materials.

Karbhari, V. et al., 2003. Durability gap analysis for fiber-reinforced polymer composites in civil infrastructure. *Journal of Composites for Construction*, pp. 238–247.

- Karbhari, V. & Zhao, L., 2000. Use of composites for 21st century civil infrastructure. *Computer methods in applied mechanics and engineering*, pp. 433-454.
- Katz, A., Berman, N. & Bank, L., 1999. Effect of high temperature on bond strength of FRP rebars. *Journal of Composites for Construction*, pp. 73-81.
- Keller, T., Tracy, C. & Huge, E., 2006. Fire endurance of loaded and liquid-cooled GFRP slabs for construction. *Composites: Part A*, p. 1055–1067.
- Kendall, D., 2007. Building the future with FRP composites. *Reinforced Plastics*, pp. 26-33.
- Kerschen, G. & Golinval, J., 2004. A model updating strategy of non-linear vibrating structures. *International Journal for numerical methods in engineering*, pp. 2147–2164 .
- Kerschen, G. et al., 2008. Toward a fundamental understanding of the Hilbert–Huang transform in nonlinear dynamics. *Journal of Vibration and Control*.
- Kerschen, G., Worden, K., Vakakis, A. & Golinval, J., 2006. Past, present and future of nonlinear system identification in structural dynamics. *Mechanical Systems and Signal Processing*, pp. 505-592.
- Kinsella, M. et al., 2001. *Mechanical properties of polymeric composites reinforced with high strength glass*. Long Beach Convention Center, Long Beach California.
- Kiss, R., Kollár, L., Jai, J. & Krawinkler, H., 2002. Masonry Strengthened with FRP Subjected to Combined Bending and Compression, Part II: Test Results and Model Predictions. *Journal of Composite Materials*, pp. 1049–1063.
- Kong, J. & Frangopol, D., 2003. Life-Cycle Reliability-Based Maintenance Cost Optimization of Deteriorating Structures with Emphasis on Bridges. *Journal of Structural Engineering*, pp. 818-828.
- Konthesingha, K. et al., 2013. Static cyclic in-plane shear response of damaged masonry walls retrofitted with NSM FRP strips – An experimental evaluation. *Engineering Structures*, pp. 126-136.

Krevaikas, T. & Triantafillou, T., 2005. Masonry Confinement with Fiber-Reinforced Polymers. *Journal of Composites for Construction*, pp. 128-135.

Kuzik, M. E. A. R. C. J., 2003. Cyclic Flexure Tests of Masonry Walls Reinforced with Glass Fiber Reinforced Polymer Sheets. *ASCE Journal of Composites for Construction*, pp. 20–30.

Kwan, B. S., 2009. Reading in preparation for writing a PhD thesis: Case studies of experiences. *Journal of English for Academic Purposes*, pp. pages 180-191.

Lacy, S. & Bernstein, D., 2005. Subspace identification for non-linear systems with measured-input non-linearities. *International Journal of Control*, pp. 906-926.

Lagomarsino, S. et al., 2010. *PERPETUATE Project: the proposal of a performance-based approach to earthquake protection of cultural heritage*.

Lang, Z. & Billings, S., 2005. Energy transfer properties of non-linear systems in the frequency domain. *International Journal of Control*, pp. 345-362.

Larko, J. & Cotoni, V., 2007. *Vibroacoustic response of the NASA ACTS spacecraft antenna to launch acoustic excitation..* Cairns, Australia.

Li, G. et al., 2002. Stiffness Degradation of FRP Strengthened RC Beams Subjected to Hygrothermal and Aging Attacks. *Journal of Composite Materials*, pp. 795-812.

Lin, Z., Kanda, T. & Li, V., 1999. On interface property characterization and performance of fiber-reinforced cementitious composites. *Concrete Science and Engineering*, pp. 173-174.

Li, T., Galati, N. & Nanni, A., 2004. *Research on FRP strengthening of URM walls with opening..* Venezia, Italy, Proceedings of the International Symposium.

Li, V., 2003. On Engineered Cementitious Composites (ECC). *Journal of Advanced Concrete Technology*, pp. 215-230.

Ljung, L., 1999. *System Identification – Theory for the User*. Upper Saddle River, NY, USA: Prentice Hall.

- Ljung, L., 1999. *System Identification – Theory for the User*. Upper Saddle River, NY, USA: Prentice Hall.
- Lourenço, P., 2005. Assessment, diagnosis and strengthening of Outeiro Church, Portugal. *Construction and Building Materials*, pp. 634–645.
- Lourenço, P. & Poças Martins, J., 2001. *Strengthening of the architectural heritage with composite materials..* Porto, Portugal.
- Luciano, R., Marfia, S. & Sacco, E., 2001. *Reinforcement of masonry arches by FRP materials: experimental tests and numerical investigations*. Porto, Portugal.
- Luciano, R. & Sacco, E., 1998. Damage of masonry panels reinforced by FRP sheets. *International Journal of Solids and Structures*, pp. 1723–1741.
- M.W.Sracic, M., 2014. Identifying parameters of multi-degree-of-freedom nonlinear structural dynamic systems using linear time periodic approximations. *Mechanical Systems and Signal Processing*, pp. 325-343.
- Mahini, S., Ronagh, H. & Eslami, A., 2007. *Seismic rehabilitation of historical masonry vaults using FRP - a case study*. Asia-Pacific Conference on FRP in Structures (APFIS 2007), S.T. Smith (ed), pp. 565-570.
- Maia, N. & Silva, J., 1997. *Theoretical and Experimental Modal Analysis*. Baldock, UK: Research Studies Press.
- Mallardo, V., Malvezzi, R., Milani, E. & Milani, G., 2008. Seismic vulnerability of historical masonry buildings: A case study in Ferrara. *Engineering Structures*, pp. 2223–2241.
- Mallick, P., 1997. *Composite Engineering Handbook*. Dearborn, Michigan: CRC Press.
- Manno, A., 2013. *Seismic retrofitting of bell-towers based on experimentally verified models (Master thesis)*. Torino: Politecnico di Torino.
- Marcari, G., Manfredi, G., Prota, A. & Pecce, M., 2007. In-plane shear performance of masonry panels strengthened with FRP. *Composites: Part B*, pp. 887–901.

Marchesiello, S. & Garibaldi, L., 2008. A time domain approach for identifying nonlinear vibrating structures by subspace methods. *Mechanical Systems and Signal Processing*, pp. 81-101.

Masri, S. & Caughey, T., 2010. A Nonparametric Identification Technique for Nonlinear Dynamic Problems. *Journal of Applied Mechanics*, 46(2), pp. 433-447.

Matthews, F. & Rawlings, R., 1999. *Composite materials: engineering and science*. Chapman & Hall.

Micelli, F., De Lorenzis, L. & La Tegola, A., 2004. FRP-confined masonry columns under axial loads: experimental results and analytical model. *Masonry International*, pp. 95–108.

Micelli, F. & La Tegola, A., 2007. Structural strengthening of masonry columns: A comparison between steel strands and FRP composites. *ICE Construction Materials*, pp. 47-55.

Micelli, F. & Nanni, A., 2004. Durability of FRP rods for concrete structures. *Construction and Building Materials*, pp. 491-503.

MIL-HDBK-17-5, D. o. D., 2002. *Handbook of Composite Materials*. Washington, DC: Department of Defense.

Mininni, M., Gabriele, S., Lopes, H. & Araújo dos Santos, J., 2016. Damage identification in beams using peckle shearography and an optimal spatial sampling. *Mechanical Systems and Signal Processing*, pp. 47-64.

Ministero dei Beni Culturali ed Ambientali, 1997. *Istruzioni generali per la redazione dei progetti di restauro nei beni architettonici di valore storico-artistico in zona sismica*.

Miracle, D. & Donaldson, S., 2001. Introduction to Composites. In: *Composites*. Material Park, Ohio: ASM International, pp. 1-16.

Mishalani, R. & Madanat, S., 2002. Computation of Infrastructure Transition Probabilities Using Stochastic Duration Models. *Journal of Infrastructures Systems*, pp. 139-148.

Modena, C., 1995. Joint International Workshop on Evaluation and Strengthening of Existing Masonry Structures.

Modena, C. et al., 2010. *Emergency Actions and Definitive Intervention Criteria for the Preservation of Cultural Heritage Constructions subjected to Seismic Actions - Abruzzo 2009*. Porto, Portugal.

Modena, C. & Valluzzi, M., 2008. Repair techniques and long-term damage of massive structures. In: *Learning from failure - Long term behaviour of heavy masonry structures*. Ashurst Lodge, Ashurst, Southampton, UK: WIT Press, pp. 175-201.

Modena, C., Valluzzi, M., Da Porto, F. & Casarin, F., 2011. Structural Aspects of The Conservation of Historic Masonry Constructions in Seismic Areas: Remedial Measures and Emergency Actions. *International Journal of Architectural Heritage*, pp. 539–558.

Modena, C., Valluzzi, M., Tongini Folli, R. & Binda, L., 2002. Design choices and intervention techniques for repairing and strengthening of the Monza cathedral bell-tower. *Construction and Building Materials*, pp. 385–395.

Mosallam, A., 2007. Out-of-plane flexural behavior of unreinforced red brick walls strengthened with FRP composites.. *Composites: Part B*, pp. 559–574.

Nagasankar, P., Balasivananadha, P. & Velmurugan, R., 2014. The effect of the strand diameter on the damping characteristics of fibre reinforced polymer matrix composite: theoretical and experimental study. *International Journal of Mechanical Sciences*, pp. 279-288.

Nayfeh, A. & Mook, D., 1995. *Nonlinear Oscillations*. New York: John Wiley & Sons.

Nciri, M. et al., 2017. Modelling and characterisation of dynamic behaviour of short-fibre-reinforced composites. *Composite Structures*, pp. 516-528.

Niroumand, H., 2009. *Fibre Reinforced Polymer (FRP) in Civil, Structure & Geotechnical Engineering*. Seoul, s.n., pp. 451-456.

Nishizaki, I., Takeda, N., Ishizuka, Y. & Shimomura, T., 2006. *A Case Study of Life Cycle Cost based on a Real FRP Bridge*. Miami, Florida, USA, pp. 99-102.

Nivitex.Fibreglass.and.Resins, 2017. *Nivitex Fibreglass and Resins*. [Online] Available at: <http://www.nivitex.com/index.html>

Noël, J. & Kerschen, G., 2017. Non linear system identification in structural dynamics: 10 more years of progress. *Mechanical Systems and Signal Processing*, Issue 83, pp. 2–35.

Norden Huang, N. et al., 1998. *The empirical mode decomposition and the Hilbert spectrum for nonlinear and non-stationary time series analysis*.

Nurchi, A. & Valdes, M., 2005. *Strengthening of stone masonry columns by means of cement-based composite wrapping*. Lyon, France., Proceedings of the 3rd International Conference.

Nystrom, H., Watkins, S., Nanni, A. & Murray, S., 2003. Financial Viability of Fiber-Reinforced Polymer (FRP) Bridges. *Journal of Management in Engineering*, pp. 2-8.

Ochola, R., Marcus, K., Nurick, G. & Franz, T., 2004. Mechanical behaviour of glass and carbon fibre reinforced composites at varying strain rates. *Composite Structures*, pp. 455–467.

Oliveira, B. & Creus, G., 2004. An analytical–numerical framework for the study of ageing in fibre reinforced polymer composites. *Composite Structures*, pp. 443-457.

Oliveira, D., Basilio, I. & Lourenço, P., 2006. *FRP strengthening of masonry arches towards an enhanced behaviour*. Porto, Portugal.

Oliveira, D., Basilio, I. & Lourenço, P., 2010. Experimental Behavior of FRP Strengthened Masonry Arches. *Journal of Composites for Construction*, pp. 312-322.

Oliveira, D., Basilio, I. & Lourenço, P., 2011. Experimental Bond Behavior of FRP Sheets Glued on Brick Masonry. *Journal of Composites for Construction*, pp. 32-41.

Olympus, S., 2016. *Olympus, innovative materials for structural reinforcement and restoration & engineering services*. [Online] Available at: <http://www.olympus-frp.com/>

OSRAM, 2017. *OSRAM*. [Online] Available at: [http://www.osram.it/osram\\_it/](http://www.osram.it/osram_it/)

OwensCorning, 1999. *Owens Corning-Innovation for living*. [Online] Available at: <http://www.ocvreinforcements.com/>

Paduart, J. et al., 2010. Identification of nonlinear systems using Polynomial Nonlinear State Space models. *Automatica*, pp. 647-656.

Palucka, T. & Bensaude-Vincent, B., 2002. *Composite Overview*. [Online] Available at: [http://authors.library.caltech.edu/5456/1/hrst.mit.edu/hrs/materials/public/composites/Composites\\_Overview.htm#1st\\_generation](http://authors.library.caltech.edu/5456/1/hrst.mit.edu/hrs/materials/public/composites/Composites_Overview.htm#1st_generation)

Pambaguian, L. & Mervel, R., 1996. Fibre strength selection and the mechanical resistance of fibre-reinforced metal matrix composites. *Journal of Material Science*, pp. 5215-5220.

Papanicolaou, C., Triantafillou, T. & Lekka, M., 2011. Externally bonded grids as strengthening and seismic retrofitting materials of masonry panels,. *Construction and Building Materials*, pp. 504-514.

Parisi, M. & Piazza, M., 2002. Seismic behavior and retrofitting of joints in traditional timber roof structures. *Soil Dynamics and Earthquake Engineering*, pp. 1183–1191.

Pendhari, S., Kant, T. & Desai, Y., 2008. Application of polymer composites in civil construction: A general review. *Composite Structures*, pp. 114-124.

Peng, Z., Lang, Z. & Billings, S., 2007. Linear parameter estimation for multi-degree-of-freedom nonlinear systems using nonlinear output frequency-response functions. *Mechanical Systems and Signal Processing*, pp. 3108-3122.

Peng, Z., Lang, Z. & Billings, S., 2007. Non-linear output frequency response functions of MDOF systems with multiple non-linear components. *International Journal of Non-Linear Mechanics*, pp. 941-958.

Peng, Z., Lang, Z. & Billings, S., 2008. Nonlinear parameter estimation for multi-degree-of-freedom nonlinear systems using nonlinear output frequency-response functions. *Mechanical Systems and Signal Processing*, pp. 1582-1594.

Peng, Z. et al., 2011. Feasibility study of structural damage detection using NARMAX modelling and Nonlinear Output Frequency Response Function based analysis. *Mechanical Systems and Signal Processing*, pp. 1045–1061.

Pickering, K., Aruan Efendy, M. & Le, T., 2016. A review of recent developments in natural fibre composites and their mechanical performance. *Composites: Part A*, pp. 98–112.

Pinotti, E., Casalegno, C., R. & Surace, C., 2016. *Aramid fibers for conservative intervention on masonry structures*. Padova, Italy, CRC Press, Taylor & Francis Group.

Pintelon, R. & Schoukens, J., 2001. *System Identification: A Frequency Domain Approach*. Piscataway, NJ, USA: IEEE Press.

Platten, M., Wright, J., Cooper, J. & Dimitriadis, G., 2009. Identification of a nonlinear wing structure using an extended modal model. *Journal of Aircraft*, 46(5), pp. 1614-1626.

Platten, M., Wright, J., Dimitriadis, G. & Cooper, J., 2009. Identification of multi-degree of freedom non-linear systems using an extended modal space model. *Mechanical Systems and Signal Processing*, 23(1), pp. 8-29.

Presidenza del Consiglio dei Ministri, 2011. *Direttiva del Presidente del Consiglio dei Ministri per la valutazione e la riduzione del rischio sismico del patrimonio culturale con riferimento alle norme tecniche per le costruzioni*. Gazzetta Ufficiale, 2.

Ravikumar, C. & Thandavamoorth, T., 2014. Application of FRP for strengthening and retrofitting of civil engineering structures. *International Journal of Civil, Structural, Environmental and Infrastructure Engineering Research and Development (IJCSEIERD)*, pp. 49-60.

Rawal, S., 2001. Metal-matrix composites for space applications. *The Journal of The Minerals, Metals & Materials Society (TMS)*, pp. 14-17.

Relan, R., Vanbeylen, L., Firouz, Y. & Schoukens, J., 2015. *Characterization and nonlinear modelling of Li-Ion battery*. Lommel, Belgium.

Renson, L., Kerschen, G. & Cochelin, B., 2016. Numerical computation of nonlinear normal modes in mechanical engineering. *Journal of Sound and Vibration*, pp. 177-206.

ResinProget, 2012. *Resin Proget consolidamenti e restauri*. [Online] Available at: <http://www.resinproget.it/>

- Rice, B. et al., 2014. Measurement of Young's modulus and damping of fibres at cryogenic temperatures. *Cryogenics*, pp. 43-48.
- Richard, D. et al., 2007. Life-cycle performance model for composites in construction. *Composites: Part B*, pp. 236-246.
- Richards, C. & Singh, R., 1998. Identification of mulyi-degree-of-freedom non-linear systems under random excitations by the “reverse path” spectral method. *Journal of Sound and Vibration*, pp. 673-708.
- Roca, P. et al., 2008. Monitoring of long-term damage in long-span masonry constructions. In: *Long-term Behaviour of Heavy Masonry Structures*. Ashurst Lodge, Ashurst, Southampton, UK: WIT Press, pp. 125-151.
- Rosato, V., 1982. An Overview of Composites. In: *Handbook of composite*. Springer US, pp. 1-14.
- Russo, S. & Silvestri, M., 2008. *Perspectives Of Employment Of Pultruded FRP Structural Elements In Seismic Engineering Field*. Reggio Calabria (Italy).
- Ryngier, K. & Zdanowicz, L., 2015. Prestressing Concrete Structures with CFRP Composite Tendons. *Engineering Transactions*, pp. 407–419.
- S.I.G.I.T., S., 2015. *S.I.G.I.T. S.n.c.* [Online] Available at: <http://www.sigit.to/>
- Saadatmanesh, H., 1997. Extending service life of concrete and masonry structures with fiber composites. *Construction and Building Materials*, pp. 327–335.
- Saad, P., Al Majid, A., Thouverez, F. & Dufour, R., 2006. Equivalent rheological and restoring force models for predicting the harmonic response of elastomer specimens. *Journal of Sound and Vibration*, pp. 619-639.
- Said, M. et al., 2006. Investigation of ultra violet (UV) resistance for high strength fibers. *Advances in Space Research*, pp. 2052–2058.
- Saileysh Sivaraja, S. et al., 2013. *Preservation of Historical Monumental Structures using Fibre Reinforced Polymer (FRP) - Case Studies*. Elsevier, pp. 472 – 479.
- Salama, M., 1984. Lightweight Materials for Mooring Lines of Deepwater Tension Leg Platforms. *Marine Technology*, pp. 234-241.

Schetzen, M., 1980. *The Volterra and Wiener Theories of Nonlinear Systems*. New York, NY, USA: John Wiley & Sons.

Schulman, A. I., 2017. A. Schulman. [Online] Available at: <http://ir.aschulman.com/releasedetail.cfm?releaseid=1004602>

Schwegler, G., 1994. *Masonry construction strengthened with fiber composites in seismically endangered zones..* Rotterdam, The Netherlands, pp. 454-458.

Sciolti, M., Frigione, M. & Aiello, M., 2010. Wet Lay-Up Manufactured FRPs for Concrete and Masonry Repair: Influence of Water on the Properties of Composites and on Their Epoxy Components. *Journal of Composites for Construction*, pp. 823-833.

Scott, D., Lai, J. & Zureick, A., 1995. Creep behavior of fiber-reinforced polymeric composites: a review of the technical literature. *Journal of Reinforcement for Plastic composites*, pp. 588-617.

Selin Ravikumar, C. & Thandavamoorthy, T., 2014. Application of FRP for strengthening and retrofitting of civil engineering structures. *International Journal of Civil, Structural Environmental and Infrastructure Engineering*, pp. 49-60.

Selvaraju, S. & Ilaiyave, S., 2011. Applications of composites in marine industry. *Journal of Engineering Research and Studies*, pp. 89-91.

Sen, R., 2003. Advances in the application of FRP for repairing corrosion damage. *New Materials in Construction*, pp. 99-113.

Shrive, N., 2006. The use of fibre reinforced polymers to improve seismic resistance of masonry. *Construction and Building Materials*, pp. 269–277.

Shrive, N., Masia, M. & Lissel, S., 2001. Strengthening and rehabilitation of masonry using fibre reinforced polymers. *Historical Construction*, pp. 1047-1056.

Silva, M., 2007. Aging of GFRP laminates and confinement of concrete columns. *Composite Structures*, pp. 97–106.

Silva, M. & Biscaia, H., 2008. Degradation of bond between FRP and RC beams.. *Composite Structures*, pp. 164-174.

Sivaraja, S., Thandavamoorthy, T., Vijayakumar, C. & Aranganathan, S., 2013. *Preservation of Historical Monumental Structures using Fibre Reinforced Polymer (FRP) - Case Studies*. Solo, Jawa Tengah, Indonesia, *Procedia Engineering*, p. 472 – 479.

Song, W., Dyke, S. & Harmon, T., 2013. Application of Nonlinear Model Updating for a Reinforced Concrete Shear Wall. *Journal of Engineering Mechanics*, pp. 635-649 .

Soyoz, S., 2009. Long-Term Monitoring and Identification of Bridge Structural Parameters. *Computer-Aided Civil and Infrastructure Engineering*, pp. 82–92.

Spina, D., Valente, C. & Tomlinson, G., 1996. A new procedure for detecting nonlinearity from transient data using the gabor transform. *Nonlinear dynamics*, 11(3), p. 235–254.

Sracic, M. & Allen, M., 2011. Method for identifying models of nonlinear systems using linear time periodic approximations. *Mechanical Systems and Signal Processing*, pp. 2705–2721.

Srivastava, S. & Hoda, S., 2016. A Brief Theory on Latest Trend of Filament Winding Machine. *International Journal of Advanced Engineering Research and Science (IJAERS)*, pp. 33-38.

Stacey, M., 1988. Production and characterisation of fibres for metal matrix composites. *Materials Science and Technology*.

Suarez, S. & Gibson, R., 1984. *Computer-aided dynamic testing of composite materials*. Milwaukee, WI, USA, Proceedings SEM, pp. 118-123.

Suarez, S., Gibson, R. & Deobald, L., 1984. Random and impulse techniques for measurement of damping in composite materials. *Experimental Techniques*, pp. 19-24.

Tan, K., Patoary, M. & Roger, C., 2003. Anchorage Systems for Masonry Walls Strengthened with FRP Composite Laminates. *Journal of Reinforced Plastics and Composites*, pp. 1353–1371.

Tomažević, M. & Weiss, P., 1994. Seismic behaviour of plain and reinforced masonry buildings. *Journal of Structural Engineering ASCE*, pp. 323–338.

Tomazevic, M., 1999. *Earth quake resistano design of masonry buildings*. London, UK: Imperial College Press.

Tomaževic, M. & Lutman, M., 1996. Seismic behaviour of masonry walls: Modelling of hysteretic rules.. *Journal of Structural Engineering ASCE*, pp. 1048–1054.

Triantafillou, T., 1998. Strengthening of masonry structures using epoxy-bonded FRP laminates. *Journal of Composites for Construction*, pp. 96-104.

Triantafillou, T. & Fardis, M., 1993. *Advanced composites for strengthening historic structures*. Lisbon, Portugal, Int. Assoc. for Bridge and Struct. Engrg., pp. 541-548.

Triantafillou, T. & Fardis, M., 1997. Strengthening of historic masonry structures with composite materials. *Materials and Structures/Matériaux et Constructions*, pp. 486-496.

Tumialan, J., Galati, N. & Nanni, A., 2003. FRP Strengthening of UMR Walls Subject to Out-of-Plane Loads. *ACI Structures Journal*, pp. 312-329.

Turco, V. et al., 2006. Flexural and shear strengthening of unreinforced masonry with FRP bars. *Composites Science and Technology*, pp. 289–296.

Valluzzi, M., 2008. *Strengthening of masonry structures with Fibre Reinforced Plastics: From modern conception to historical building preservation*. London, Taylor & Francis Group, pp. 33-45.

Valluzzi, M., Binda, L. & Modena, C., 2005. Mechanical behaviour of historic masonry structures strengthened by bed joints structural repointing. *Construction and Building Materials*, pp. 63-73.

Valluzzi, M., Da Porto, F. & Modena, C., 2004. Behavior and modeling of strengthened three-leaf stone masonry walls. *Materials and Structures*, pp. 184-192.

Valluzzi, M., Tinazzi, D. & Modena, C., 2002. Shear behavior of masonry panels strengthened by FRP laminates.. *Construction and Building Materials*, pp. 409-416.

Valluzzi, M., Valdemarca, M. & Modena, C., 2001. Behavior of brick masonry vaults strengthened by FRP laminates. *Journal of Composites for Construction*, pp. 163-169.

Valluzzi, M., Valdemarca, M. & Modena, C., 2001. Behavior of brick masonry vaults strengthened by FRP laminates.. *Journal of Composites for Construction ASCE* , pp. 163-169.

Valtorta, D., Lefèvre, J. & Mazza, E., 2005. A new method for measuring damping in flexural vibration of thin fibers. *Experimental Mechanics*, pp. 433-439.

VanOverschee, P. & DeMoor, B., 1996. *Subspace Identification for Linear Systems: Theory, Implementation and Applications*. Dordrecht, TheNetherlands,: Kluwer Academic Publishers.

Velazquez-Dimas, J., Ehsani, M. & Saadatmanesh, H., 2000. Out-of-Plane Behavior of Brick Masonry Walls Strengthened with Fiber Composites. *ACI Structural Journal*, pp. 377–387.

Vintzileou, E. & Tassios, T., 1995. Three leaf stone masonry strengthened by injecting cement grouts. *Journal of Structural Engineering ASCE*, pp. 848–856.

Wallenberger, F., Watson, J., Li, H. & Industries, P., 2001. Glass Fibres. In: *ASM Handbook, Vol. 21: Composites*. Materials Park, Ohio, USA: ASM International®, pp. 27-34.

Wang, H. et al., 2012. The influence of UV radiation and moisture on the mechanical properties and micro-structure of single Kevlar fibre using optical methods. *Polymer Degradation and Stability*, pp. 1755-1761.

Wang, X. & Zheng, G., 2016. Equivalent Dynamic Stiffness Mapping technique for identifying nonlinear structural elements from frequency response functions. *Mechanical System and Signal Processing*, pp. 394–415.

Wei, C. & Kukureka, S., 2000. Evaluation of damping and elastic properties of composites and composite structures by the resonance technique. *Journal of Materials Science*, pp. 3785-3792.

Widanage, W. et al., 2011. Nonlinear system-identification of the filling phase of a wet-clutch system. *Control Engineering Practice*, pp. 1506-1516.

Więcek, T., 2014. A new method for the measurement of static and dynamic Young's moduli of long fibres. *Composites: Part A*, pp. 1-7.

Wielage, B., Lampkea, T., Utschick, H. & Soergel, L., 2003. Processing of natural-fibre reinforced polymers and the resulting dynamic–mechanical properties. *Journal of Materials Processing Technology*, pp. 140–146.

Worden, K., Hickey, D., Haroon, M. & Adams, D., 2009. Nonlinear system identification of automotive dampers: A time and frequency-domain analysis. *Mechanical Systems and Signal Processing*, pp. 104-126.

Worden, K. & Tomlinson, G., 2001. *Nonlinearity in Structural Dynamics*. IOP Publishing Ltd.

Wu, Z. & Abe, M., 2003. *Proceedings of the International Conference on Structural Health Monitoring and Intelligent Infrastructure*. Lisse, Netherlands, Swets and Zeitlinger.

Xu, B., He, J. & Dyke, S., 2015. Model-free nonlinear restoring force identification for SMA dampers with double Chebyshev polynomials: approach and validation. *Nonlinear Dynamics*, pp. 1507–1522.

Yajima, S., Omori, M., Hayashi, J. & Okamura, K., 1976. Simple Synthesis of the continuous SiC fiber with high tensile strength. *CSJ Journals*, pp. 551-554.

Yang, Z. et al., 2006. *Identification of structural free-play non-linearities using the non-linear resonant decay method*. Leuven, Belgium, Proceedings of the International Seminar on Modal Analysis (ISMA).

Yuan, H., Teng, J. G. & Seracino, R., 2004. Full-range behavior of FRP to concrete bonded joints. *Engineering Structures*, pp. 553-565.

Zanotti Fragonara, L. et al., 2017. Dynamic investigation on the Mirandola bell tower in post-earthquake scenarios. *Bulletin of Earthquake Engineering*, pp. 313–337.

Zhang, S., 2003. Fabrication of novel biomaterials through molecular self-assembly. *Nature Biotechnology*, pp. 1171 - 1178.



